iScience

CellPress

Article

Visible-Light-Induced Alkoxyl Radicals Enable α-C(sp^3)-H Bond Allylation

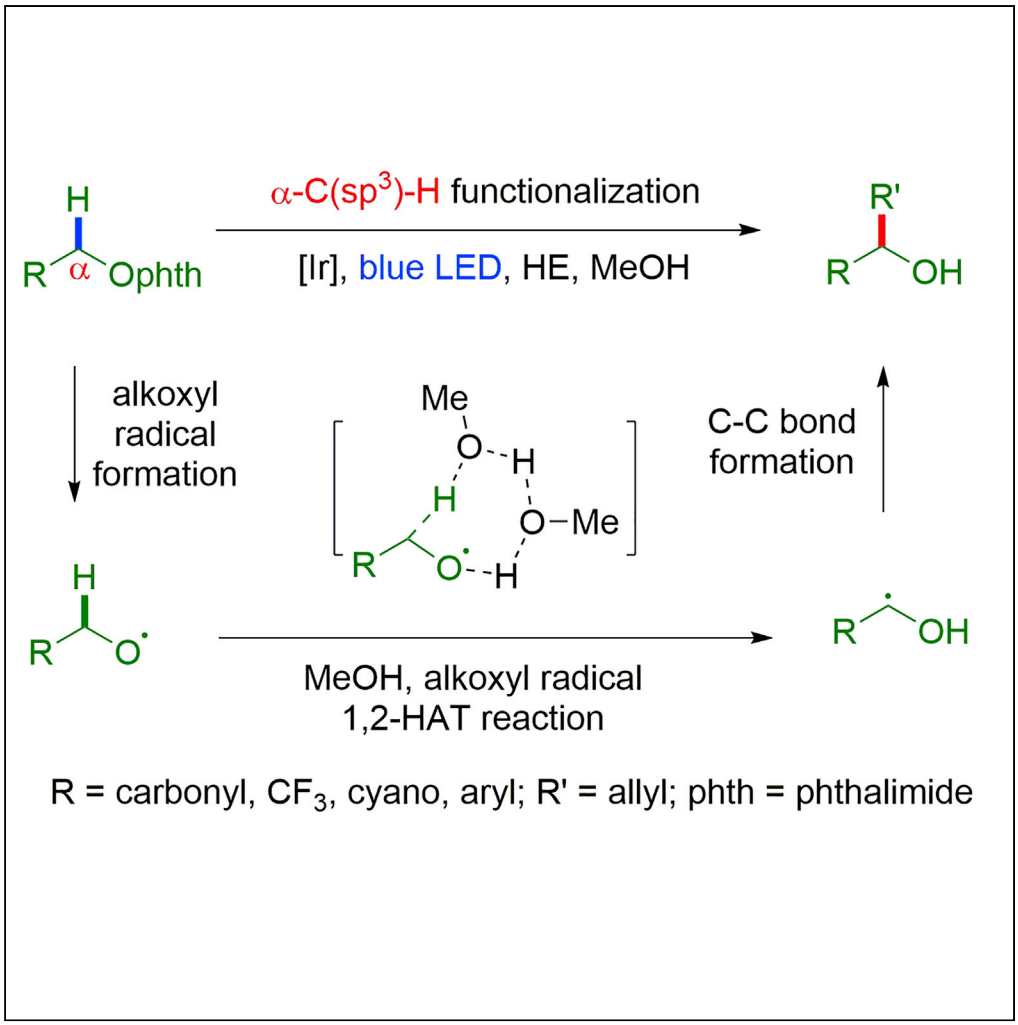

Jing Zhang, Dan Liu, Song Liu, Yuanyuan Ge, Yu Lan, Yiyun Chen

lanyu@cqu.edu.cn (Y.L.)
yiyunchen@sioc.ac.cn (Y.C.)

HIGHLIGHTS

1,2-Hydrogen atom transfer (HAT) of alkoxyl radical enables α-C(sp^3)-H allylation

α-Carbonyl, α-cyano, α-trifluoromethyl, and benzylic C(sp^3)-H bonds are applicable

Mechanistic and electron paramagnetic resonance (EPR) studies confirmed 1,2-HAT

DFT calculations explained the methanol acceleration of alkoxyl radical 1,2-HAT

Zhang et al., iScience *23*, 100755
January 24, 2020 © 2019 The Author(s).
https://doi.org/10.1016/j.isci.2019.100755

iScience

CellPress

Article

Visible-Light-Induced Alkoxyl Radicals Enable α-C(sp^3)-H Bond Allylation

Jing Zhang,[1,4] Dan Liu,[1,4] Song Liu,[2] Yuanyuan Ge,[1] Yu Lan,[2,3,*] and Yiyun Chen[1,5,*]

SUMMARY

The alkoxyl radical is an essential reactive intermediate in mechanistic studies and organic synthesis with hydrogen atom transfer (HAT) reactivity. However, compared with intramolecular 1,5-HAT or intermolecular HAT of alkoxyl radicals, the intramolecular 1,2-HAT reactivity has been limited to theoretical studies and rarely synthetically utilized. Here we report the first selective 1,2-HAT of alkoxyl radicals for α-C(sp^3)-H bond allylation of α-carbonyl, α-cyano, α-trifluoromethyl, and benzylic N-alkoxylphthalimides. The mechanistic probing experiments, electron paramagnetic resonance (EPR) studies, and density functional theory (DFT) calculations confirmed the 1,2-HAT reactivity of alkoxyl radicals, and the use of protic solvents lowered the activation energy by up to 10.4 kcal/mol to facilitate the α-C(sp^3)-H allylation reaction.

INTRODUCTION

The selective inert C(sp^3)-H bond activation for new C-C bond formation is very desirable in organic synthesis (Chen et al., 2009; Lyons and Sanford, 2010; Prier et al., 2013; Gensch et al., 2016; Yi et al., 2017). The hydroxyl groups are ubiquitous in organic molecules, and the use of hydroxyl derivatives provides an effective tool to differentiate chemically indistinguishable C-H bonds (Holmes et al., 2018; Engle et al., 2012; Ren et al., 2012; Wappes et al., 2017; Espino et al., 2001; Simmons and Hartwig, 2012a; Chen et al., 2008, 2015; Karmel et al., 2018). The alkoxyl radical is an essential reactive intermediate in mechanistic studies and organic synthesis, and its highly reactive character enables unactivated C-H bond functionalization with the hydrogen atom transfer (HAT) reactivity (Čeković, 2003, 2005; Hartung, 2001; Chiba and Chen, 2014; Lundgren et al., 2006; Salamone et al., 2011, 2012, 2013, 2014a, 2014b, 2016a, 2016b; Bietti and Salamone, 2014; Salamone and Bietti, 2015). When intramolecular δ-C-H bonds are present within the molecule, the 1,5-HAT reaction of alkoxyl radicals preferentially occurs to abstract the δ-C-H; otherwise, the intermolecular HAT reaction dominates (Scheme 1A) (Dorigo and Houk, 1988; Robertson et al., 2001; Weavers, 2001; Burke et al., 1988; Petrovic et al., 2004; Zhu et al., 2009, 2015; Rueda-Becerril et al., 2011; Hu et al., 2018; Wu et al., 2018a, 2018b; Guan et al., 2018). In contrast, the intramolecular C-H abstraction at positions other than δ-position by alkoxyl radicals has been less reported owing to the unfavorable transition states and high activation energies (Čeković, 2003, 2005; Hartung, 2001; Chiba and Chen, 2014). Currently, there are only a few reports on the 1,2-HAT reactivity of alkoxyl radicals in theoretical or biological studies, and the synthetic utilization of 1,2-HAT for new C-C bond formation remains elusive (Buszek et al., 2011; Elford and Roberts, 1996; Fernández-Ramos and Zgierski, 2002; Konya et al., 2000; Gilbert et al., 1976; Che et al., 2016, 2018). Here we report the first visible-light-induced α-C(sp^3)-H allylation reaction enabled by the selective 1,2-HAT of alkoxyl radicals, which is facilitated by protic solvents and applicable to various α-carbonyl, α-cyano, α-trifluoromethyl, and benzylic C(sp^3)-H bonds (Scheme 1B).

RESULTS AND DISCUSSION

Optimization of the Reaction Conditions

Our investigation was initiated by the serendipitous discovery with N-alkoxylphthalimide **1** as the alkoxyl radical precursor, which can be readily prepared from alcohols and are bench-stable (Scheme 2) (Zhu et al., 2009; Kim et al., 1998; Zhang et al., 2016, 2017; Wang et al., 2016; Ito et al., 2018; Han et al., 2019; Deng et al., 2019; Shi et al., 2019). Under the reaction conditions of *fac*-Ir(ppy)$_3$ and Hantzsch ester known to generate alkoxyl radicals (Zhang et al., 2016, 2017; Wang et al., 2016; Ito et al., 2018; Han et al., 2019; Deng et al., 2019; Shi et al., 2019), the ester-derived N-alkoxylphthalimide **1** gave no δ-C(sp^3)-H allylation adduct **3** with allyl sulfone **2** under blue LED irradiation. Instead, the α-C(sp^3)-H allylation adduct **4** was observed in 41% yield, together with the hydrogenation adduct alcohol **5** in 52% yield (entry 1 in Table 1) (Zhang et al., 2016). These results were in sharp contrast with our previous observation on the reactivity of alkoxyl radicals under photocatalysis conditions (Zhang et al., 2016, 2017). We then tested the addition of

[1]State Key Laboratory of Bioorganic and Natural Products Chemistry, Center for Excellence in Molecular Synthesis, Shanghai Institute of Organic Chemistry, University of Chinese Academy of Sciences, Chinese Academy of Sciences, 345 Lingling Road, Shanghai 200032, China

[2]School of Chemistry and Chemical Engineering, Chongqing University, Chongqing 400030, China

[3]Green Catalysis Center, College of Chemistry, Zhengzhou University, Zhengzhou, Henan 450001, China

[4]These authors contributed equally

[5]Lead Contact

*Correspondence: lanyu@cqu.edu.cn (Y.L.), yiyunchen@sioc.ac.cn (Y.C.)

https://doi.org/10.1016/j.isci.2019.100755

This is an open access article under the CC BY license (http://creativecommons.org/licenses/by/4.0/).

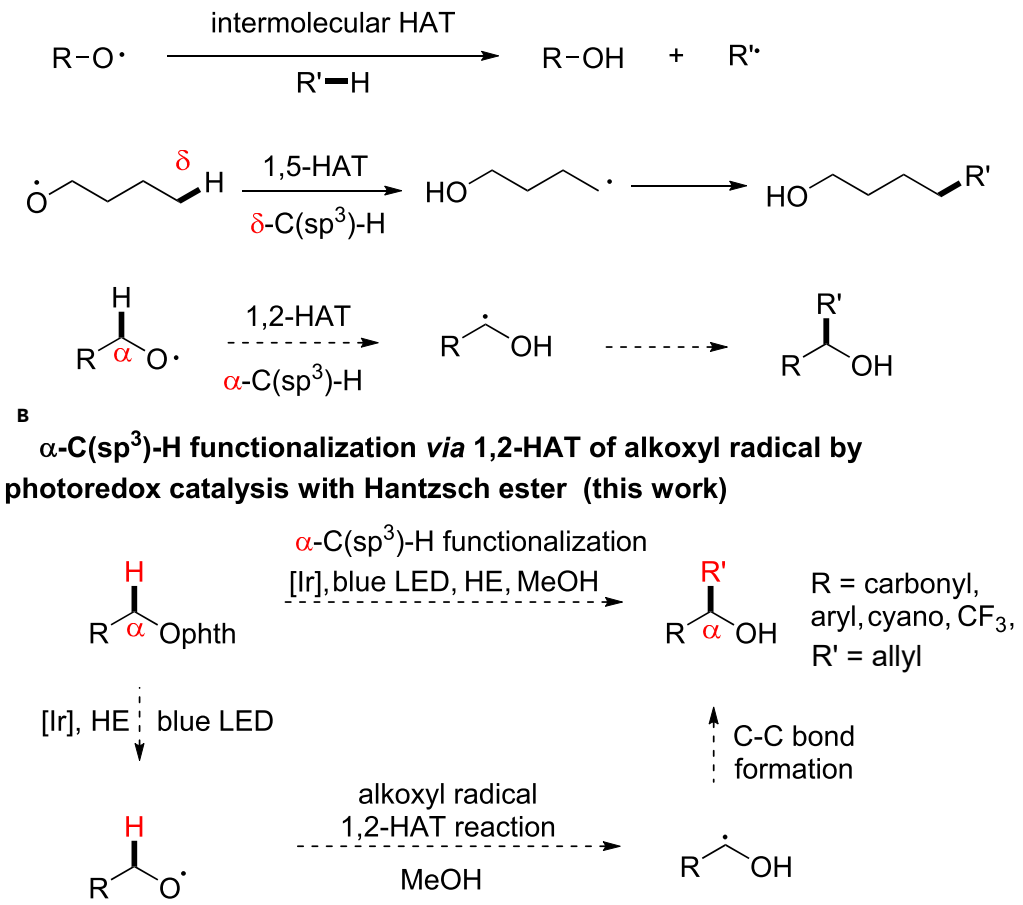

Scheme 1. Selective C(sp^3)-H Functionalization via Hydrogen Atom Transfer of Alkoxyl Radicals

phth, Phthalimide. (A) Alkoxyl radicals enable C(sp^3)-H functionalization with intermolecular HAT, intramolecular 1,5-HAT or 1,2-HAT. (B) α-C(sp^3)-H allylation via 1,2-HAT of alkoxyl radical by photoredox catalysis with Hantzsch ester.

acids or bases to the reaction and found the outcomes of the reaction were not significantly affected (entries 2–3). The further screen of different Hantzsch ester derivatives has little effect on the reaction (entries 4–6) (Chen et al., 2016). Significantly, the use of ethanol or methanol as solvents dramatically improved the α-C(sp^3)-H allylation adduct to 93%–97% yields (93% isolated yield, entries 7–8) and minimalized the hydrogenation adduct alcohol **5** formations. The mixed protic solvents were also beneficial that the addition of methanol or water improved the reaction of dioxane from 41% to 52%–66% yields (entries 9–10) (see Tables S2 and S3).

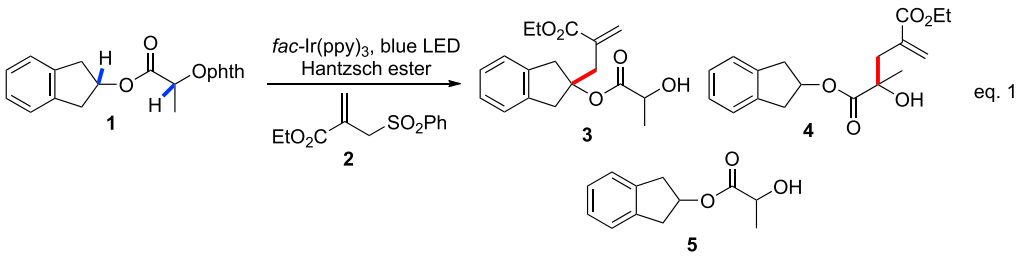

Scheme 2. 1,2-HAT Reaction of N-alkoxylphthalimide 1

Entry	Conditions[a]	4 Yield (%)[b]	5 Yield (%)[b]
1	Dioxane	41	52
2	Entry 1, 2.0 equiv. Na_2CO_3	56	42
3	Entry 1, 2.0 equiv. HCO_2H	40	56
4	Entry 1, COOMe-HE	43	56
5	Entry 1, COO^{i}Pr-HE	47	52
6	Entry 1, COO^{t}Bu-HE	45	54
7	EtOH	93	7
8	MeOH	97 (93)	<5
9	MeOH/dioxane = 1:9	52	45
10	H_2O/dioxane = 1:9	66	33

Table 1. Discovery and Optimization of the 1,2-HAT of Alkoxyl Radicals for α-C(sp^3)-H Allylation

[a]Reaction conditions: **1** (0.10 mmol, 1.0 equiv.), **2** (0.30 mmol, 3.0 equiv.), *fac*-Ir(ppy)$_3$ (0.001 mmol, 1%), and Hantzsch ester (0.15 mmol, 1.5 equiv.) in 1.0 mL solvent under nitrogen with 4 W blue LED irradiation at ambient temperature for 3 h, conversion was >95%, unless otherwise noted.

[b]Conversion and yields were determined by ^{1}H NMR analysis, and isolated yields are in parentheses.

Scope

We next explored the scope of this 1,2-HAT reaction for other substrates (Scheme 3). The glycol-derived **6** without ring strain at the δ-C-H bonds afforded **7** in 89% yield, without the observation of the δ-C-H allylation adducts. The benzyl ester **8** with the activated benzylic δ-C-H bonds gave the α-C(sp^3)-H allylation adduct **9** in 92% yield. The N-alkoxylphthalimides **10** and **12** provided 88% and 95% yields of α-C-H allylation adducts, successfully, with the ketone or the free hydroxyl group unaffected. The N-alkoxylphthalimide **14** with the amide linkage provided the 1,2-HAT adduct **15** smoothly in 52% yield, together with 17% yield of hydrogenation adduct as the side product (See Figures S1–S26).

The 1,2-HAT reaction is also applicable to N-alkoxylphthalimides without the ester or amide linkages. The N-alkoxylphthalimide **16** with benzyl C(sp^3)-H bonds gave the α-C(sp^3)-H allylation adduct **17** in 66% yield (Scheme 3). The incorporation of electron-rich methoxyl group on the phenyl ring slightly improved the reaction to give **19** in 71% yield, whereas the electron-deficient fluorides decreased the reaction to give **21** in 52% yield. The α- and β-substituted naphthalenes reacted nicely to give **23** and **25** in 68%–73% yields. The heterocyclic furans and thiophenes reacted to provide **27** and **29** in 71%–75% yields. The secondary-alcohol-derived N-alkoxylphthalimides **30** and **32** gave the corresponding tertiary homoallylic alcohols **31** and **33** in 51% and 53% yields, respectively (See Figures S27–S64).

This reaction is particularly valuable for the homoallylic alcohol synthesis when the corresponding aldehydes are inaccessible by the nucleophilic addition methods (Yamamoto and Asao, 1993; Yus et al., 2011). The cyano-substituted homoallylic alcohol **35** can be obtained from the stable N-alkoxylphthalimide **34** by 1,2-HAT reaction smoothly in 59% yield, and the corresponding formyl cyanide **36** is unstable and cannot be synthetically utilized (Scheme 4) (Lewis-Bevan et al., 1992). Similarly, the trifluoromethyl-substituted homoallylic alcohol **37** can be prepared from the stable N-alkoxylphthalimide **38** in 39% yield, whereas the trifluoromethyl aldehyde **39** is very unstable and volatile (Scheme 5) (Ishikawa et al., 1984; Loh and Li, 1999). We also tested a structurally complexed steroid derivative **40** with multiple tertiary and allylic C-H bonds, which are challenging substrates to differentiate the targeted α-C-H bonds by intermolecular HAT reactions (Scheme 6) (Roberts, 1999; Chu and Rovis, 2018). Gratifyingly, the α-C(sp^3)-H allylation adduct **41** was selectively obtained in 62% yield, leaving other six tertiary C-H and four allylic C-H bonds untouched (see Figures S65–S78).

Mechanistic Investigations

We next carried out mechanistic investigations (Scheme 7). The possible intermolecular hydrogen atom transfer pathway instead of the 1,2-HAT was first evaluated by crossover experiments (Schemes 7A and

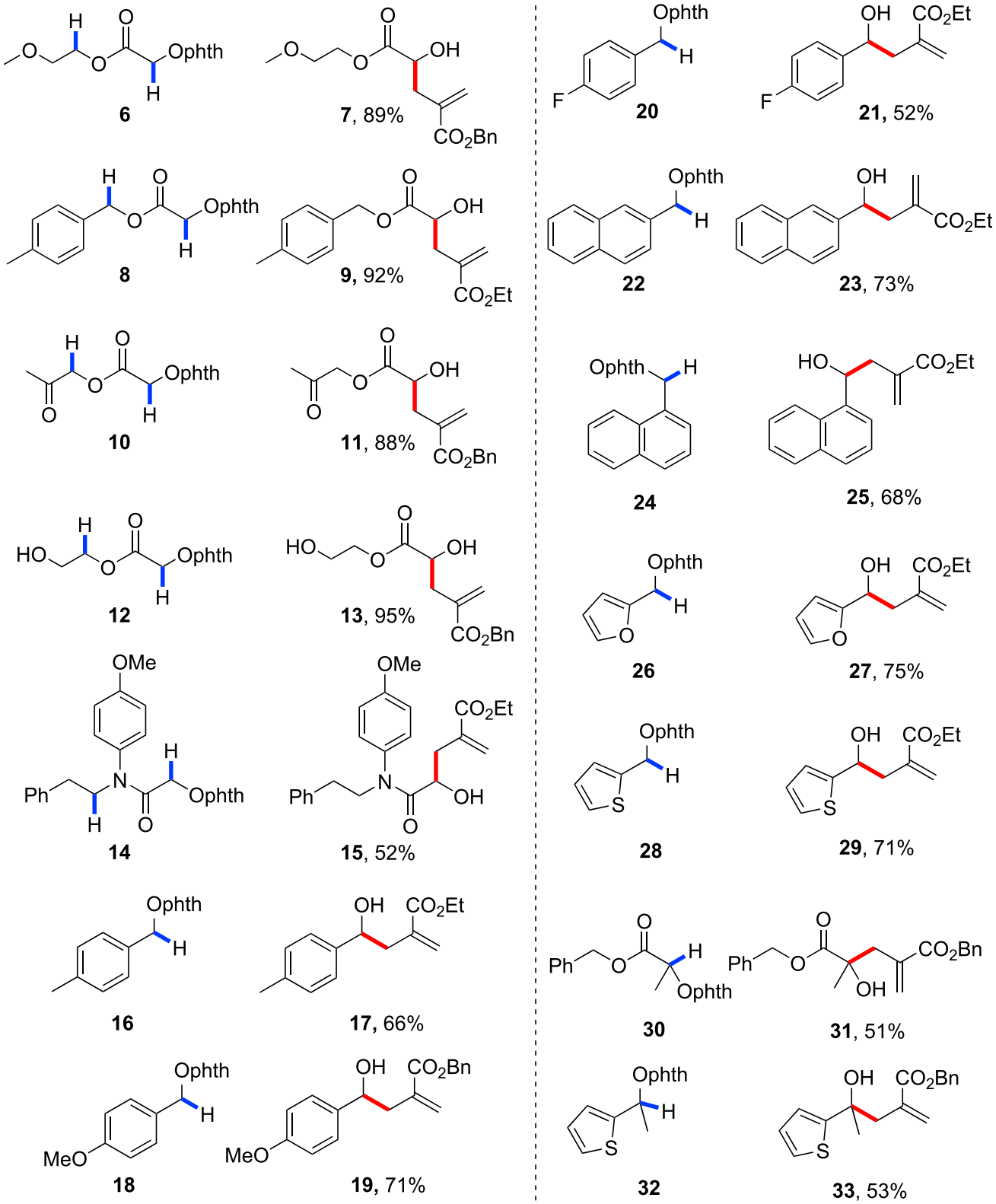

Scheme 3. Substrate Scope of the 1,2-HAT Reactions

Reaction condition is in entry 8 in Table 1, and isolated yields are reported.

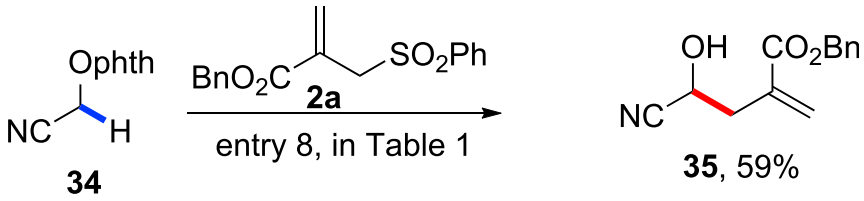

Scheme 4. 1,2-HAT Reaction of N-alkoxylphthalimide 34

S1). With N-alkoxylphthalimide **16** and a structurally similar alcohol **42**, the reaction with allylsulfone **2** gave the exclusive homoallylic alcohol **17** from **16** in 69% yield, whereas the formation of **23** from **42** was not observed. This result together with the chemoselective α-C(sp^3)-H allylation demonstrated in Scheme 6 excluded the intermolecular HAT reaction pathway. We then compared the 1,2-HAT with other potential reaction pathways of alkoxyl radicals in different N-alkoxylphthalimides (Scheme 7B). With benzyl alcohol-derived N-alkoxylphthalimide **43** bearing a pendant alkene at the δ-position, the tetrahydrofuran **44** was obtained via the preferential 5-exo cyclization of alkoxyl radicals, whereas neither the α-C(sp^3)-H allylation adduct nor the oxidized ketone adduct **45** was observed (Zlotorzynska and Sammis, 2011). With benzyl alcohol-derived N-alkoxylphthalimide **46** bearing activated δ-C-H bonds, the α-C(sp^3)-H allylation adduct **47** was observed in 36% yield, together with the δ-C(sp^3)-H allylation adduct **48** in 15% yield (see Scheme S3 for details). These results confirmed the presence of alkoxyl radicals and suggested other alkoxyl radical reaction pathways may be favored over 1,2-HAT pathway in certain substrates (the KIE (k_H/k_D) with deuterated N-alkoxylphthalimide was measured to be 0.87, suggesting the cleavage of the C-H bond was not the rate-determining step, see Table S1, Scheme S2 and Simmons and Hartwig, 2012b) (see Figures S79–S96).

We further investigated the radical intermediates in the reaction by the electron paramagnetic resonance measurements (EPR) using 5,5-dimethyl-pyrroline N-oxide (DMPO) **50** as the radical spin trap. Scheme 8 illustrates the EPR spectrum from the addition of DMPO to the reaction of N-alkoxylphthalimide **49** (see Schemes S11–S13). The spectrum can be fit as the admixture of a triplet of doublets (a_N = 14.1 G, a_H = 9.6 G) and a triplet of doublets (a_H = 14.2 G, a_H = 19.7 G) in dioxane. The first triplet of doublets is attributed to DMPO-trapped alkoxyl radical **51** (asterisk * signals in the left panel), and the second triplet of doublets is attributed to DMPO-trapped ketyl radical **52**. However, only the ketyl radical trapping adduct **51** (right panel) could be observed in methanol. These results were consistent with the increased hydrogenation adduct from alkoxyl radicals in dioxane compared with in methanol, which indicated that the 1,2-HAT process of alkoxyl radicals to yield ketyl radicals was accelerated in methanol (the Stern-Volmer plots suggest the Hantzsch ester quenched the photoexcited fac-Ir$(ppy)_3$ more effectively than N-alkoxylphthalimides and allyl sulfones; see Schemes S4–S8 for details).

We then performed density functional theory (DFT) calculations to investigate the free energy profiles of the alkoxyl radical generation (Scheme 9A). From computational studies, the N-alkoxylphthalimide **1** first undergoes single electron reduction to generate the radical anion **CP1**. After protonation by the Hantzsch ester radical cation, the alkyl radical intermediate **CP2** was formed with 5.8 kcal/mol endothermically (black line) (Azizi et al., 2015; McSkimming and Colbran, 2013; Zheng and You, 2012; Turovska et al., 2008; Zhu et al., 1999). The N-O bond was then homolytically cleaved to form the alkoxyl radical **CP3** via the transition state **TS1** with an activation energy of 18.8 kcal/mol. Alternatively, the radical anion **CP1** may form the intermediate **CP6** via the transition state **TS3** with 39.5 kcal/mol of activation energy, and the following redox

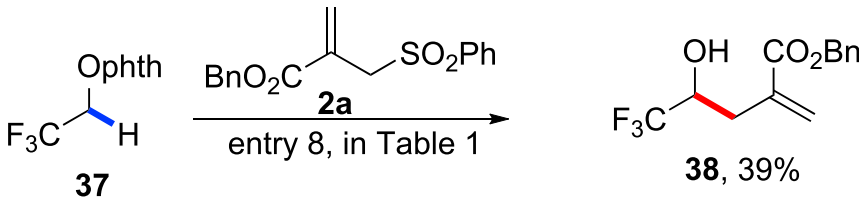

Scheme 5. 1,2-HAT Reaction of N-alkoxylphthalimide 38

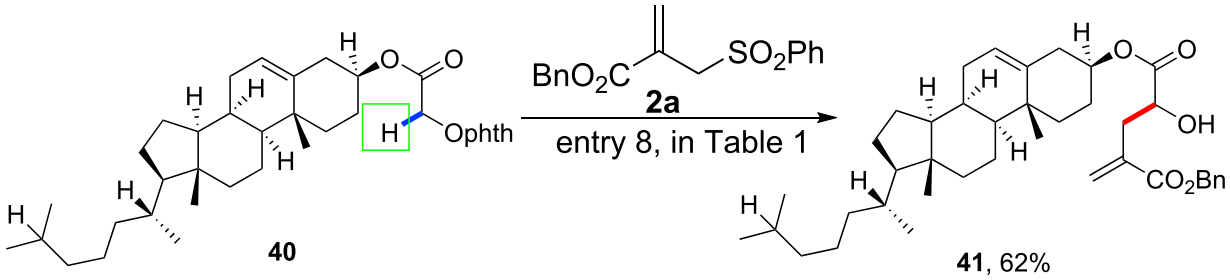

Scheme 6. 1,2-HAT Reaction of N-alkoxylphthalimide 40

fragmentation generates the ketoester **CP7** (red line) (Qi and Chen, 2016). However, the prohibitively high 39.5 kcal/mol of activation energy of **TS3** excludes it as the major reaction pathway, which is consistent with the experimental observation of the preferential formation of alkoxyl radicals in different substrates.

The methanol-assisted 1,2-HAT of alkoxyl radicals was next investigated by computational studies (Scheme 9B). The direct hydrogen atom transfer to form the ketyl radical **CP5** was calculated to have 16.4 kcal/mol of activation energy in **TS2**. In contrast, the involvement of methanol dramatically affects the energy diagram with hydrogen bonds. With one molecule of methanol participation, a 3.5-kcal/mol decrease of activation energy can be obtained in **TS5**. Significantly, two methanol molecules reduce the activation energy by 10.4 kcal/mol to merely 6.0 kcal/mol in **TS6** with multiple hydrogen bond formation, and three methanol molecules can lower the activation energy by 7.8 kcal/mol in **TS7**. From the computational studies mentioned above, the methanol facilitates the alkoxyl radical **CP3** rearrangement to ketyl radical **CP5** with hydrogen bonds, and an up to 10.4 kcal/mol decrease of activation energy can be obtained with the methanol assistance (the involvement of one methanol and one water molecule decreased the activation barrier to 6.9 kcal/mol; see Scheme S14. The α-C-H functionalization product distribution in different solvents is not only determined by the 1,2-HAT reactivity, but also affected by the alkoxyl radical generation) (see Tables S4, S5, S6, and S7).

With mechanistic experiments and DFT calculations mentioned above, we propose the reaction is initiated from the reductive quenching of the photoexcited Ir(III)* to Ir(II) by Hantzsch ester, and Ir(II) subsequently

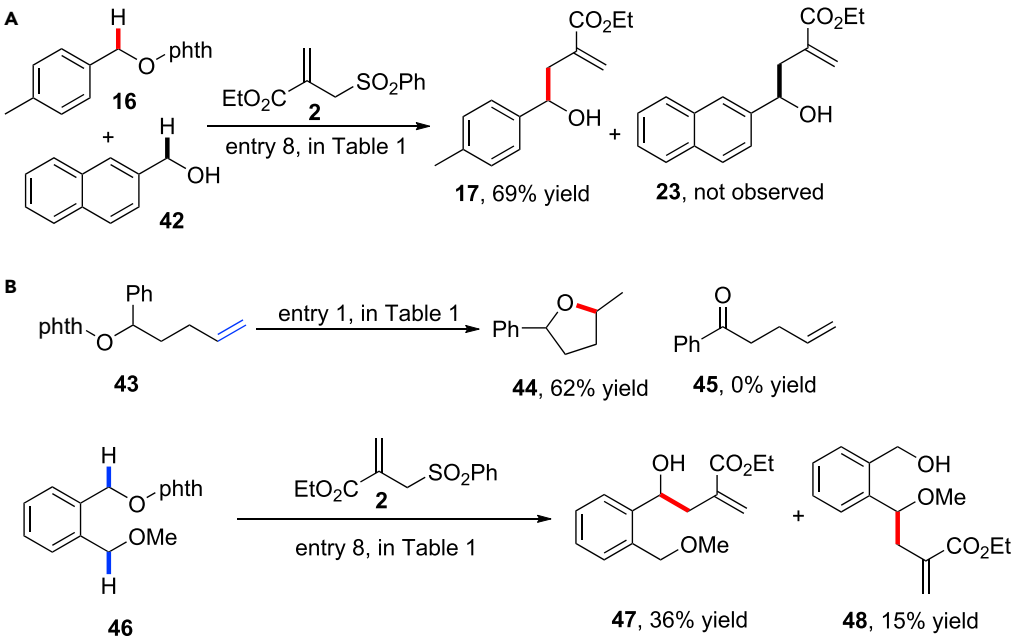

Scheme 7. Mechanistic Investigations of the 1,2-HAT of Alkoxyl Radicals

(A) The crossover experiment with N-alkoxylphthalimide **16** and alcohol **42**. (B) The investigation of potential reaction pathways of alkoxyl radicals.

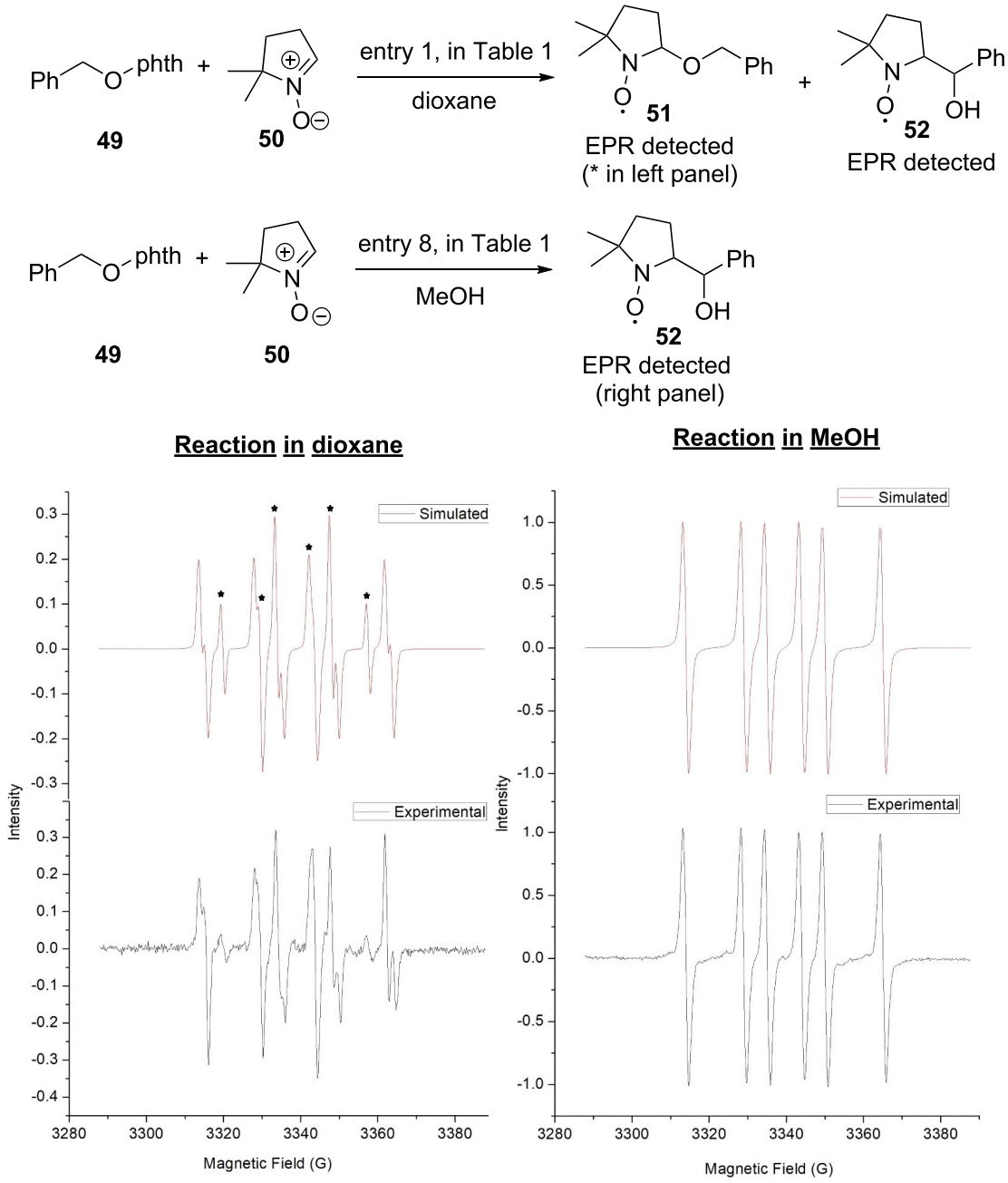

Scheme 8. EPR Studies of the 1,2-HAT of Alkoxyl Radicals

reduces the N-alkoxylphthalimides to the radical anion (Scheme 10). The radical anion undergoes proton transfer with Hantzsch ester radical cation and subsequent N-O bond cleavage to form the alkoxyl radical (Fukuzumi et al., 1983; Lackner et al., 2015; Pratsch et al., 2015; Taylor et al., 2018, and see Schemes S4–S10 for details). Two methanol molecules then assist the 1,2-HAT reaction with hydrogen bonds at the α-carbonyl, α-cyano, α-trifluoromethyl, or benzylic C(sp^3)-H bonds to form ketyl radicals for new C-C bond formations (Poutsma, 2007; Nechab et al., 2014).

Conclusions

In conclusion, we have developed the first regioselective α-C(sp^3)-H functionalization enabled by 1,2-HAT of alkoxyl radicals using photoredox catalysis. The 1,2-HAT of alkoxyl radicals was confirmed by various

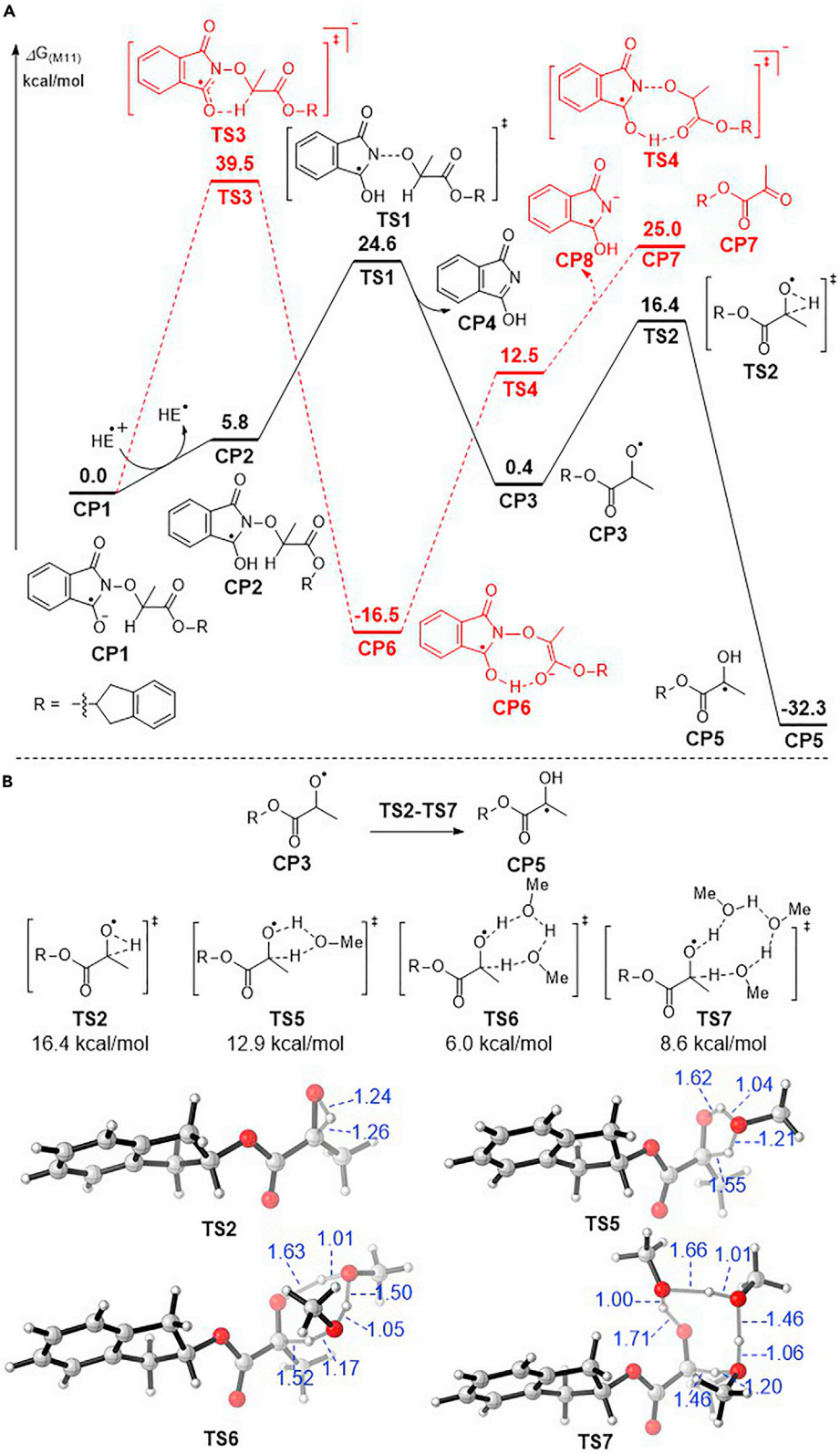

Scheme 9. DFT Calculation of the 1,2-HAT of Alkoxyl Radicals

(A) The free energy profile of two reaction pathways of N-alkoxylphthalimides. (B) The free energy profile of methanol-assisted 1,2-HAT of alkoxyl radicals.

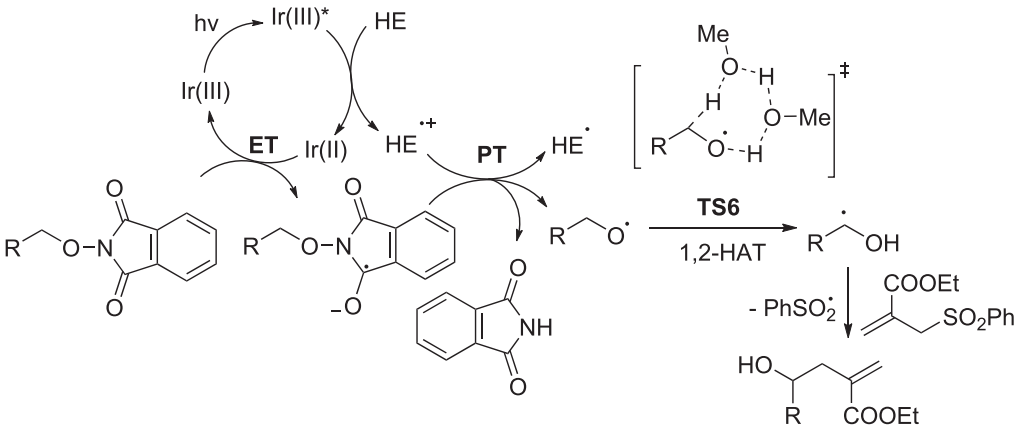

Scheme 10. Mechanistic Proposals

mechanistic investigations including EPR studies and was useful for the new C-C bond formation of α-carbonyl, α-cyano, α-trifluoromethyl, and benzylic N-alkoxylphthalimides. The computational studies indicate the assistance of protic solvents significantly facilities the 1,2-HAT reaction of alkoxyl radicals for new C-C bond formations. Further investigations are ongoing to explore this new 1,2-HAT reactivity of alkoxyl radicals.

Limitations of the Study

The 1,2-HAT pathway is not always favored for alkoxyl radicals; other alkoxyl radical reaction pathways may complete over 1,2-HAT pathway in different substrates. The existence of the carbonyl intermediate cannot be completely excluded; however, it is not the main reaction pathway from the performed computational and experimental studies.

METHODS

All methods can be found in the accompanying Transparent Methods supplemental file.

SUPPLEMENTAL INFORMATION

Supplemental Information can be found online at https://doi.org/10.1016/j.isci.2019.100755.

ACKNOWLEDGMENTS

Financial support was provided by the National Natural Science Foundation of China 21622207, 91753126, 21472230 and the Strategic Priority Research Program of the Chinese Academy of Sciences XDB20020200 to Y.C.; National Natural Science Foundation of China 21822303, 21772020, and Fundamental Research Funds for the Central Universities (Chongqing University) 2018CDXZ0002, 2018CDPTCG0001/4 to Y.L. We thank Dr. Yanxia Zhang (SIOC) for her help on EPR studies.

AUTHOR CONTRIBUTIONS

J.Z., D,L., Y.L., and Y.C. designed the research, analyzed the data, and wrote the manuscript. J.Z., D.L., and Y.G. performed the experimental studies. S.L. performed the computational studies.

DECLARATION OF INTERESTS

The authors declare no competing interests.

Received: July 30, 2019
Revised: November 8, 2019
Accepted: November 27, 2019
Published: January 24, 2020

REFERENCES

Azizi, S., Ulrich, G., Guglielmino, M., le Calve, S., Hagon, J.P., Harriman, A., and Ziessel, R. (2015). Photoinduced proton transfer promoted by peripheral subunits for some Hantzsch esters. J. Phys. Chem. A *119*, 39–49.

Bietti, M., and Salamone, M. (2014). Reaction pathways of alkoxyl radicals. The role of solvent effects on C–C bond fragmentation and hydrogen atom transfer reactions. Synlett *25*, 1803–1816.

Burke, S.D., Silks, L.A., and Strickland, S.M.S. (1988). Remote functionalization and molecular modeling: observations relevant to the barton and hypoiodite reactions. Tetrahedron Lett. *29*, 2761–2764.

Buszek, R.J., Sinha, A., and Francisco, J.S. (2011). The isomerization of methoxy radical: intramolecular hydrogen atom transfer mediated through acid catalysis. J. Am. Chem. Soc. *133*, 2013–2015.

Čeković, Ž. (2003). Reactions of δ-carbon radicals generated by 1,5-hydrogen transfer to alkoxyl radicals. Tetrahedron *59*, 8073–8090.

Čeković, Ž. (2005). Reactions of carbon radicals generated by 1,5-transposition of reactive centers. J. Serb. Chem. Soc. *70*, 287–318.

Che, C., Huang, Q., Zheng, H., and Zhu, G. (2016). Copper-catalyzed cascade annulation of unsaturated α-bromocarbonyls with enynals: a facile access to ketones from aldehydes. Chem. Sci. *7*, 4134–4139.

Che, C., Qian, Z., Wu, M., Zhao, Y., and Zhu, G. (2018). Intermolecular oxidative radical addition to aromatic aldehydes: direct access to 1,4- and 1,5-diketones via silver-catalyzed ring-opening acylation of cyclopropanols and cyclobutanols. J. Org. Chem. *83*, 5665–5673.

Chen, K., Richter, J.M., and Baran, P.S. (2008). 1,3-Diol synthesis via controlled, radical-mediated C-H functionalization. J. Am. Chem. Soc. *130*, 7247–7249.

Chen, X., Engle, K.M., Wang, D.H., and Yu, J.Q. (2009). Palladium(II)-catalyzed C-H activation/C-C cross-coupling reactions: versatility and practicality. Angew. Chem. Int. Ed. *48*, 5094–5115.

Chen, Z., Wang, B., Zhang, J., Yu, W., Liu, Z., and Zhang, Y. (2015). Transition metal-catalyzed C–H bond functionalizations by the use of diverse directing groups. Org. Chem. Front. *2*, 1107–1295.

Chen, W., Liu, Z., Tian, J., Li, J., Ma, J., Cheng, X., and Li, G. (2016). Building congested ketone: substituted Hantzsch ester and nitrile as alkylation reagents in photoredox catalysis. J. Am. Chem. Soc. *138*, 12312–12315.

Chiba, S., and Chen, H. (2014). sp^3 C–H oxidation by remote H-radical shift with oxygen- and nitrogen-radicals: a recent update. Org. Biomol. Chem. *12*, 4051–4060.

Chu, J.C.K., and Rovis, T. (2018). Complementary strategies for directed C(sp^3)-H functionalization: a comparison of transition-metal-catalyzed activation, hydrogen atom transfer, and carbene/nitrene transfer. Angew. Chem. Int. Ed. *57*, 62–101.

Deng, Y., Nguyen, M.D., Zou, Y., Houk, K.N., and Smith, A.B., III (2019). Generation of dithianyl and dioxolanyl radicals using photoredox catalysis: application in the total synthesis of the danshenspiroketallactones via radical relay chemistry. Org. Lett. *21*, 1708–1712.

Dorigo, A.E., and Houk, K.N. (1988). The relationship between proximity and reactivity. An ab initio study of the flexibility of the OH· + CH4 hydrogen abstraction transition state and a force-field model for the transition states of intramolecular hydrogen abstractions. J. Org. Chem. *53*, 1650–1664.

Elford, P.E., and Roberts, B.P. (1996). EPR studies of the formation and transformation of isomeric radicals [C3H5O]˙. Rearrangement of the allyloxyl radical in non-aqueous solution involving a formal 1,2-hydrogen-atom shift promoted by alcohols. J. Chem. Soc. *2*, 2247–2256.

Engle, K.M., Mei, T.S., Wasa, M., and Yu, J.Q. (2012). Weak coordination as a powerful means for developing broadly useful C-H functionalization reactions. Acc. Chem. Res. *45*, 788–802.

Espino, C.G., Wehn, P.M., Chow, J., and Du Bois, J. (2001). Synthesis of 1,3-difunctionalized amine derivatives through selective C—H bond oxidation. J. Am. Chem. Soc. *123*, 6935–6936.

Fernández-Ramos, A., and Zgierski, M.Z. (2002). Theoretical study of the rate constants and kinetic isotope effects of the 1,2-hydrogen-atom shift of methoxyl and benzyloxyl radicals assisted by water. J. Phys. Chem. A *106*, 10578–10583.

Fukuzumi, S., Hironaka, K., and Tanaka, T. (1983). Photoreduction of alkyl halides by an NADH model compound. An electron-transfer chain mechanism. J. Am. Chem. Soc. *105*, 4722–4727.

Gensch, T., Hopkinson, M.N., Glorius, F., and Wencel-Delord, J. (2016). Mild metal-catalyzed C-H activation: examples and concepts. Chem. Soc. Rev. *45*, 2900–2936.

Gilbert, B.C., Holmes, R.G.G., Laue, H.A.H., and Norman, R.O.C. (1976). Electron spin resonance studies. Part L. Reactions of alkoxyl radicals generated from alkyl hydroperoxides and titanium(III) ion in aqueous solution. J. Chem. Soc. *2*, 1047–1052.

Guan, H., Sun, S., Mao, Y., Chen, L., Lu, R., Huang, J., and Liu, L. (2018). Iron(II)-catalyzed site-selective functionalization of unactivated C(sp^3)-H bonds guided by alkoxyl radicals. Angew. Chem. Int. Ed. *57*, 11413–11417.

Han, J.B., Guo, A., and Tang, X.Y. (2019). Alkylation of allyl/Alkenyl sulfones by deoxygenation of alkoxyl radicals. Chem. Eur. J. *25*, 2989–2994.

Hartung, J. (2001). Stereoselective construction of the tetrahydrofuran nucleus by alkoxyl radical cyclizations. Eur. J. Org. Chem. *2001*, 619–632.

Holmes, M., Schwartz, L.A., and Krische, M.J. (2018). Intermolecular metal-catalyzed reductive coupling of dienes, allenes, and enynes with carbonyl compounds and imines. Chem. Rev. *118*, 6026–6052.

Hu, A., Guo, J.J., Pan, H., Tang, H., Gao, Z., and Zuo, Z. (2018). δ-Selective functionalization of alkanols enabled by visible-light-induced ligand-to-metal charge transfer. J. Am. Chem. Soc. *140*, 1612–1616.

Ishikawa, N., Moon, G.K., Kitazume, T., and Sam, K.C. (1984). Preparation of trifluoromethylated allylic alcohols from trifluoroacetaldehyde and organometallic compounds. J. Fluor. Chem. *24*, 419–430.

Ito, Y., Kimura, A., Osawa, T., and Hari, Y. (2018). Photoredox-catalyzed deformylative 1,4-addition of 2′-Deoxy-5′- O-phthalimidonucleosides for synthesis of 5′-carba analogs of nucleoside 5′-phosphates. J. Org. Chem. *83*, 10701–10708.

Karmel, C., Li, B., and Hartwig, J.F. (2018). Rhodium-catalyzed regioselective silylation of alkyl C-H bonds for the synthesis of 1,4-diols. J. Am. Chem. Soc. *140*, 1460–1470.

Kim, S., Lee, T.A., and Song, Y. (1998). Facile Generation of alkoxy radicals from N-alkoxyphthalimides. Synlett *1998*, 471–472.

Konya, K.G., Paul, T., Lin, S.Q., Lusztyk, J., and Ingold, K.U. (2000). Laser flash photolysis studies on the first superoxide thermal source. First direct measurements of the rates of solvent-assisted 1,2-hydrogen atom shifts and a proposed new mechanism for this unusual rearrangement. J. Am. Chem. Soc. *122*, 7518–7527.

Lackner, G.L., Quasdorf, K.W., Pratsch, G., and Overman, L.E. (2015). Fragment coupling and the construction of quaternary carbons using tertiary radicals generated from tert-alkyl N-phthalimidoyl oxalates by visible-light photocatalysis. J. Org. Chem. *80*, 6012–6024.

Lewis-Bevan, W., Gaston, R.D., Tyrrell, J., Stork, W.D., and Salmon, G.L. (1992). Formyl cyanide: a stable species. Experimental and theoretical studies. J. Am. Chem. Soc. *114*, 1933–1938.

Loh, T.-P., and Li, X.-R. (1999). A simple and practical synthesis of α-trifluoromethylated alcohols in water. Tetrahedron *55*, 5611–5622.

Lundgren, C.V., Koner, A.L., Tinkl, M., Pischel, U., and Nau, W.M. (2006). Reaction of singlet-excited 2,3-diazabicyclo[2.2.2]oct-2-ene and tert-butoxyl radicals with aryl-substituted benzofuranones. J. Org. Chem. *71*, 1977–1983.

Lyons, T.W., and Sanford, M.S. (2010). Palladium-catalyzed ligand-directed C-H functionalization reactions. Chem. Rev. *110*, 1147–1169.

McSkimming, A., and Colbran, S.B. (2013). The coordination chemistry of organo-hydride donors: new prospects for efficient multi-electron reduction. Chem. Soc. Rev. *42*, 5439–5488.

Nechab, M., Mondal, S., and Bertrand, M.P. (2014). 1,n-hydrogen-atom transfer (HAT) reactions in which n≠5: an updated inventory. Chem. Eur. J. *20*, 16034–16059.

Petrovic, G., Saicic, R., Dosen-Micovic, L., and Čeković, Ž. (2004). Stereoselective free radical

phenylsulfenylation of a nonactivated δ-carbon atom. J. Serb. Chem. Soc. *69*, 737–747.

Poutsma, M.L. (2007). Evaluation of the kinetic data for intramolecular 1,x-hydrogen shifts in alkyl radicals and structure/reactivity predictions from the carbocyclic model for the transition state. J. Org. Chem. *72*, 150–161.

Pratsch, G., Lackner, G.L., and Overman, L.E. (2015). Constructing quaternary carbons from N-(acyloxy)phthalimide precursors of tertiary radicals using visible-light photocatalysis. J. Org. Chem. *80*, 6025–6036.

Prier, C.K., Rankic, D.A., and MacMillan, D.W. (2013). Visible light photoredox catalysis with transition metal complexes: applications in organic synthesis. Chem. Rev. *113*, 5322–5363.

Qi, L., and Chen, Y. (2016). Polarity-reversed allylations of aldehydes, ketones, and imines enabled by Hantzsch ester in photoredox catalysis. Angew. Chem. Int. Ed. *55*, 13312–13315.

Ren, Z., Mo, F., and Dong, G. (2012). Catalytic functionalization of unactivated sp^3 C-H bonds via *exo*-directing groups: synthesis of chemically differentiated 1,2-diols. J. Am. Chem. Soc. *134*, 16991–16994.

Roberts, B.P. (1999). Polarity-reversal catalysis of hydrogen-atom abstraction reactions: concepts and applications in organic chemistry. Chem. Soc. Rev. *28*, 25–35.

Robertson, J., Pillai, J., and Lush, R.K. (2001). Radical translocation reactions in synthesis. Chem. Soc. Rev. *30*, 94–103.

Rueda-Becerril, M., Leung, J.C., Dunbar, C.R., and Sammis, G.M. (2011). Alkoxy radical cyclizations onto silyl enol ethers relative to alkene cyclization, hydrogen atom transfer, and fragmentation reactions. J. Org. Chem. *76*, 7720–7729.

Salamone, M., and Bietti, M. (2015). Tuning reactivity and selectivity in hydrogen atom transfer from aliphatic C-H bonds to alkoxyl radicals: role of structural and medium effects. Acc. Chem. Res. *48*, 2895–2903.

Salamone, M., Anastasi, G., Bietti, M., and DiLabio, G.A. (2011). Diffusion controlled hydrogen atom abstraction from tertiary amines by the benzyloxyl radical. The importance of C-H/N hydrogen bonding. Org. Lett. *13*, 260–263.

Salamone, M., Martella, R., and Bietti, M. (2012). Hydrogen abstraction from cyclic amines by the cumyloxyl and benzyloxyl radicals. The role of stereoelectronic effects and of substrate/radical hydrogen bonding. J. Org. Chem. *77*, 8556–8561.

Salamone, M., Milan, M., DiLabio, G.A., and Bietti, M. (2013). Reactions of the cumyloxyl and benzyloxyl radicals with tertiary amides. Hydrogen abstraction selectivity and the role of specific substrate-radical hydrogen bonding. J. Org. Chem. *78*, 5909–5917.

Salamone, M., Amorati, R., Menichetti, S., Viglianisi, C., and Bietti, M. (2014a). Structural and medium effects on the reactions of the cumyloxyl radical with intramolecular hydrogen bonded phenols. The interplay between hydrogen-bonding and acid-base interactions on the hydrogen atom transfer reactivity and selectivity. J. Org. Chem. *79*, 6196–6205.

Salamone, M., Milan, M., DiLabio, G.A., and Bietti, M. (2014b). Absolute rate constants for hydrogen atom transfer from tertiary amides to the cumyloxyl radical: evaluating the role of stereoelectronic effects. J. Org. Chem. *79*, 7179–7184.

Salamone, M., Carboni, G., and Bietti, M. (2016a). Fine control over site and substrate selectivity in hydrogen atom transfer-based functionalization of aliphatic C-H bonds. J. Org. Chem. *81*, 9269–9278.

Salamone, M., Mangiacapra, L., Carboni, G., and Bietti, M. (2016b). Hydrogen atom transfer from tertiary alkanamides to the cumyloxyl radical. The role of substrate structure on alkali and alkaline earth metal ion induced C–H bond deactivation. Tetrahedron *72*, 7757–7763.

Shi, J.L., Wang, Z., Zhang, R., Wang, Y., and Wang, J. (2019). Visible-light-promoted ring-opening alkynylation, alkenylation, and allylation of cyclic hemiacetals through b-scission of alkoxy radicals. Chem. Eur. J. *25*, 8992–8995.

Simmons, E.M., and Hartwig, J.F. (2012a). Catalytic functionalization of unactivated primary C-H bonds directed by an alcohol. Nature *483*, 70–73.

Simmons, E.M., and Hartwig, J.F. (2012b). On the interpretation of deuterium kinetic isotope effects in C−H bond functionalizations by transition-metal complexes. Angew. Chem. Int. Ed. *51*, 3066–3072.

Taylor, M.T., Nelson, J.E., Suero, M.G., and Gaunt, M.J. (2018). A protein functionalization platform based on selective reactions at methionine residues. Nature *562*, 563–568.

Turovska, B., Goba, I., Turovskis, I., Grinberga, S., Belyakov, S., Stupnikova, S., Liepinsh, E., and Stradins, J. (2008). Electrochemical oxidation of 4-monoalkyl-substituted 1,4-dihydropyridines. Chem. Heterocycl. Comp. *44*, 1483–1490.

Wang, C., Harms, K., and Meggers, E. (2016). Catalytic asymmetric Csp^3-H functionalization under photoredox conditions by radical translocation and stereocontrolled alkene addition. Angew. Chem. Int. Ed. *55*, 13495–13498.

Wappes, E.A., Nakafuku, K.M., and Nagib, D.A. (2017). Directed β C-H amination of alcohols via radical relay chaperones. J. Am. Chem. Soc. *139*, 10204–10207.

Weavers, R.T. (2001). Laurenanes: fenestranes with a twist. J. Org. Chem. *66*, 6453–6461.

Wu, X., Wang, M., Huan, L., Wang, D., Wang, J., and Zhu, C. (2018a). Tertiary-alcohol-directed functionalization of remote C(sp^3)-H bonds by sequential hydrogen atom and heteroaryl migrations. Angew. Chem. Int. Ed. *57*, 1640–1644.

Wu, X., Zhang, H., Tang, N., Wu, Z., Wang, D., Ji, M., Xu, Y., Wang, M., and Zhu, C. (2018b). Metal-free alcohol-directed regioselective heteroarylation of remote unactivated C(sp^3)-H bonds. Nat. Commun. *9*, 3343–3350.

Yamamoto, Y., and Asao, N. (1993). Selective reactions using allylic metals. Chem. Rev. *93*, 2207–2293.

Yi, H., Zhang, G., Wang, H., Huang, Z., Wang, J., Singh, A.K., and Lei, A. (2017). Recent advances in radical C-H activation/radical cross-coupling. Chem. Rev. *117*, 9016–9085.

Yus, M., Gonzalez-Gomez, J.C., and Foubelo, F. (2011). Catalytic enantioselective allylation of carbonyl compounds and imines. Chem. Rev. *111*, 7774–7854.

Zhang, J., Li, Y., Zhang, F., Hu, C., and Chen, Y. (2016). Generation of alkoxyl radicals by photoredox catalysis enables selective C(sp^3)-H functionalization under mild reaction conditions. Angew. Chem. Int. Ed. *55*, 1872–1875.

Zhang, J., Li, Y., Xu, R., and Chen, Y. (2017). Donor-Acceptor complex enables alkoxyl radical generation for metal-free C(sp^3)-C(sp^3) cleavage and allylation/alkenylation. Angew. Chem. Int. Ed. *56*, 12619–12623.

Zheng, C., and You, S.L. (2012). Transfer hydrogenation with Hantzsch esters and related organic hydride donors. Chem. Soc. Rev. *41*, 2498–2518.

Zhu, X.-Q., Liu, Y.-C., and Cheng, J.-P. (1999). Which hydrogen atom is first transferred in the NAD(P)H model Hantzsch ester mediated reactions via one-step and multistep hydride transfer? J. Org. Chem. *64*, 8980–8981.

Zhu, H., Wickenden, J.G., Campbell, N.E., Leung, J.C., Johnson, K.M., and Sammis, G.M. (2009). Construction of carbo- and heterocycles using radical relay cyclizations initiated by alkoxy radicals. Org. Lett. *11*, 2019–2022.

Zhu, H., Leung, J.C., and Sammis, G.M. (2015). Strategies to control alkoxy radical-initiated relay cyclizations for the synthesis of oxygenated tetrahydrofuran motifs. J. Org. Chem. *80*, 965–979.

Zlotorzynska, M., and Sammis, G., M. (2011). Photoinduced Electron-Transfer- Promoted Redox Fragmentation of N-Alkoxyphthalimides. Org. Lett. *13*, 6264–6267.

ISCI, Volume *23*

Supplemental Information

Visible-Light-Induced Alkoxyl Radicals Enable α-C(sp^3)-H Bond Allylation

Jing Zhang, Dan Liu, Song Liu, Yuanyuan Ge, Yu Lan, and Yiyun Chen

I. Spectra of New Compounds

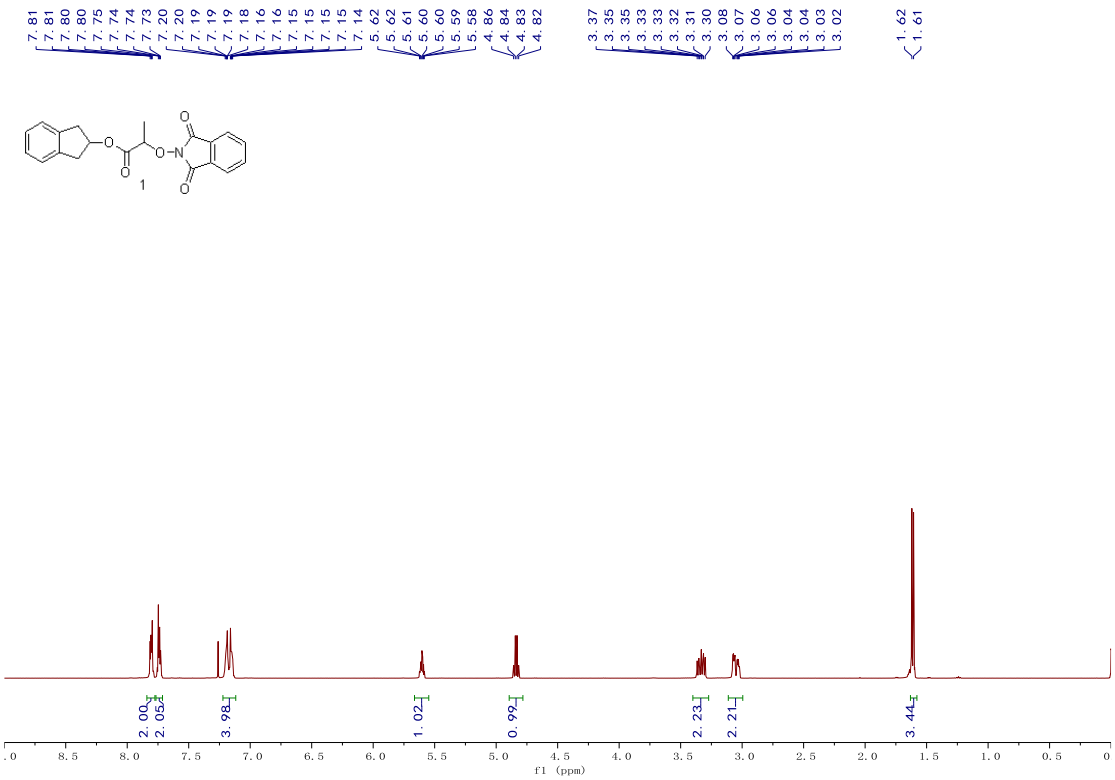

Figure S1. ^{1}H NMR (500 MHz, CDCl3) spectrum of compound 1, related to Scheme 2.

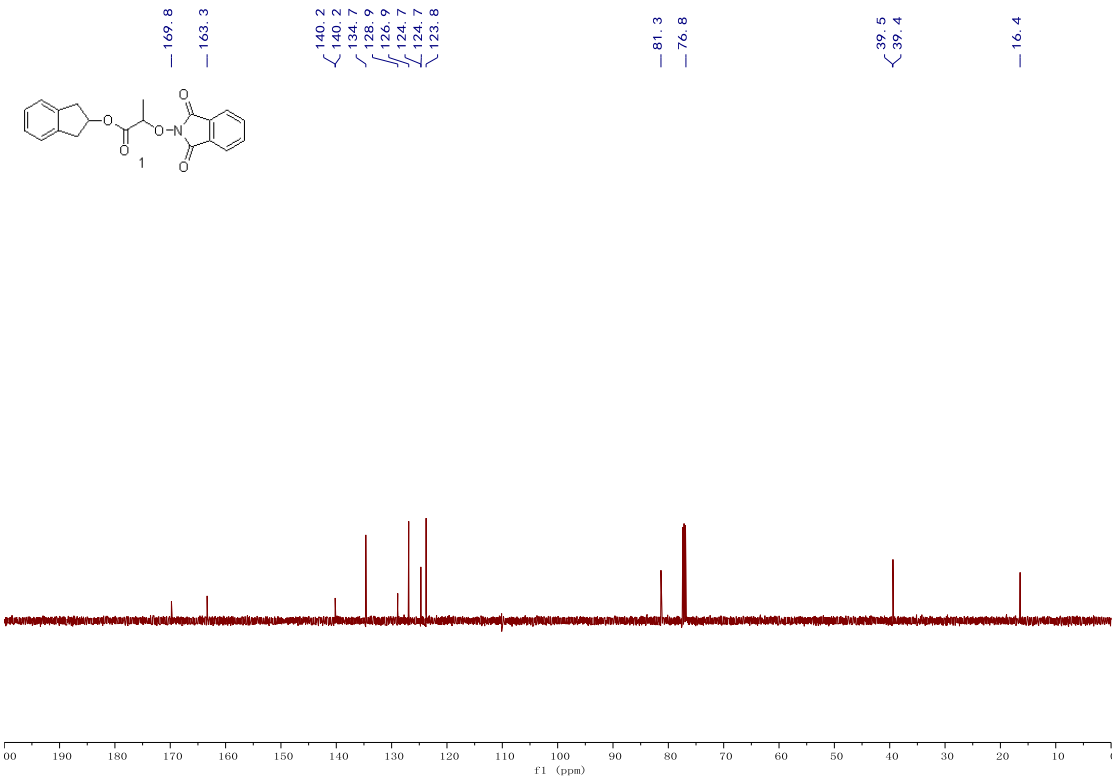

Figure S2. ^{13}C NMR (126 MHz, CDCl3) spectrum of compound 1, related to Scheme 2.

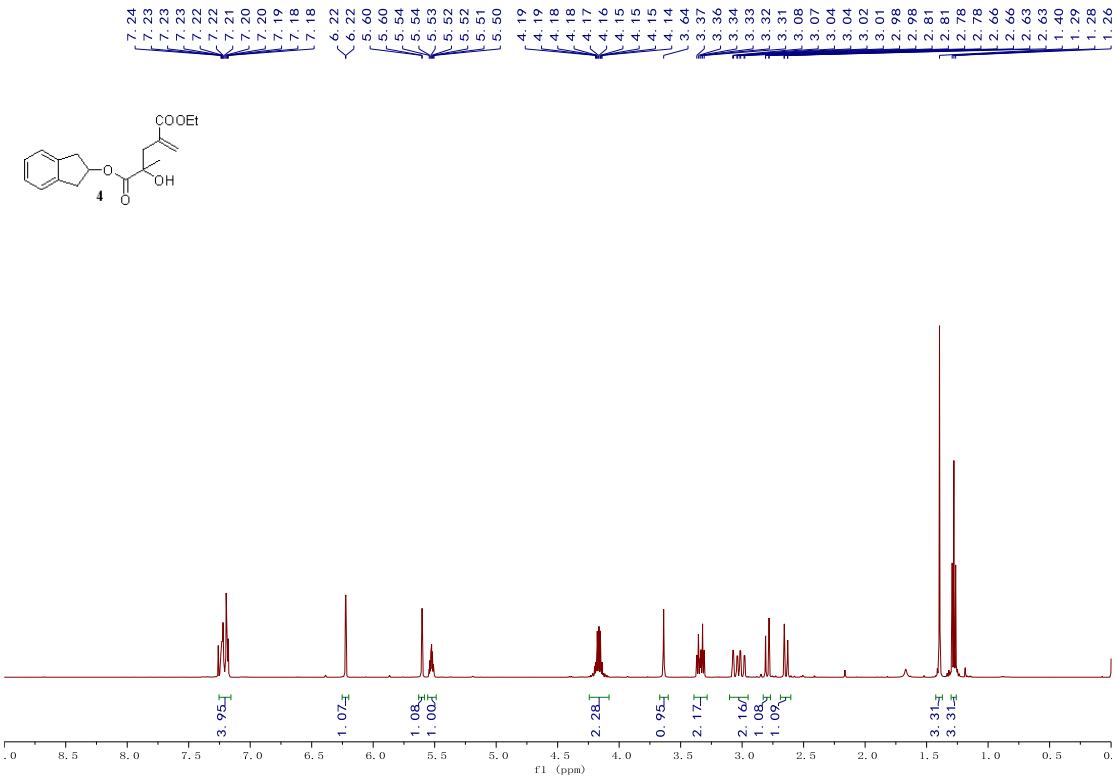

Figure S3. ^{1}H NMR (500 MHz, CDCl3) spectrum of compound 4, related to Scheme 2.

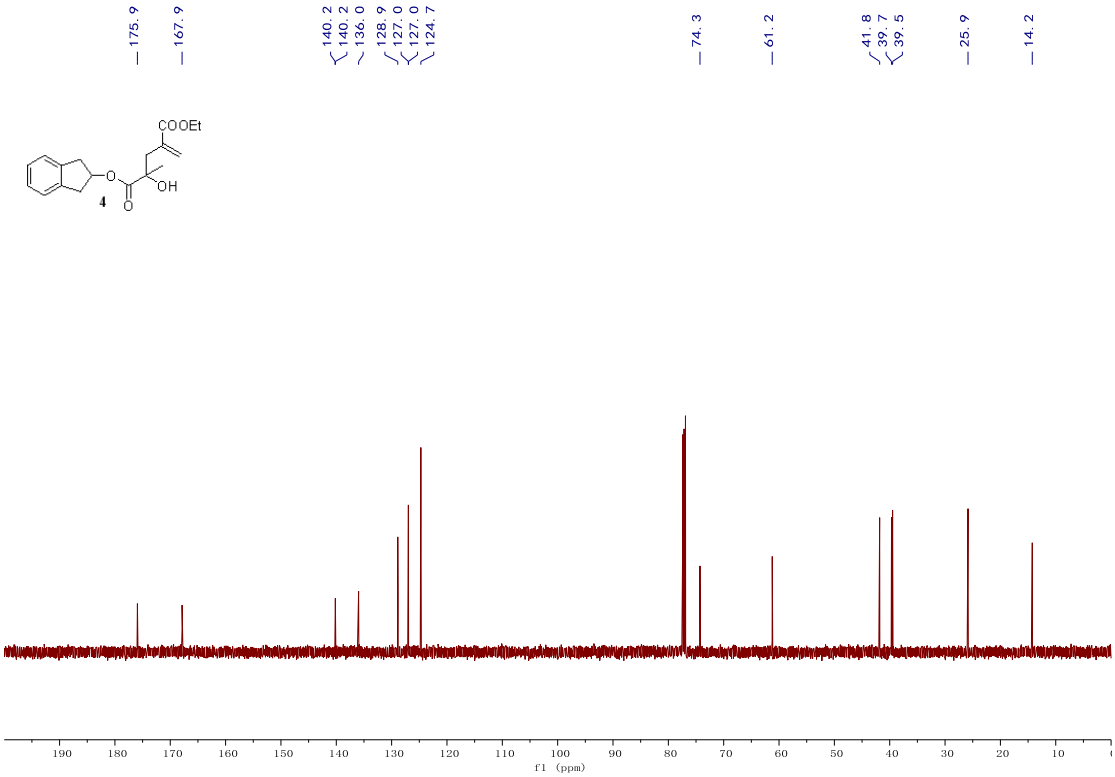

Figure S4. ^{13}C NMR (126 MHz, CDCl3) spectrum of compound 4, related to Scheme 2.

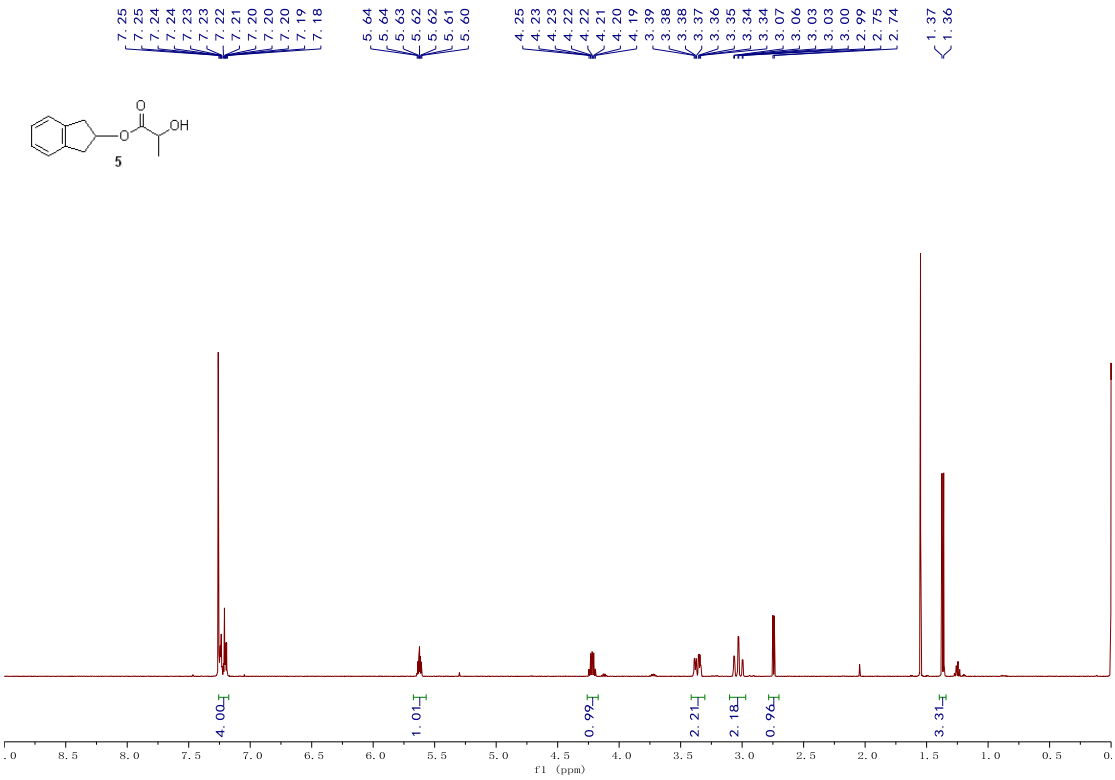

Figure S5. ^{1}H NMR (500 MHz, CDCl3) spectrum of compound 5, related to Scheme 2.

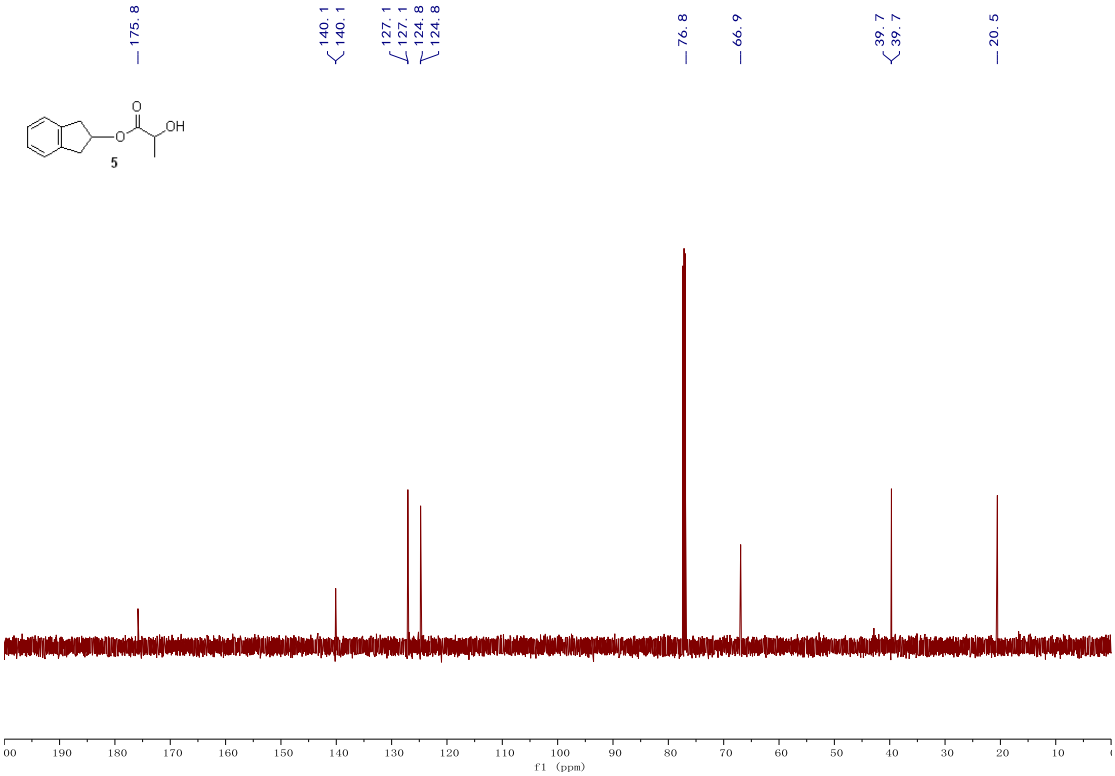

Figure S6. ^{13}C NMR (126 MHz, CDCl3) spectrum of compound 5, related to Scheme 2.

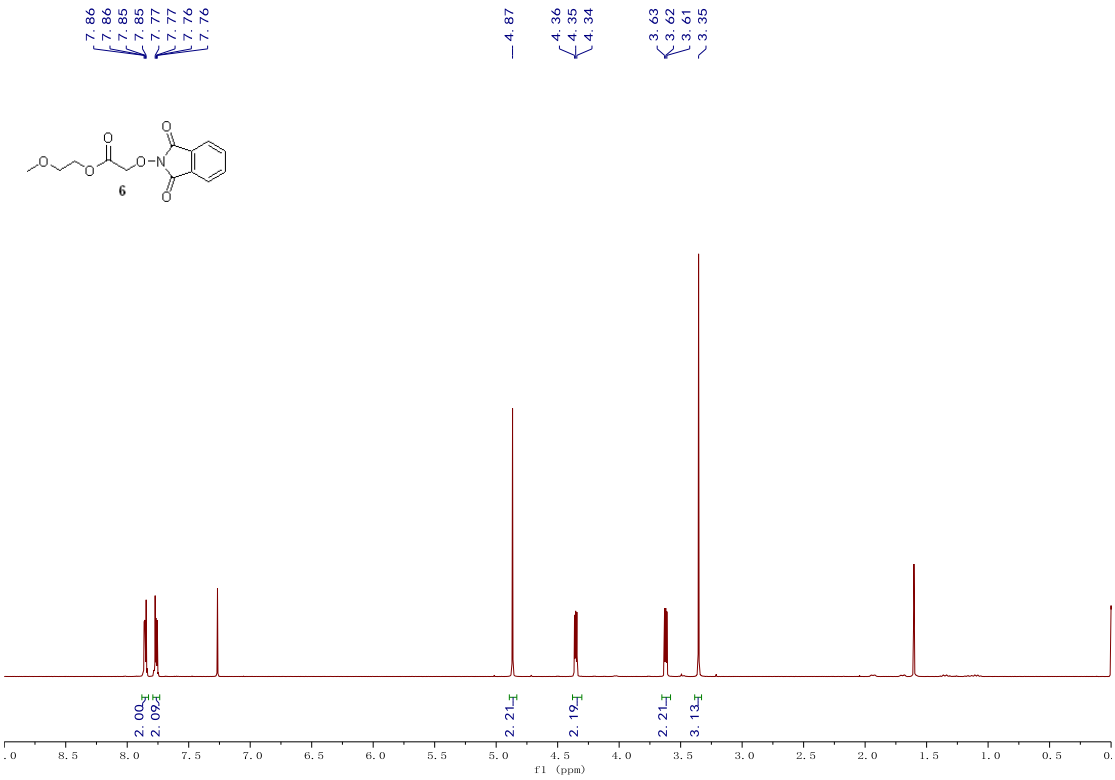

Figure S7. ^{1}H NMR (500 MHz, CDCl3) spectrum of compound 6, related to Scheme 2.

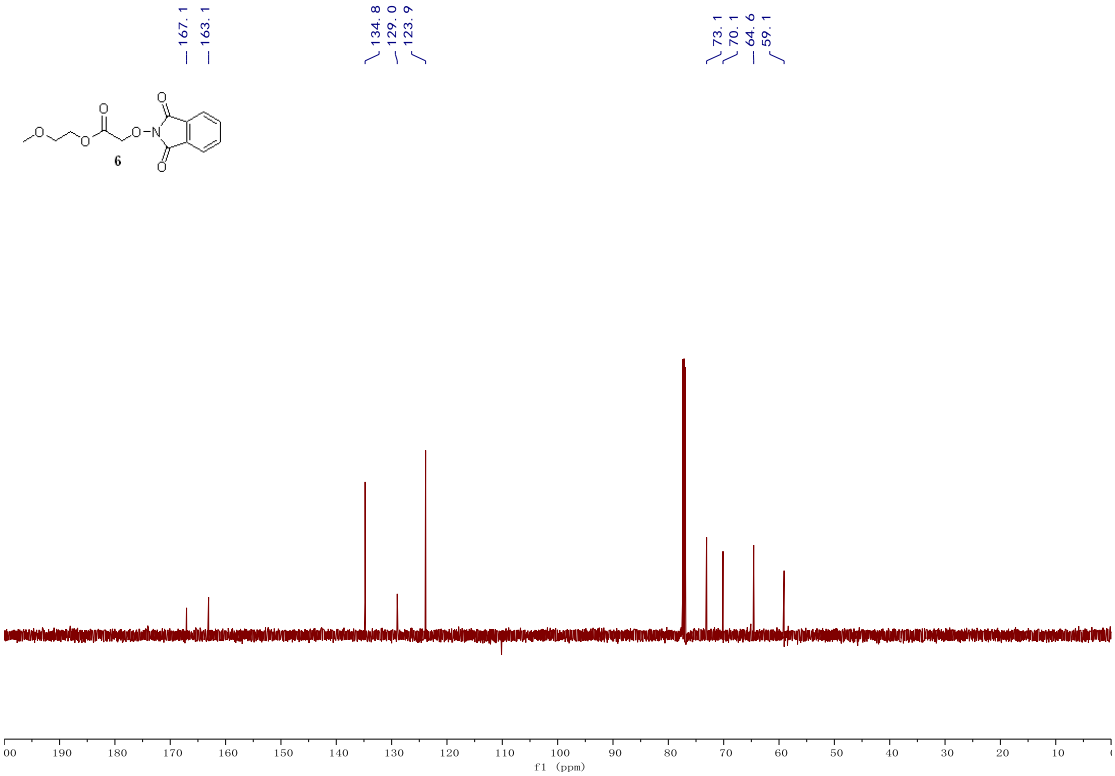

Figure S8. ^{13}C NMR (126 MHz, CDCl3) spectrum of compound 6, related to Scheme 2.

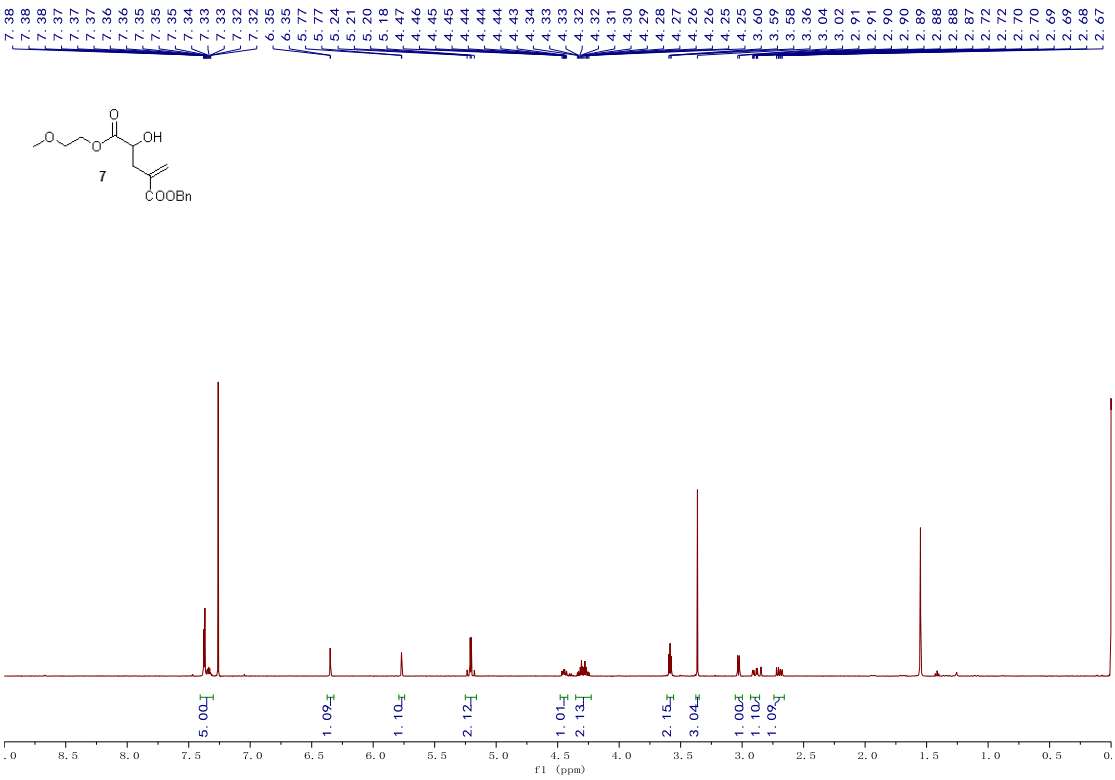

Figure S9. ^{1}H NMR (500 MHz, CDCl3) spectrum of compound 7, related to Scheme 2.

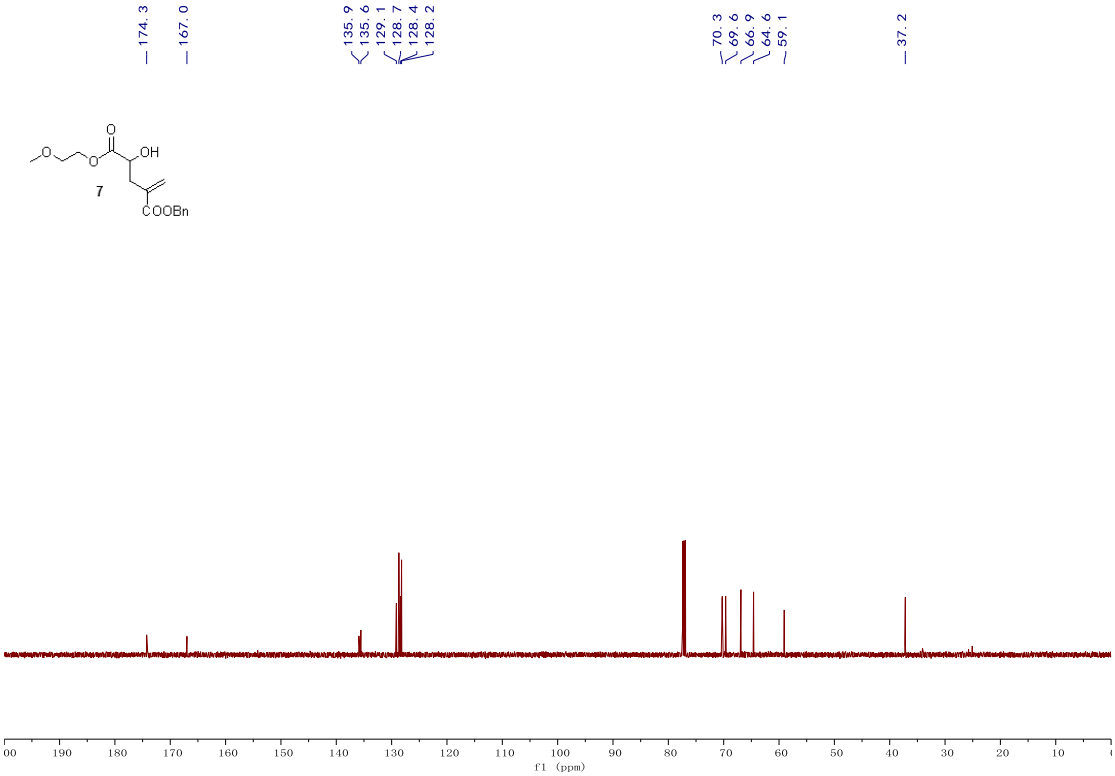

Figure S10. ^{13}C NMR (126 MHz, CDCl3) spectrum of compound 7, related to Scheme 2.

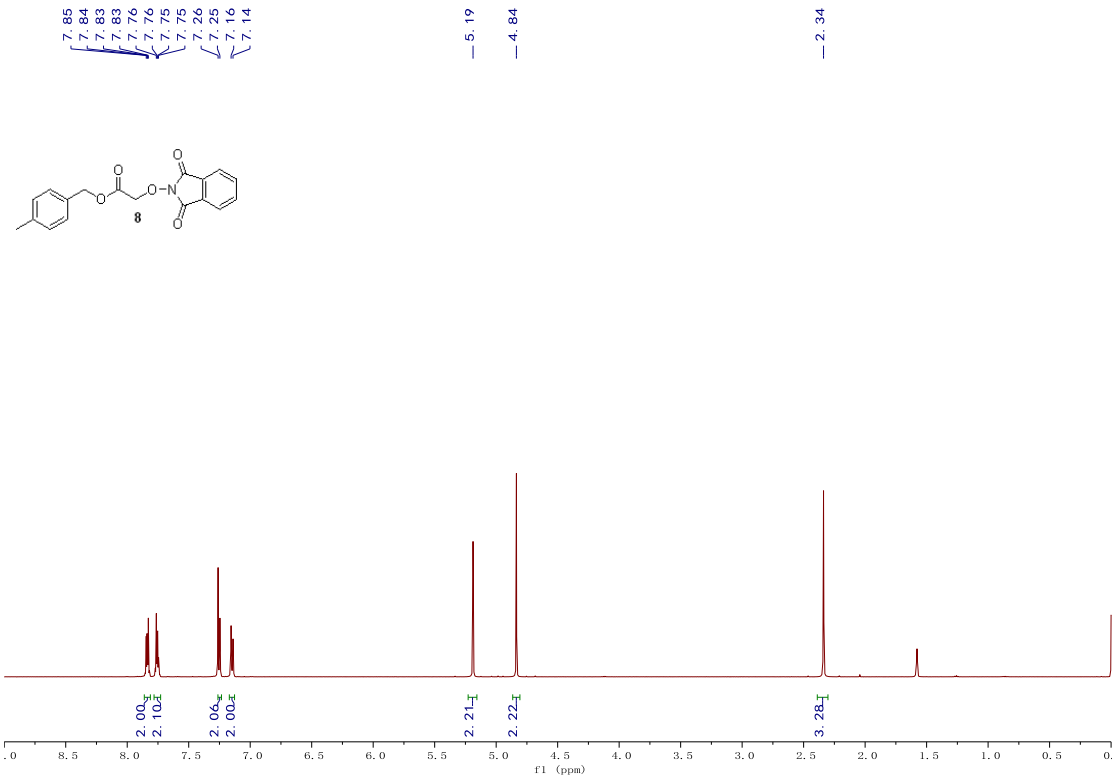

Figure S11. ^{1}H NMR (500 MHz, CDCl3) spectrum of compound 8, related to Scheme 2.

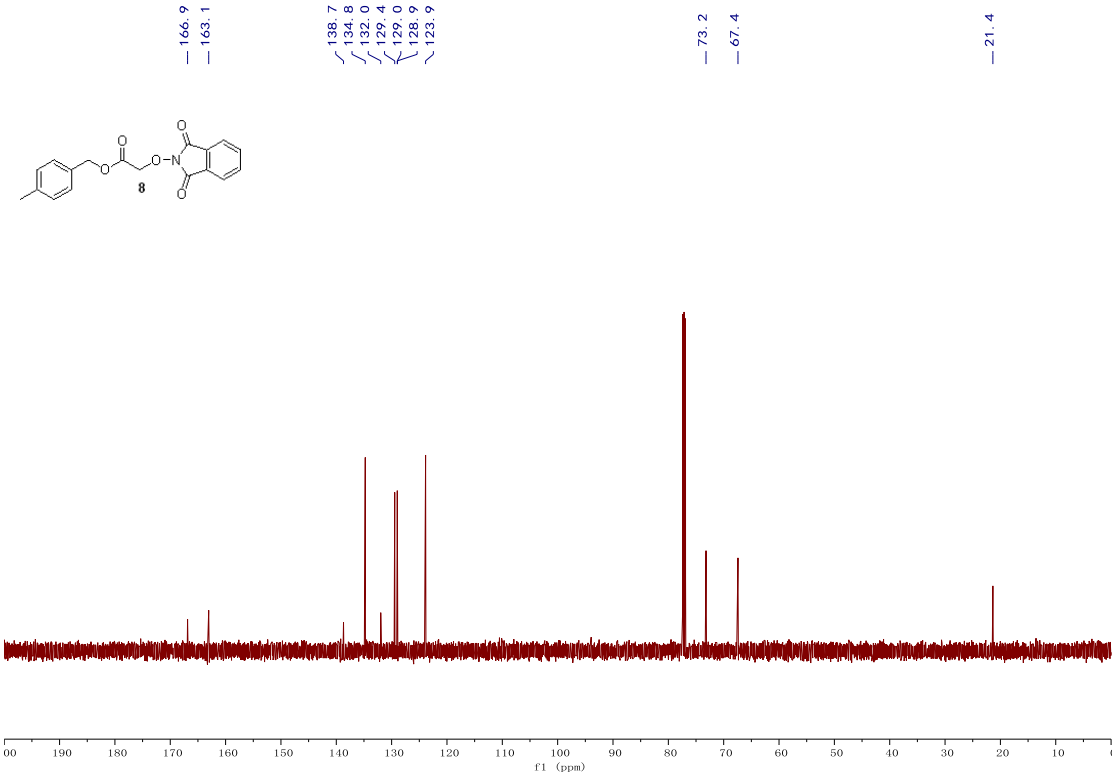

Figure S12. ^{13}C NMR (126 MHz, CDCl3) spectrum of compound 8, related to Scheme 2.

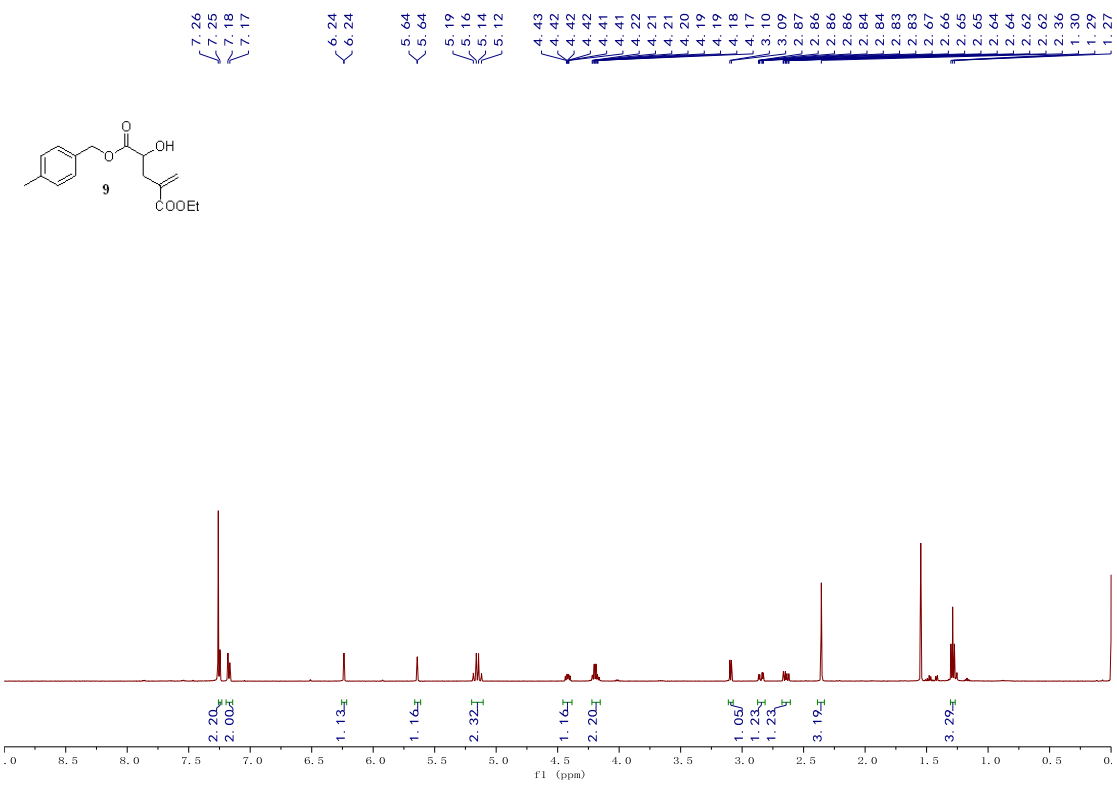

Figure S13. ^{1}H NMR (500 MHz, CDCl3) spectrum of compound 9, related to Scheme 2.

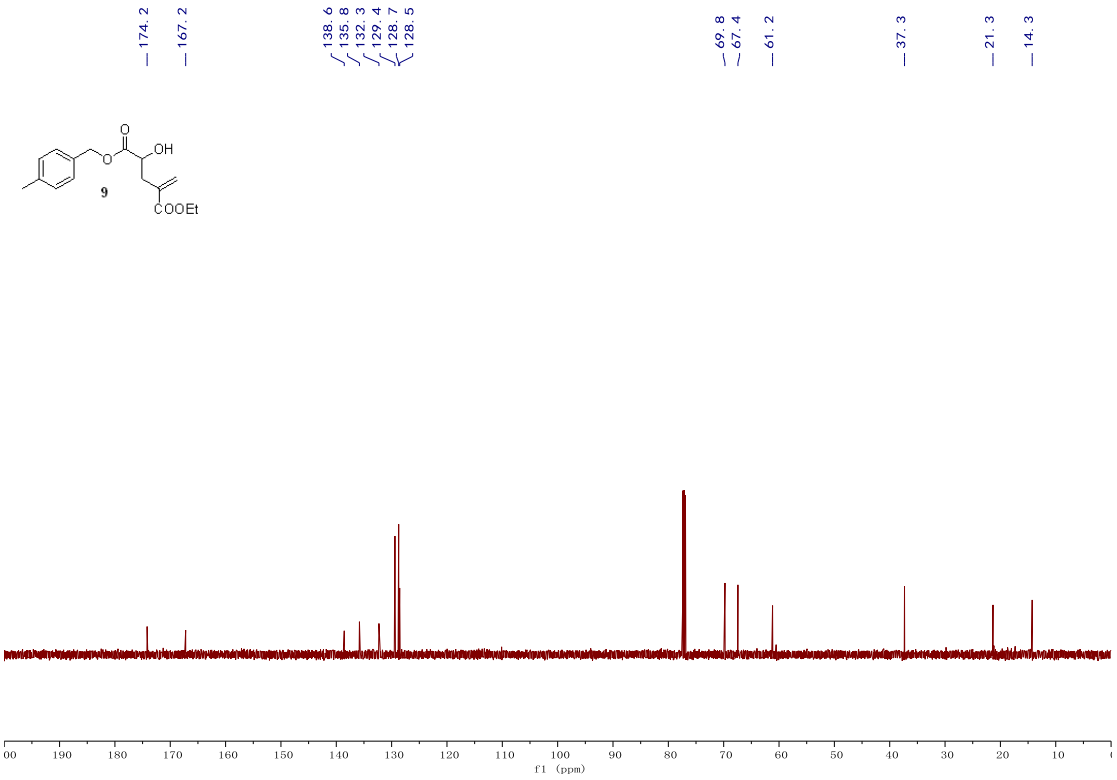

Figure S14. ^{13}C NMR (126 MHz, CDCl3) spectrum of compound 9, related to Scheme 2.

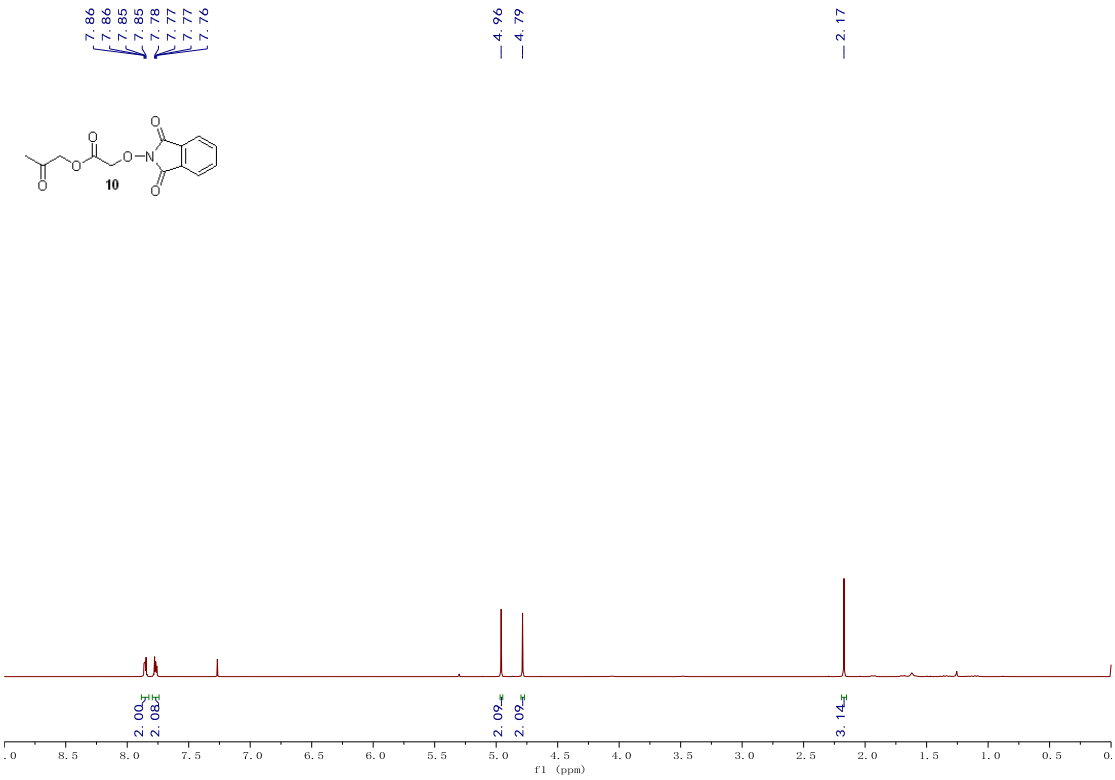

Figure S15. ^{1}H NMR (500 MHz, CDCl3) spectrum of compound 10, related to Scheme 2.

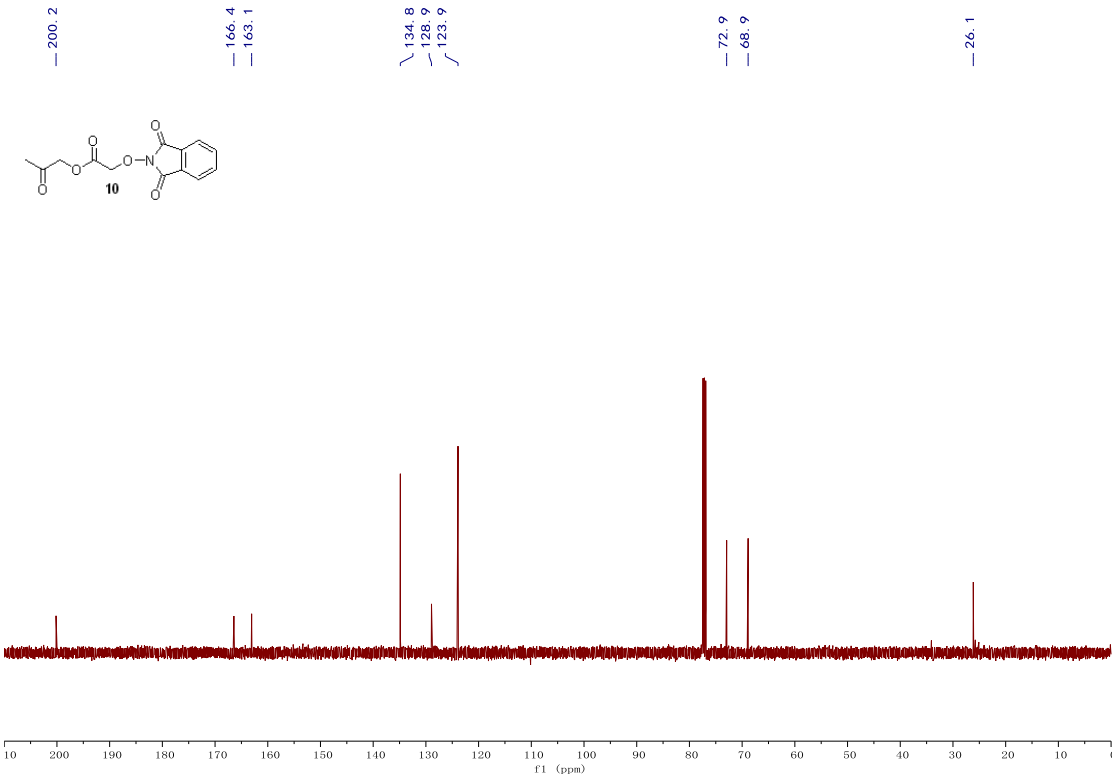

Figure S16. ^{13}C NMR (126 MHz, CDCl3) spectrum of compound 10, related to Scheme 2.

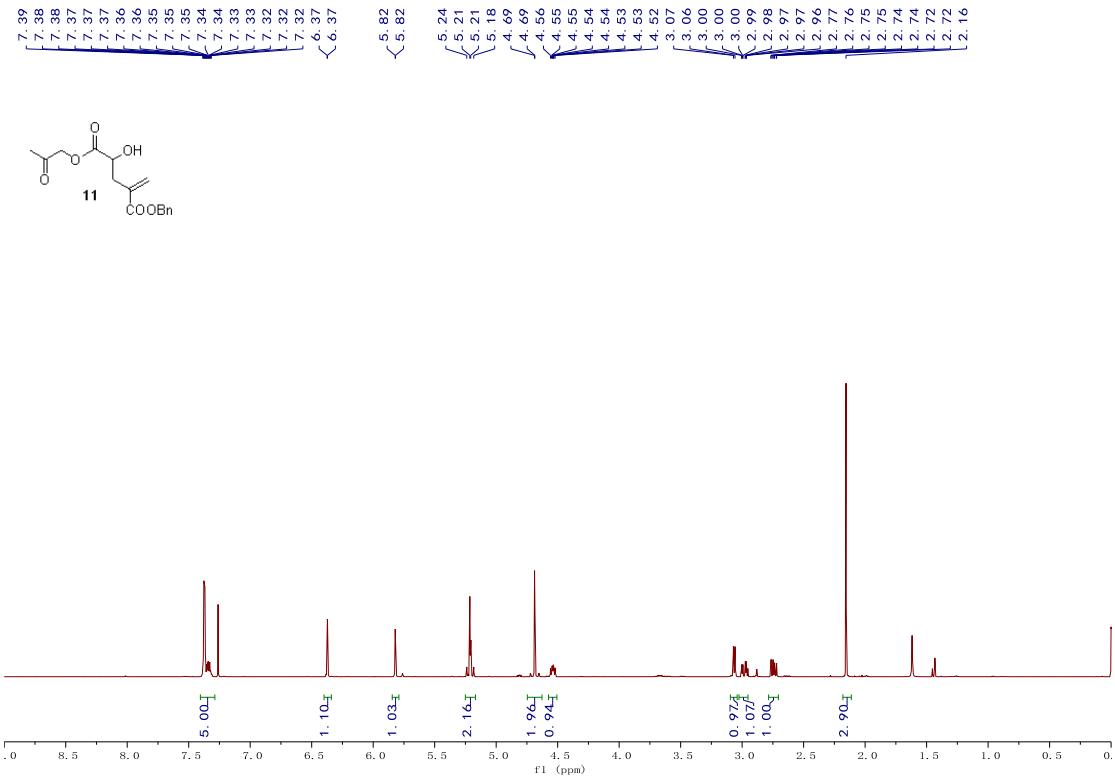

Figure S17. ^{1}H NMR (500 MHz, CDCl3) spectrum of compound 11, related to Scheme 2.

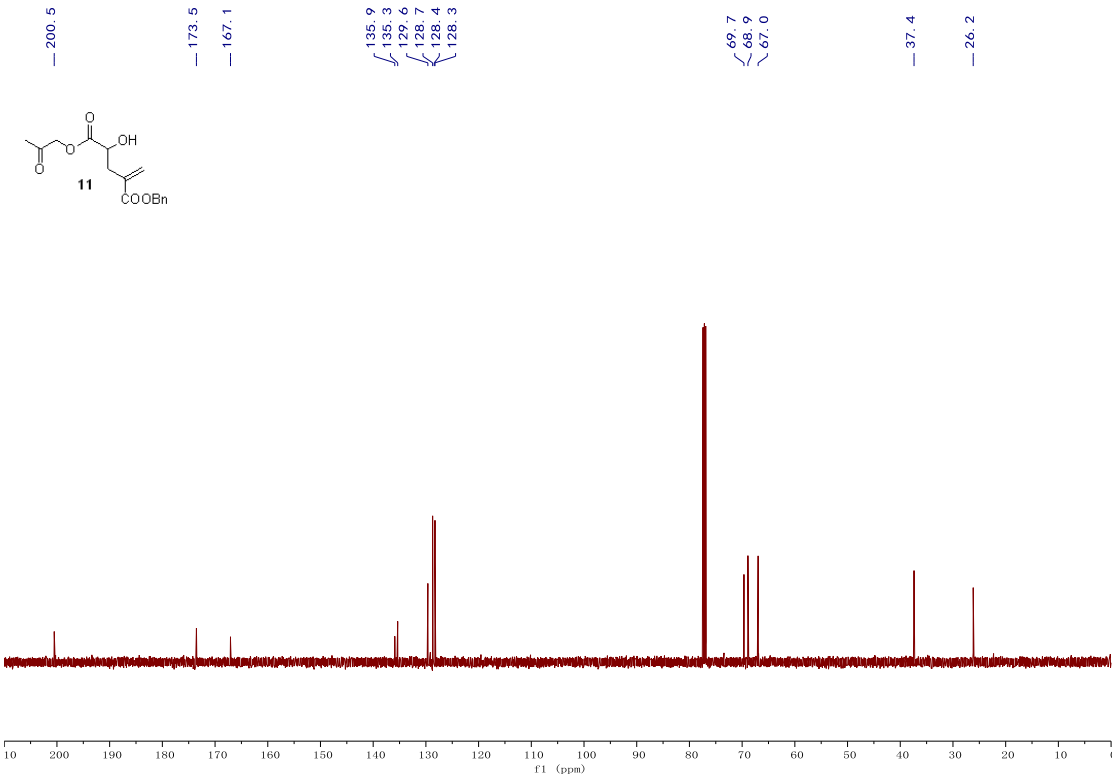

Figure S18. ^{13}C NMR (126 MHz, CDCl3) spectrum of compound 11, related to Scheme 2.

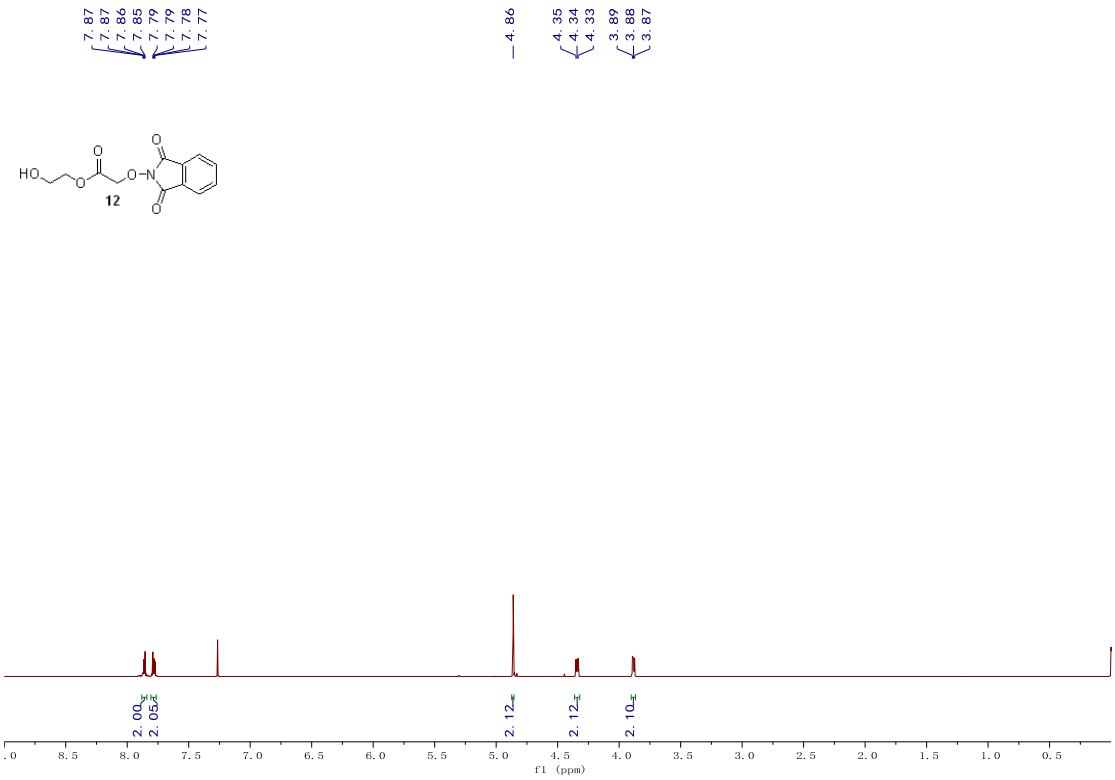

Figure S19. ^{1}H NMR (500 MHz, CDCl3) spectrum of compound 12, related to Scheme 2.

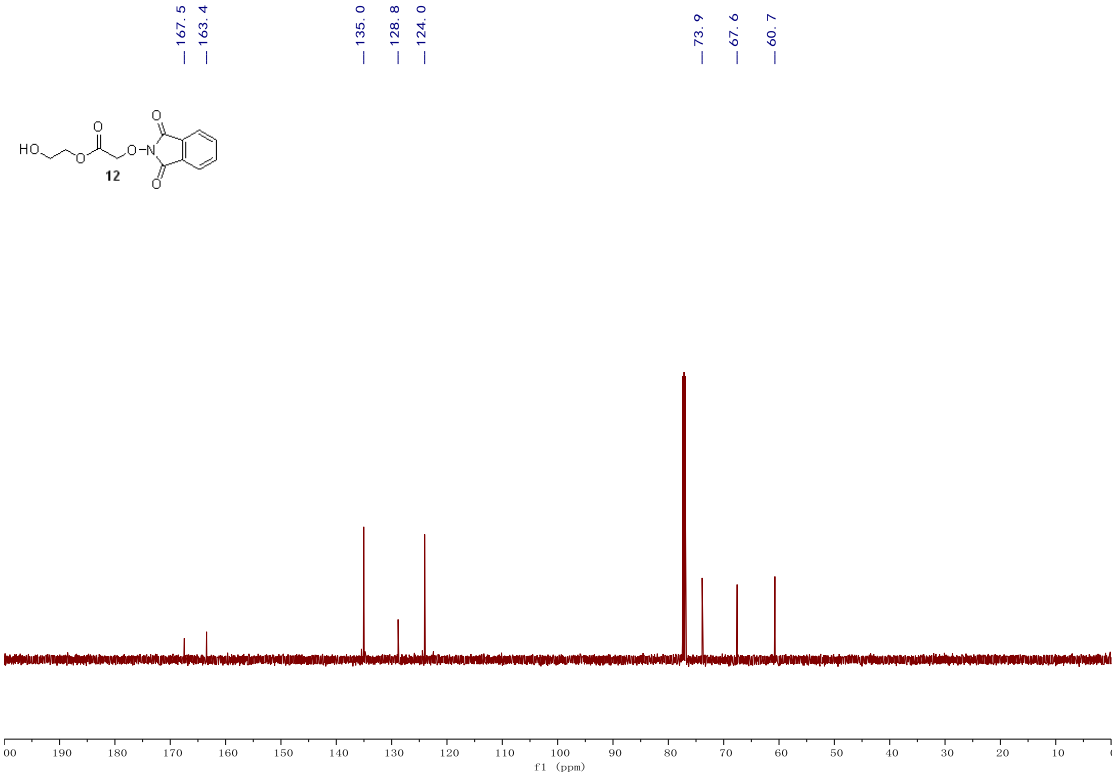

Figure S20. ^{13}C NMR (126 MHz, CDCl3) spectrum of compound 12, related to Scheme 2.

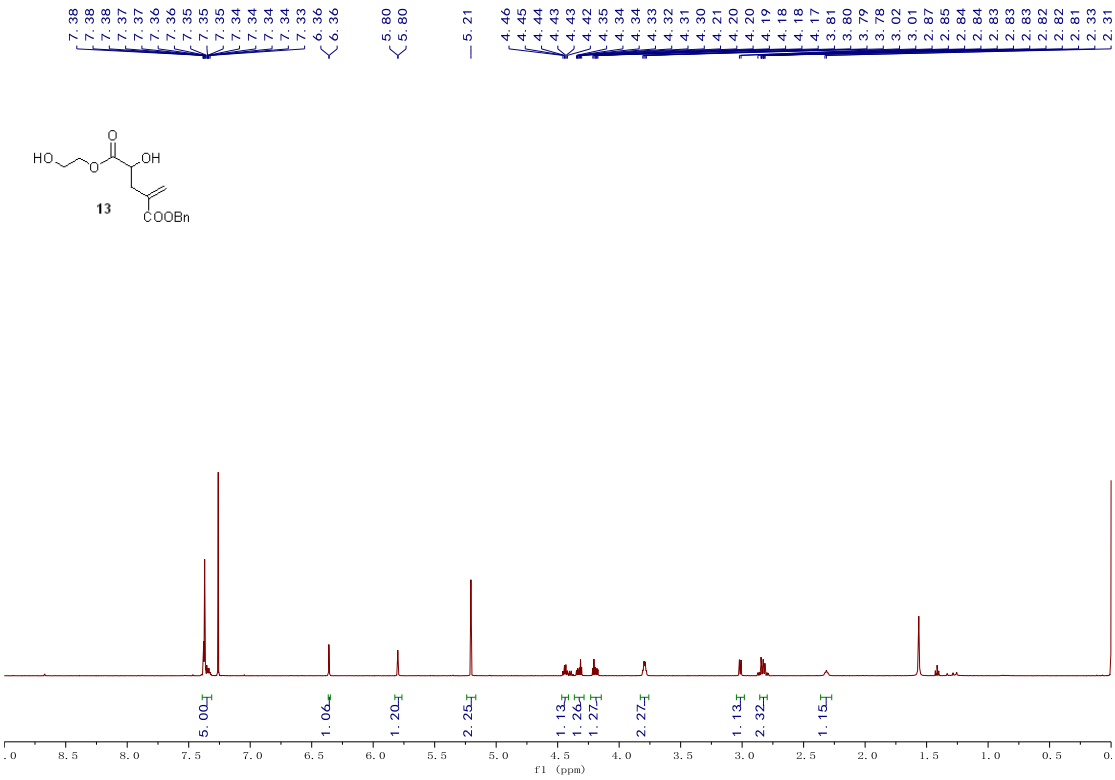

Figure S21. ^{1}H NMR (500 MHz, CDCl3) spectrum of compound 13, related to Scheme 2.

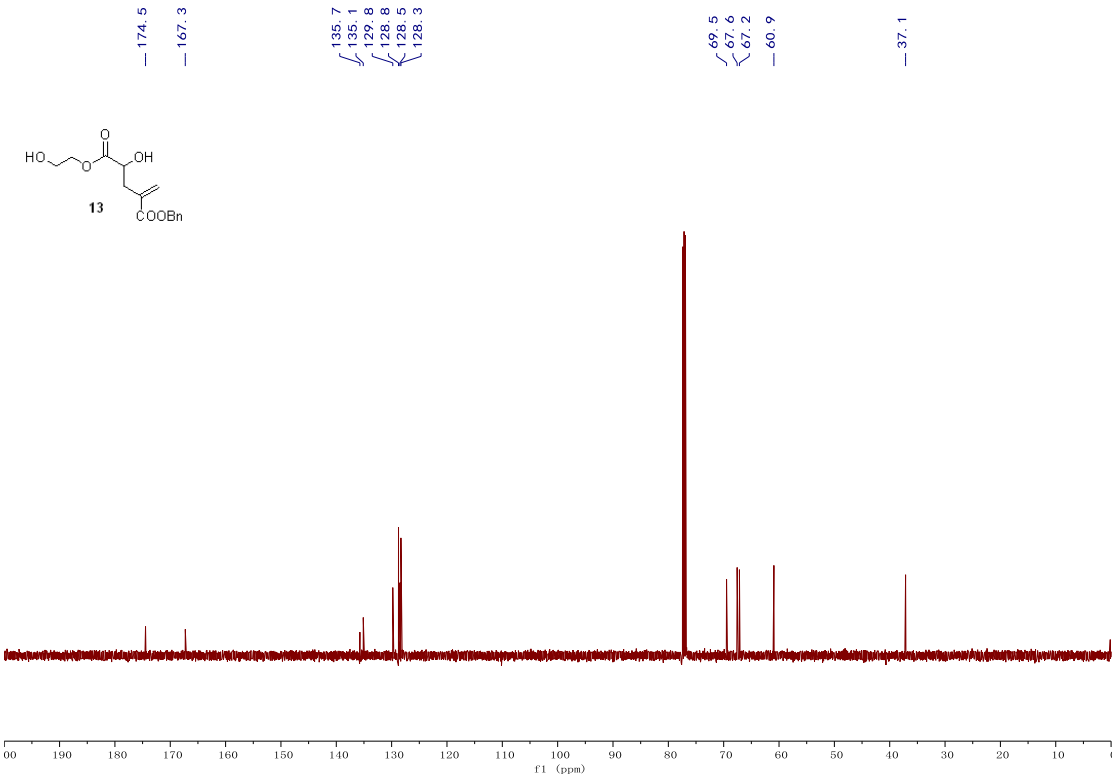

Figure S22. ^{13}C NMR (126 MHz, CDCl3) spectrum of compound 13, related to Scheme 2.

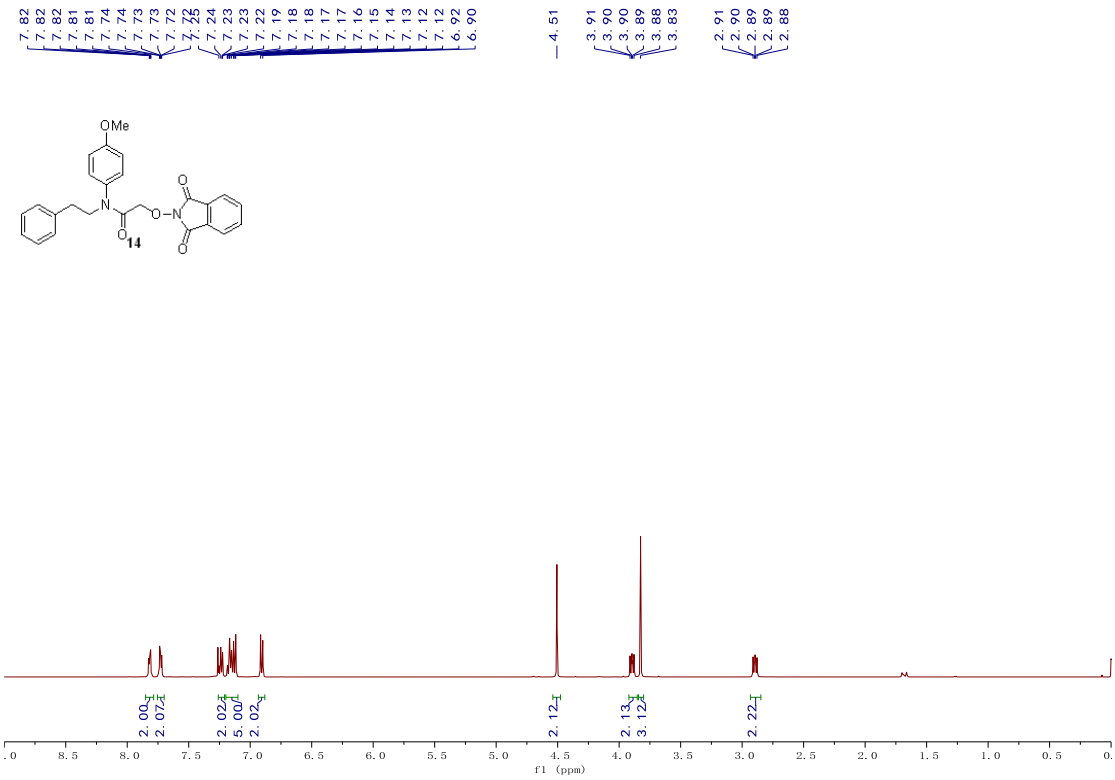

Figure S23. ^{1}H NMR (500 MHz, CDCl3) spectrum of compound 14, related to Scheme 2.

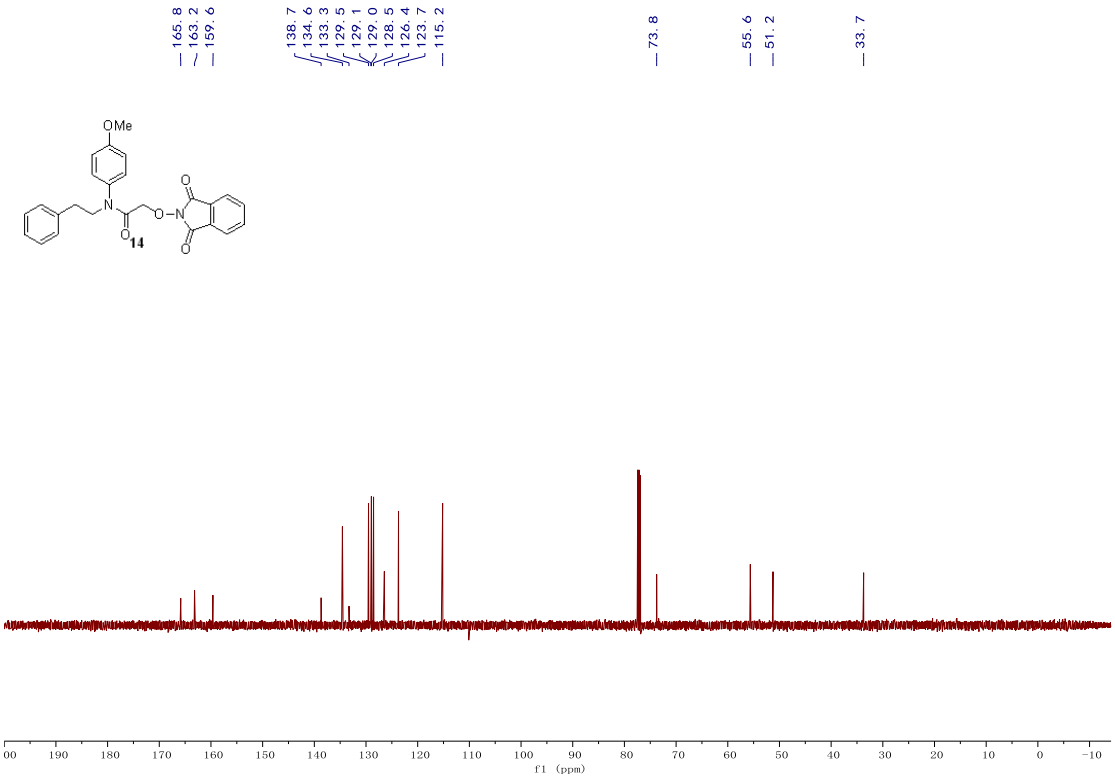

Figure S24. ^{13}C NMR (126 MHz, CDCl3) spectrum of compound 14, related to Scheme 2.

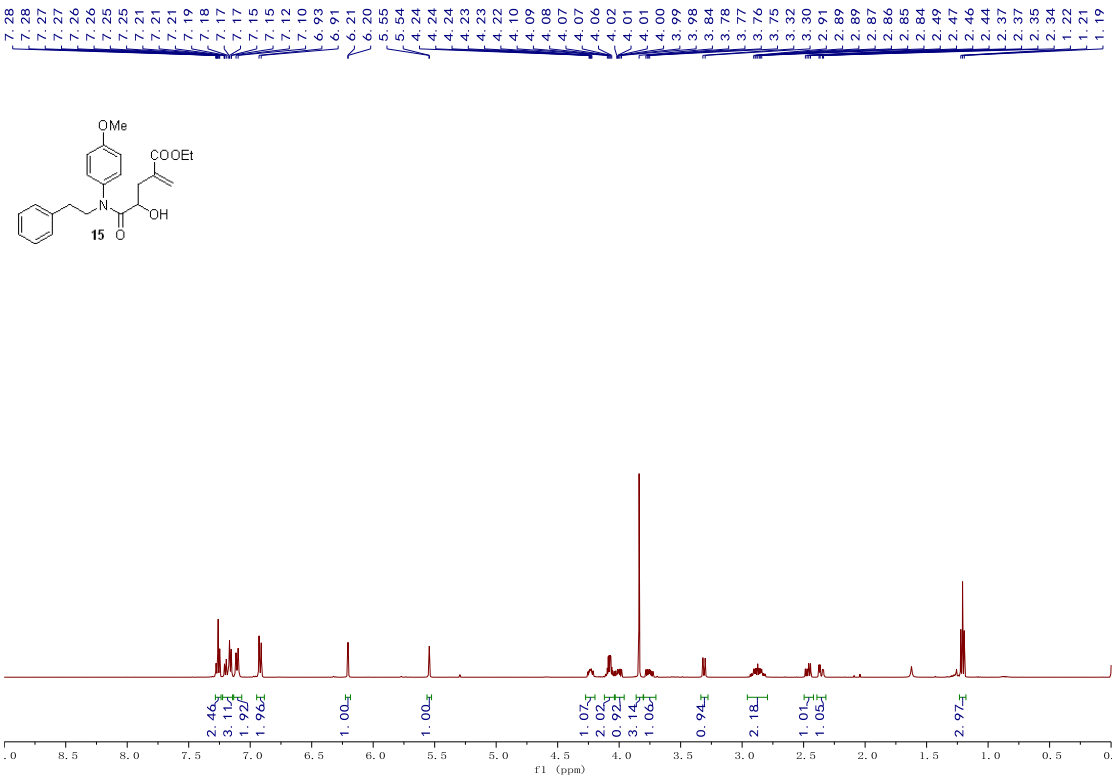

Figure S25. ^{1}H NMR (500 MHz, CDCl3) spectrum of compound 15, related to Scheme 2.

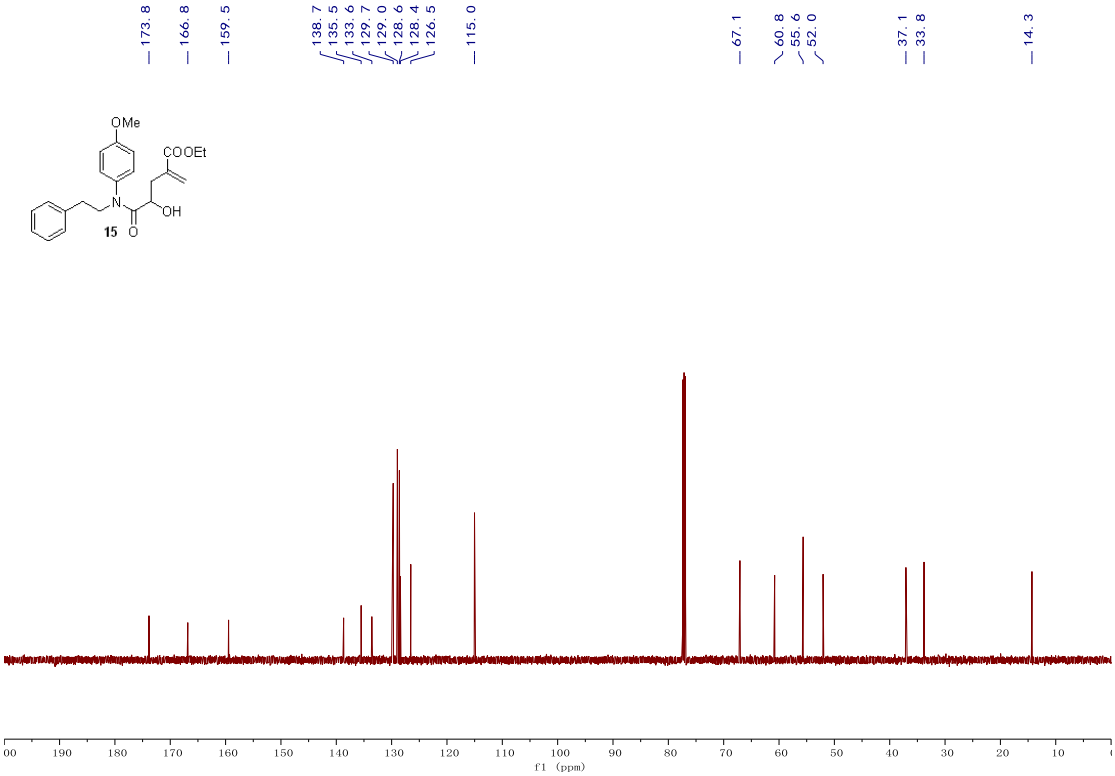

Figure S26. ^{13}C NMR (126 MHz, CDCl3) spectrum of compound 15, related to Scheme 2.

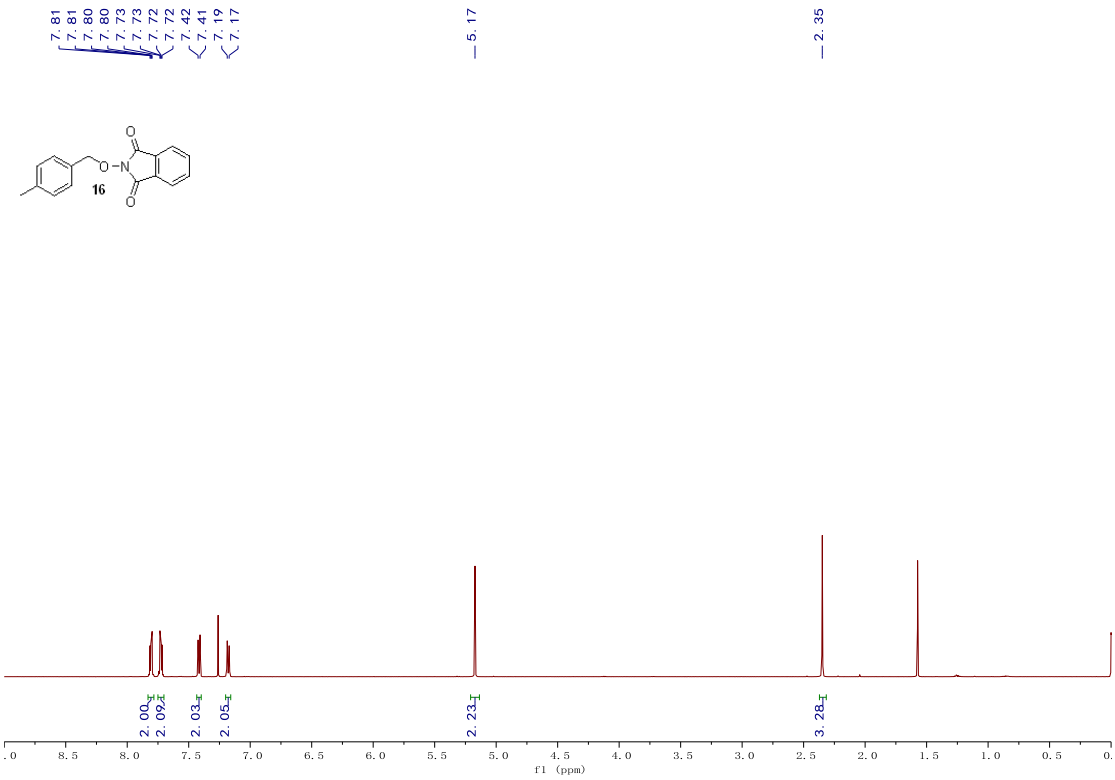

Figure S27. ^{1}H NMR (500 MHz, CDCl3) spectrum of compound 16, related to Scheme 2.

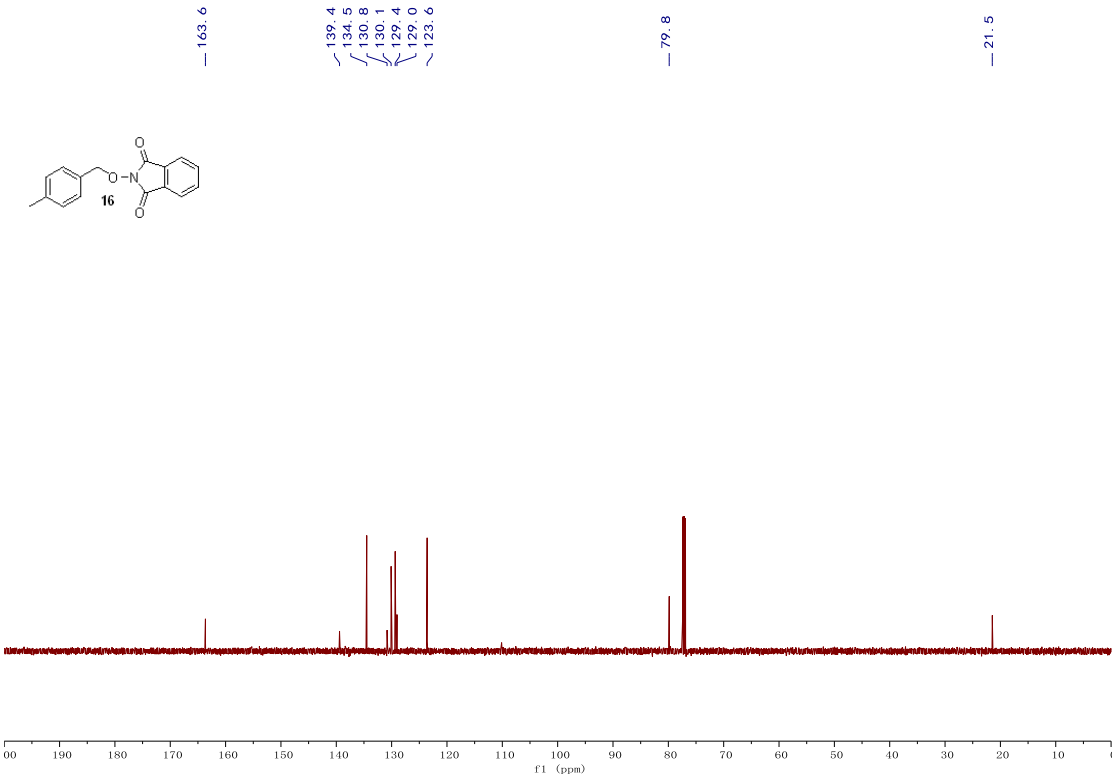

Figure S28. ^{13}C NMR (126 MHz, CDCl3) spectrum of compound 16, related to Scheme 2.

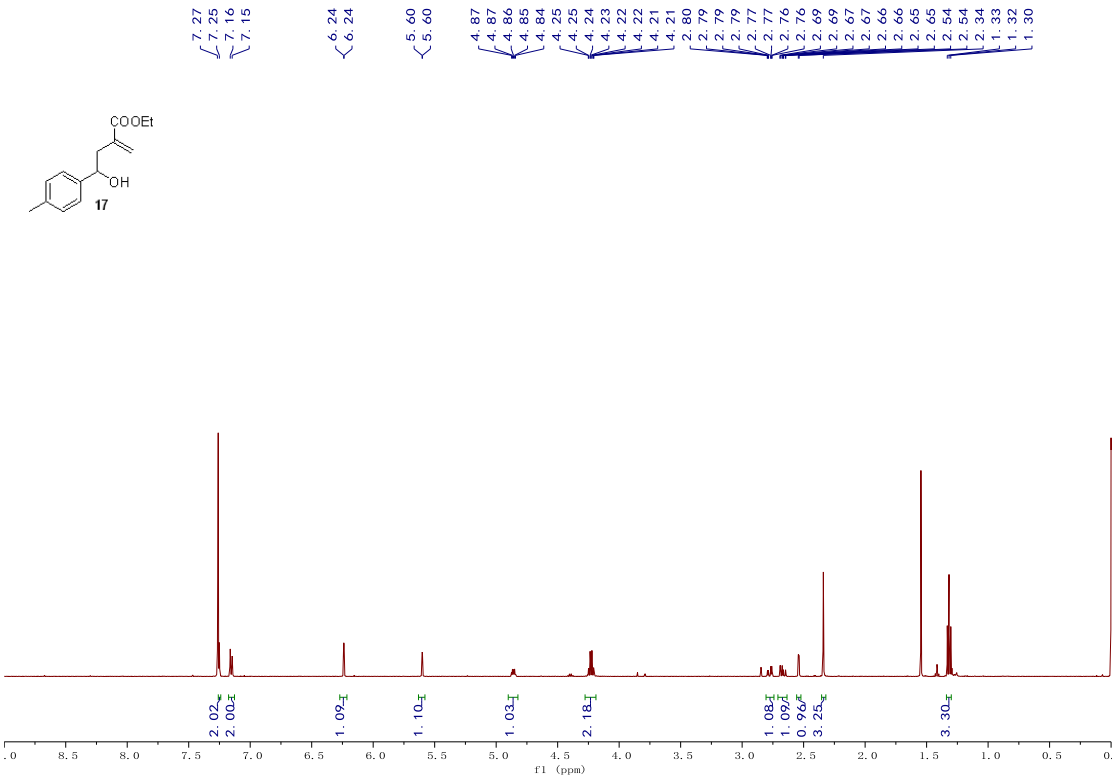

Figure S29. ^{1}H NMR (500 MHz, CDCl3) spectrum of compound 17, related to Scheme 2.

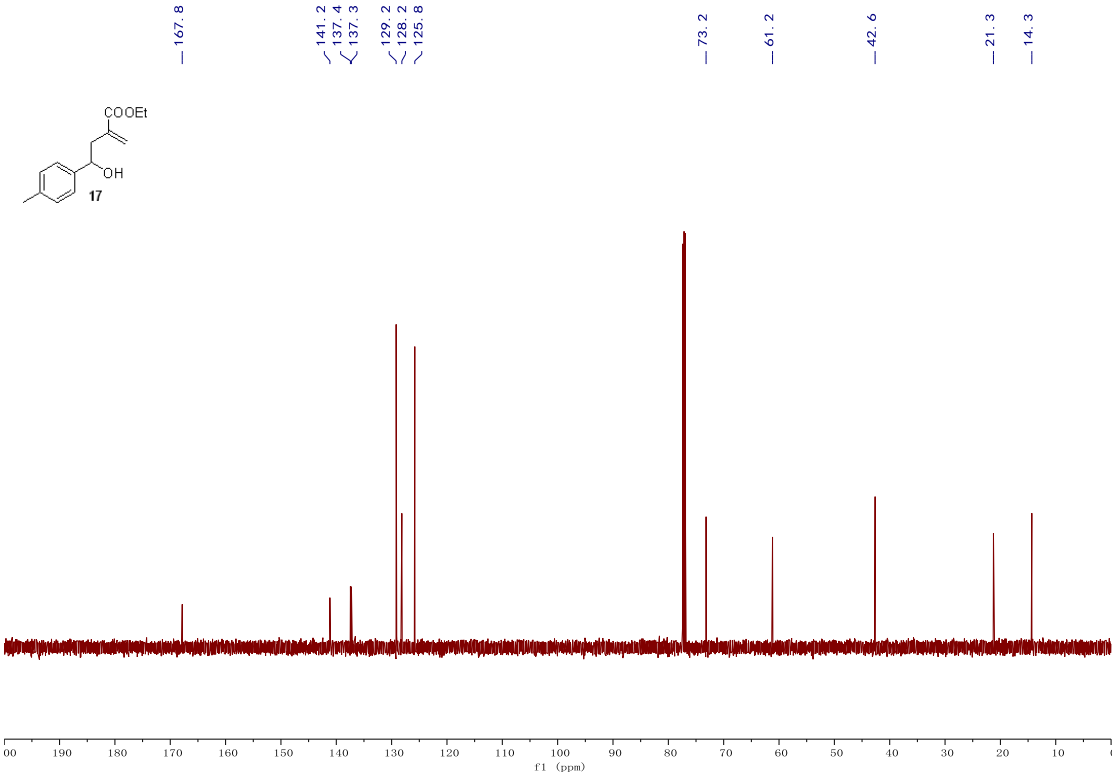

Figure S30. ^{13}C NMR (126 MHz, CDCl3) spectrum of compound 17, related to Scheme 2.

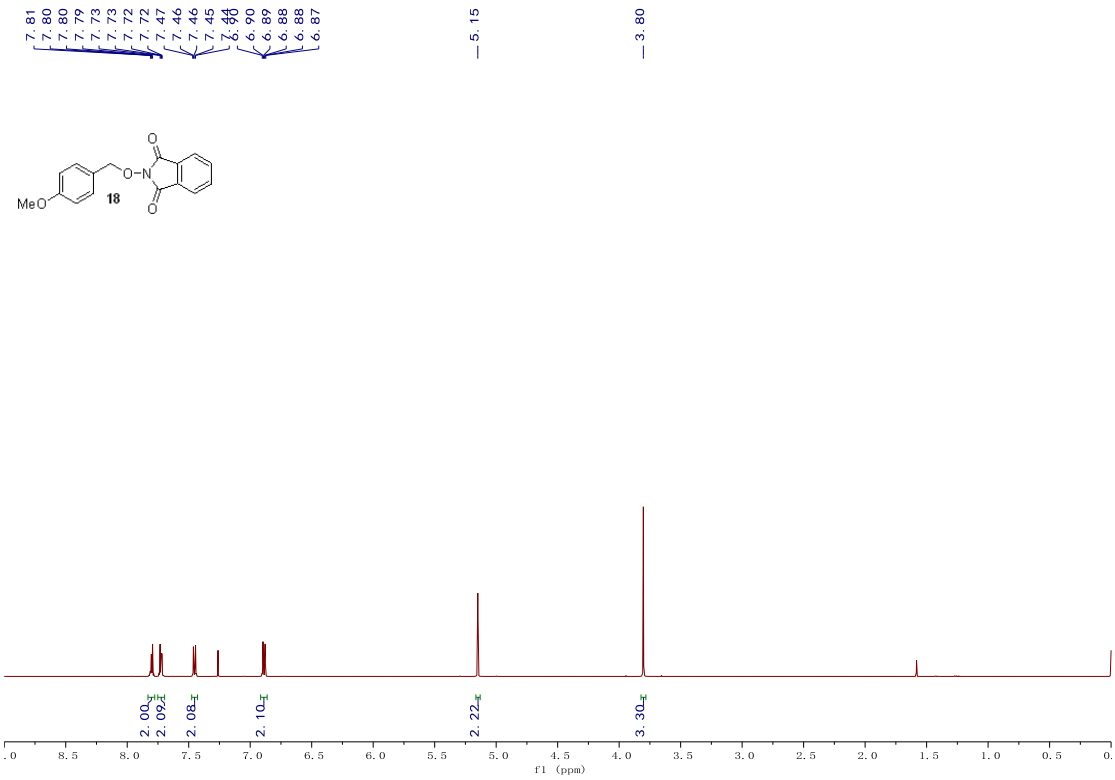

Figure S31. ^{1}H NMR (500 MHz, CDCl3) spectrum of compound 18, related to Scheme 2.

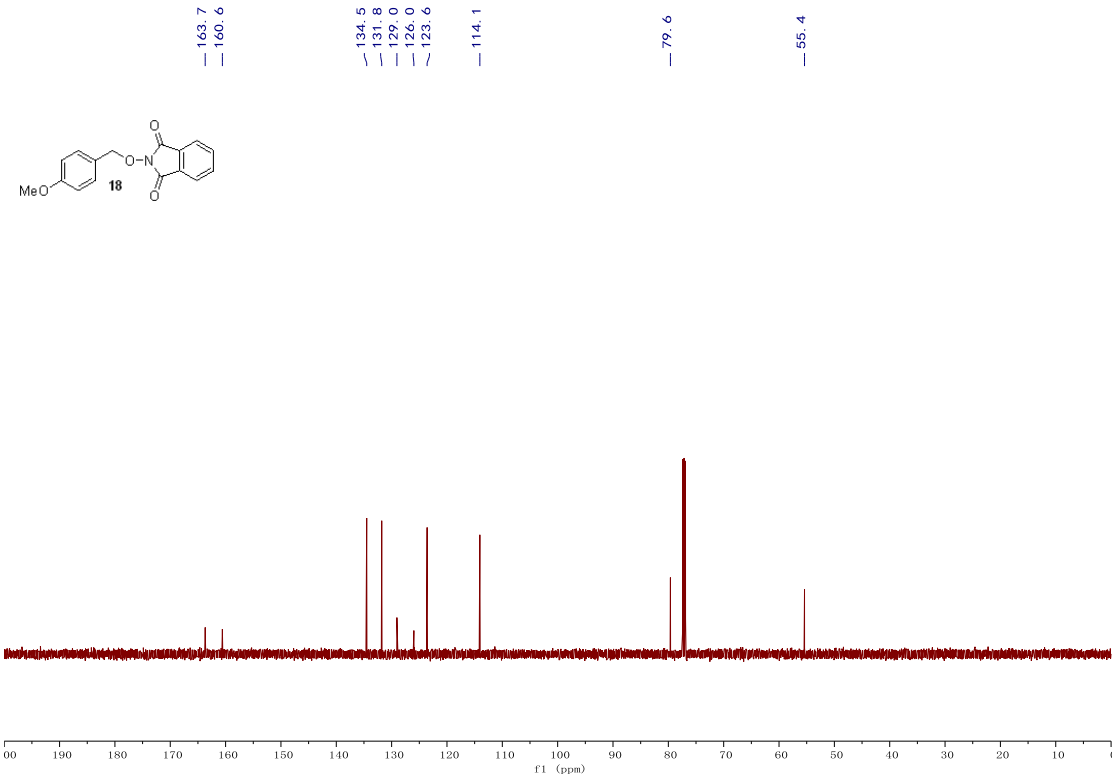

Figure S32. ^{13}C NMR (126 MHz, CDCl3) spectrum of compound 18, related to Scheme 2.

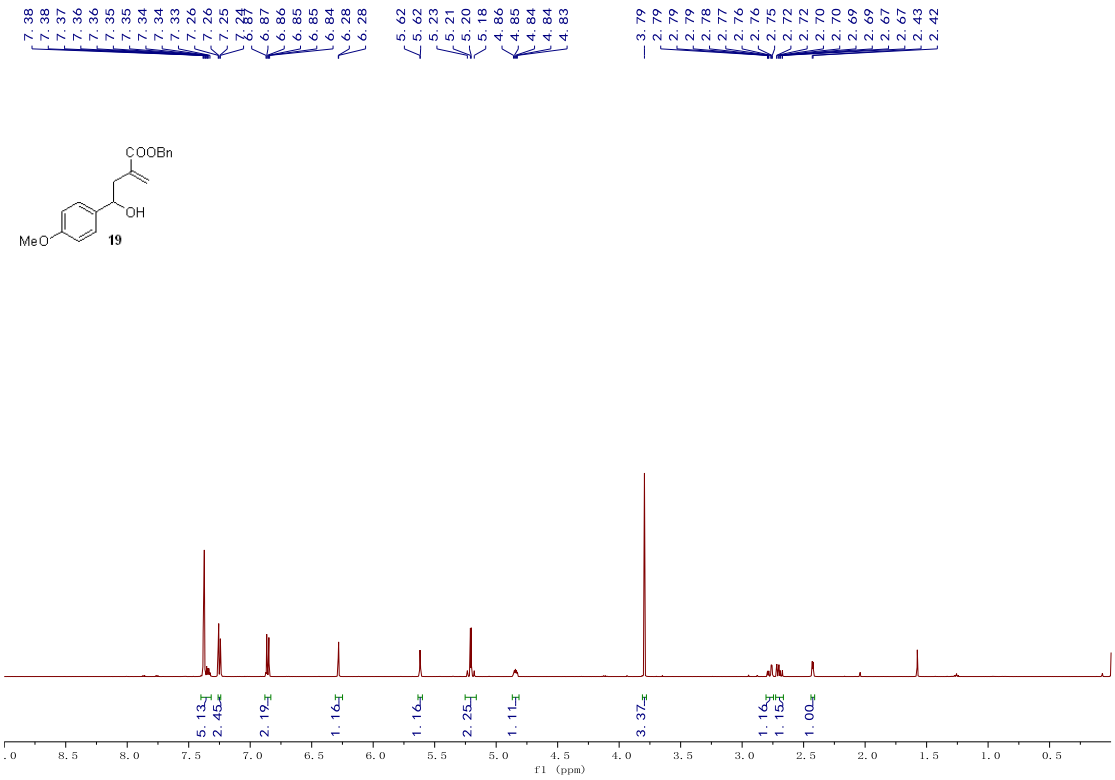

Figure S33. ^{1}H NMR (500 MHz, CDCl3) spectrum of compound 19, related to Scheme 2.

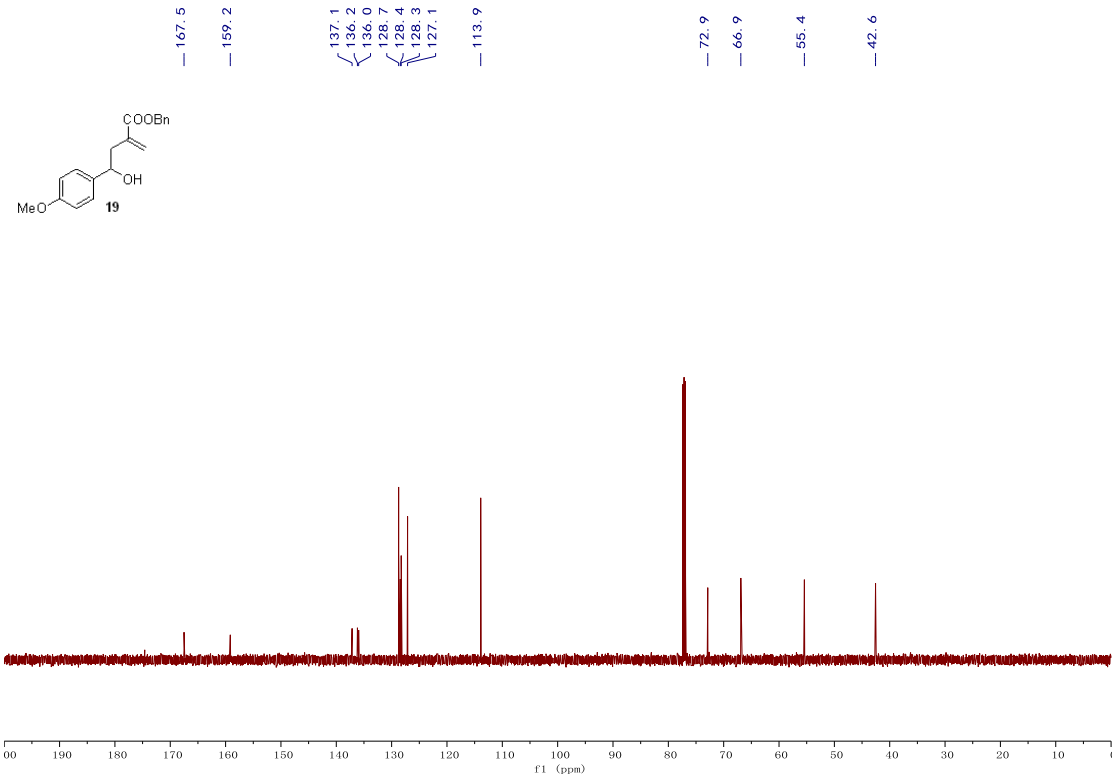

Figure S34. ^{13}C NMR (126 MHz, CDCl3) spectrum of compound 19, related to Scheme 2.

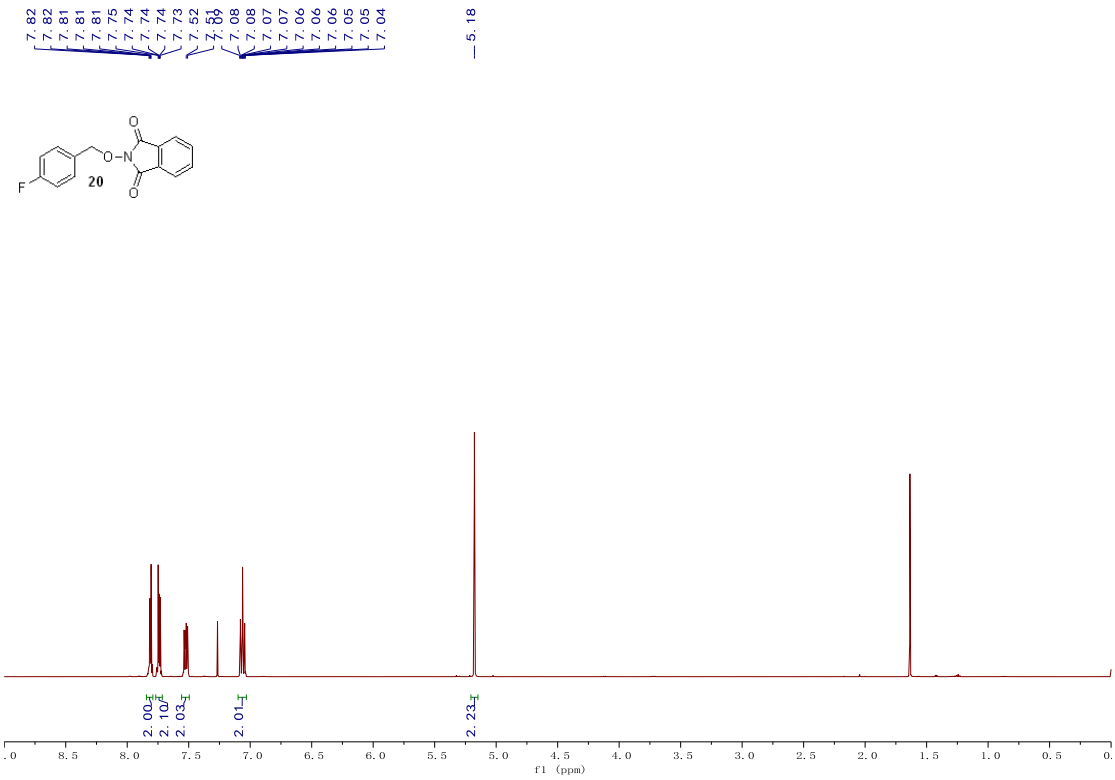

Figure S35. ^{1}H NMR (500 MHz, CDCl3) spectrum of compound 20, related to Scheme 2.

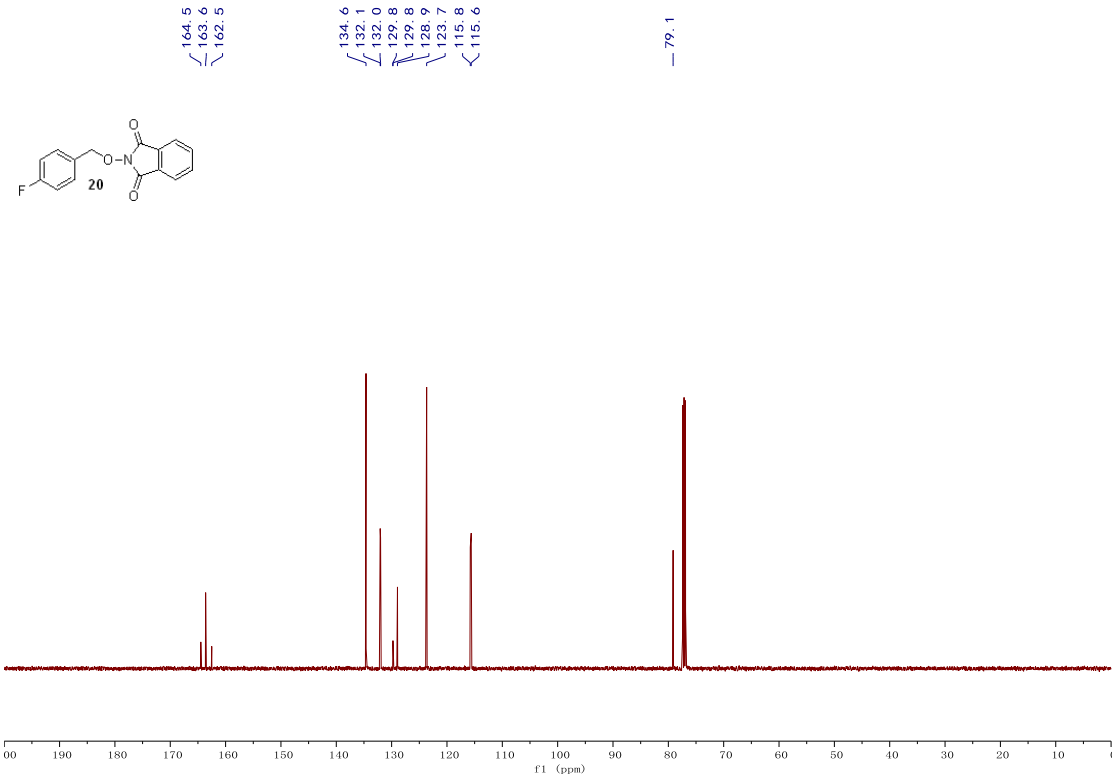

Figure S36. ^{13}C NMR (126 MHz, CDCl3) spectrum of compound 20, related to Scheme 2.

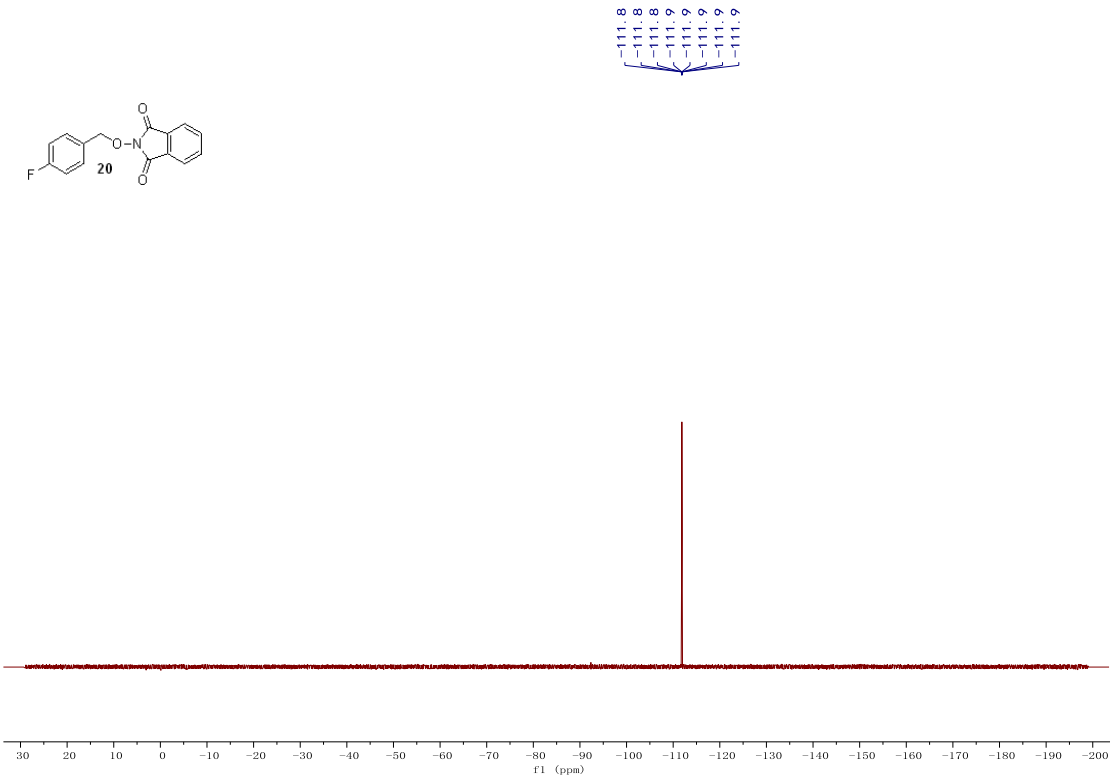

Figure S37. ^{19}F NMR (376 MHz, CDCl3) spectrum of compound 20, related to Scheme 2.

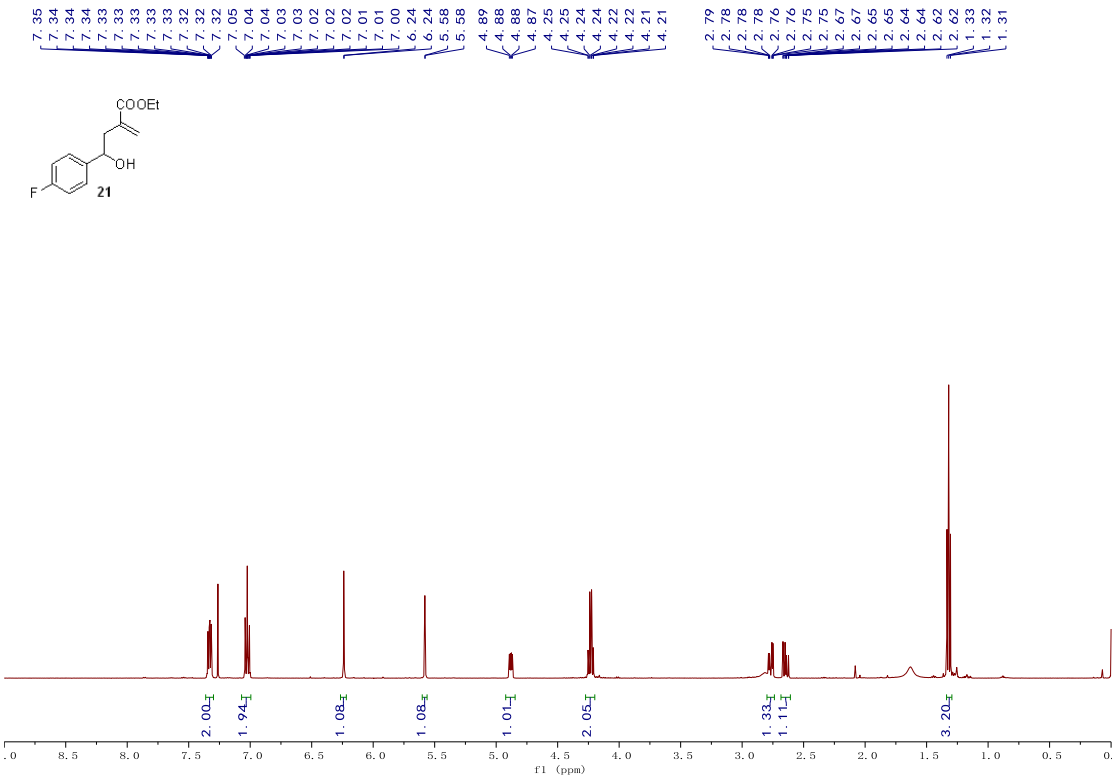

Figure S38. ^{1}H NMR (500 MHz, CDCl3) spectrum of compound 21, related to Scheme 2.

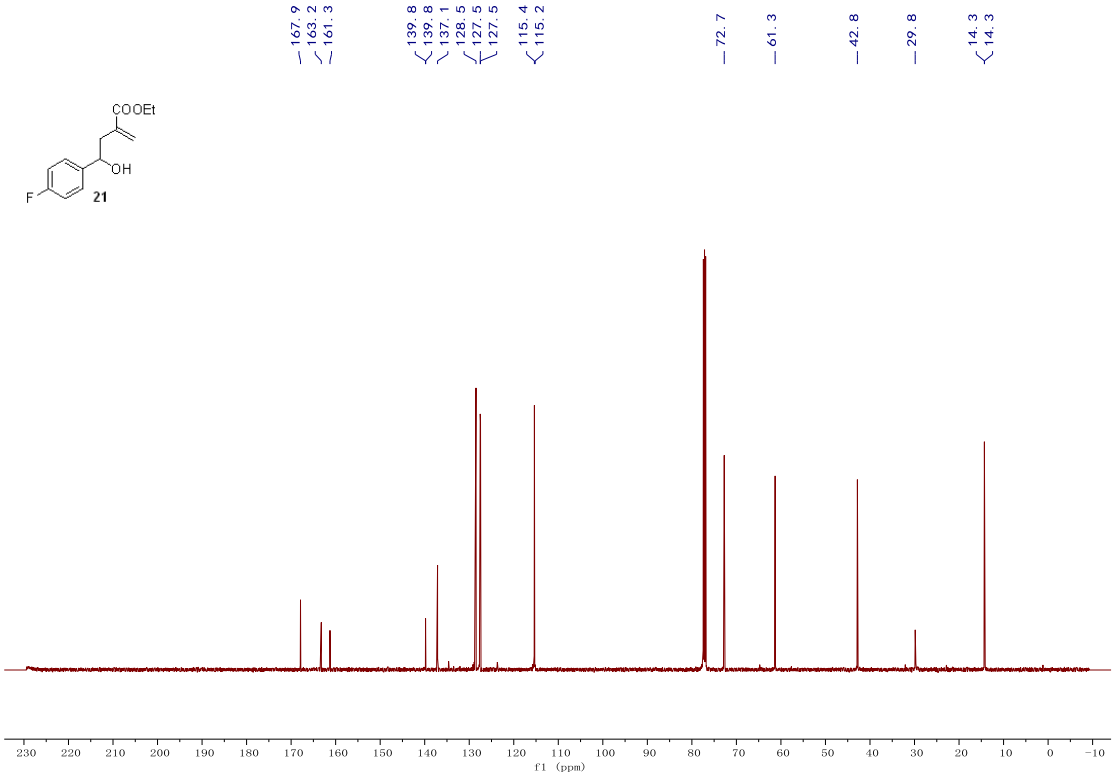

Figure S39. ^{13}C NMR (126 MHz, CDCl3) spectrum of compound 21, related to Scheme 2.

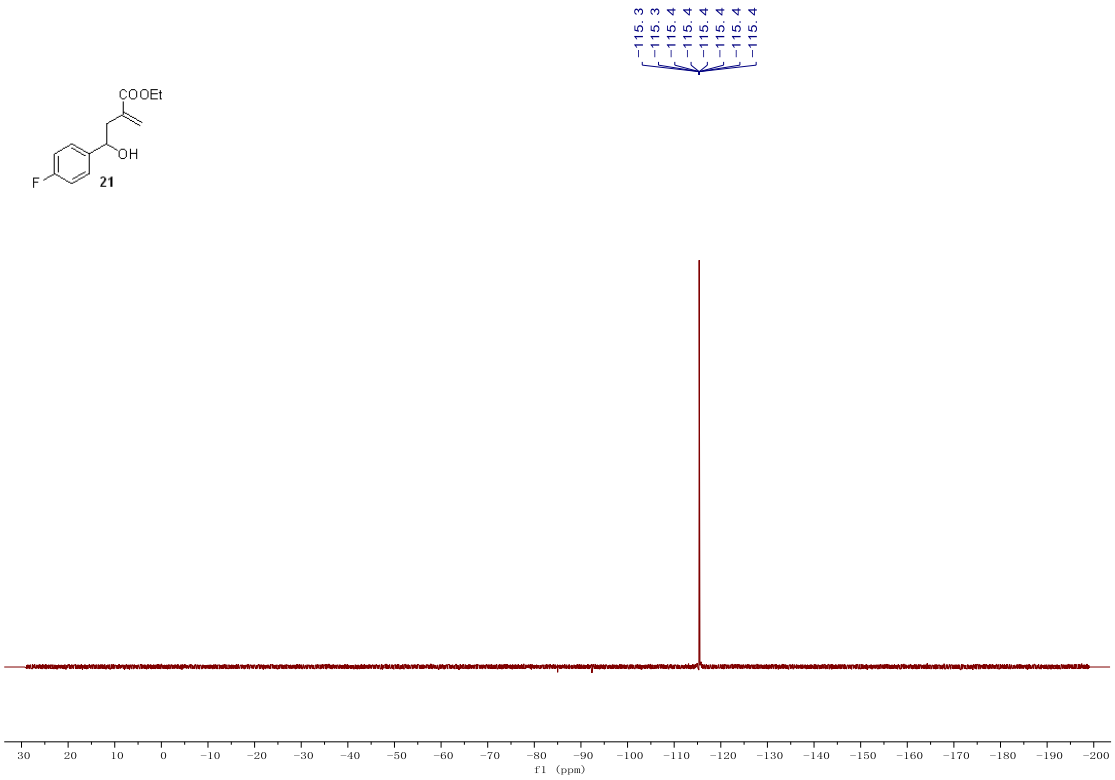

Figure S40. ^{19}F NMR (376 MHz, CDCl3) spectrum of compound 21, related to Scheme 2

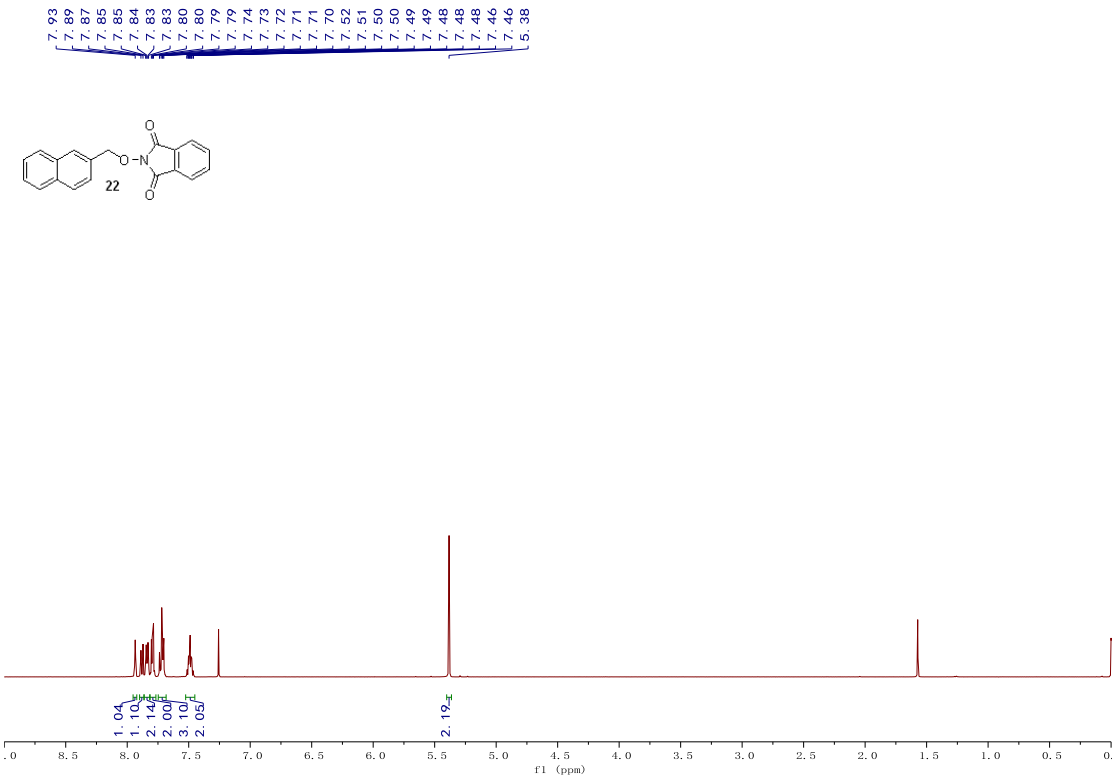

Figure S41. ^{1}H NMR (500 MHz, CDCl3) spectrum of compound 22, related to Scheme 2.

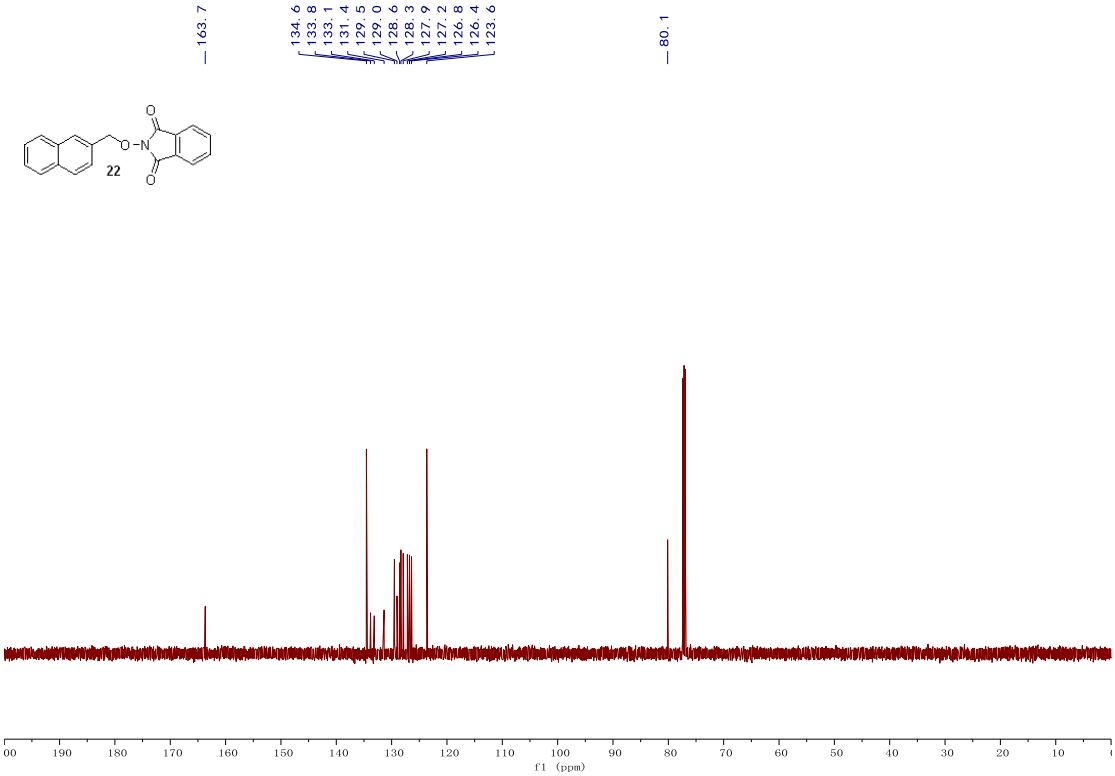

Figure S42. ^{13}C NMR (126 MHz, CDCl3) spectrum of compound 22, related to Scheme 2.

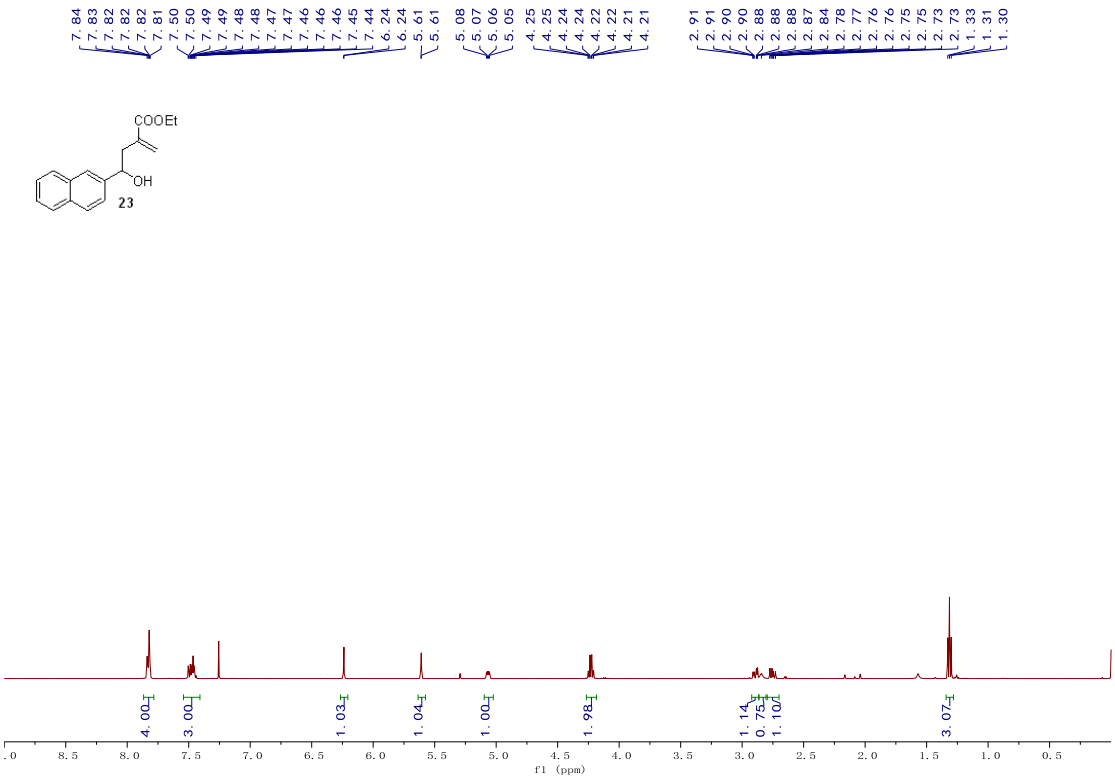

Figure S43. ^{1}H NMR (500 MHz, CDCl3) spectrum of compound 23, related to Scheme 2.

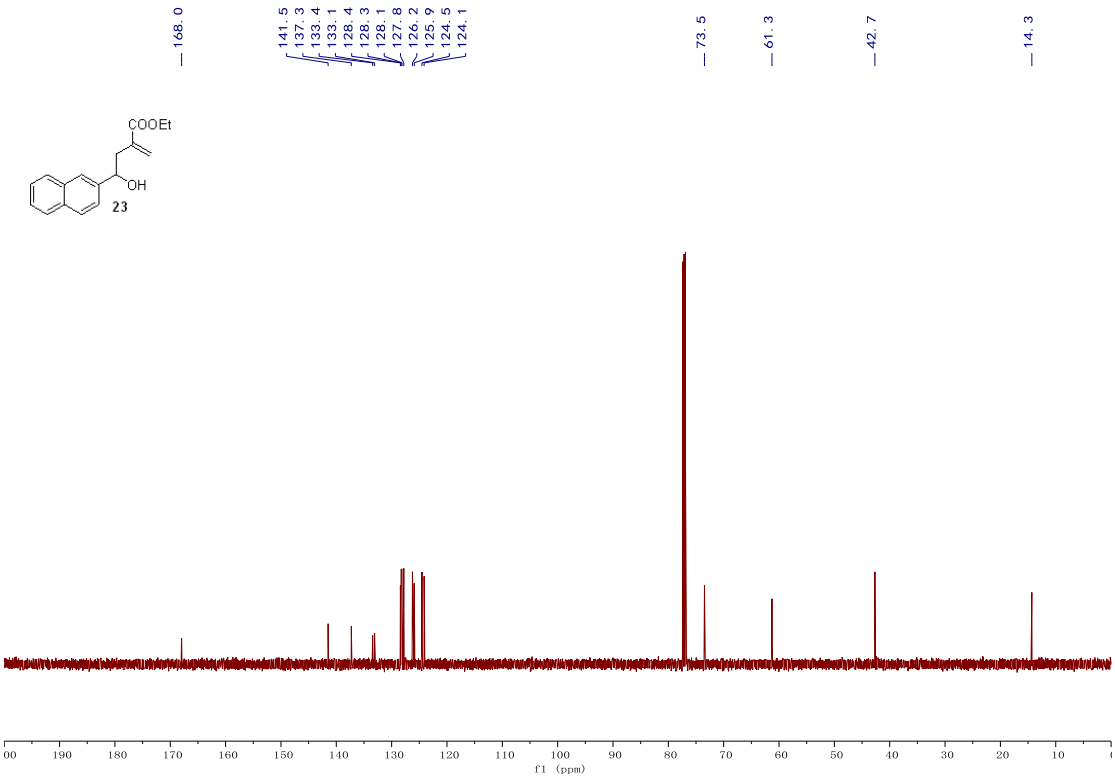

Figure S44. ^{13}C NMR (126 MHz, CDCl3) spectrum of compound 23, related to Scheme 2.

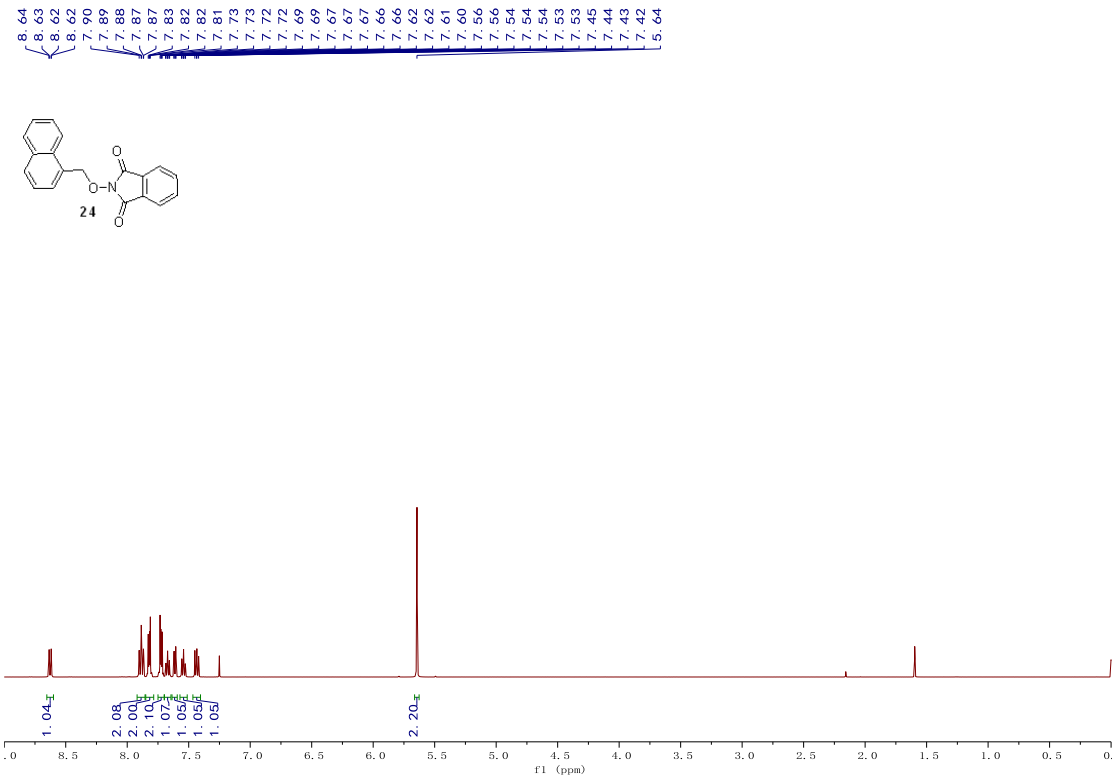

Figure S45. ^{1}H NMR (500 MHz, CDCl3) spectrum of compound 24, related to Scheme 2.

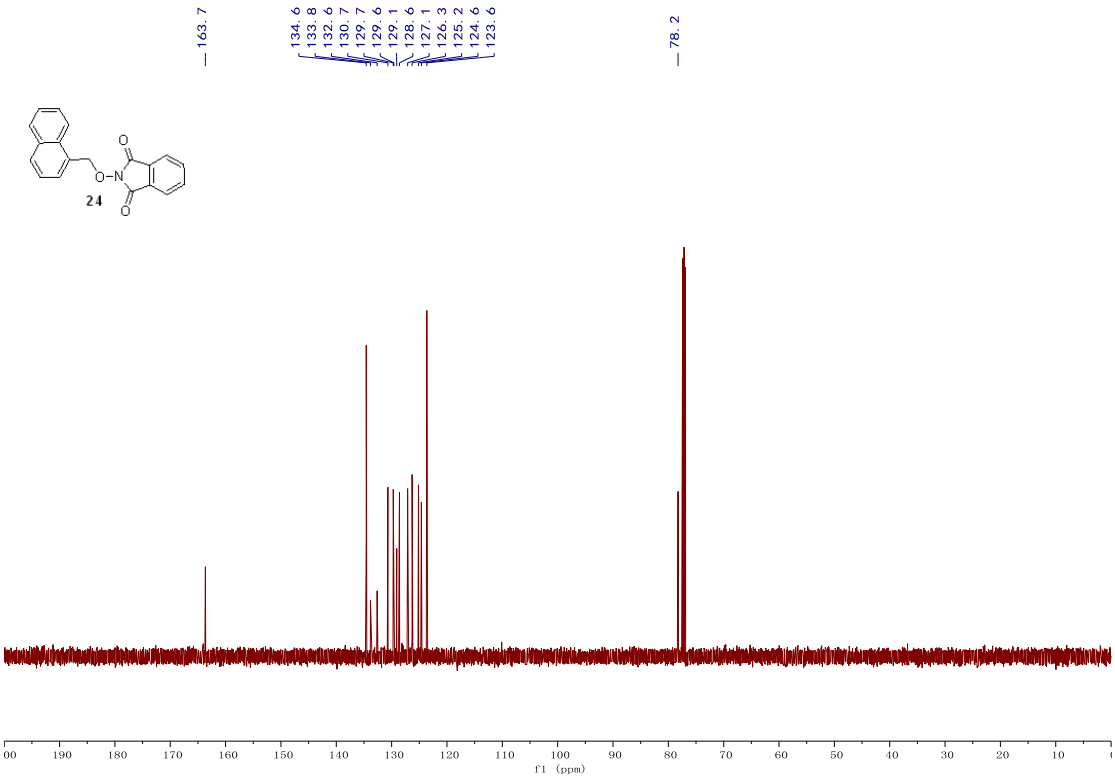

Figure S46. ^{13}C NMR (126 MHz, CDCl3) spectrum of compound 24, related to Scheme 2.

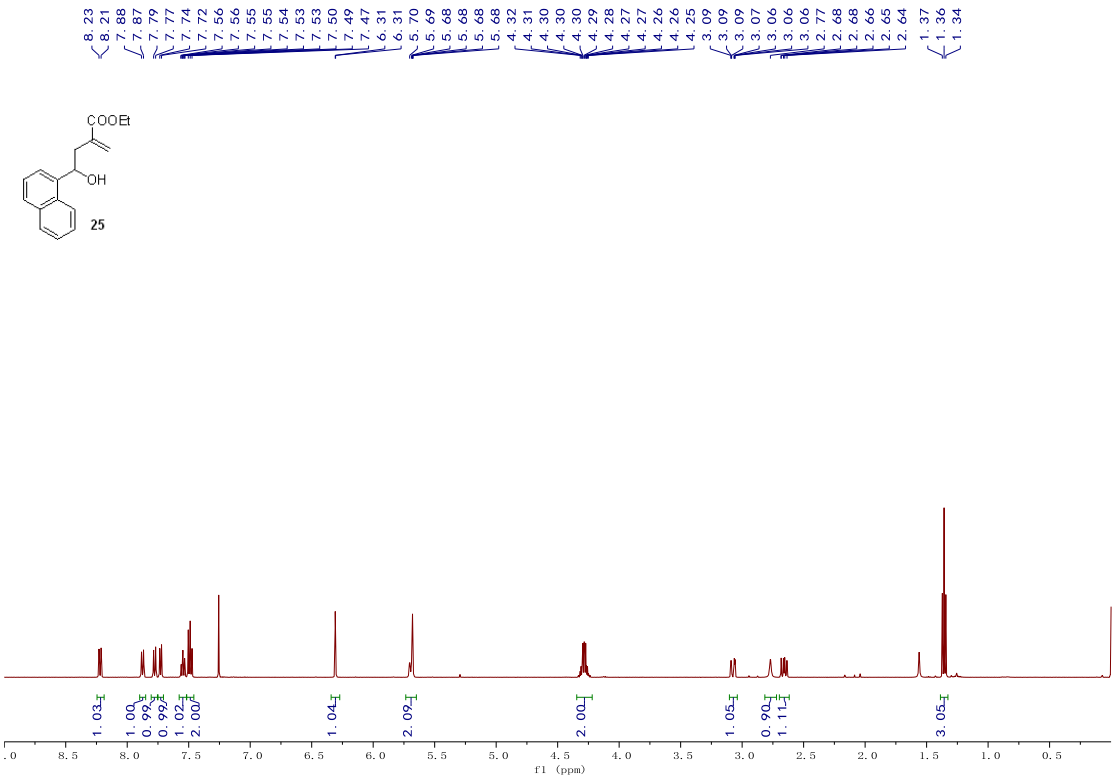

Figure S47. ^{1}H NMR (500 MHz, CDCl3) spectrum of compound 25, related to Scheme 2.

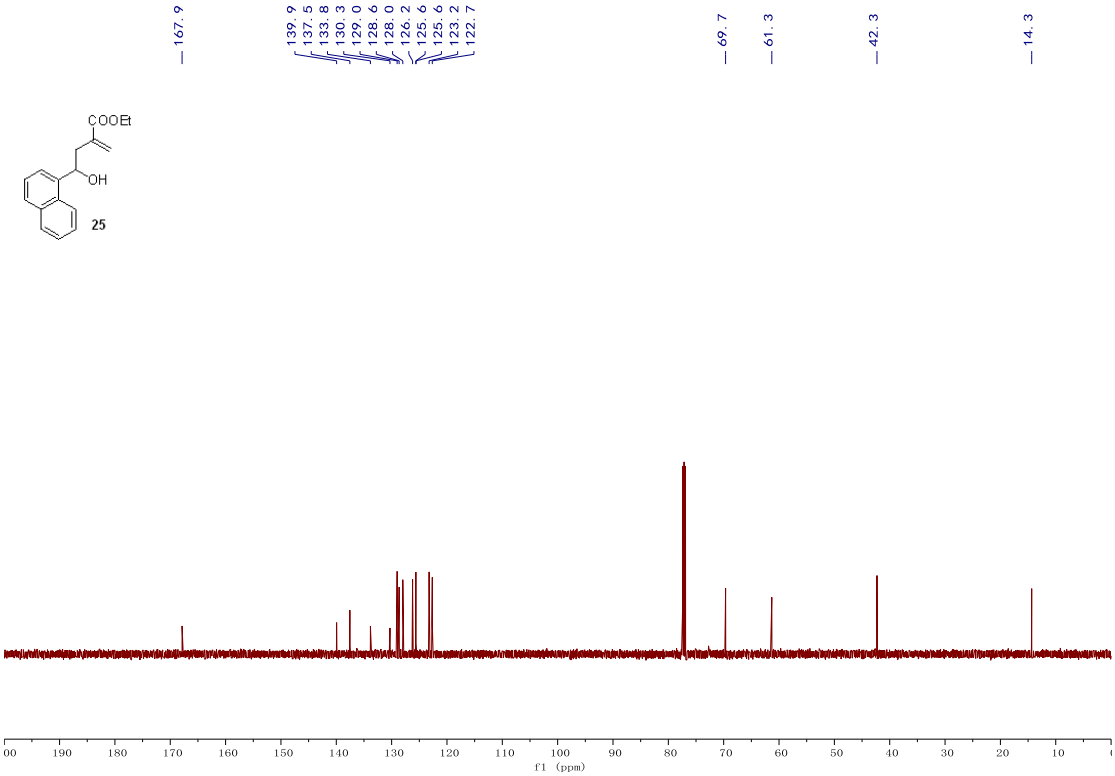

Figure S48. ^{13}C NMR (126 MHz, CDCl3) spectrum of compound 25, related to Scheme 2.

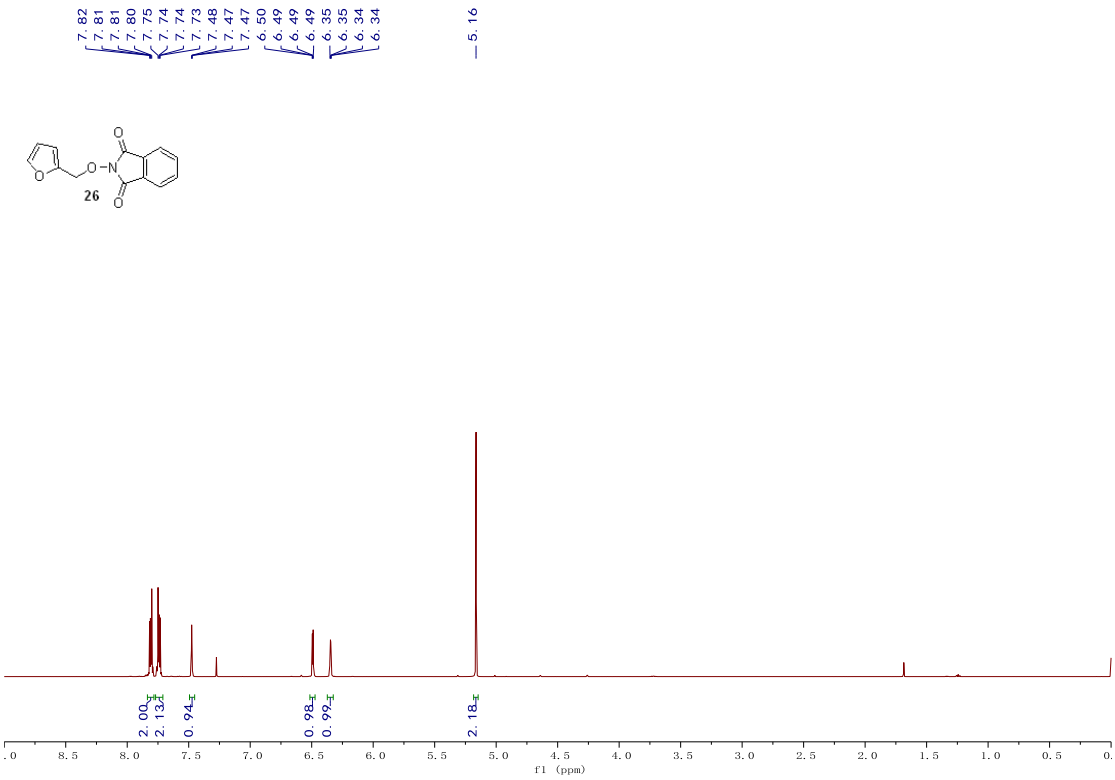

Figure S49. ^{1}H NMR (500 MHz, CDCl3) spectrum of compound 26, related to Scheme 2.

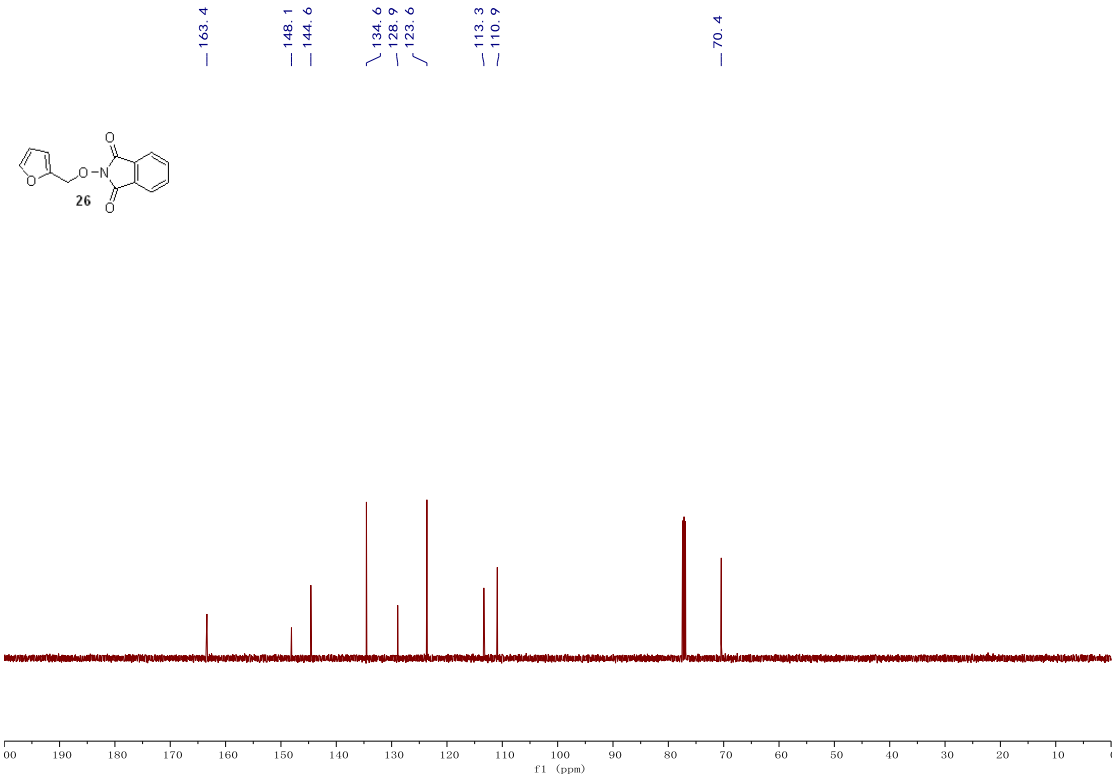

Figure S50. ^{13}C NMR (126 MHz, CDCl3) spectrum of compound 26, related to Scheme 2.

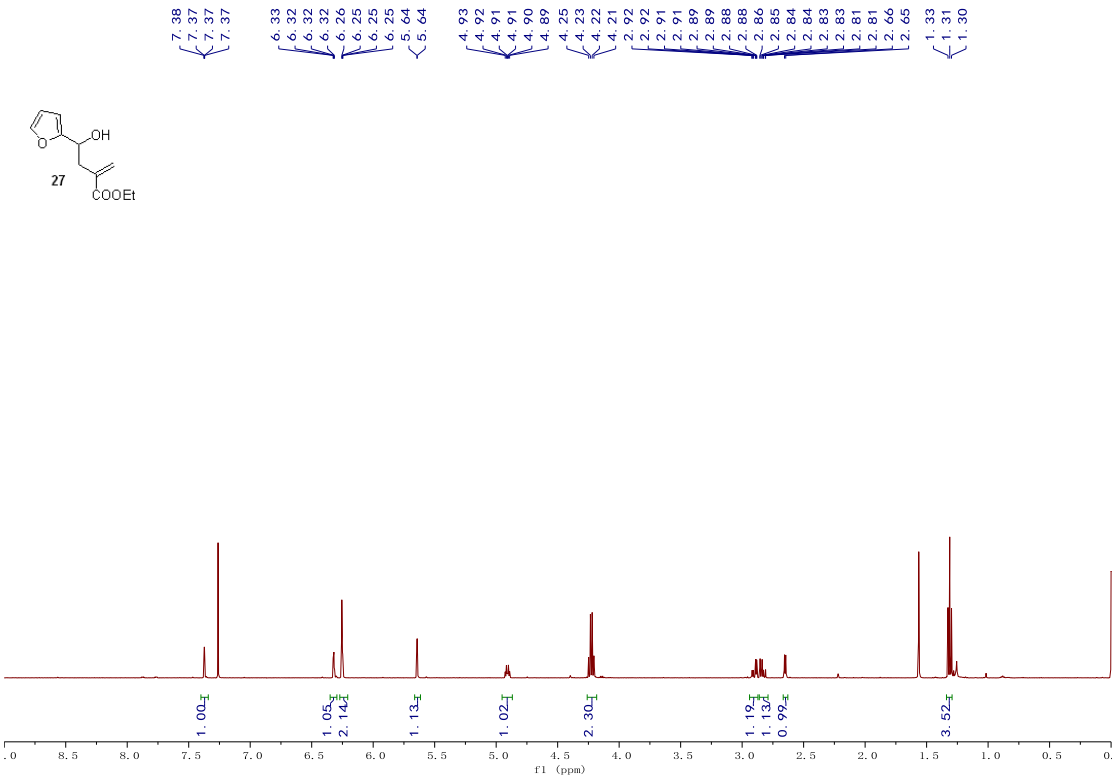

Figure S51. ^{1}H NMR (500 MHz, CDCl3) spectrum of compound 27, related to Scheme 2.

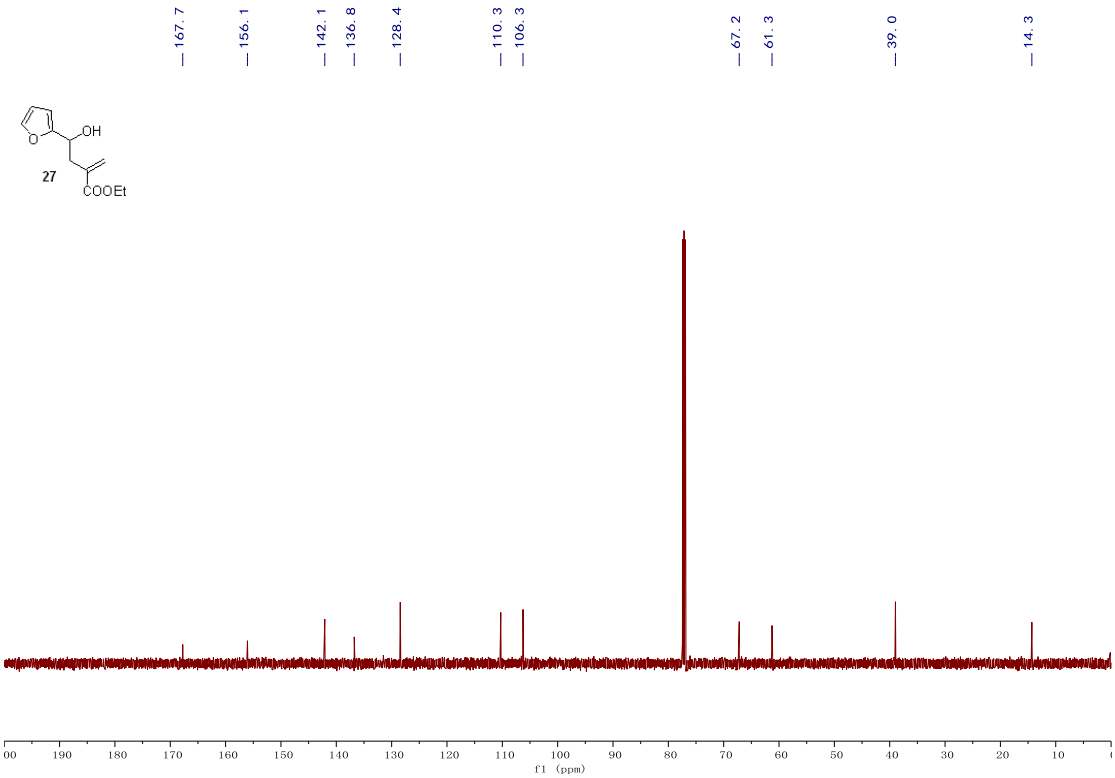

Figure S52. ^{13}C NMR (126 MHz, CDCl3) spectrum of compound 27, related to Scheme 2.

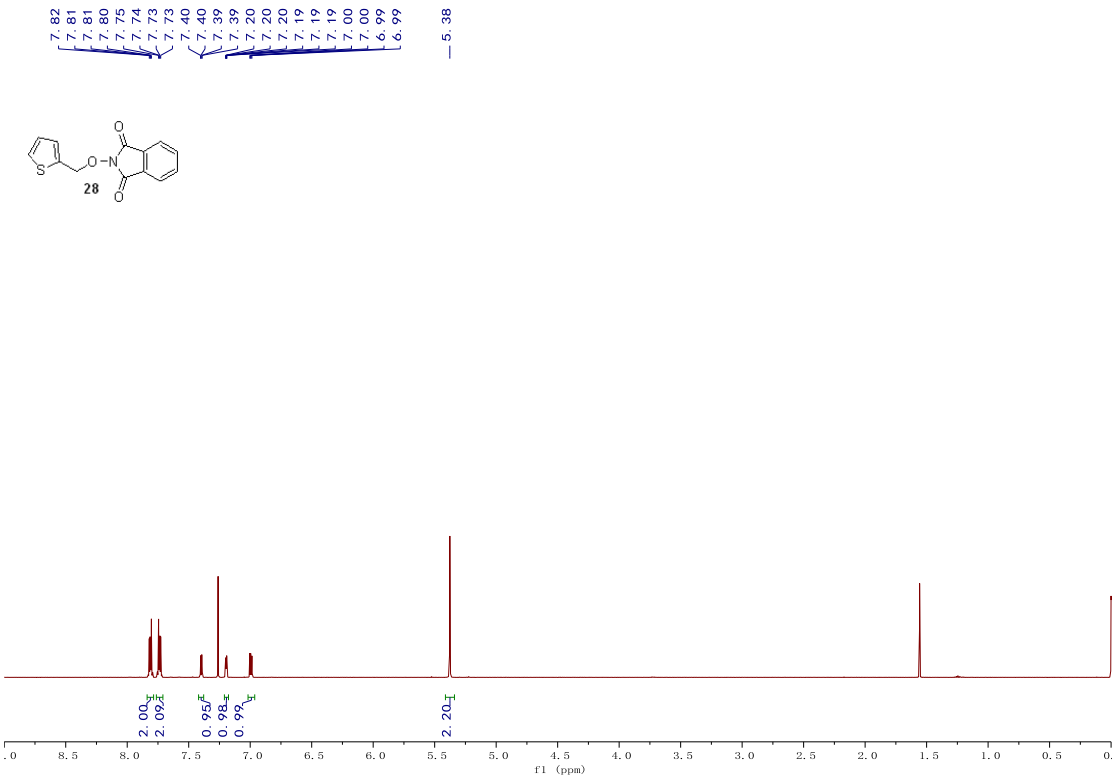

Figure S53. ^{1}H NMR (500 MHz, CDCl3) spectrum of compound 28, related to Scheme 2.

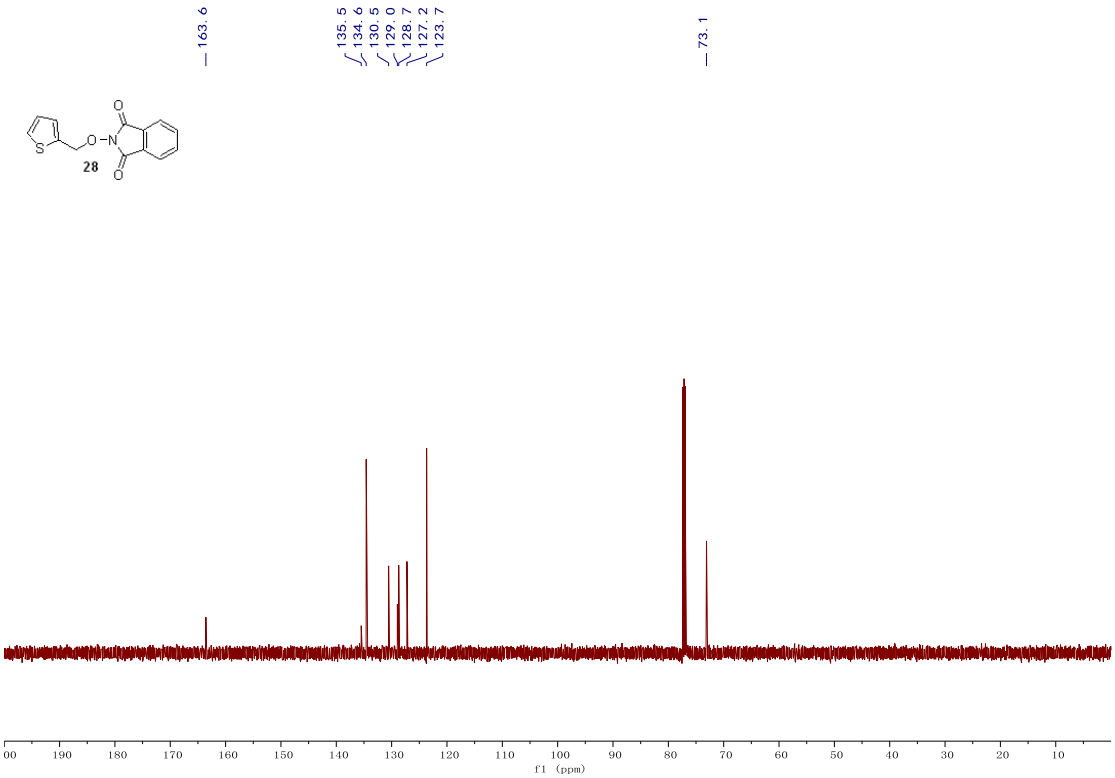

Figure S54. ^{13}C NMR (126 MHz, CDCl3) spectrum of compound 28, related to Scheme 2.

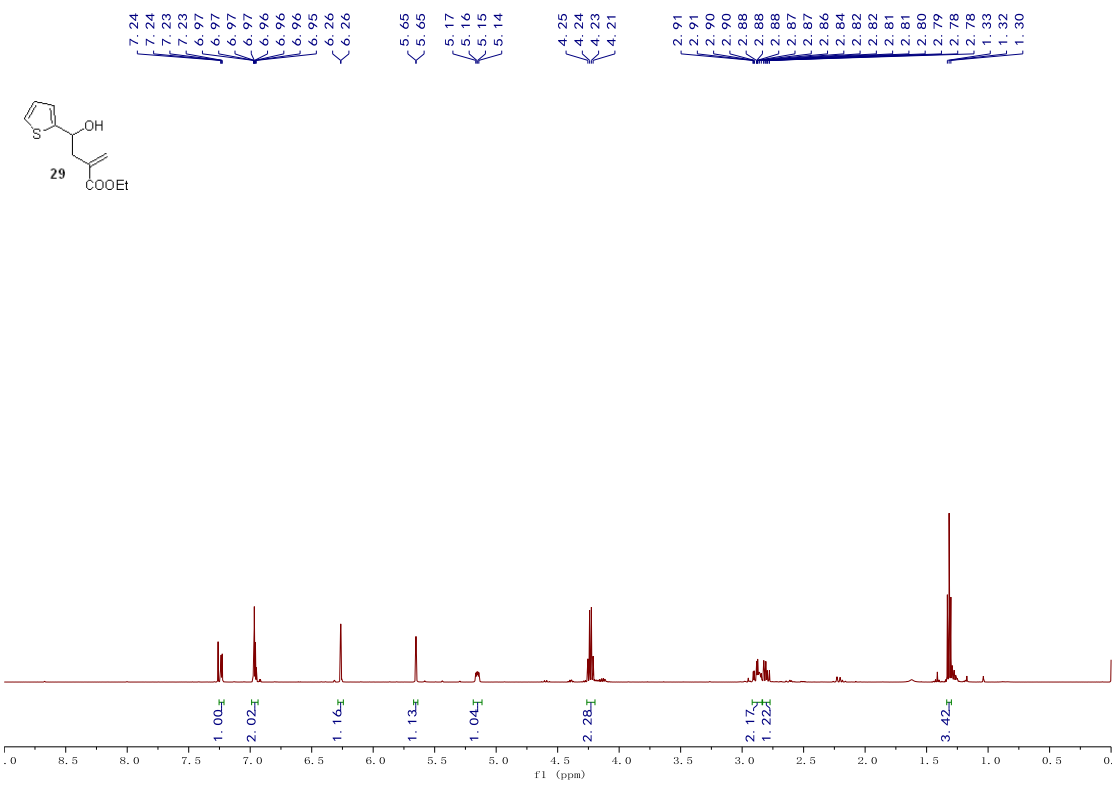

Figure S55. ^{1}H NMR (500 MHz, CDCl3) spectrum of compound 29, related to Scheme 2.

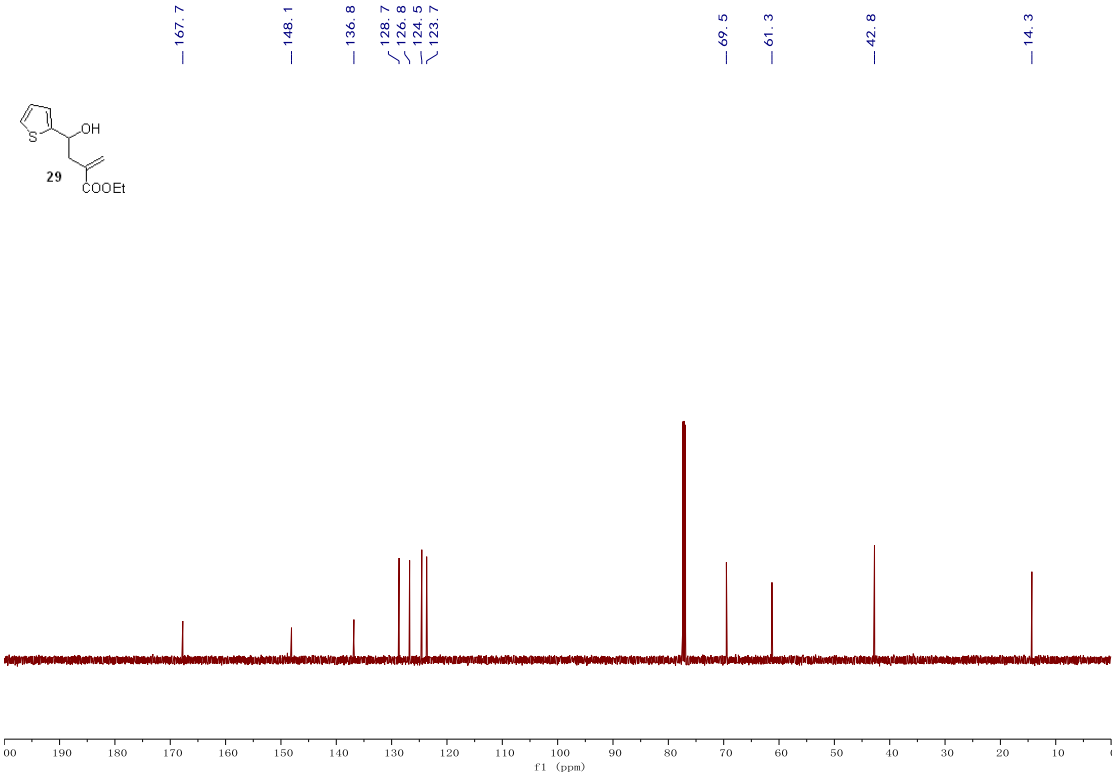

Figure S56. ^{13}C NMR (126 MHz, CDCl3) spectrum of compound 29, related to Scheme 2.

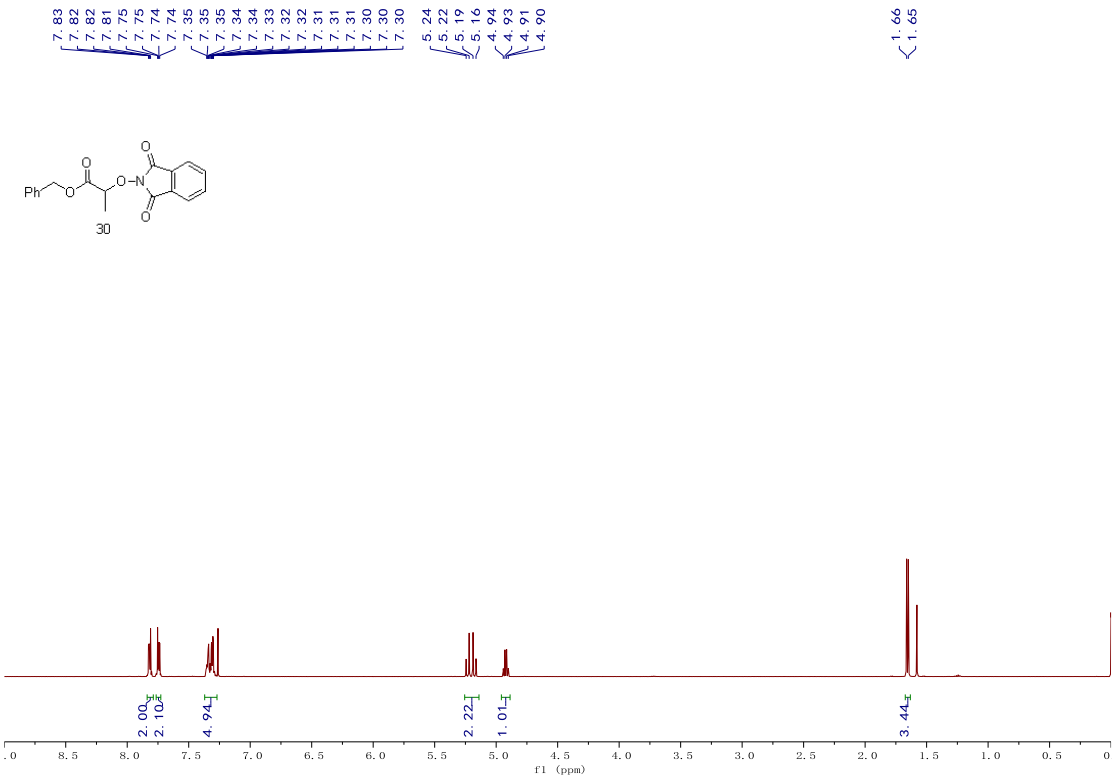

Figure S57. ^{1}H NMR (500 MHz, CDCl3) spectrum of compound 30, related to Scheme 2.

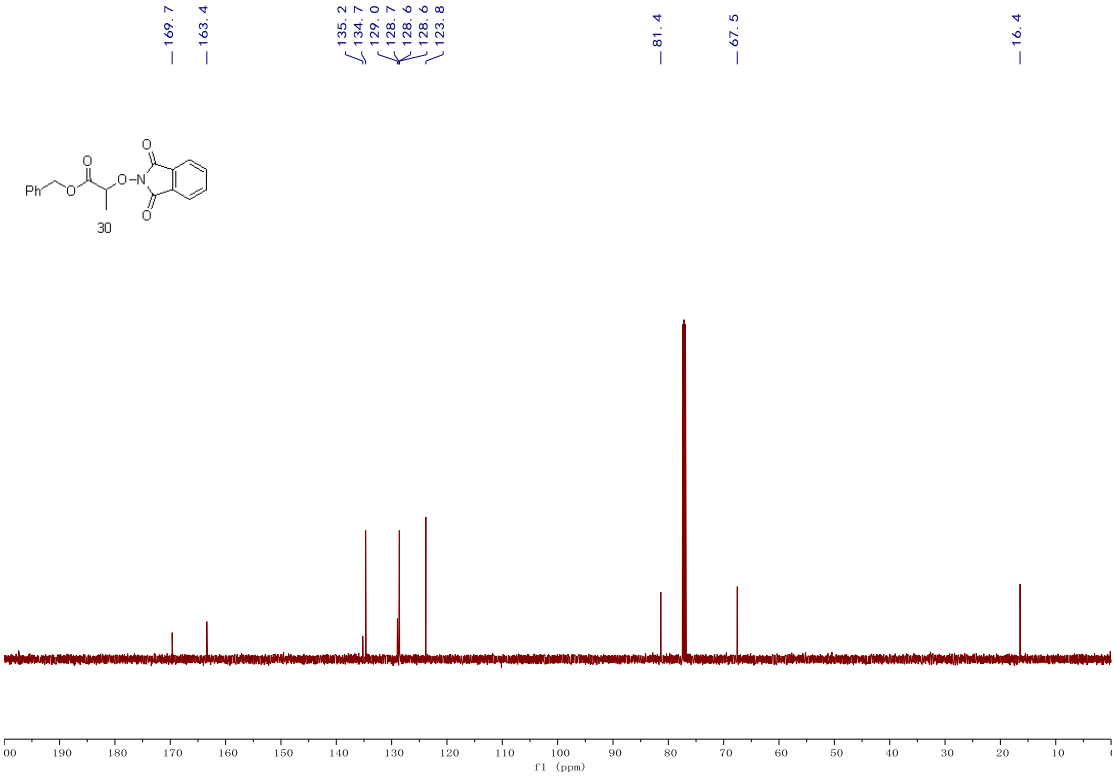

Figure S58. ^{13}C NMR (126 MHz, CDCl3) spectrum of compound 30, related to Scheme 2.

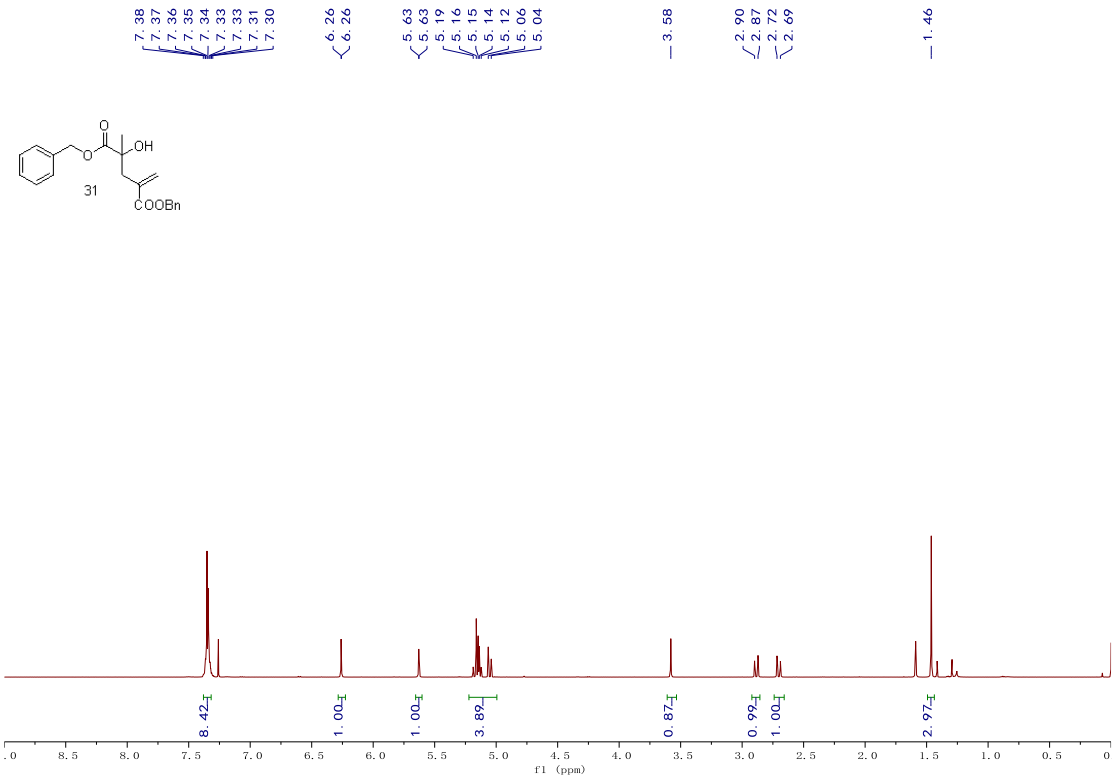

Figure S59. ^{1}H NMR (500 MHz, CDCl3) spectrum of compound 31, related to Scheme 2.

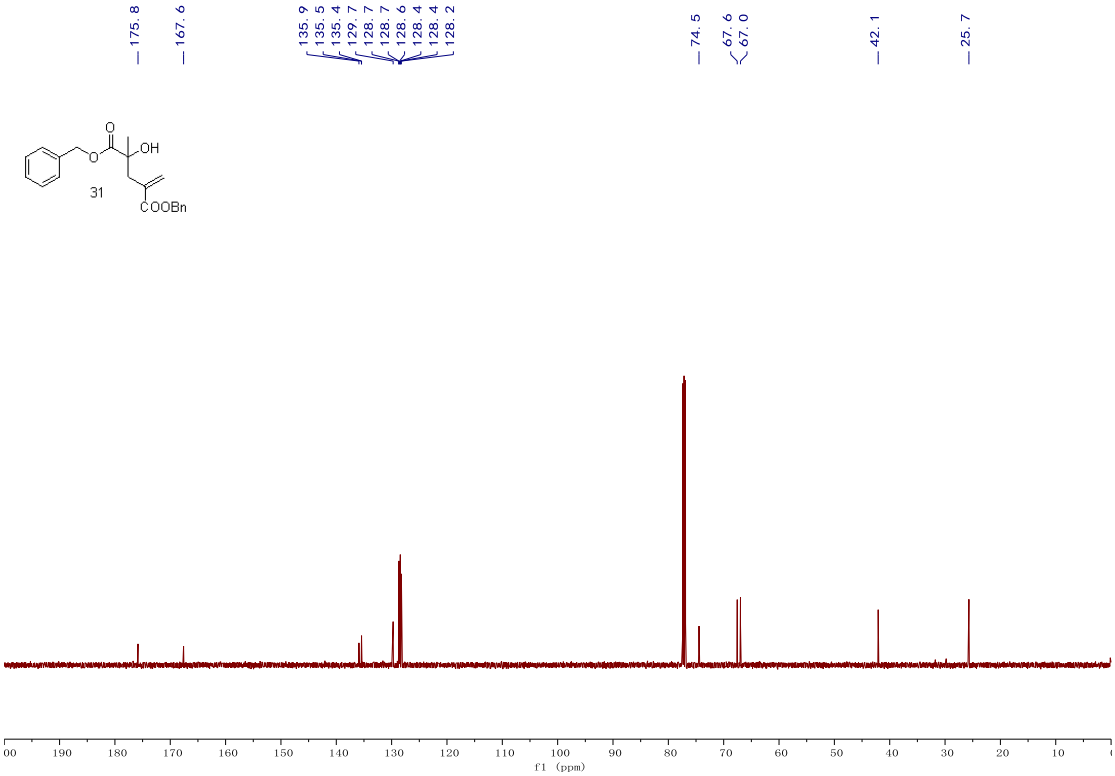

Figure S60. ^{13}C NMR (126 MHz, CDCl3) spectrum of compound 31, related to Scheme 2.

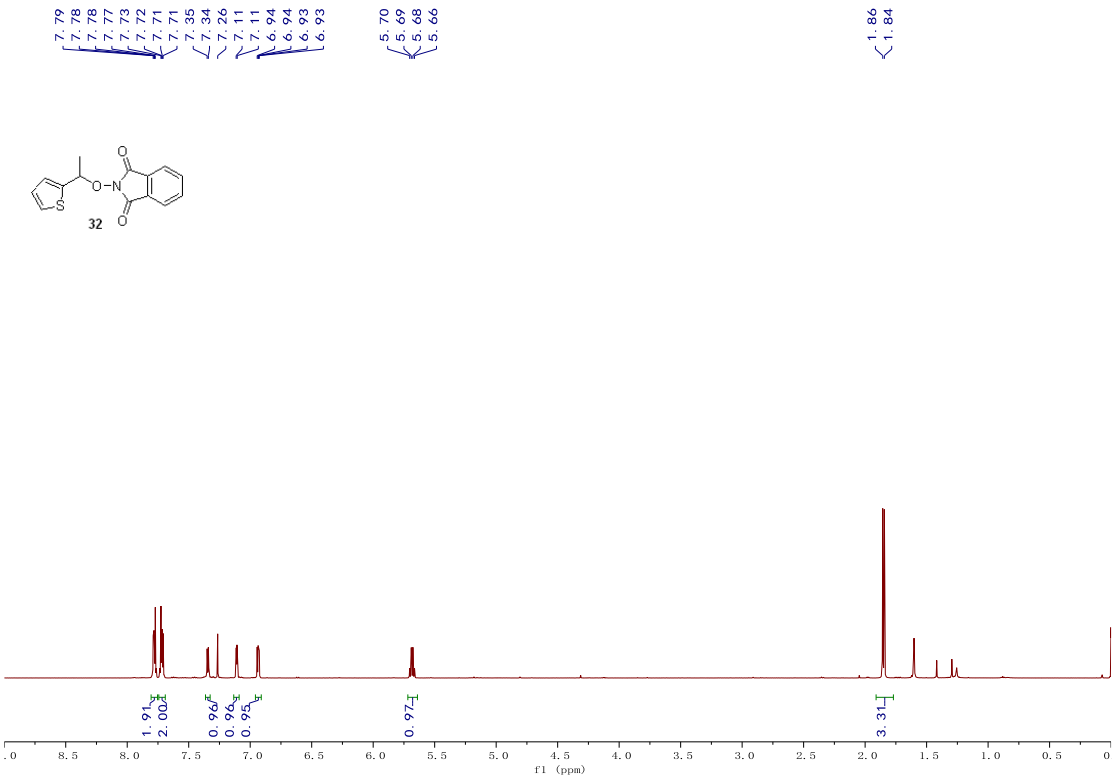

Figure S61. ^{1}H NMR (500 MHz, CDCl3) spectrum of compound 32, related to Scheme 2.

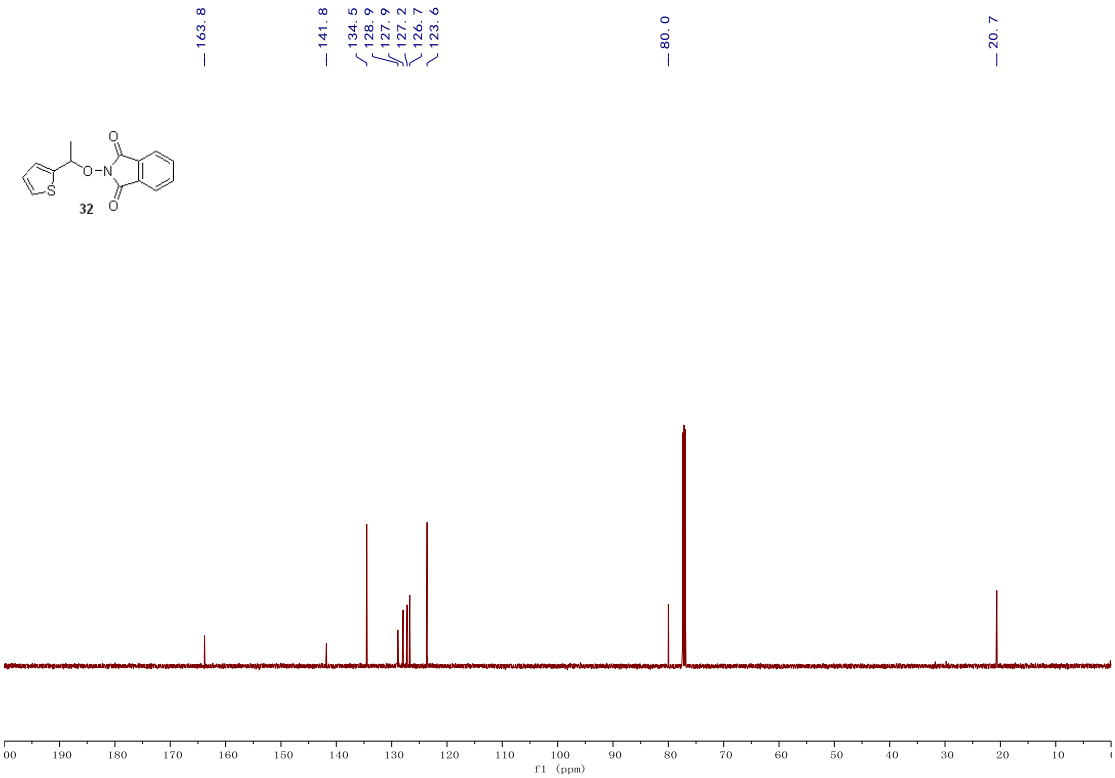

Figure S62. ^{13}C NMR (126 MHz, CDCl3) spectrum of compound 32, related to Scheme 2.

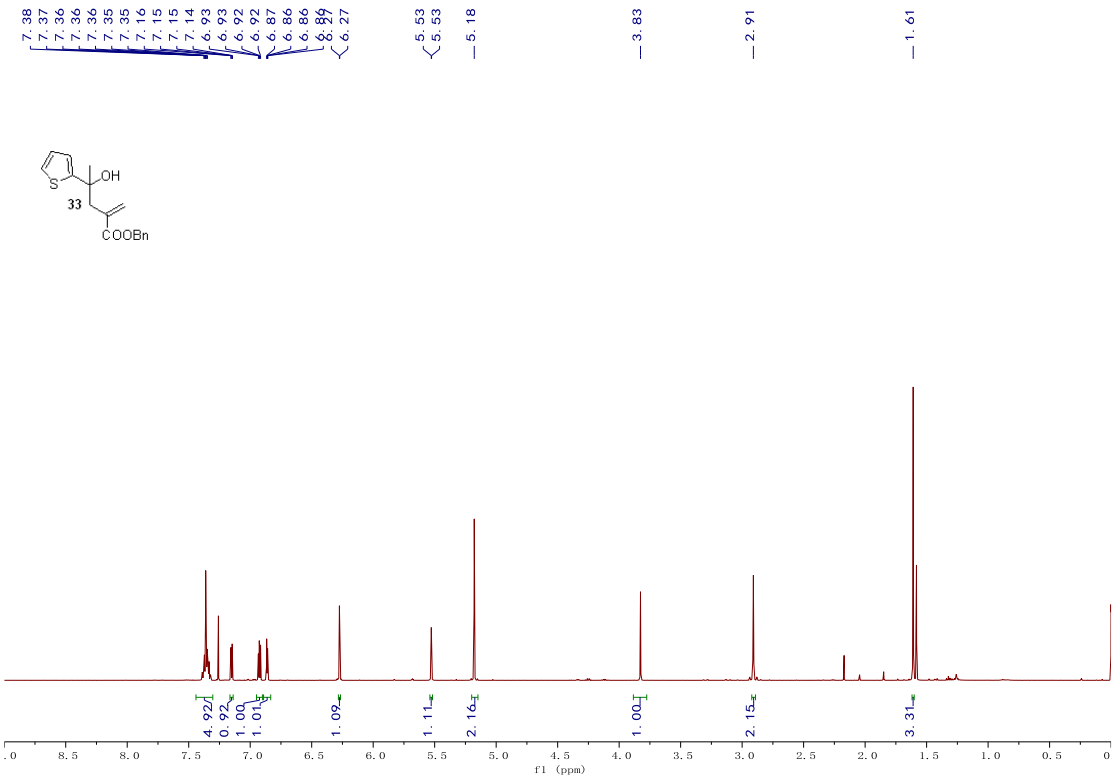

Figure S63. ^{1}H NMR (500 MHz, CDCl3) spectrum of compound 33, related to Scheme 2.

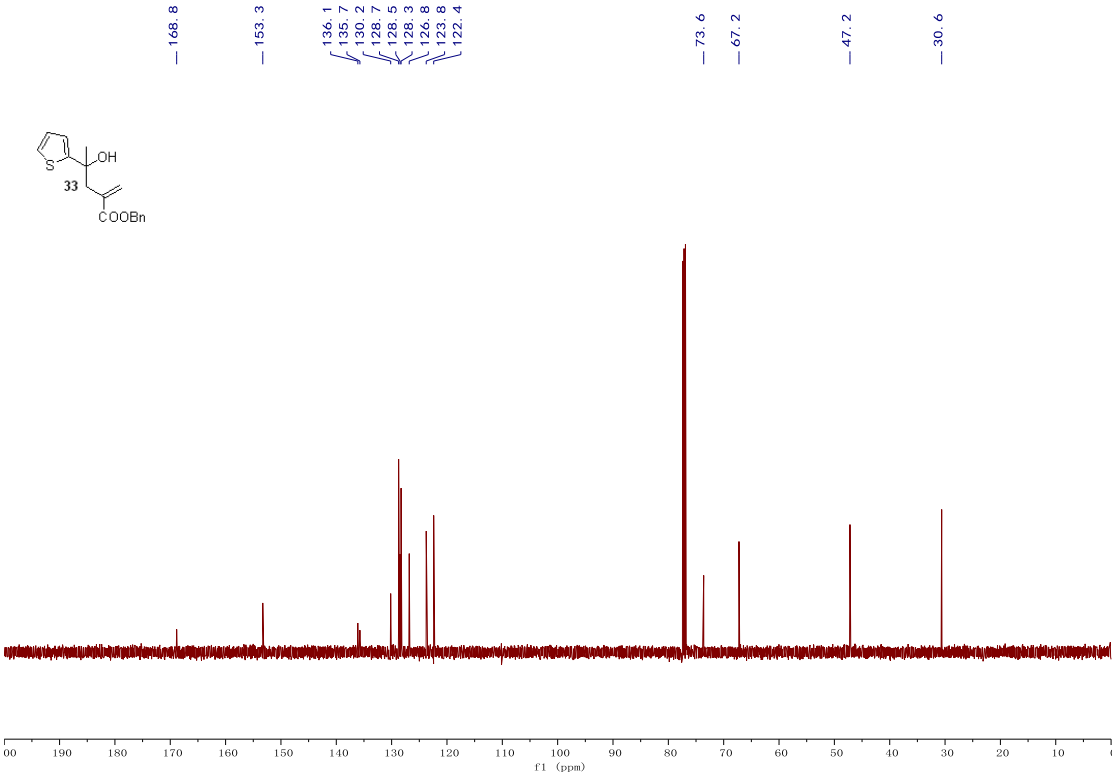

Figure S64. ^{13}C NMR (126 MHz, CDCl3) spectrum of compound 33, related to Scheme 2.

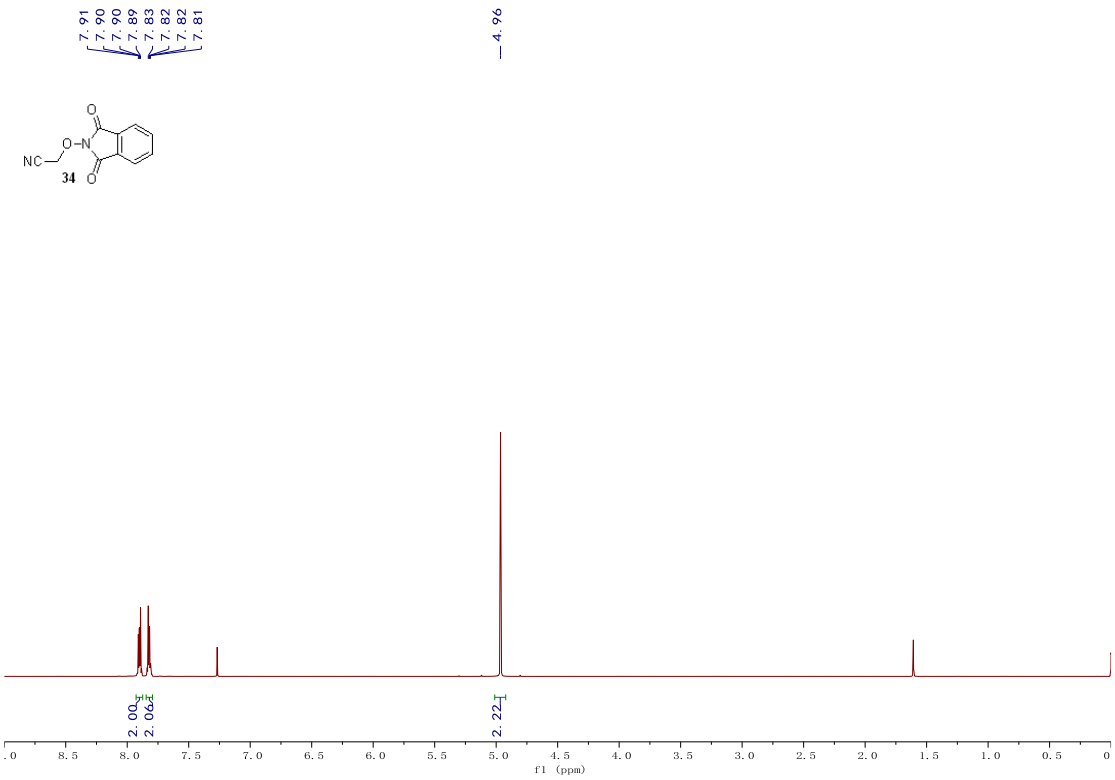

Figure S65. ^{1}H NMR (500 MHz, CDCl3) spectrum of compound 34, related to Scheme 2.

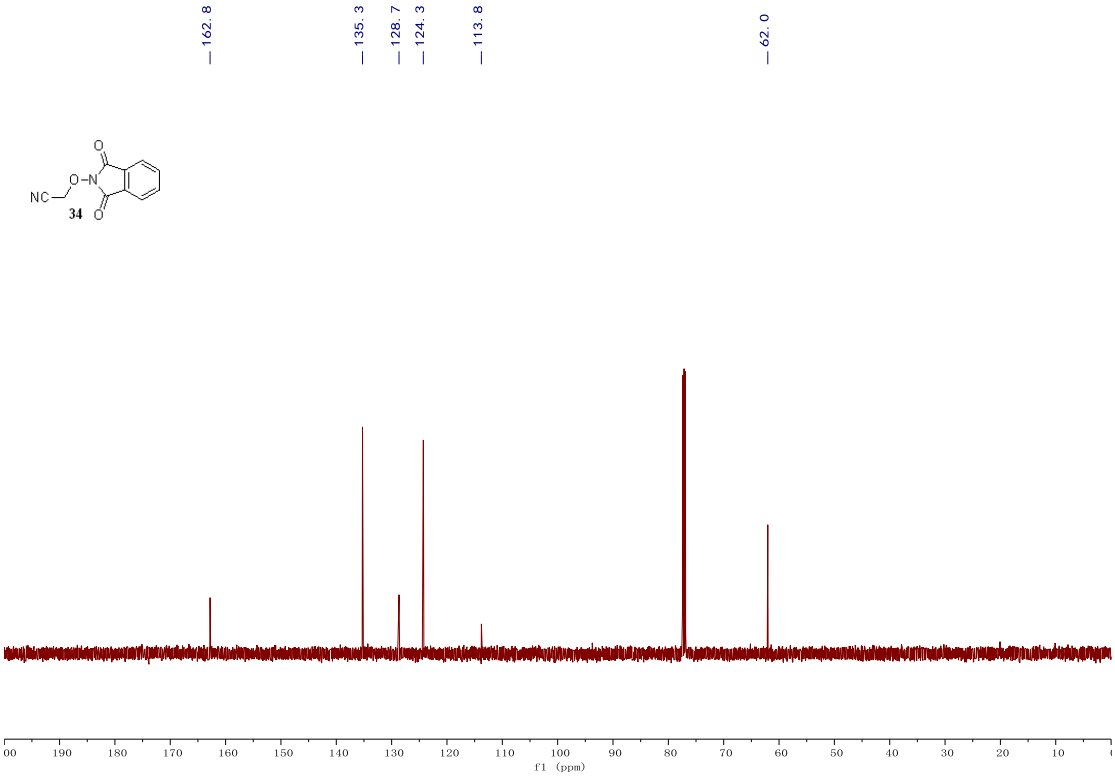

Figure S66. ^{13}C NMR (126 MHz, CDCl3) spectrum of compound 34, related to Scheme 2.

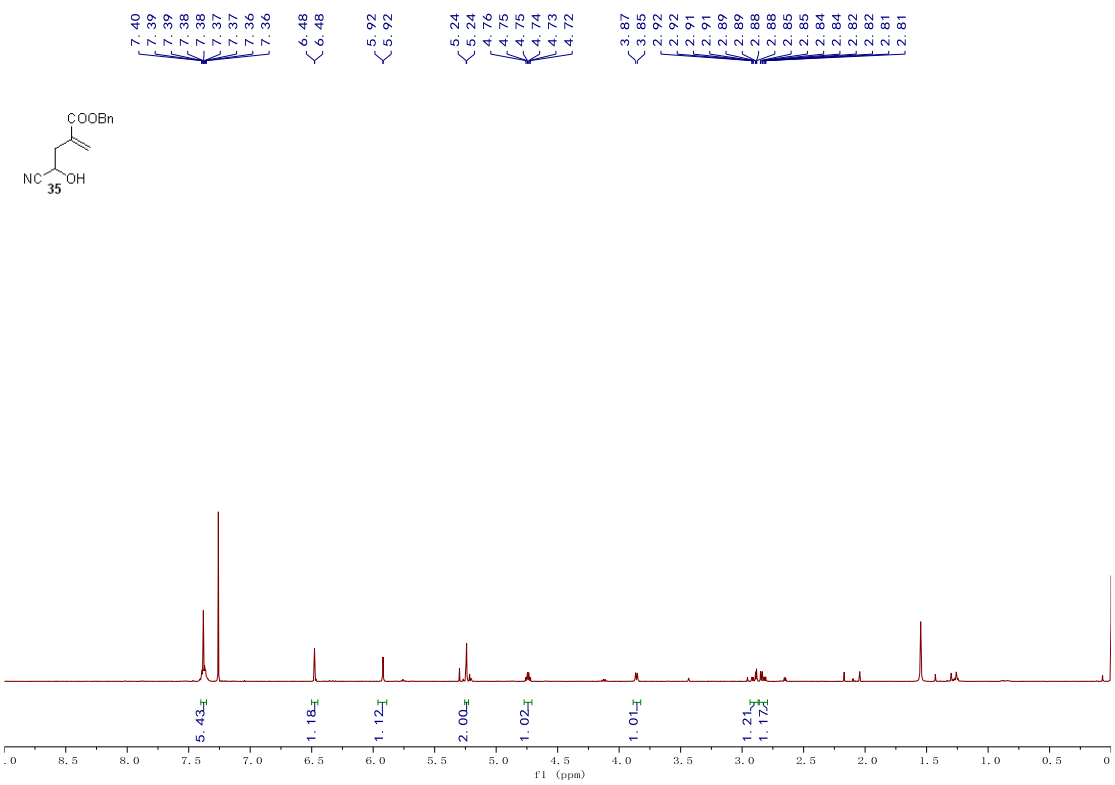

Figure S67. ^{1}H NMR (500 MHz, CDCl3) spectrum of compound 35, related to Scheme 2.

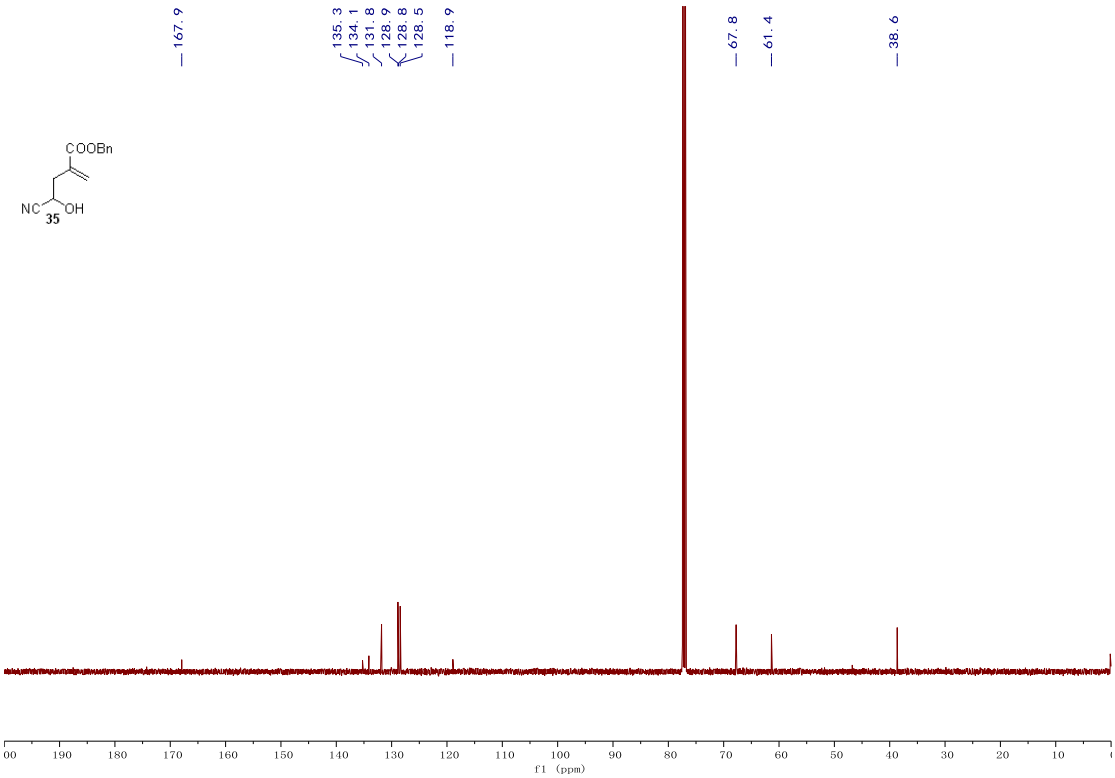

Figure S68. ^{13}C NMR (126 MHz, CDCl3) spectrum of compound 36, related to Scheme 2.

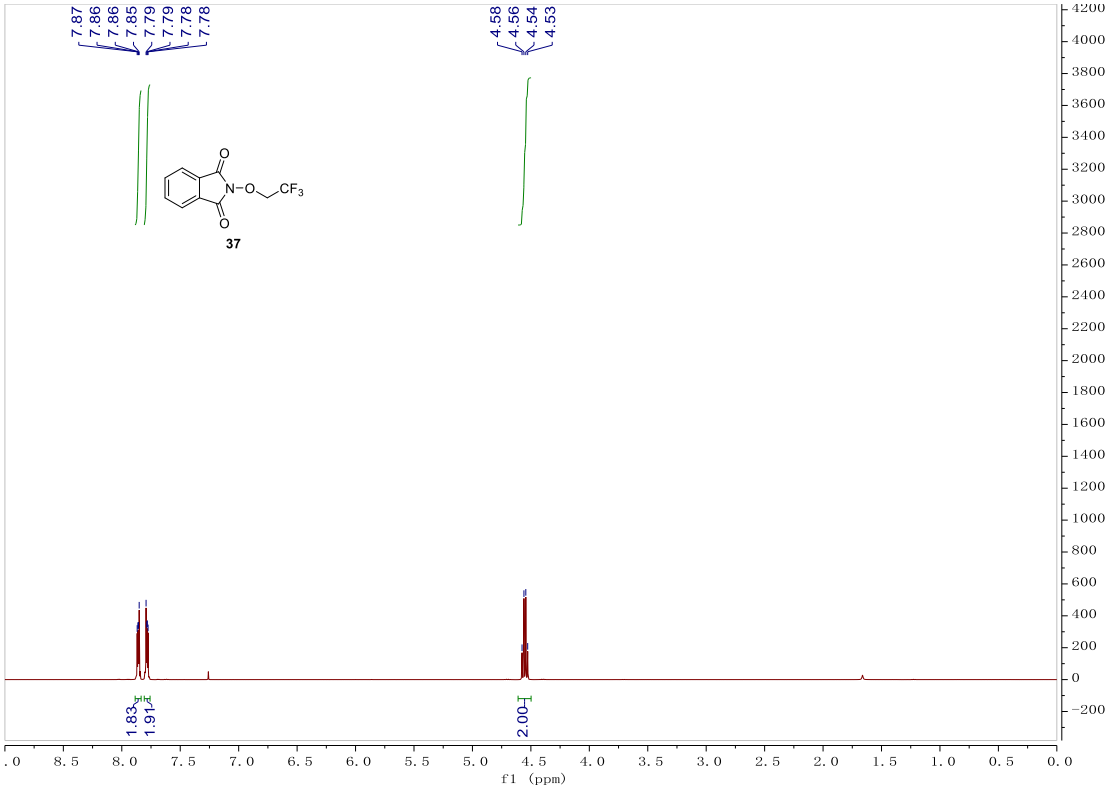

Figure S69. ^{1}H NMR (500 MHz, CDCl3) spectrum of compound 37, related to Scheme 2.

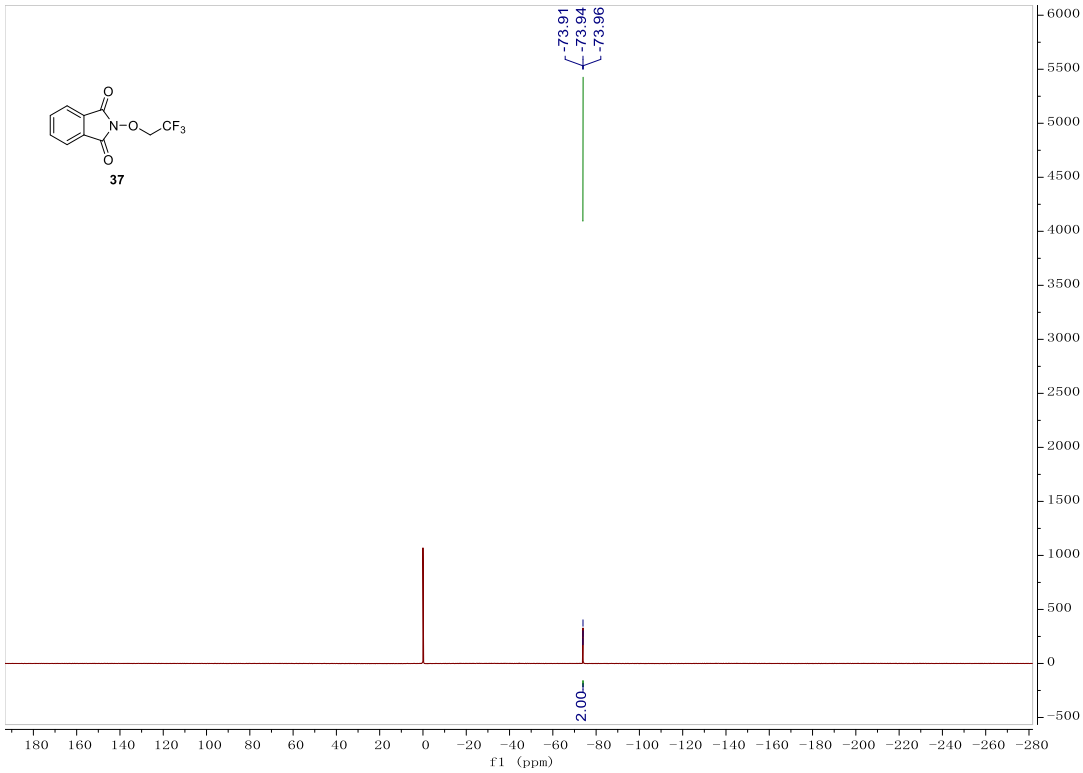

Figure S70. ^{13}C NMR (126 MHz, CDCl3) spectrum of compound 37, related to Scheme 2.

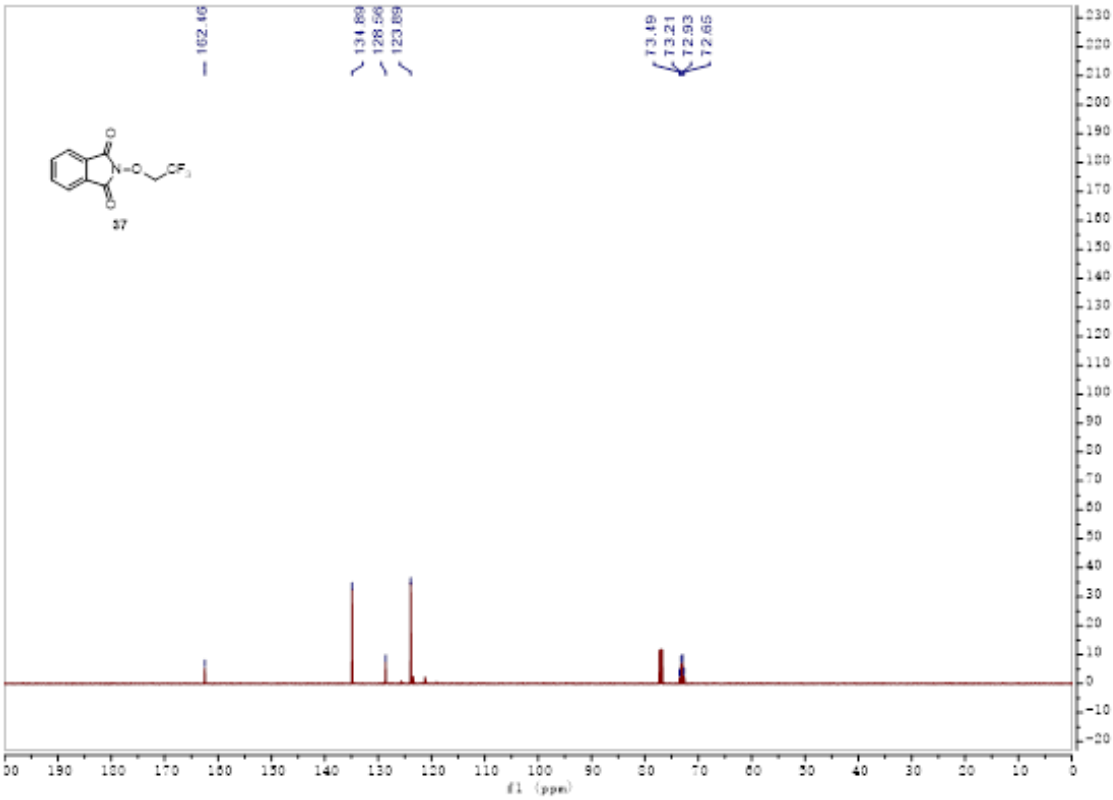

Figure S71. ^{19}F NMR (376 MHz, CDCl3) spectrum of compound 37, related to Scheme 2

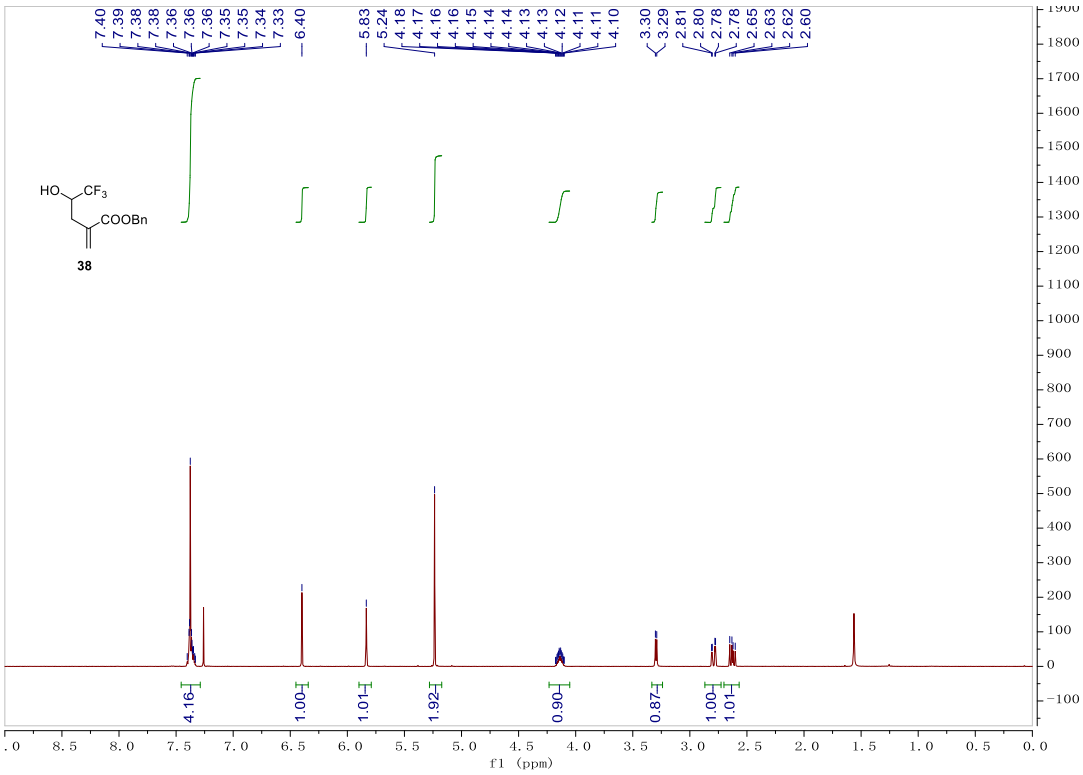

Figure S72. 1H NMR (500 MHz, CDCl3) spectrum of compound 38, related to Scheme 2.

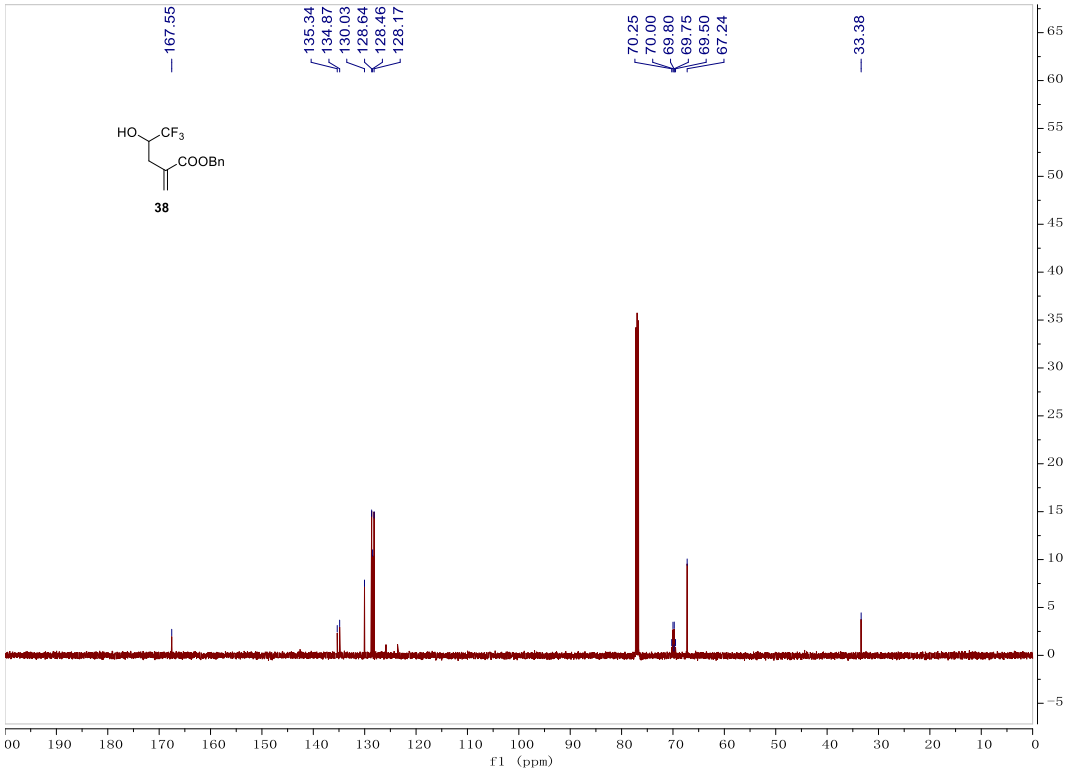

Figure S73. ^{13}C NMR (126 MHz, CDCl3) spectrum of compound 38, related to Scheme 2.

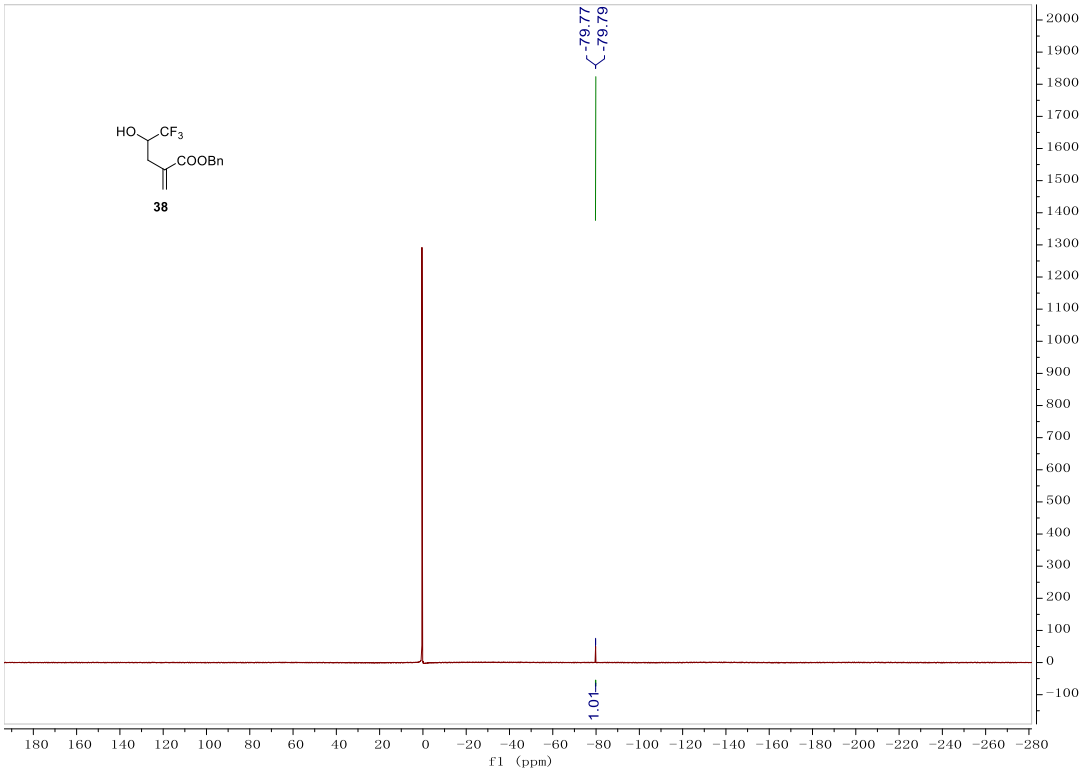

Figure S74. ^{19}F NMR (376 MHz, CDCl3) spectrum of compound 38, related to Scheme 2

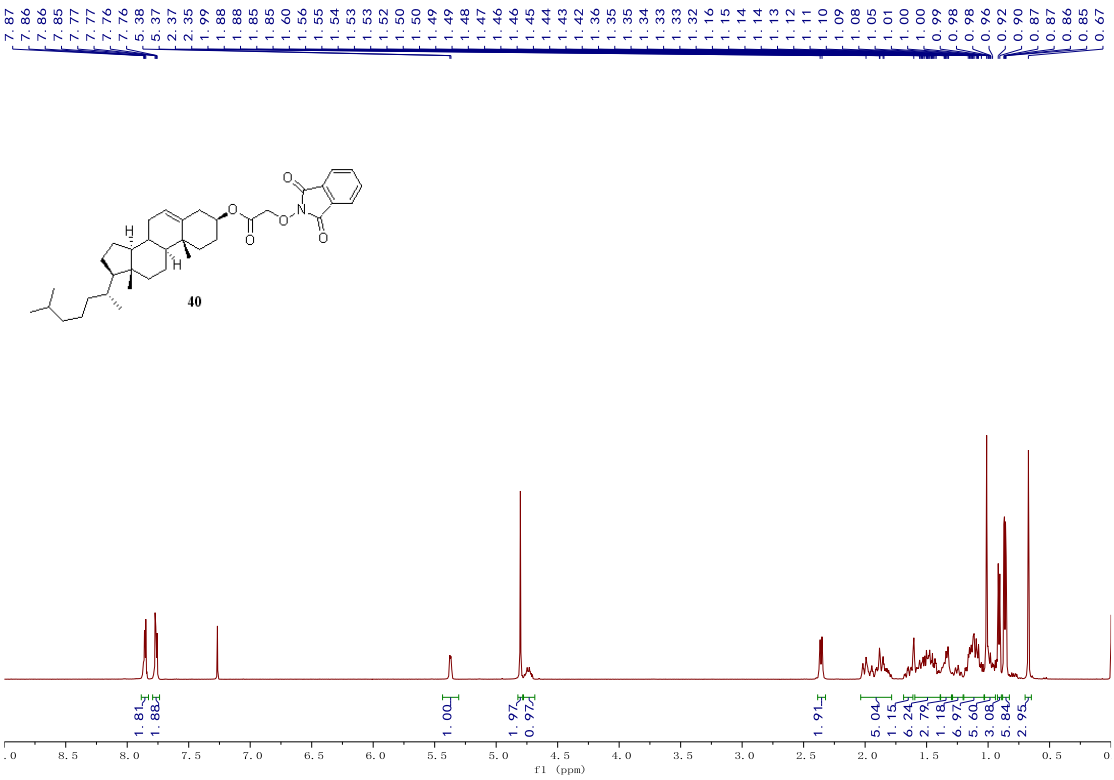

Figure S75. ^{1}H NMR (500 MHz, CDCl3) spectrum of compound 40, related to Scheme 2.

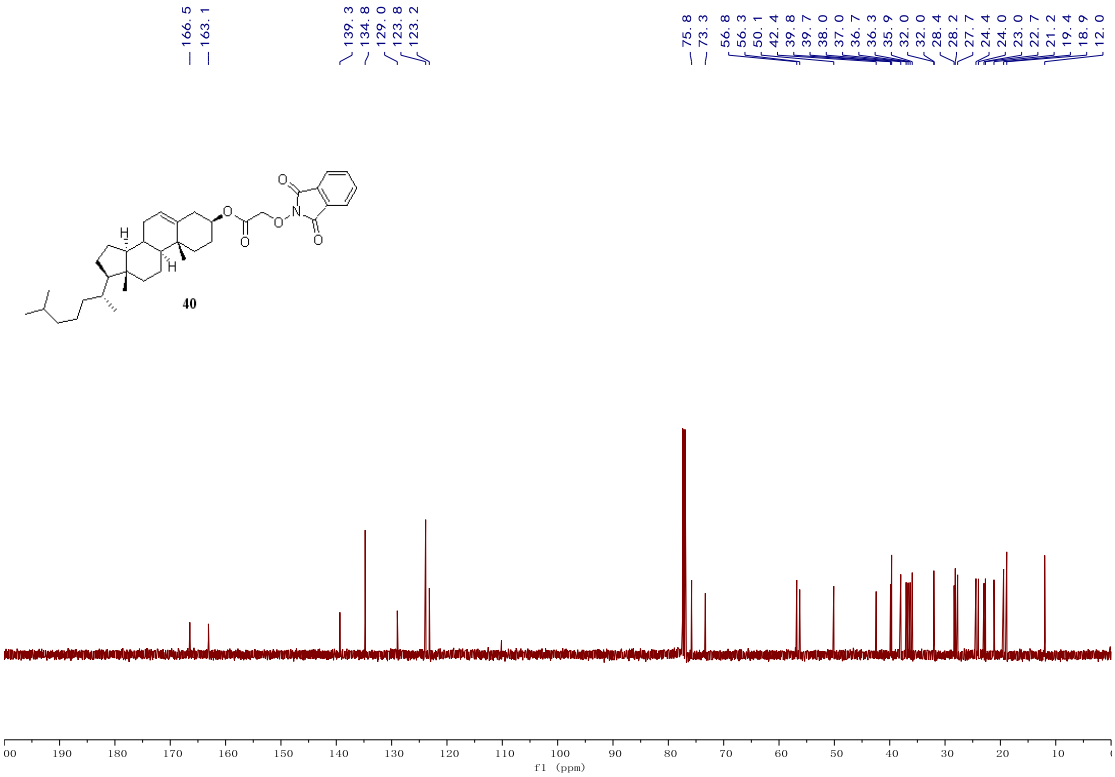

Figure S76. ^{13}C NMR (126 MHz, CDCl3) spectrum of compound 40, related to Scheme 2.

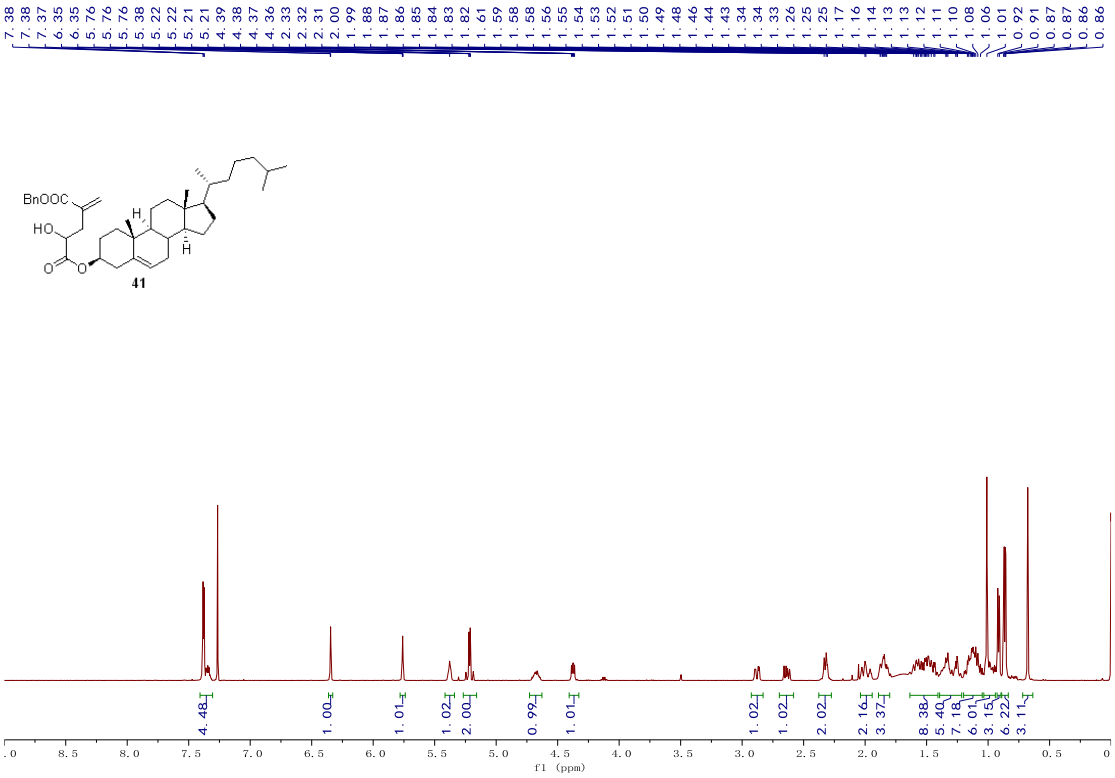

Figure S77. ^{1}H NMR (500 MHz, CDCl3) spectrum of compound 41, related to Scheme 2.

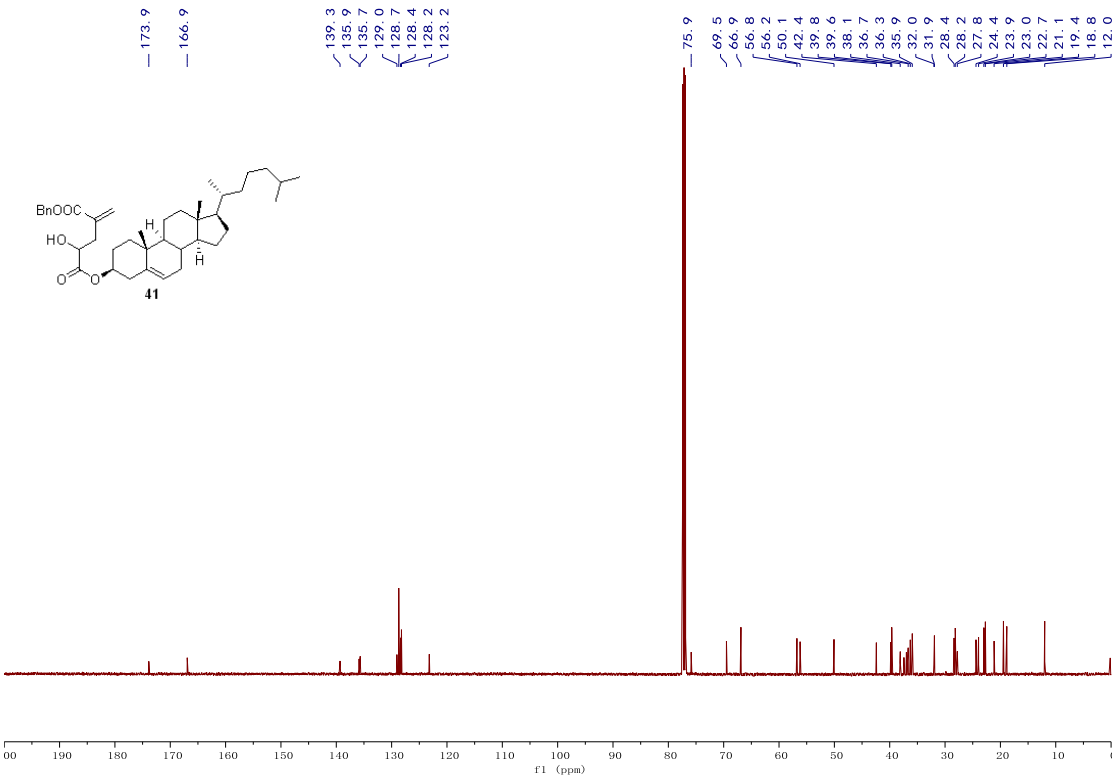

Figure S78. ^{13}C NMR (126 MHz, CDCl3) spectrum of compound 41, related to Scheme 2.

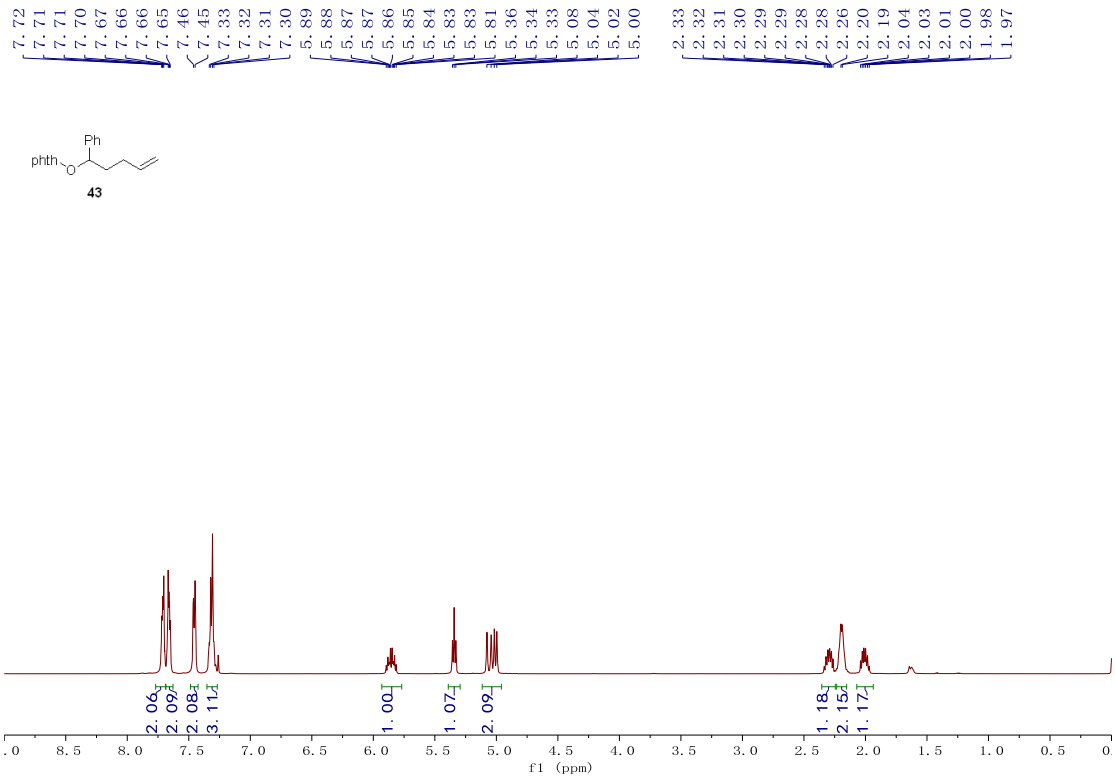

Figure S79. ^{1}H NMR (500 MHz, CDCl3) spectrum of compound 43, related to Scheme 3.

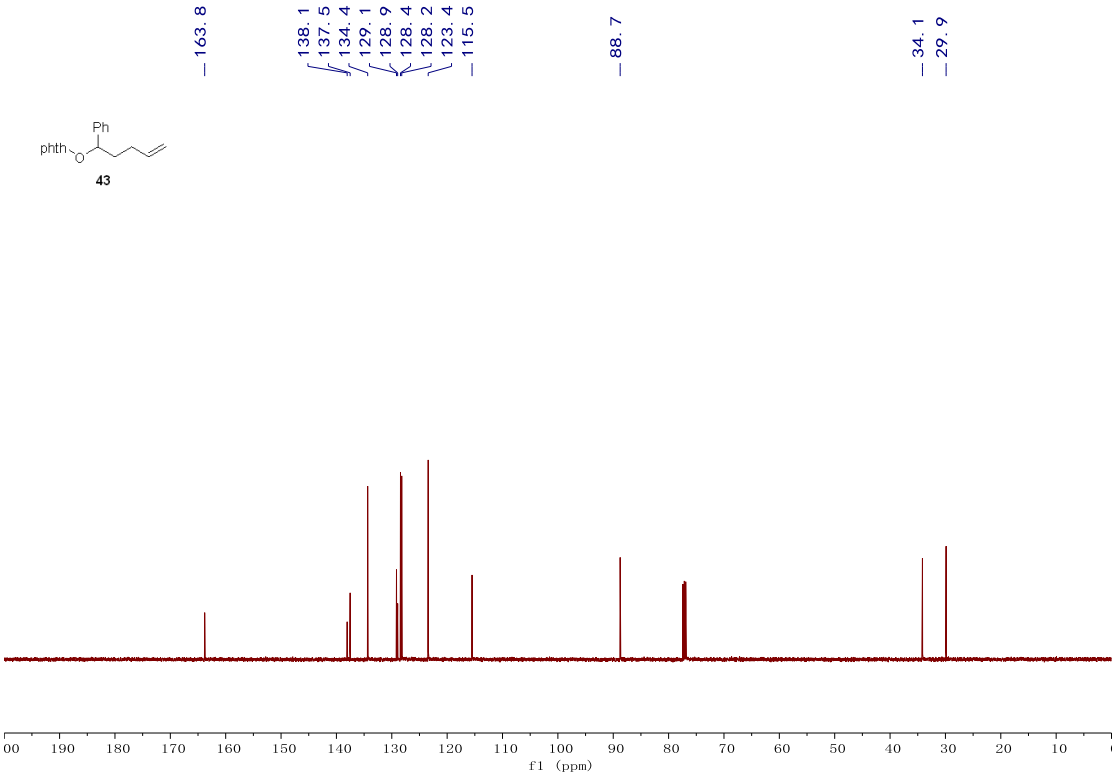

Figure S80. ^{13}C NMR (126 MHz, CDCl3) spectrum of compound 43, related to Scheme 2.

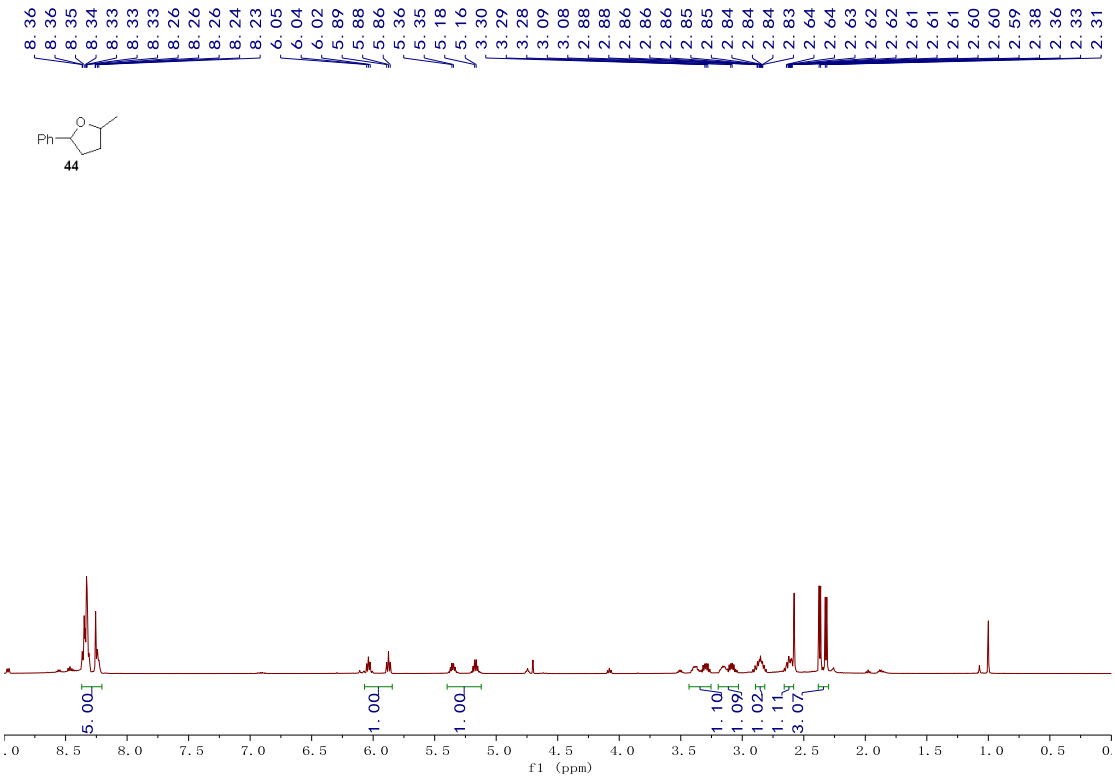

Figure S81. ^{1}H NMR (500 MHz, CDCl3) spectrum of compound 44, related to Scheme 3.

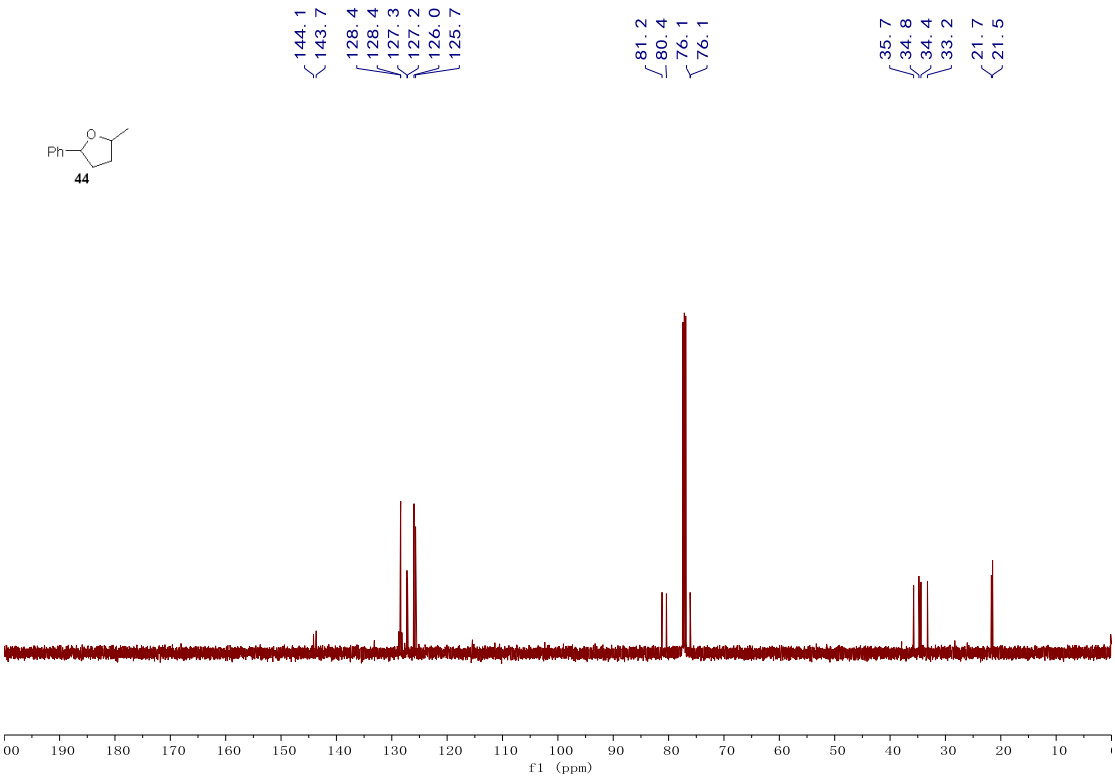

Figure S82. ^{13}C NMR (126 MHz, CDCl3) spectrum of compound 44, related to Scheme 3.

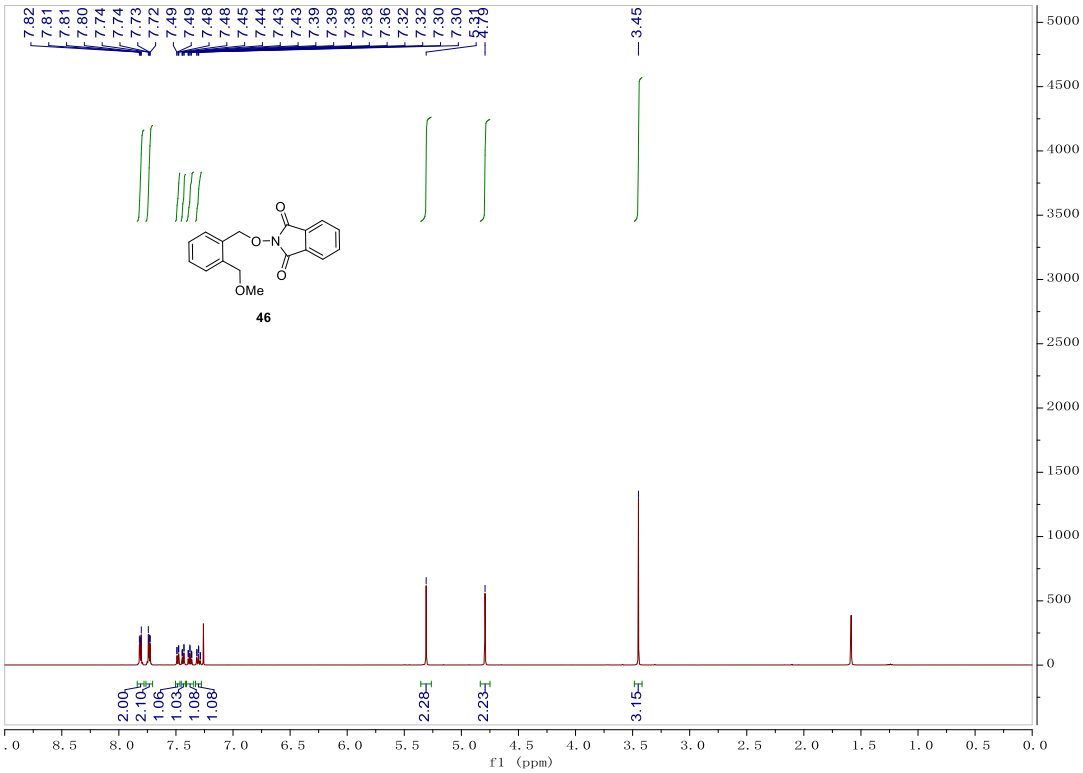

Figure S83. ^{1}H NMR (500 MHz, CDCl3) spectrum of compound 46, related to Scheme 3.

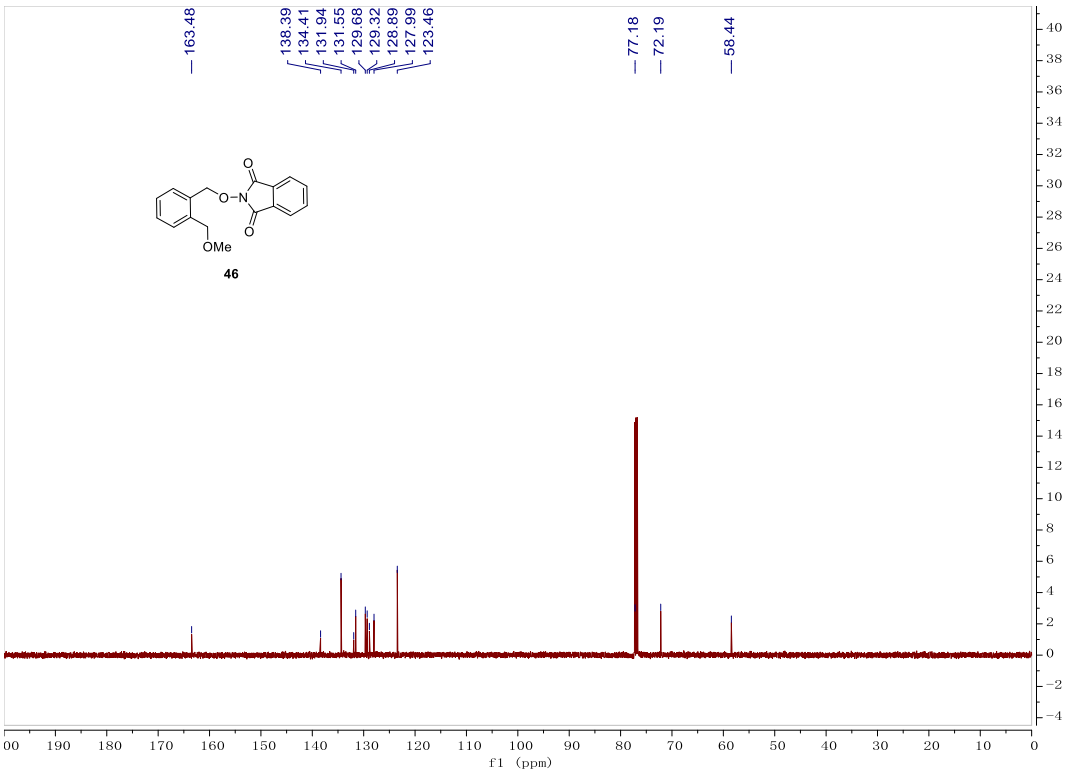

Figure S84. ^{13}C NMR (126 MHz, CDCl3) spectrum of compound 46, related to Scheme 3.

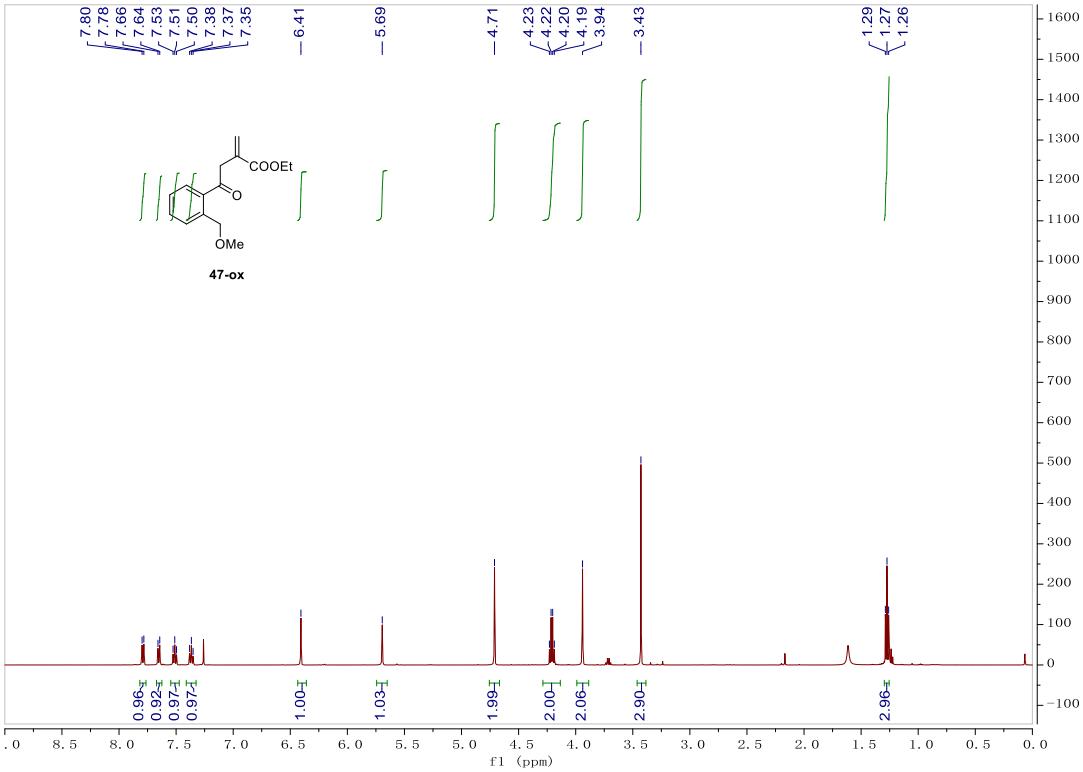

Figure S85. ^{1}H NMR (500 MHz, CDCl3) spectrum of compound 47-ox, related to Scheme 3.

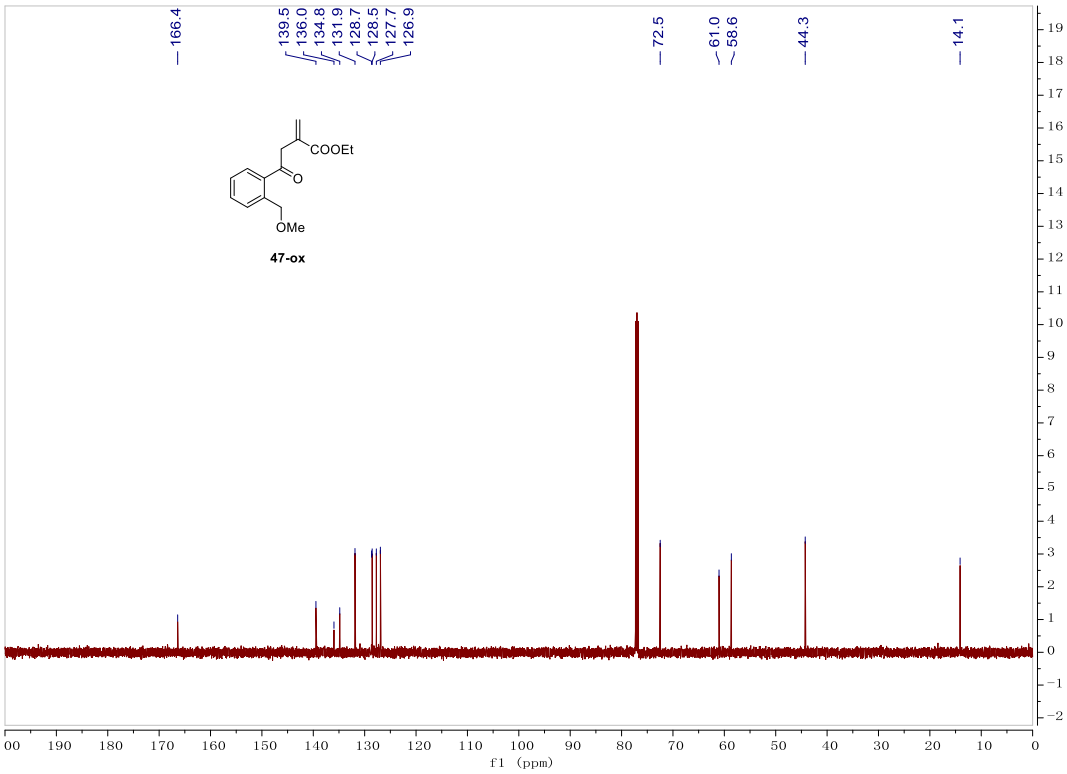

Figure S86. ^{13}C NMR (126 MHz, CDCl3) spectrum of compound 47-ox, related to Scheme 3.

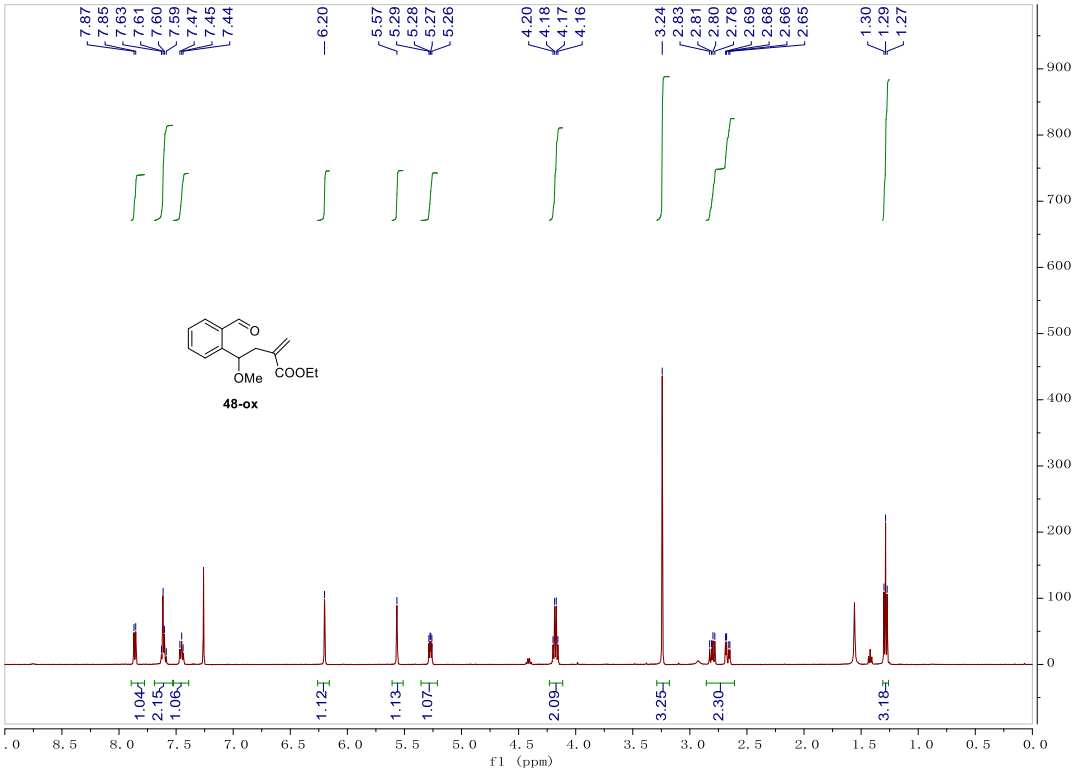

Figure S87. ^{1}H NMR (500 MHz, CDCl3) spectrum of compound 48-ox, related to Scheme 3.

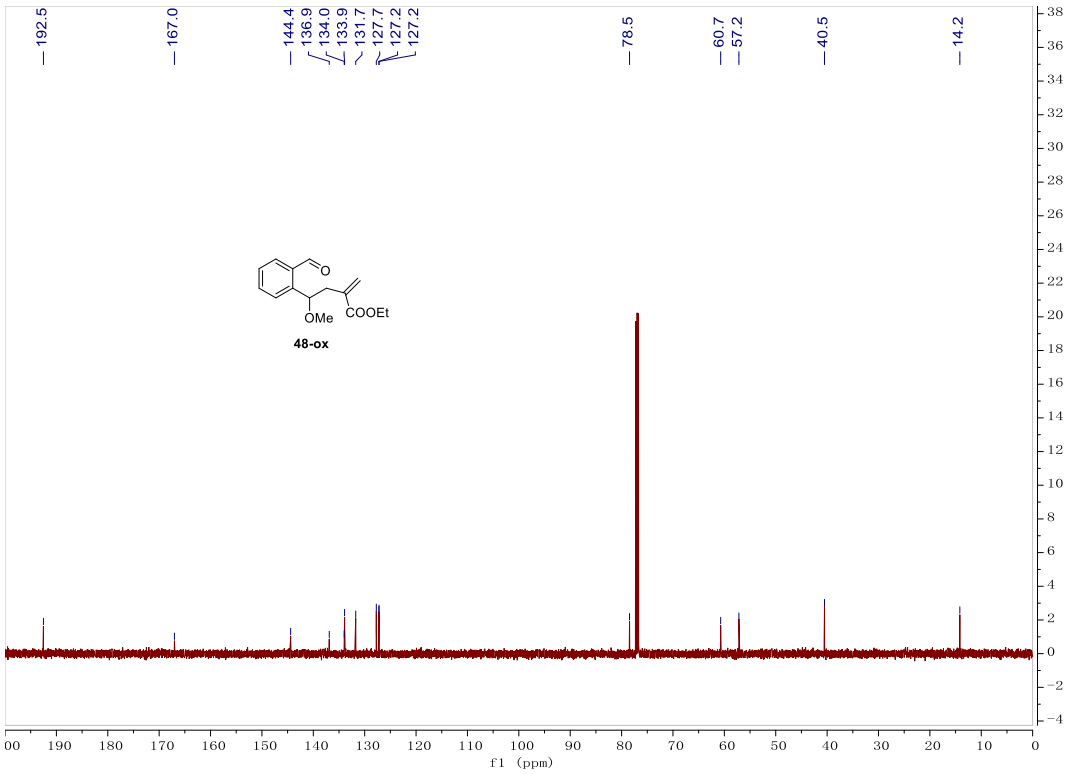

Figure S88. ^{13}C NMR (126 MHz, CDCl3) spectrum of compound 48-ox, related to Scheme 3.

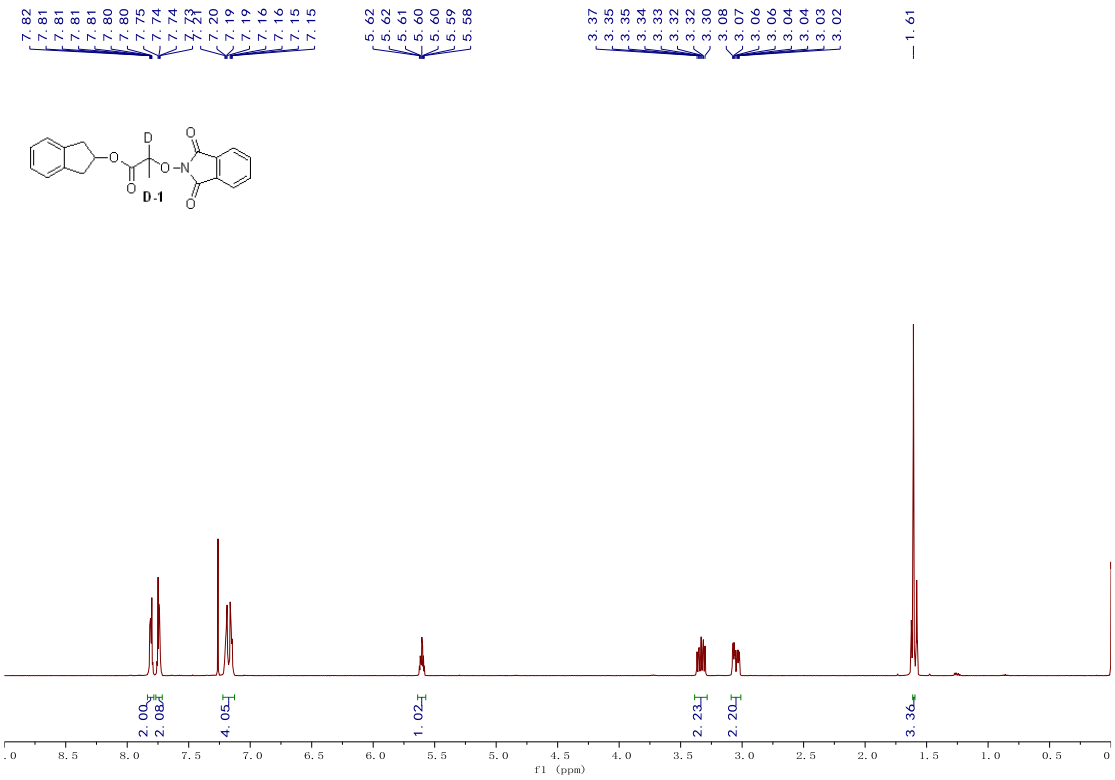

Figure S89. ^{1}H NMR (500 MHz, CDCl3) spectrum of compound D-1, related to Scheme 3.

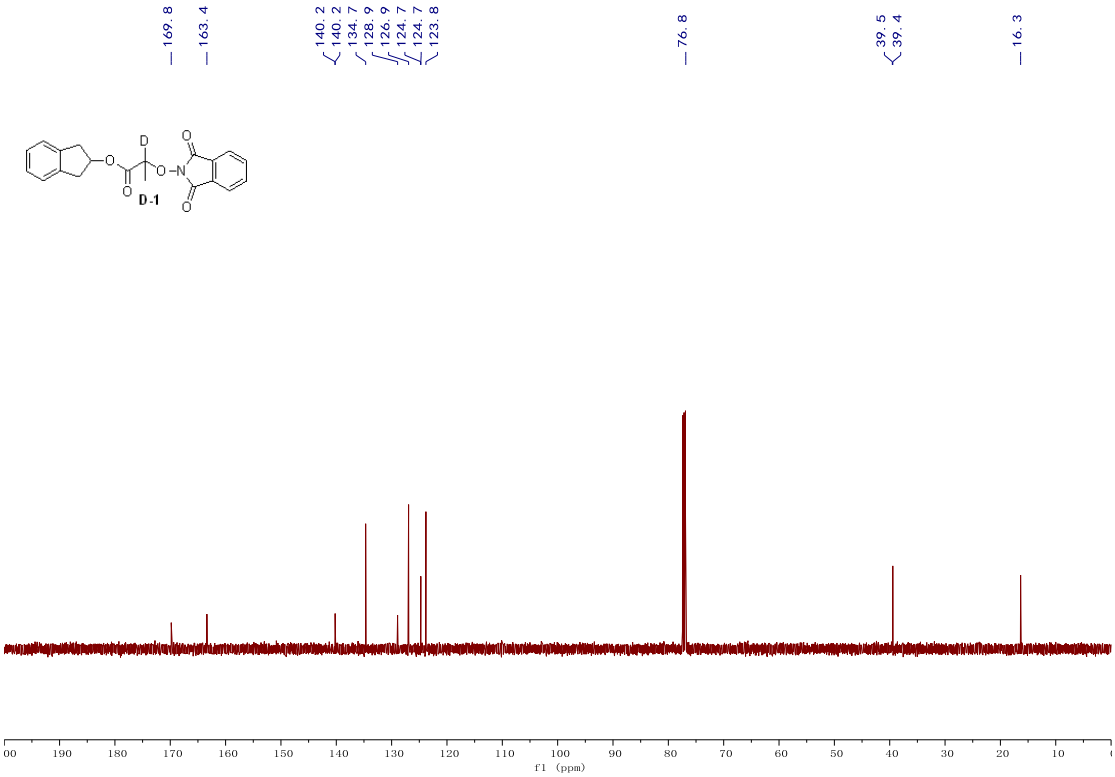

Figure S90. ^{13}C NMR (126 MHz, CDCl3) spectrum of compound D-1, related to Scheme 3.

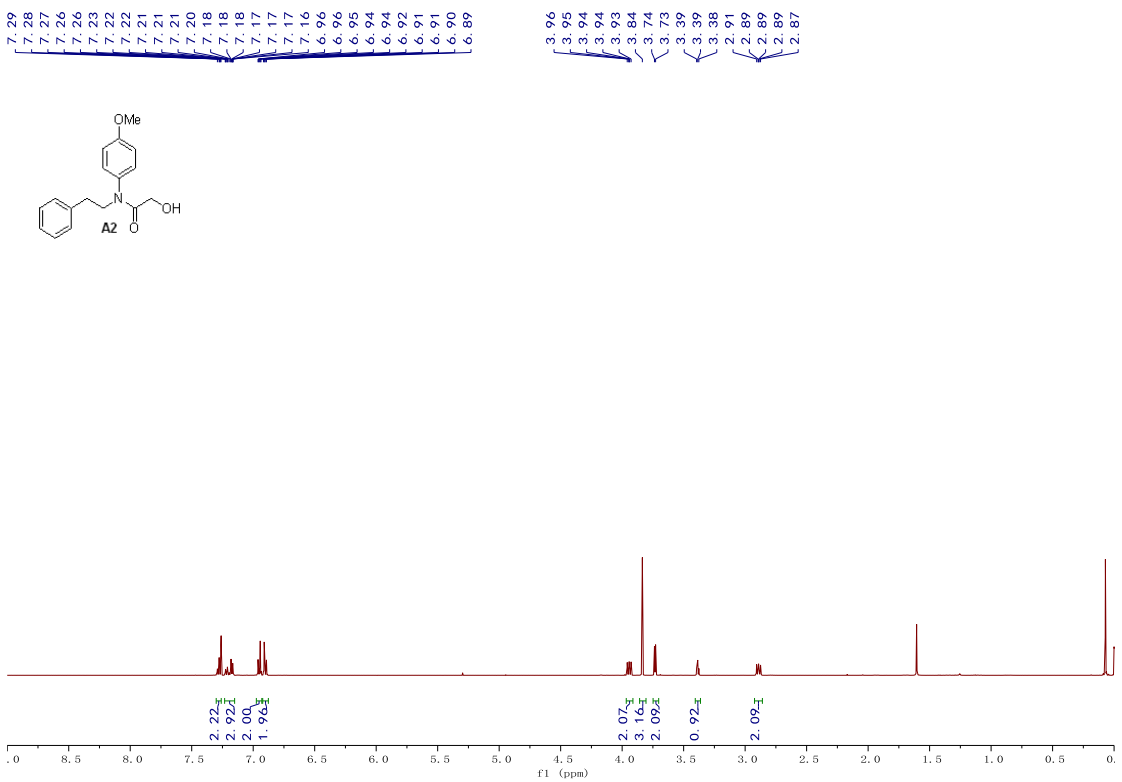

Figure S91. ^{1}H NMR (500 MHz, CDCl3) spectrum of compound A2, related to Scheme 2.

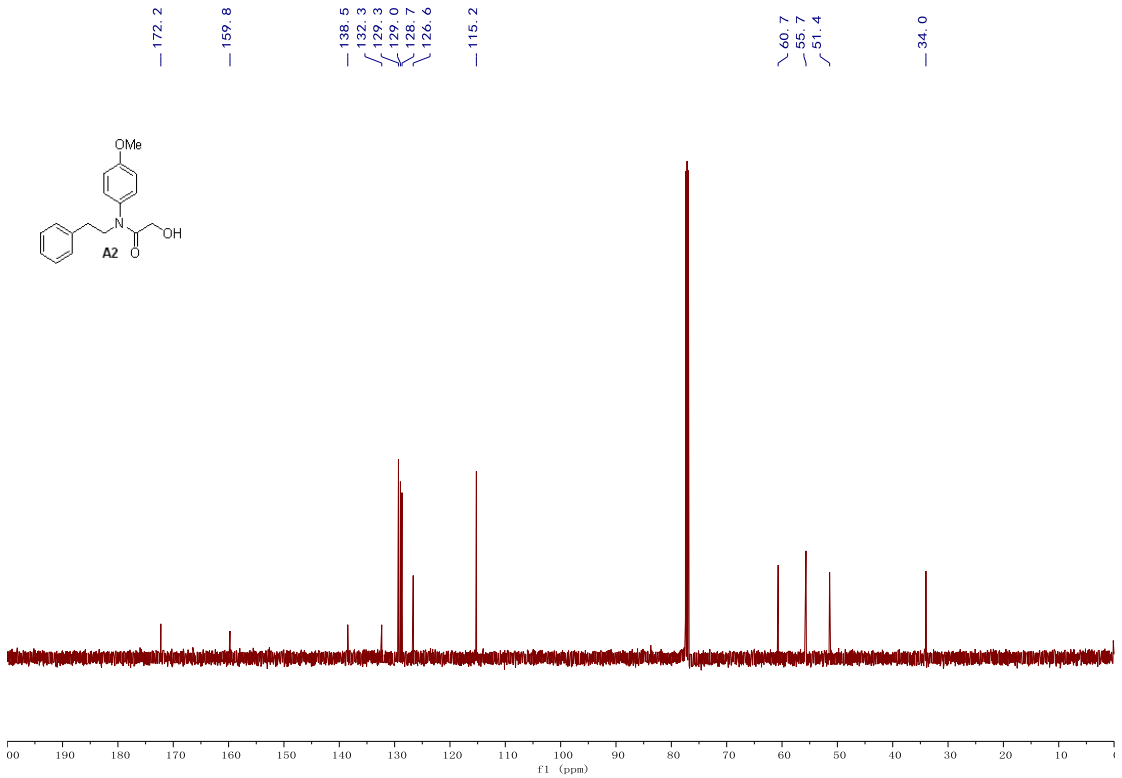

Figure S92. ^{13}C NMR (126 MHz, CDCl3) spectrum of compound A2, related to Scheme 2.

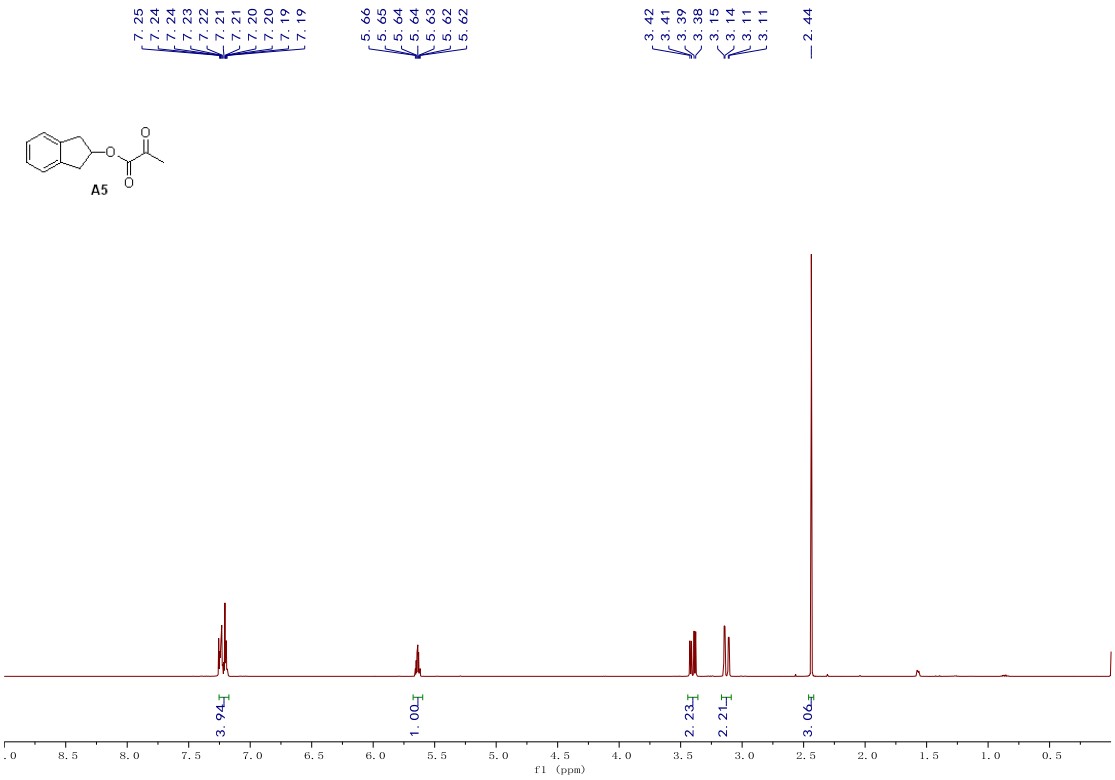

Figure S93. ^{1}H NMR (500 MHz, CDCl3) spectrum of compound A5, related to Scheme 2.

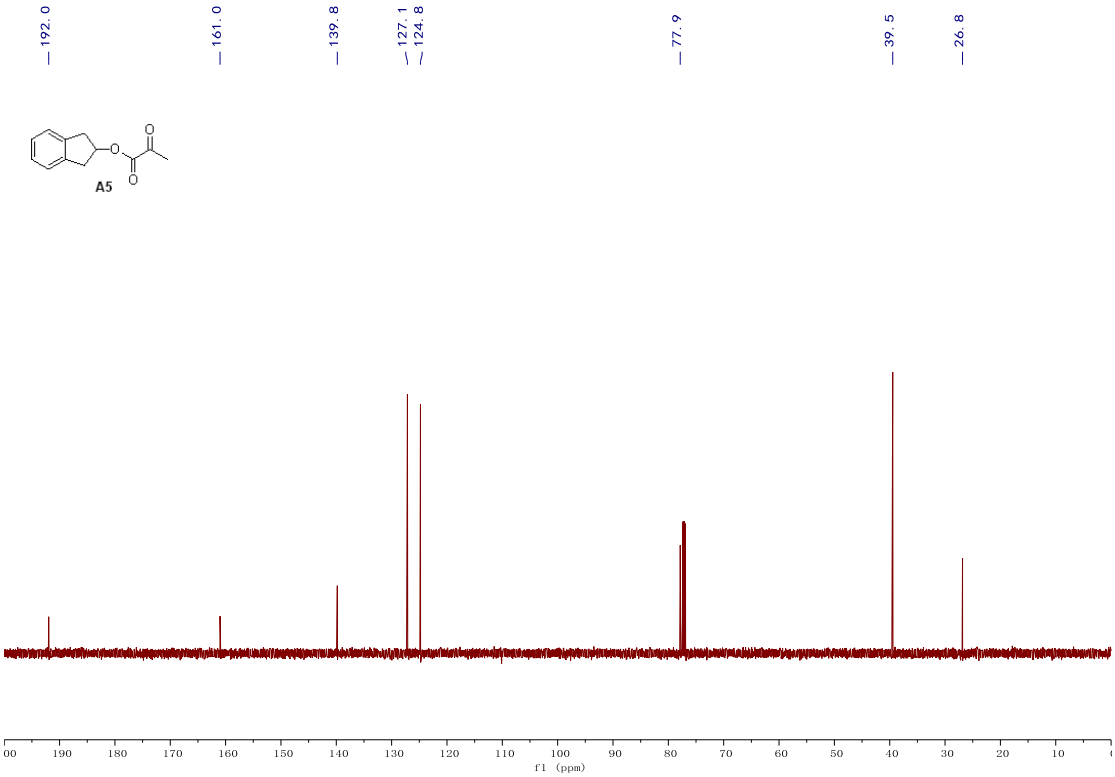

Figure S94. ^{13}C NMR (126 MHz, CDCl3) spectrum of compound A5, related to Scheme 2.

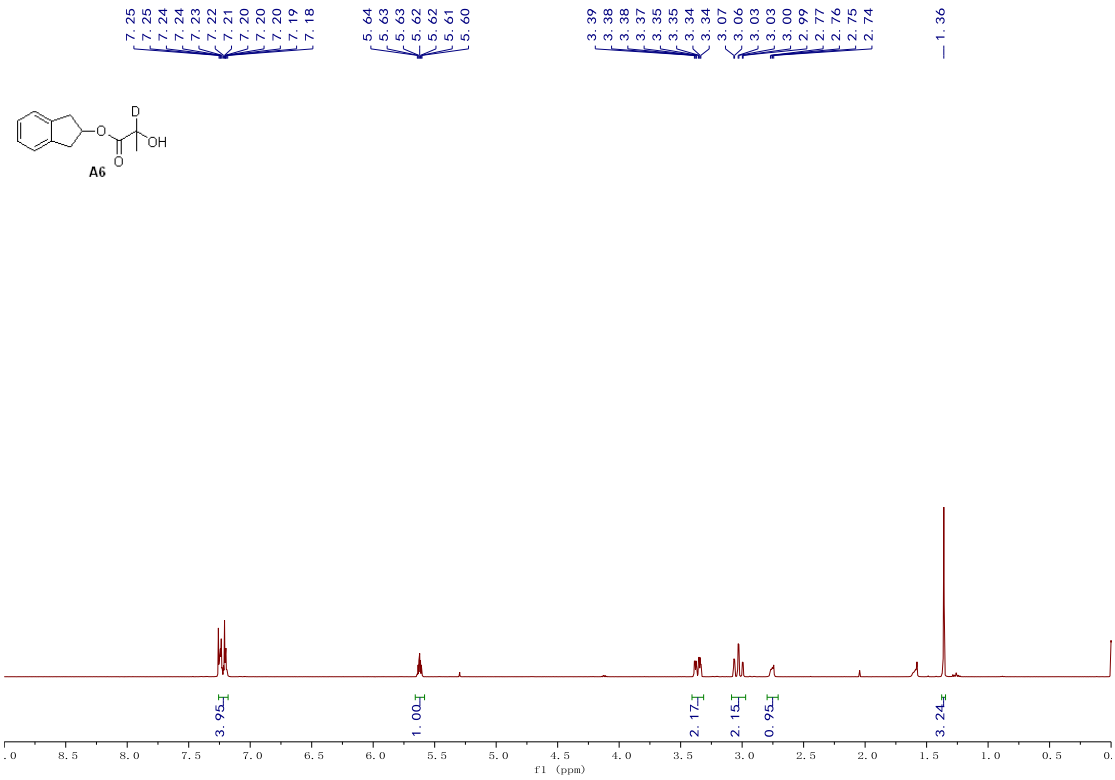

Figure S95. ^{1}H NMR (500 MHz, CDCl3) spectrum of compound A6, related to Scheme 3.

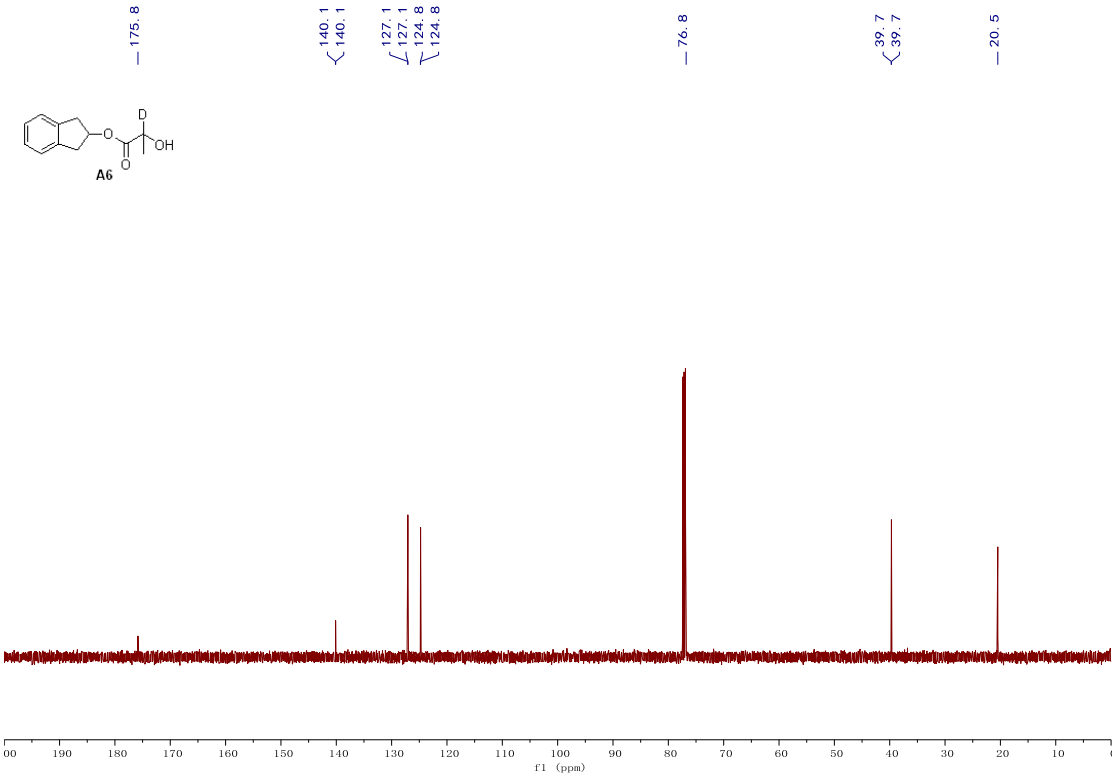

Figure S96. ^{13}C NMR (126 MHz, CDCl3) spectrum of compound A6, related to Scheme 3.

II. Mechanistic Investigations

The Cross-Over Experiment

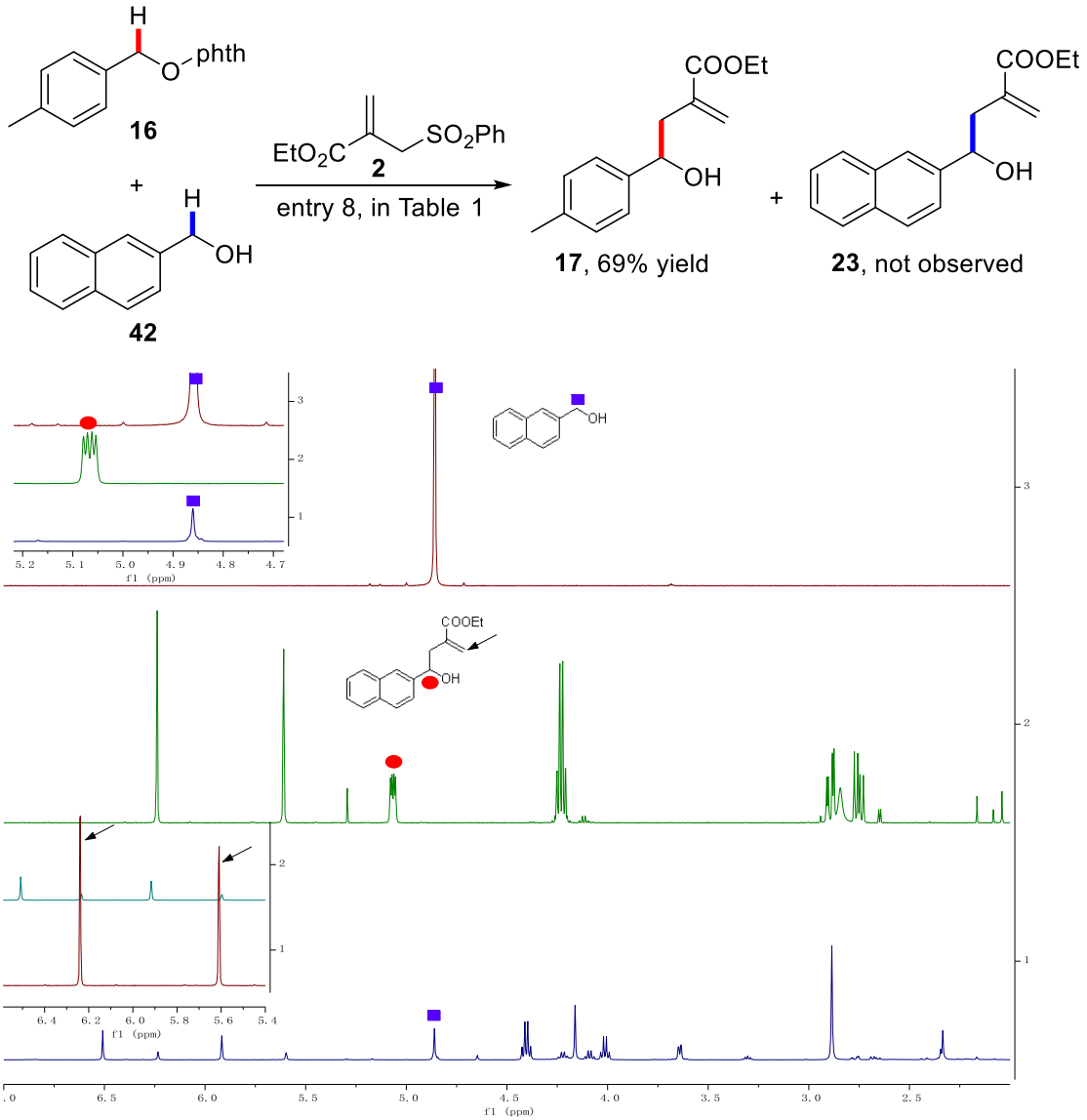

Scheme S1. The NMR spectra of the Cross-Over Experiment, Related to Scheme 3.

The allylation adduct **17** in 69% yield and no occurrence of **23** from crude NMR spectra.

KIE experiments

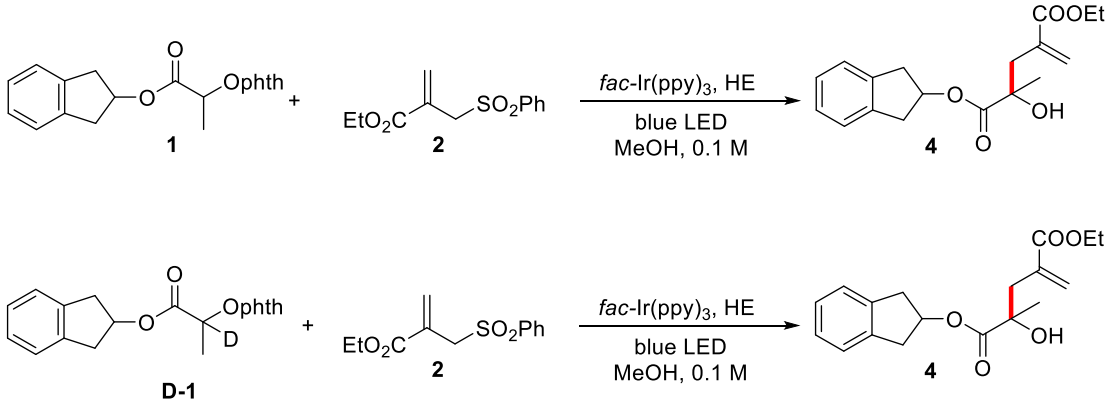

Reaction Time (min)	Yield of Sub **1** (%)	Yied of Sub **D-1** (%)
10	9	9
20	12	18
30	19	24
40	26	27

Table S1. The NMR Yield of the KIE Experiment, Related to Scheme 3.

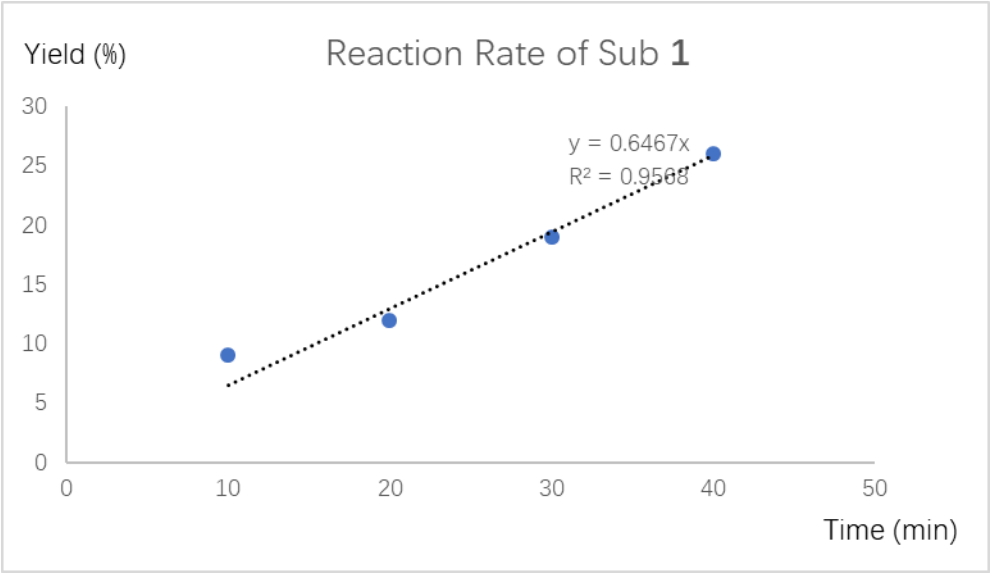

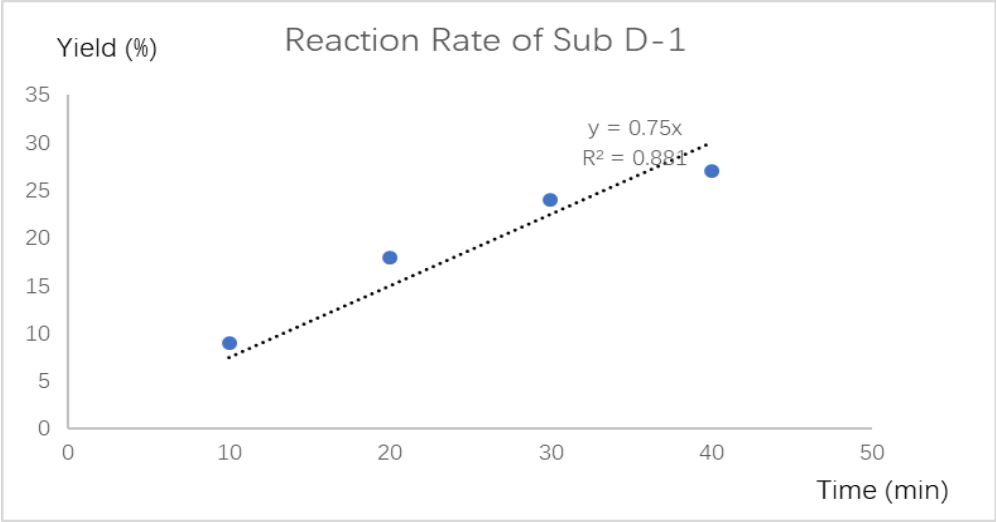

Scheme S2. Deuterium labeling experimtns, Related to Scheme 3.

The KIE value was calculated as K_H/K_D = 0.65/ 0.75 = 0.87, suggesting that the cleavage of the α-C(sp^3)-H bond was not the rate determining step.

1,2-HAT Competes with Other Alkoxyl Radical Reaction Pathways

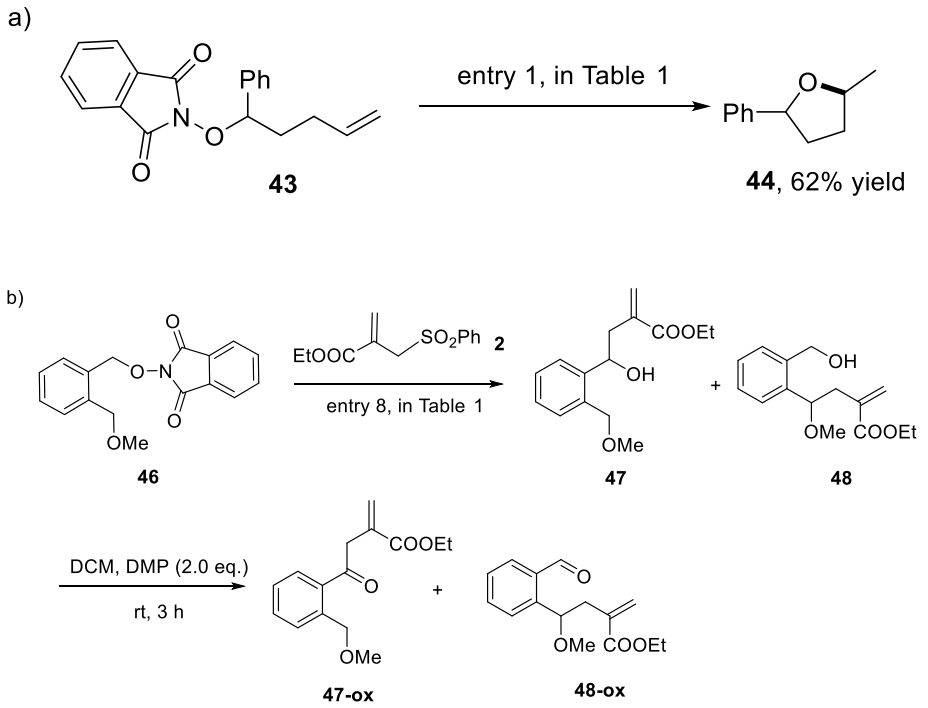

entry	conditions	conversion	NMR yield of 47	NMR yield of 48
1	Entry 8, in table 1	> 95 %	37%	14 %
2	Entry 1, in table 1	> 95 %	28 %	53 %

Scheme S3. 1,2-HAT Competes with 1,5-HAT, Related to Scheme 3.

Luminescence Quenching Experiments

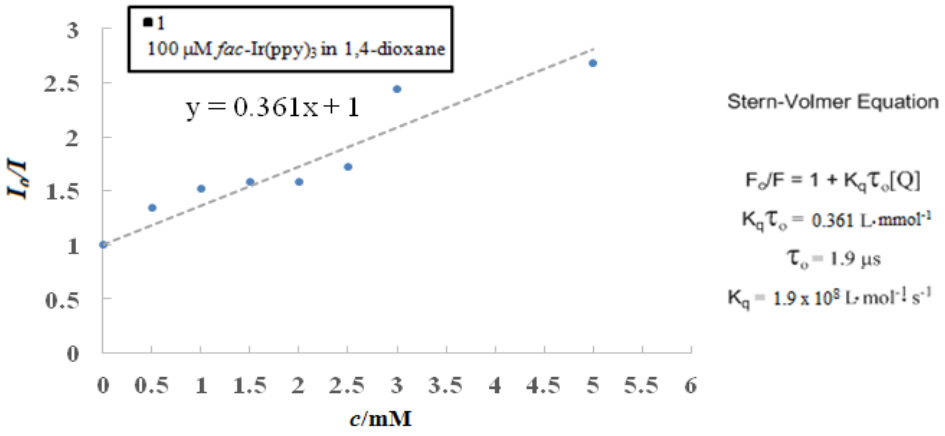

Scheme S4. *fac*-Ir(ppy)$_3$ Emission Quenching by *N*-alkoxyphthalimide 1, Related to Scheme 6.

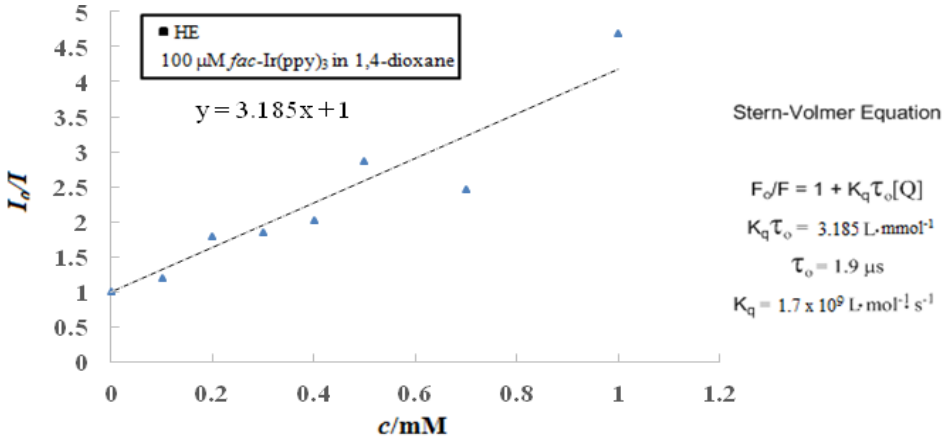

Scheme S5. *fac*-Ir(ppy)$_3$ Emission Quenching by Hanztsch Ester (HE), Related to Scheme 6.

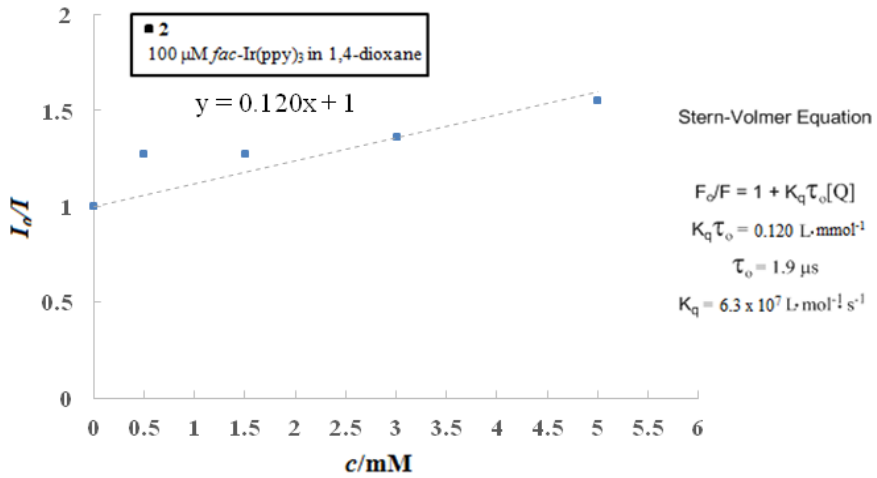

Scheme S6. *fac*-Ir(ppy)$_3$ Emission Quenching by Allyl Sulfone 2, Related to Scheme 6.

Cyclic Voltammetry Data

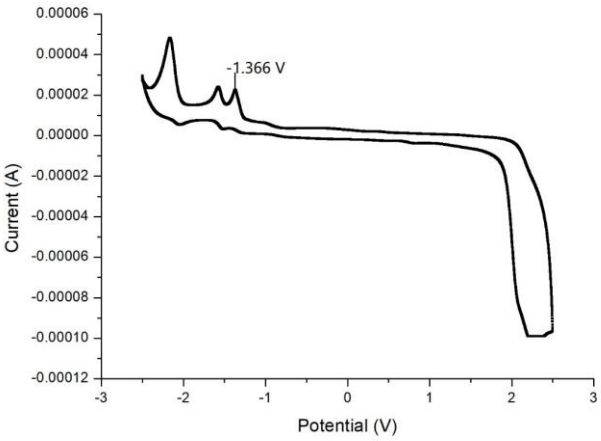

Scheme S7. Cyclic Voltammogram of *N*-alkoxyphthalimide 1, Related to Scheme 6.

$E_{1/2}^{red}$ (1) = -1.37 V vs. SCE in CH_3CN

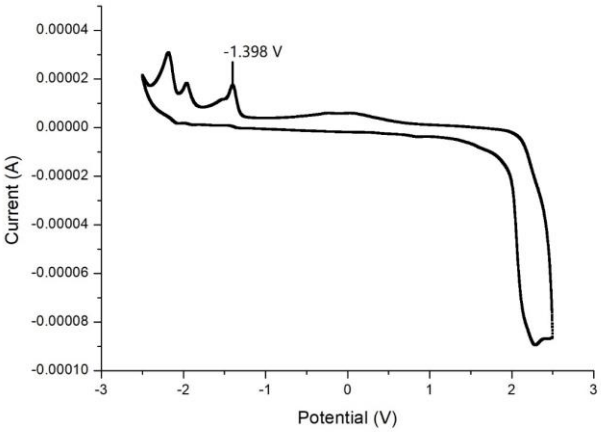

Scheme S8. Cyclic Voltammogram of *N*-alkoxyphthalimide 16, Related to Scheme 6.

$E_{1/2}^{red}$ (1) = -1.40 V vs. SCE in CH_3CN

The Quantum Yield Measurement

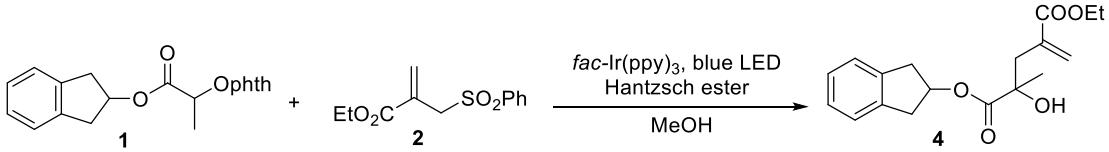

$$\Phi = \frac{N_{\text{prod}}}{N_{abs,\text{photon}}} = \frac{n_{\text{x}}}{n_{p}}$$

Scheme S9. The Quantum Yield Measurement, Related to Scheme 6.
The quantum yield is calculated to be 1.96.

The On-Off-Light Experiments

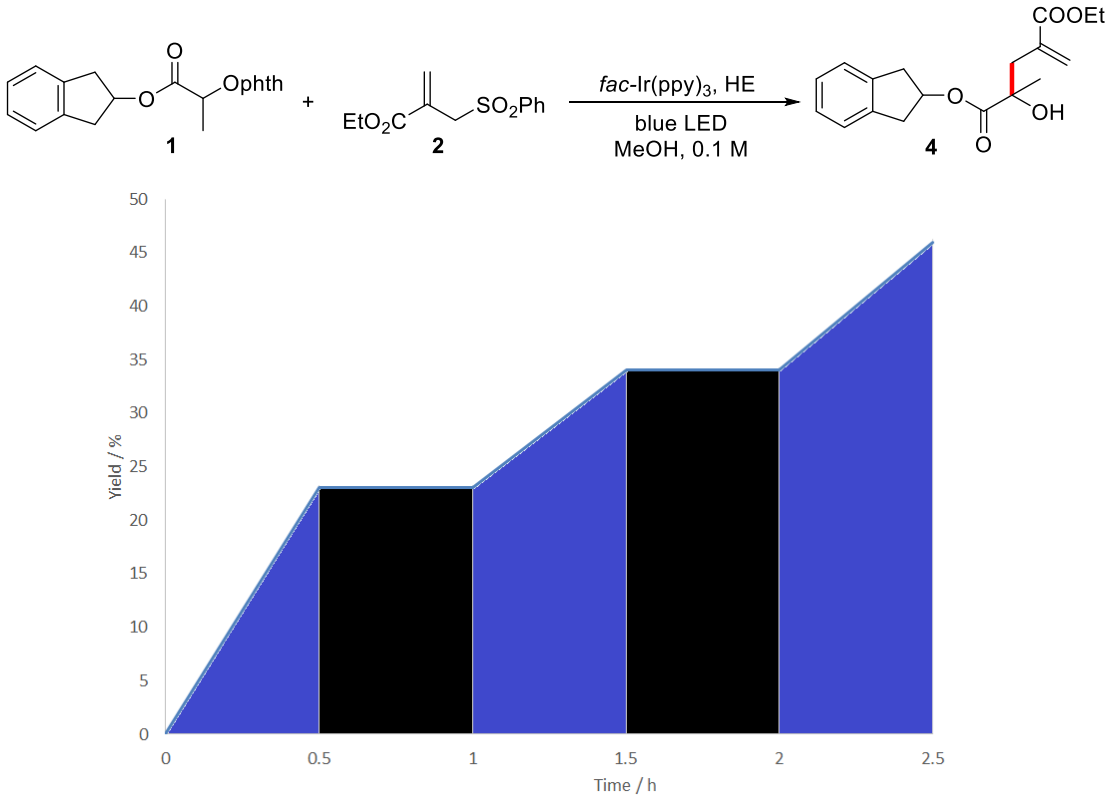

Scheme S10. The On-off-light Experiments, Related to Scheme 6.

The results suggest the radical chain may exist, however the chain length is short.

Detailed Reaction Optimizations

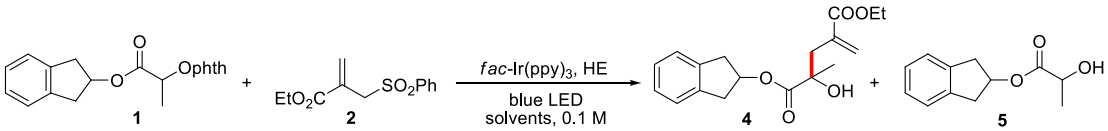

entry	conditions[a]	conversion	**4** yield (%)[b]	**5** yield (%)[b]
1	HE, 1,4-dioxane	>95%	41%	52%
2	entry 1, 0.05 M	>95%	36%	60%
3	entry 1, 0.2 M	>95%	49%	48%
4	entry 1, CH_3CN	>95%	37%	56%
5	entry 1, DCM	>95%	60%	33%
6	entry 1, EtOH	>95%	93%	7%
7	entry 1, MeOH	>95%	97%	<5%
8	entry 1, $CHCl_3$	>95%	66%	25%
9	entry 7, 0.05 M	>95%	89%	11%

[a]Reaction conditions: 1 (0.10 mmol, 1.0 equiv.), 2 (0.30 mmol, 3.0 equiv.), *fac*-Ir(ppy)$_3$ (0.001 mmol, 1%) and Hantzsch ester (0.15 mmol, 1.5 equiv.) in 1.0 mL solvent under nitrogen with 4 W blue LED irradiation at ambient temperature for 3 h, conversion was >95%, unless otherwise noted. [b]Conversion and yields were determined by ^{1}H NMR analysis and isolated yields were in parentheses. [c]Hantzsch ester (HE)

Table S2. Detailed Reaction Optimizations, Related to Table 1.

The Effect of Water Addition for the Reaction

entry	conditions	conversion[b]	**4** (%)[b]	**5** (%)[b]
1	ultra dry MeOH	>95%	>95%	<5%
2	ultra dry MeOH : H_2O = 9:1	>95%	93%	<5%
3	ultra dry MeOH : H_2O = 1:1	>95%	89%	9%
4	ultra dry 1,4-dioxane	>95%	29%	67%
5	ultra dry 1,4-dioxane : H_2O = 9:1	>95%	66%	33%
6	ultra dry 1,4-dioxane : H_2O = 1:1	>95%	76%	11%

[a]Reaction conditions: **1** (0.10 mmol), **2** (0.30 mmol), HE (0.15 mmol) in 1.0 mL solvents under nitrogen with 4 W blue LED irradiation at ambient temperature.
[b]Conversions and yields were determined by ^{1}H NMR analysis.

Table S3. The Effect of Water Addition, Related to Table 1.

EPR studies

The ketyl radical addition adduct **52** was found in MeOH. Instrumental parameters: ν = 9.37 GHz, modulation frequency = 100 kHz, modulation amplitude = 1.00 G, microwave power = 7.96 mW, conversion time = 58.59 ms, time constant = 0 ms, sweep time = 60 s. The hyperfine coupling constants determined after simulation correspond to an adduct DMPO-CH (a_N = 14.9 G and $a_{H\beta}$ = 21.1 G, g = 2.00538). The simulated EPR signals were obtained by Xepr software.

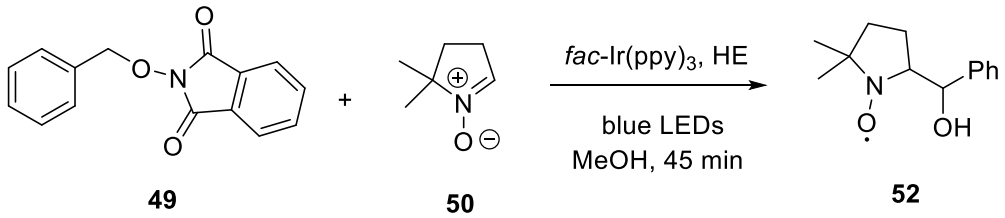

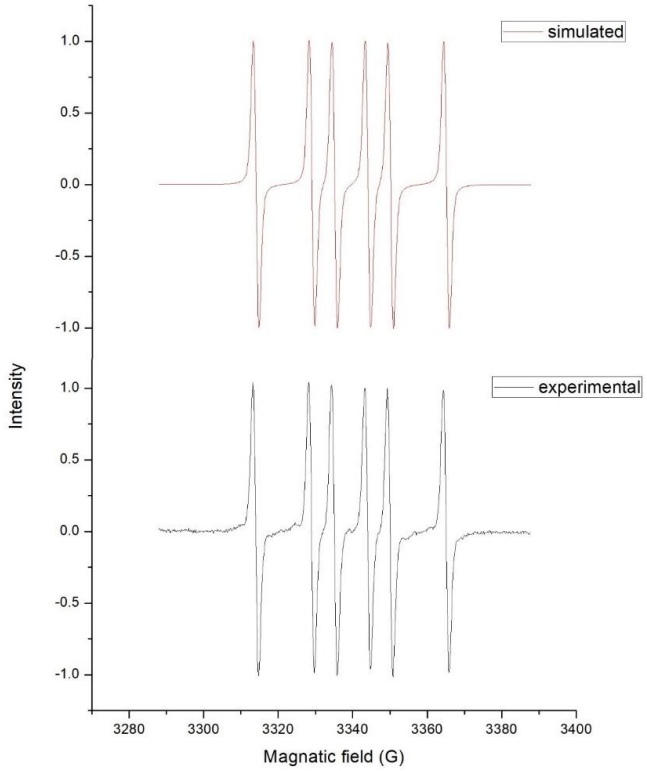

Scheme S11. EPR Spectrum of Spin Adducts in MeOH, Related to Scheme 4.

The alkoxyl radical and the ketyl radical addition adducts **51** and **52** were found in dioxane. Instrumental parameters: ν = 9.37 GHz, modulation frequency = 100 kHz, modulation amplitude = 1.00 G, microwave power = 0.50 mW, conversion time = 58.59 ms, time constant = 0 ms, sweep time = 60 s. The hyperfine coupling constants determined after simulation correspond to a mixture of adduct DMPO-OCH (a_N = 14.1 G and $a_{H\beta}$ = 9.6 G, g = 2.00585) and adduct DMPO-CH (a_N = 14.2 G, and $a_{H\beta}$ = 19.7 G, g = 2.00573). The asterisks peaks are assigned to the alkoxyl radical addition adduct **47**. The simulated EPR signals were obtained by Xepr software.

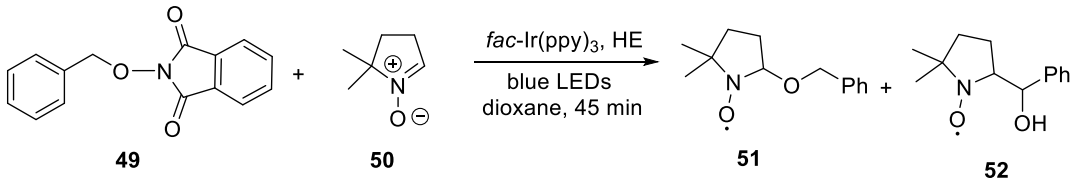

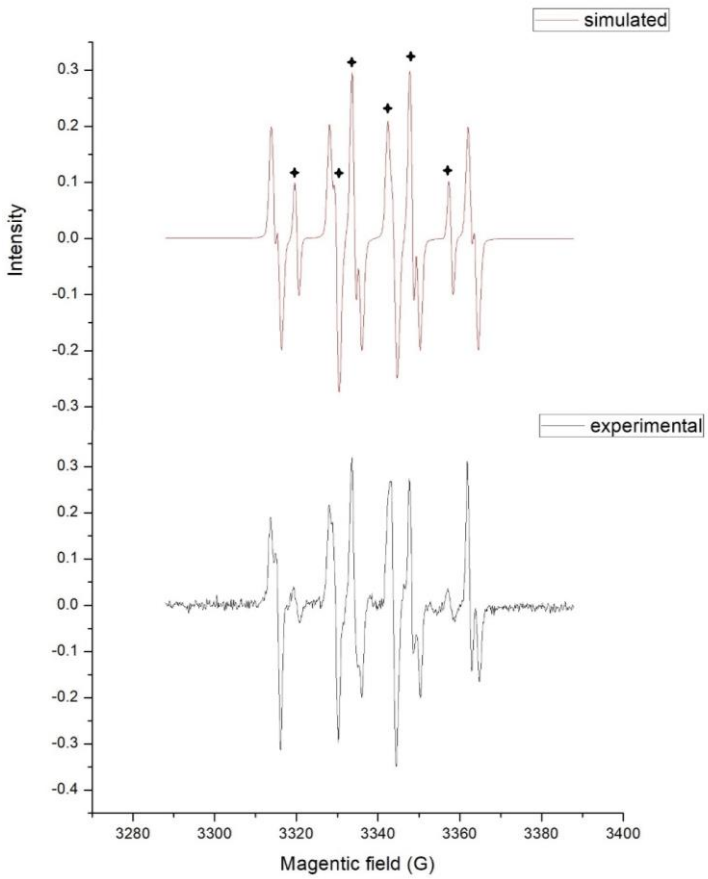

Scheme S12. EPR Spectrum of Spin Adducts in Dioxane, Related to Scheme 4.

The alkyl radical addition adduct **43-adduct** was found. Instrumental parameters: ν = 9.37 GHz, modulation frequency = 100 kHz, modulation amplitude = 1.00 G, microwave power = 7.96 mW, conversion time = 58.59 ms, time constant = 0 ms, sweep time = 60 s. The coupling constants of adduct DMPO-CH is a_N = 14.3 G and $a_{H\beta}$ = 20.1 G.

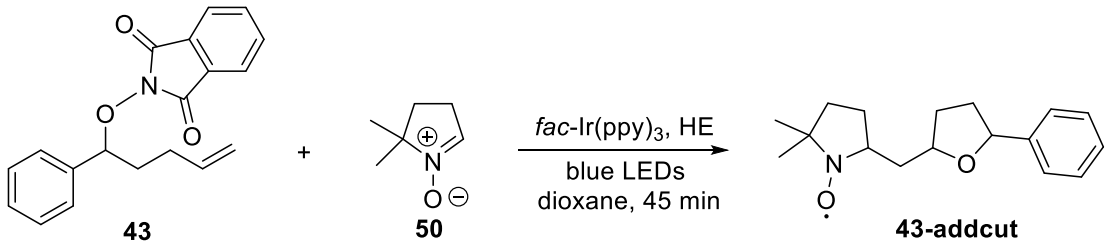

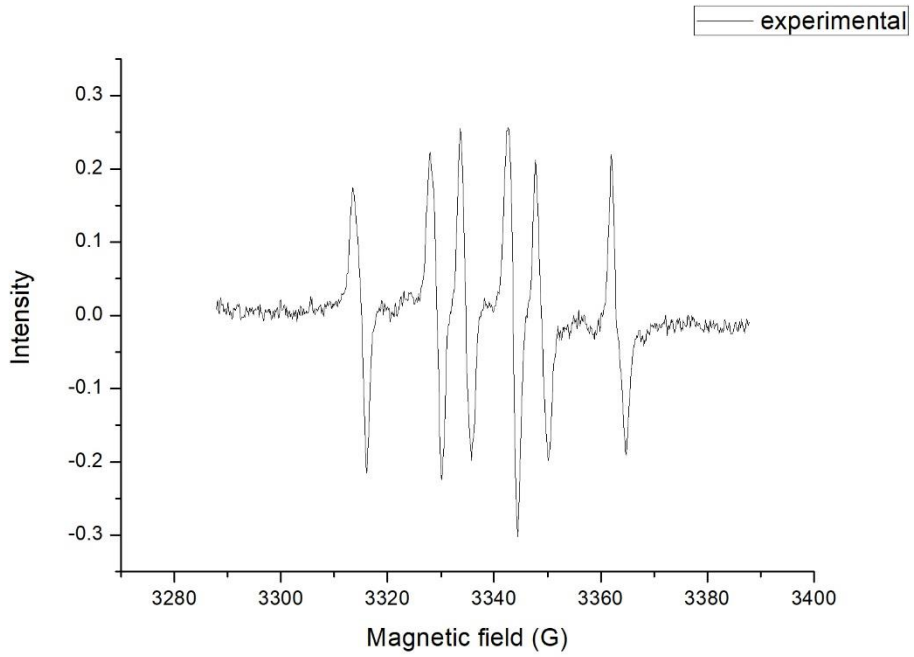

Scheme S13. EPR Spectrum of Spin Adduct in Dioxane, Related to Scheme 4.

DFT Calculation

Geometry	$E_{(elec\text{-}B3LYP)}$[1]	$H_{(corr\text{-}B3LYP)}$[2]	$G_{(corr\text{-}B3LYP)}$[3]	$E_{(solv\text{-}M11)}$[4]	IF[5]
CP1	-1203.234367	0.356076	0.279012	-1203.054513	-
$HE^{\cdot+}$	-862.231455	0.330610	0.258334	-862.095451	-
CP2	-1203.749639	0.369532	0.291021	-1203.493082	-
$E^{\cdot}$	-861.846357	0.316992	0.245785	-861.647058	-
TS1	-1203.725890	0.366709	0.287669	-1203.459777	-654.9
CP3	-690.707331	0.241721	0.184576	-690.528852	-
CP4	-513.047076	0.124823	0.083306	-512.948779	-
TS2	-690.660762	0.236711	0.179942	-690.499607	-2017.5
CP5	-690.748343	0.242768	0.186119	-690.583403	-
TS3	-1203.174837	0.352692	0.276452	-1202.988998	-338.5
CP6	-1203.206799	0.354285	0.277336	-1203.016213	-
TS4	-1203.198201	0.351380	0.275214	-1202.994127	-398.4
CP7	-690.167476	0.230970	0.174412	-690.007959	-
CP8	-513.070911	0.121791	0.079440	-513.072304	-
MeOH	-115.712204	0.055708	0.028753	-115.704694	-
TS5	-806.401221	0.294046	0.228819	-806.230046	-1206.9
TS6	-922.153016	0.352611	0.277625	-921.965704	-743.9
TS7	-1037.893693	0.410793	0.325078	-1037.684964	-752.6
TS8	-690.692319	0.240238	0.185178	-690.522421	-64.8
CP9	-690.700720	0.241164	0.185274	-690.530673	-
TS9	-690.690385	0.235426	0.179987	-690.521347	-1362.4
CP10	-690.718053	0.241179	0.183760	-690.557158	-

Table S4. B3LYP geometries for all the optimized compounds and transition states, Related to Scheme 5.

[1]The electronic energy calculated by B3LYP in gas phase.

[2]The thermal correction to enthalpy calculated by B3LYP in gas phase.

[3]The thermal correction to Gibbs free energy calculated by B3LYP in gas phase.

[4]The electronic energy calculated by M11 in methanol solvent.

[5]The B3LYP calculated imaginary frequencies for the transition states.

Table S5. B3LYP and M11 absolute calculation energies, enthalpies, and free energies, Related to Scheme 5.

The Gibbs free energy profiles for the MeOH/H_2O-assisted 1,2-HAT reaction are shown in Scheme S14. The direct hydrogen atom transfer to form the ketyl radical

CP5-1 was calculated to have 16.0 kcal/mol of activation barrier in **TS2-1** (red line). With one molecule of H_2O assisted (blue line), the activation barrier of the hydrogen atom transfer transition state **TS3-1** could be increased to be 16.2 kcal/mol. Significantly, one methanol and one H_2O molecules decrease the activation barrier to 6.9 kcal/mol in **TS4-1** (black line), while two methanol and one H_2O molecules can lower the activation barrier to 9.4 kcal/mol in **TS5-1** (purple line). The calculated results indicate that one methanol and one H_2O molecules decrease the activation barrier to merely 6.9 kcal/mol with multiple hydrogen bonds formation.

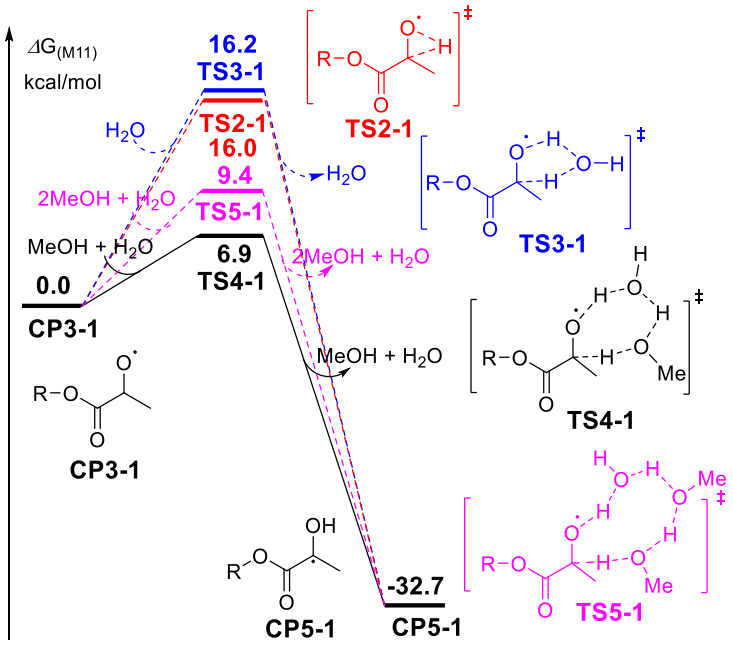

Scheme S14. Gibbs Free Energy Profiles for the MeOH/H_2O-assisted 1,2-HAT reaction, Related to Scheme 5.

Geometry	$E_{(elec\text{-}B3LYP)}$[1]	$H_{(corr\text{-}B3LYP)}$[2]	$G_{(corr\text{-}B3LYP)}$[3]	$E_{(solv\text{-}M11)}$[4]	IF[5]
CP3-1	-690.708645	0.241817	0.184734	-690.529933	-
TS2-1	-690.660762	0.236711	0.179942	-690.499607	-2017.5
TS3-1	-767.093055	0.262944	0.202253	-766.952305	-1363.3
H_2O	-76.407024	0.024920	0.002821	-76.433519	-
TS4-1	-882.849357	0.322367	0.252417	-882.693235	-746.6
MeOH	-115.712204	0.055708	0.028753	-115.704694	-
TS5-1	-998.589743	0.380337	0.299903	-998.412740	-748.4
CP5-1	-690.748343	0.242768	0.186119	-690.583403	-

Table S6 B3LYP and M11 absolute calculation energies, enthalpies, and free energies, Related to Scheme 5.

[1]The electronic energy calculated by B3LYP in gas phase.
[2]The thermal correction to enthalpy calculated by B3LYP in gas phase.
[3]The thermal correction to Gibbs free energy calculated by B3LYP in gas phase.
[4]The electronic energy calculated by M11 in methanol solvent.
[5]The B3LYP calculated imaginary frequencies for the transition states.

Table S7. B3LYP geometries for all the optimized compounds and transition states, Related to Scheme 5.

III. Transparant Methods:

General Procedures

Unless otherwise noted, all reactions of substrates preparation were conducted in flame-dried glassware under a nitrogen atmosphere using anhydrous solvent passed through an activated alumina column (Innovative Technology). Commercially available anhydrous MeOH was treated by 4 Å MS. Commercially available reagents were used without further purification. Hantzsch ester (HE) was recrystallized from ethanol and 1,4-dioxane was distilled over sodium. Thin layer chromatography (TLC) was performed using Jiangyou TLC silica gel plates HSG F_{254} and visualized using UV light, and potassium permanganate. Flash chromatography was performed on Lisure science EZ purification system using the Santai technologies silica gel cartridge. Preparative thin layer chromatography separations were carried out on 0.25 or 0.50 mm E. Merck silica gel plates (60F-254). Photochemical reactions were carried with 4.8 W blue LED (ZL-3036R) obtained from Beijing Jolly Lighting Engineering Co. Ltd. ^{1}H and ^{13}C NMR spectra were recorded in $CDCl_3$, unless otherwise noted, on a Bruker AV-400 MHz or an Agilent 500 MHz spectrometer. Chemical shifts in ^{1}H NMR spectra were reported in parts per million (ppm) on the δ scale from an internal standard of residual $CDCl_3$ (7.26 ppm). Data for ^{1}H NMR were reported as follows: chemical shift, multiplicity (s = singlet, d = doublet, t = triplet, q = quartet, m = multiplet), coupling constant in Herts (Hz) and integration. Data for ^{13}C NMR spectra were reported in terms of chemical shift in ppm from the central peak of $CDCl_3$ (77.16 ppm). IR spectra were recorded on a Thermo Scientific Nicolet 380 FT-IR spectrometer. MS experiments were performed on a Bruker maXis 4G instrument for HRMS-ESI, an Agilent 5973N instrument for EI-MS, and a Waters Micromass GCT Premier instrument for HRMS-EI. Cyclic Voltammetry was performed on a CH Instruments Electrochemical Workstation model CHI600E.

Synthesis of *N*-alkoxyphthalimide Precursors

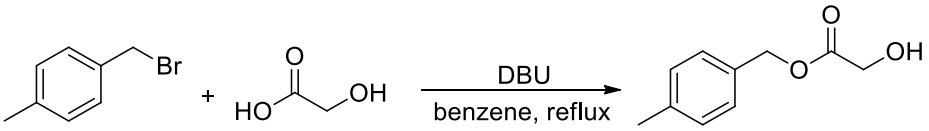

Scheme S15. Synthetic Procedure, Related to Scheme 2

To a solution of 4-methylbenzyl bromide (1.11 g, 6.0 mmol) and DBU (0.76 g, 5.0 mmol) in benzene (12 mL) was stirred for 15 min at room temperature. The reaction mixture was slowly added glycolic acid (0.38 g, 5.0 mmol) and refluxed for 6 hours. The resulting reaction mixture was extracted with 1 M aqueous HCl (2 x 20 mL). The organic layers were washed with brine, dried over anhydrous Na_2SO_4, and concentrated in vacuo. The crude product was purified by column chromatography on silica gel (20% hexanes/EtOAc) to give **A1** as a colorless oil.

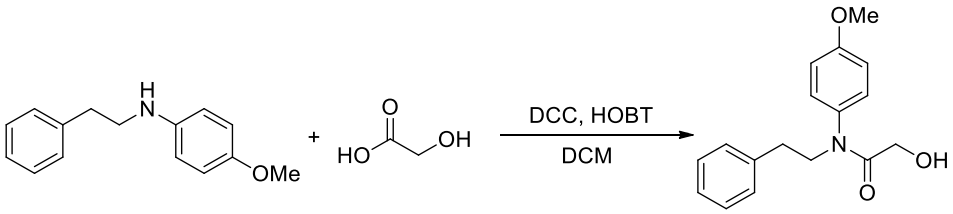

Scheme S16. Synthetic Procedure, Related to Scheme 2

To a solution of 4-methoxy-*N*-phenethylaniline (0.68 g, 3.0 mmol), glycolic acid (0.19 g, 2.5 mmol) and 1-hydroxybenzotriazole (0.68 g, 5.0 mmol) in DCM (10 mL) was added dicyclohexylcarbodiimide (0.78 g, 3.8 mmol) at 0 ^{o}C. The resulting suspension was filtered and the filtrate was concentrated in vacuo. The crude product was purified by column chromatography on silica gel (20% hexanes/EtOAc) to give **A2** as a colorless oil.

Synthesis of N-alkoxyphthalimide substrates

Method A

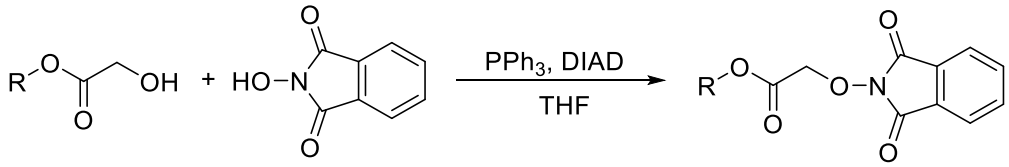

Scheme S17. Synthetic Procedure, Related to Scheme 2

To a solution of the alcohol (10.0 mmol), PPh_3 (3.15 g, 12.0 mmol), and N-hydroxyphthalimide (1.96 g, 12.0 mmol) in THF (30 mL) was added diisopropyl azodicarboxylate (2.4 mL, 12.0 mmol) over 10 min at room temperature. The resulting mixture was stirred for 3-24 h, taken up in EtOAc (20 mL), and washed with saturated $NaHCO_3$ (3 x 20 mL) and brine (2 x 30 mL). The organic layers were dried over anhydrous Na_2SO_4, concentrated in vacuo, and subjected to flash chromatography to afford the *N*-alkoxyphthalimides.

Method B

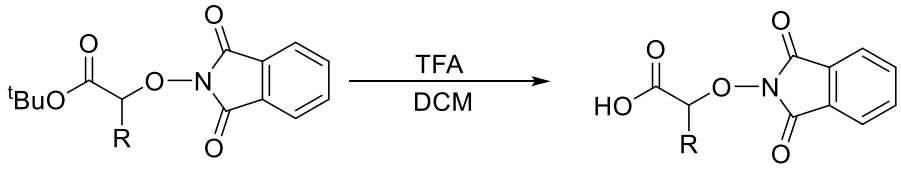

Scheme S18. Synthetic Procedure, Related to Scheme 2

To a solution of *N*-alkoxyphthalimides (33 mmol) in 110 mL DCM was slowly added TFA (37.0 mL, 495 mmol) at 0 ^{o}C. The reaction mixture was stirred at room temperature under N_2 for 2 hours. The reaction was then concentrated and azeotroped with DCM to afford *N*-alkoxyphthalimides and the crude product was directly subjected to the next reaction without further purification.

Method C

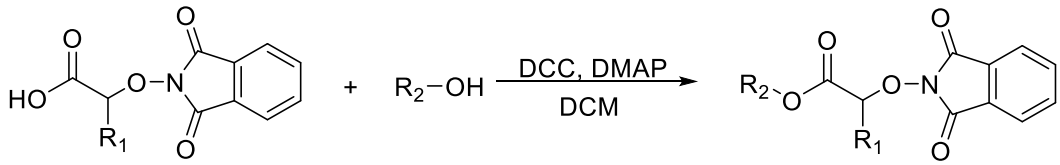

Scheme S19. Synthetic Procedure, Related to Scheme 2

To a solution of *N*-alkoxyphthalimides (1.5 mmol), alcohol (1.0 mmol) and DMAP (61.1 mg, 0.5 mmol) in 10 mL DCM was added N,N'-dicyclohexylcarbodiimide (0.31 g, 1.5 mmol) at 0 ^{o}C. The reaction mixture was stirred at 0 ^{o}C for 30 min and continued stirring at 25 ^{o}C overnight. The resulting suspension was filtered and the filtrate was concentrated in vacuo. Purification by column chromatography afforded the *N*-alkoxyphthalimides.

Method D

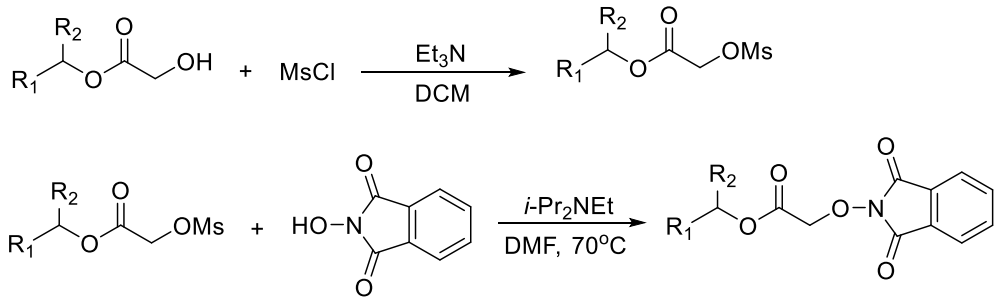

Scheme S20. Synthetic Procedure, Related to Scheme 2

To a solution of the alcohol (10 mmol) and Et_3N (2.2 mL, 16 mmol) in CH_2Cl_2 (30 mL) was added methanesulfonyl chloride (0.93 mL, 12 mmol) dropwise over 5 min at 0 °C. The reaction mixture was then allowed to warm to ambient temperature and stirred for 1 h. It was then washed with brine (3 x 30 mL). The organic layer was dried over Na_2SO_4, the solvent was removed by rotary evaporation to provide a yellow oil. The crude mesylate and directly mixed with N-hydroxyphthalimide (2.61 g, 16.0 mmol) and diisopropylethylamine (3.5 mL, 20 mmol) in DMF (20 mL). The resulting reaction mixture was stirred at 70 °C for 3 h and allowed to cool to room

temperature. The mixture was then taken up in Et_2O (50 mL), washed with sat. $NaHCO_3$ solution (3 x 25 mL), and brine (50 mL). It was then dried over Na_2SO_4, concentrated in vacuo, puried by column chromatography to afford the *N*-alkoxyphthalimides.

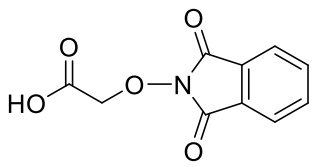

2-((1,3-dioxoisoindolin-2-yl)oxy)acetic acid (A3). Following the general method B, the reaction of *tert*-butyl 2-((1,3-dioxoisoindolin-2-yl)oxy)acetate (9.12 g, 33.0 mmol) afforded *N*-alkoxyphthalimides **A3** as a white solid (7.49 g, 100% yield) and the crude product was directly subjected to the next reaction without further purification.

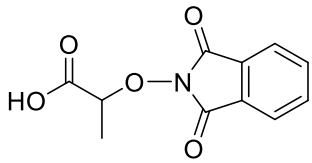

2-((1,3-dioxoisoindolin-2-yl)oxy)acetic acid (A4). Following the general method B, the reaction of *tert*-butyl 2-((1,3-dioxoisoindolin-2-yl)oxy)propanoate (6.89 g, 23.6 mmol) afforded *N*-alkoxyphthalimides **A4** as a white solid (5.54 g, 100% yield) and the crude product was directly subjected to the next reaction without further purification.

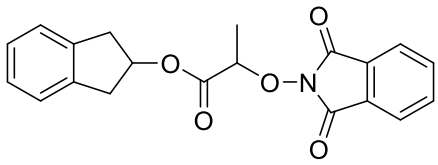

2,3-Dihydro-1*H*-inden-2-yl 2-((1,3-dioxoisoindolin-2-yl)oxy)propanoate (1). Following the general method C, the reaction of 2-indanol (1.34 g, 10.0mmol) afforded *N*-alkoxyphthalimides **1** as a white solid**.**

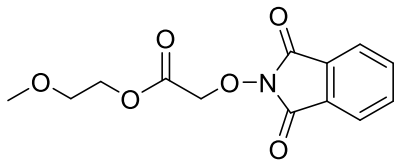

2-Methoxyethyl 2-((1,3-dioxoisoindolin-2-yl)oxy)acetate (6). Following the general method C, the reaction of 2-methoxyethanol (0.23 g, 3.0 mmol) afforded N-alkoxyphthalimides **6** as a white solid.

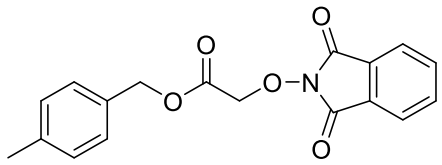

4-Methylbenzyl 2-((1,3-dioxoisoindolin-2-yl)oxy)acetate (8). Following the general method D, the reaction of **A1** (0.62 g, 3.5 mmol) afforded *N*-alkoxyphthalimides **8** as a white solid**.**

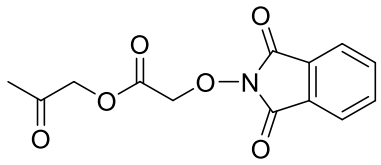

2-Oxopropyl 2-((1,3-dioxoisoindolin-2-yl)oxy)acetate (10). Following the general method C, the reaction of hydroxyacetone (0.15 g, 1.0 mmol) afforded *N*-alkoxyphthalimides **10** as a white solid.

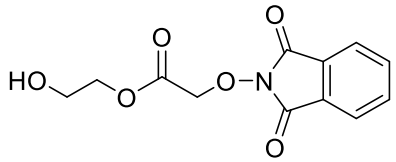

2-Hydroxyethyl 2-((1,3-dioxoisoindolin-2-yl)oxy)acetate (12). Following the general method C, the reaction of ethylene glycol (0.16 g, 2.5 mmol) and *N*-alkoxyphthalimides **12** (0.83 g, 3.8 mmol) afforded *N*-alkoxyphthalimides **12** as a white solid.

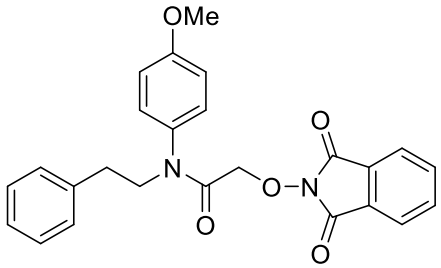

2-((1,3-Dioxoisoindolin-2-yl)oxy)-*N*-(4-methoxyphenyl)-N-phenethylacetamide (14). Following the general method A, the reaction of **A2** (0.43 g, 1.5 mmol) afforded *N*-alkoxyphthalimides **14** as a white solid**.**

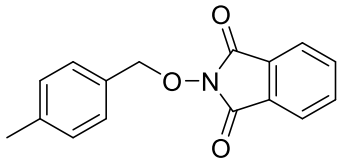

2-((4-Methylbenzyl)oxy)isoindoline-1,3-dione (16). Following the generalmethod A, the reaction of 4-methylbenzyl alcohol (1.22 g, 10.0 mmol) afforded *N*-alkoxyphthalimides **16** as a white solid**.**

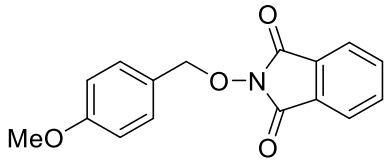

2-((4-Methoxybenzyl)oxy)isoindoline-1,3-dione (18). Following the general method A, the reaction of 4-methoxybenzyl alcohol (1.38 g, 10.0 mmol) afforded *N*-alkoxyphthalimides **18** as a white solid.

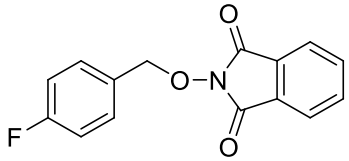

2-(4-fluorobenzyloxy)isoindoline-1,3-dione (20). Following the general method A, the reaction of 4-fluorobenzyl alcohol (1.26 g, 10.0 mmol) afforded *N*-alkoxyphthalimides **20** as a white solid.

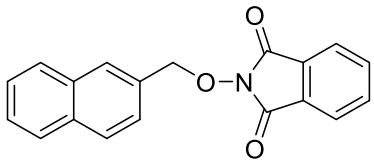

2-(Naphthalen-2-ylmethoxy)isoindoline-1,3-dione (22). Following the general method A, the reaction of 2-naphthalenemethanol (0.40 g, 2.6 mmol) afforded *N*-alkoxyphthalimides **22** as a white solid.

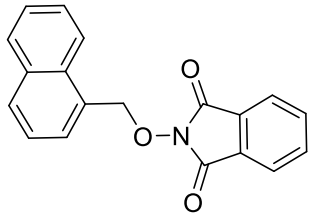

2-(Naphthalen-1-ylmethoxy)isoindoline-1,3-dione (24). Following the general method A, the reaction of 1-naphthalenemethanol (0.79 g, 5.0 mmol) afforded *N*-alkoxyphthalimides **24** as a white solid.

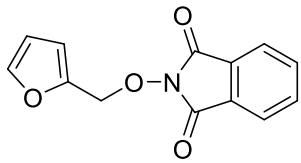

2-(Furan-2-ylmethoxy)isoindoline-1,3-dione (26). Following the general method A, the reaction of furfuryl alcohol (0.98 g, 10.0 mmol) afforded *N*-alkoxyphthalimides **26** as a white solid.

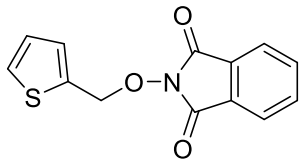

2-(Thiophen-2-ylmethoxy)isoindoline-1,3-dione (28). Following the general method A, the reaction of 2-thiophenemethanol (1.14 g, 10.0 mmol) afforded *N*-alkoxyphthalimides **28** as a white solid**.**

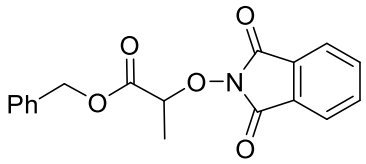

Benzyl 2-((1,3-dioxoisoindolin-2-yl)oxy)propanoate (30). Following the general method A, the reaction of benzyl 2-hydroxypropanoate (0.53 g, 3.0 mmol) afforded *N*-alkoxyphthalimides **30** as a white solid.

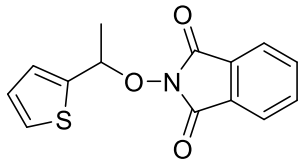

2-(1-(thiophen-2-yl)ethoxy)isoindoline-1,3-dione (32). Following the general method A, the reaction of 1-(thiophen-2-yl)ethan-1-ol (1.28 g, 10.0 mmol) afforded *N*-alkoxyphthalimides **32** as a white solid.

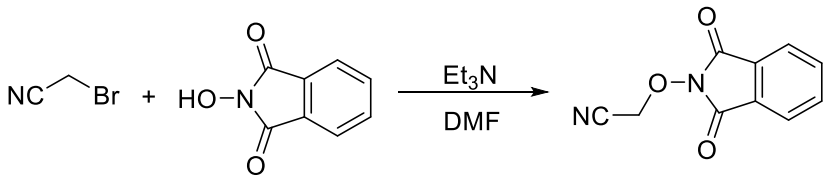

Scheme S21. Synthetic Procedure, Related to Scheme 2

To a solution of the N-hydroxyphthalimide (1.63 g, 10.0 mmol) in DMF (10 mL) was added Et_3N (3.1 mL, 22.0 mmol) and bromoacetonitrile (1.44 g, 12.0 mmol) at 0 ºC. The reaction mixture was warmed to room temperature and stirred overnight. The mixture was then taken up in EtOAc (100 mL), washed with H_2O (3 x 30 mL), and brine (30 mL). It was then dried over Na_2SO_4, concentrated in vacuo, puried by column chromatography to afford **34** as a white solid.

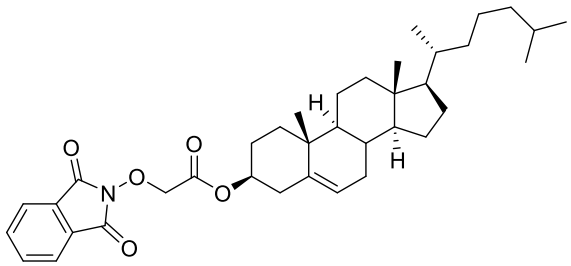

(3S,9S,10R,13R,14S,17R)-10,13-dimethyl-17-(6-methylheptan-2-yl)-2,3,4,7,8,9,10,11,12,13,14,15,16,17-tetradecahydro-1H-cyclopenta[a]phenanthren-3-yl 2-((1,3-dioxoisoindolin-2-yl)oxy)acetate (40). Following the general method C, the reaction of cholesterol (0.77 g, 2.0mmol) afforded *N*-alkoxyphthalimides **40** as a white solid**.**

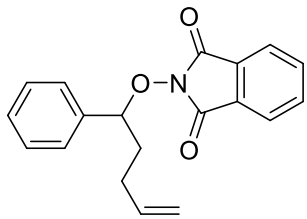

2-((1-Phenylpent-4-en-1-yl)oxy)isoindoline-1,3-dione (43). Following the general method A, the reaction of 1-phenylpent-4-en-1-ol (1.26 g, 8.0 mmol) afforded *N*-alkoxyphthalimides **43** as a white solid.

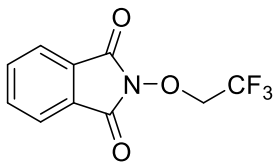

2-(2,2,2-trifluoroethoxy)isoindoline-1,3-dione(37). Following the general method D, the reaction of 2,2,2-trifluoroethan-1-ol (1.00 g, 10.0 mmol) afforded *N*-alkoxyphthalimides **37** as a white solid.

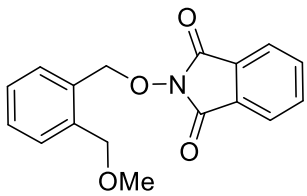

2-((2-(methoxymethyl)benzyl)oxy)isoindoline-1,3-dione. (46) Following the general method A, the reaction of (2-(methoxymethyl)phenyl)methanol (1.52 g, 10.0 mmol) afforded *N*-alkoxyphthalimides **46** as a white solid.

Synthesis of Allyl Sulfones

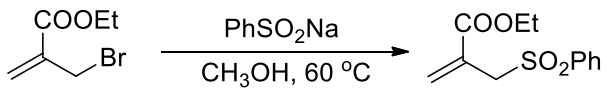

Scheme S22. Synthetic Procedure, Related to Scheme 2

Ethyl-2-((phenylsulfonyl)methyl)acrylate (2). To a solution of **B2** (1.99 g, 10.4 mmol) in dry methanol (25 mL) was added sodium phenylsulfinate (2.50 g, 15.2 mmol). After 2.5 h of reflux, the mixture was concentrated under reduced pressure, the obtained residue was dissolved in EtOAc and the mixture was washed with water, brine, dried with Na_2SO_4, filtered and the filtrate was evaporated and purified by chromatography (50% EtOAc/hexanes) to give **2** as a viscous oil.

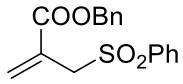

Benzyl-2-((phenylsulfonyl)methyl)acrylate (2-a). Following the above procedure, the reaction of benzylacrylate (3.24 g, 20.0 mmol) afforded **2-a** as a white solid.

Procedure for Allylation

standard procedure for allylation:

A solution of *N*-alkoxyphthalimides (0.1 mmol, 1.0 equiv.), allyl sulfone (0.3 mmol, 3.0 equiv.) and Hantzsch ester (38.0 or 76.0 mg, 0.15 or 0.3 mmol, 1.5 or 3.0 equiv.) was placed in a 5 mL clear-colored glass vial. After 1.0 mL MeOH (bubbled with nitrogen gas for 30 minutes to remove oxygen) was added, the vial was sealed and exposed to 4W blue LED at room temperature with stirring for appropriate hours. The reaction mixture was concentrated and purified directly by column chromatography to afford the allylation adduct.

*The heating effect from LED irradiation conditions above is minimal. With 6-12 hours irradiation, the increase of temperature is less than 5°C.

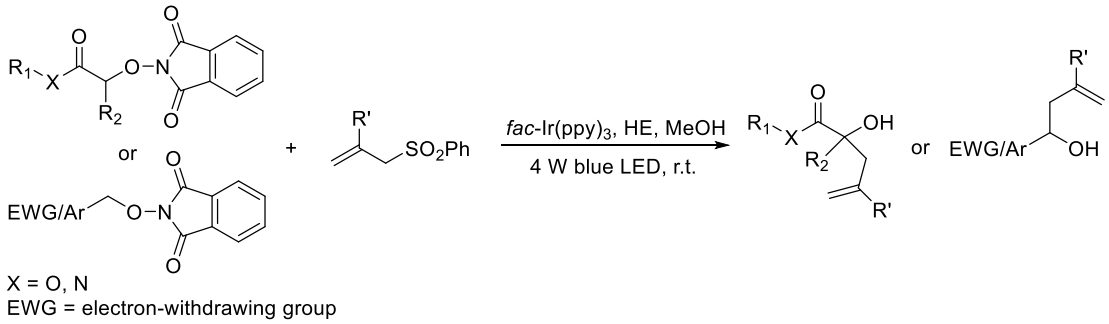

Scheme S23. Synthetic Procedure, Related to Scheme 2

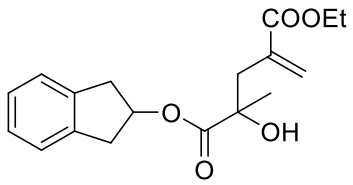

1-(2,3-Dihydro-1*H*-inden-2-yl) 5-ethyl 2-hydroxy-2-methyl-4-methylenepentane-dioate (4). Following the standard procedure, the reaction of *N*-alkoxyphthalimides **1** (35.1 mg, 0.1 mmol), Hantzsch ester (38.0 mg, 0.15 mmol) and allyl sulfone **2** (76.2 mg, 0.3 mmol) in 1 mL MeOH for 3 h afforded target product **4** as a colorless oil .

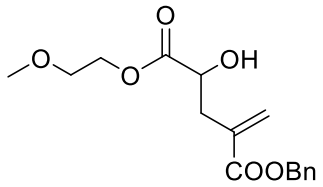

1-Benzyl 5-(2-methoxyethyl) 4-hydroxy-2-methylenepentanedioate (7). Following the standard procedure, the reaction of *N*-alkoxyphthalimides **6** (27.9 mg, 0.1 mmol), Hantzsch ester (38.0 mg, 0.15 mmol) and allyl sulfone **2-a** (94.8 mg, 0.3 mmol) in 1 mL MeOH for 3 h afforded target product **7** as a light yellow oil.

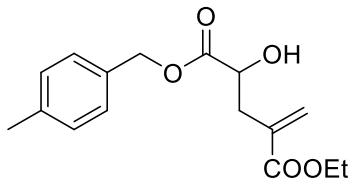

1-Ethyl 5-(4-methylbenzyl) 4-hydroxy-2-methylenepentanedioate (9). Following the standard procedure, the reaction of *N*-alkoxyphthalimides **8** (32.5 mg, 0.1 mmol), Hantzsch ester (38.0 mg, 0.15 mmol) and allyl sulfone **2** (76.2 mg, 0.3 mmol) in 1 mL MeOH for 3 h afforded target product **9** as a light yellow oil.

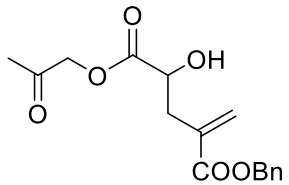

1-Benzyl 5-(2-oxopropyl) (*S*)-4-hydroxy-2-methylenepentanedioate (11).

Following the standard procedure, the reaction of *N*-alkoxyphthalimides **10** (27.7 mg, 0.1 mmol), Hantzsch ester (38.0 mg, 0.15 mmol) and allyl sulfone **2-a** (94.8 mg, 0.3 mmol) in 1 mL MeOH for 3 h afforded target product **11** as a light yellow oil.

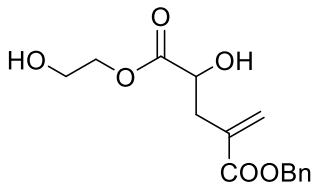

1-Benzyl 5-(2-hydroxyethyl) 4-hydroxy-2-methylenepentanedioate (13). Following the standard procedure, the reaction of *N*-alkoxyphthalimides **12** (26.5 mg, 0.1 mmol), Hantzsch ester (38.0 mg, 0.15 mmol) and allyl sulfone **2-a** (94.8 mg, 0.3 mmol) in 1 mL MeOH for 3 h afforded target product **13** as a light yellow oil.

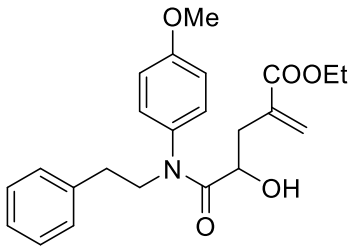

Ethyl 4-hydroxy-5-((4-methoxyphenyl)(phenethyl)amino)-2-methylene-5-oxopentanoate (15). Following the standard procedure, the reaction of *N*-alkoxyphthalimides **14** (43.0 mg, 0.1 mmol), Hantzsch ester (38.0 mg, 0.15 mmol) and allyl sulfone **2** (76.2 mg, 0.3 mmol) in 1 mL MeOH for 3 h afforded target product **15** as a light yellow oil.

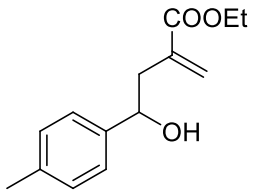

Ethyl 4-hydroxy-2-methylene-4-(p-tolyl)butanoate (17). Following the standard procedure, the reaction of *N*-alkoxyphthalimides **16** (26.7 mg, 0.1 mmol), Hantzsch

ester (38.0 mg, 0.15 mmol) and allyl sulfone **2** (76.2 mg, 0.3 mmol) in 1 mL MeOH for 6 h afforded target product **17** as a light yellow oil.

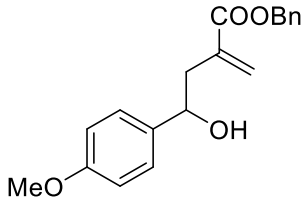

Benzyl 4-hydroxy-4-(4-methoxyphenyl)-2-methylenebutanoate (19). Following the standard procedure, the reaction of *N*-alkoxyphthalimides **18** (28.3 mg, 0.1 mmol), Hantzsch ester (38.0 mg, 0.15 mmol) and allyl sulfone **2-a** (94.8 mg, 0.3 mmol) in 1 mL MeOH for 6 h afforded target product **19** as a light yellow oil.

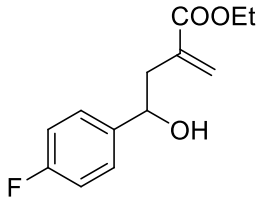

Ethyl 4-(4-fluorophenyl)-4-hydroxy-2-methylenebutanoate (21). Following the standard procedure, the reaction of *N*-alkoxyphthalimides **20** (27.1 mg, 0.1 mmol), Hantzsch ester (38.0 mg, 0.15 mmol) and allyl sulfone **2** (76.2 mg, 0.3 mmol) in 1 mL MeOH for 3 h afforded target product **21** as a light yellow oil.

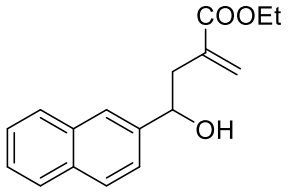

Ethyl 4-hydroxy-2-methylene-4-(naphthalen-2-yl)butanoate (23). Following the standard procedure, the reaction of *N*-alkoxyphthalimides **22** (30.3 mg, 0.1 mmol), Hantzsch ester (76.0 mg, 0.3 mmol) and allyl sulfone **2** (76.2 mg, 0.3 mmol) in 1 mL MeOH for 12 h afforded target product **23** as a light yellow oil.

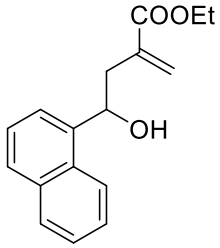

Ethyl 4-hydroxy-2-methylene-4-(naphthalen-1-yl)butanoate (25). Following the standard procedure, the reaction of *N*-alkoxyphthalimides **24** (30.3 mg, 0.1 mmol), Hantzsch ester (38.0 mg, 0.15 mmol) and allyl sulfone **2** (76.2 mg, 0.3 mmol) in 1 mL MeOH for 6 h afforded target product **25** as a light yellow oil.

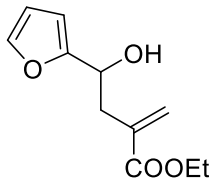

Ethyl 4-(furan-2-yl)-4-hydroxy-2-methylenebutanoate (27). Following the standard procedure, the reaction of *N*-alkoxyphthalimides **26** (24.3 mg, 0.1 mmol), Hantzsch ester (76.0 mg, 0.3 mmol) and allyl sulfone **2** (76.2 mg, 0.3 mmol) in 1 mL MeOH for 12 h afforded target product **27** as a light yellow oil.

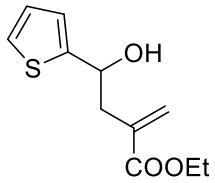

Ethyl 4-hydroxy-2-methylene-4-(thiophen-2-yl)butanoate (29). Following the standard procedure, the reaction of *N*-alkoxyphthalimides **28** (25.9 mg, 0.1 mmol), Hantzsch ester (38.0 mg, 0.15 mmol) and allyl sulfone **2** (76.2 mg, 0.3 mmol) in 1 mL MeOH for 6 h afforded target product **29** as a light yellow oil.

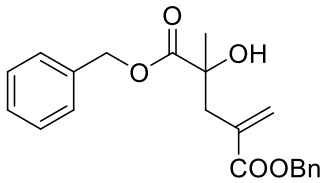

Dibenzyl 2-hydroxy-2-methyl-4-methylenepentanedioate (31). Following the standard procedure, the reaction of *N*-alkoxyphthalimides **30** (32.5 mg, 0.1 mmol), Hantzsch ester (38.0 mg, 0.15 mmol) and allyl sulfone **2-a** (94.8 mg, 0.3 mmol) in 1 mL MeOH for 3 h afforded target product **31** as a colourless oil.

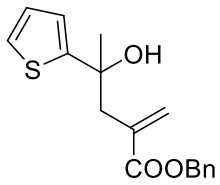

Benzyl 4-hydroxy-2-methylene-4-(thiophen-2-yl)pentanoate (33). Following the standard procedure, the reaction of *N*-alkoxyphthalimides **32** (27.3 mg, 0.1 mmol), Hantzsch ester (38.0 mg, 0.15 mmol) and allyl sulfone **2-a** (94.8 mg, 0.3 mmol) in 1 mL MeOH for 12 h afforded target product **33** as a colourless oil.

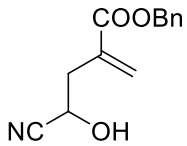

Benzyl 4-cyano-4-hydroxy-2-methylenebutanoate (35). Following the standard procedure, the reaction of *N*-alkoxyphthalimides **34** (20.2 mg, 0.1 mmol), Hantzsch ester (38.0 mg, 0.15 mmol) and allyl sulfone **2-a** (94.8 mg, 0.3 mmol) in 1 mL MeOH for 6 h afforded target product **35** as a light yellow oil.

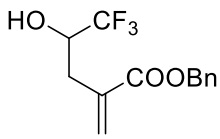

benzyl 5,5,5-trifluoro-4-hydroxy-2-methylenepentanoate (**38**). Following the standard procedure, the reaction of *N*-alkoxyphthalimides **37** (25.4 mg, 0.1 mmol), Hantzsch ester (38.0 mg, 0.15 mmol) and allyl sulfone **2-a** (94.8 mg, 0.3 mmol) in 1 mL MeOH for 6 h afforded target product **38** as a colourless oil.

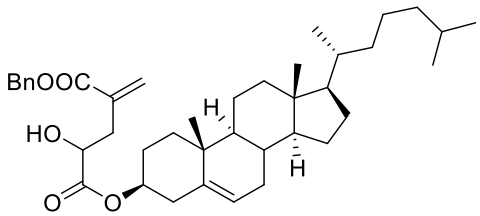

1-Benzyl 5-((3S,9S,10R,13R,14S,17R)-10,13-dimethyl-17-(6-methylheptan-2-yl)-2,3,4,7,8,9,10,11,12,13,14,15,16,17-tetradecahydro-1H-cyclopenta[a]phenanthren-3-yl) 4-hydroxy-2-methylenepentanedioate (41). Following the standard procedure, the reaction of *N*-alkoxyphthalimides **40** (58.9 mg, 0.1 mmol), Hantzsch ester (38.0 mg, 0.15 mmol) and allyl sulfone **2-a** (94.8 mg, 0.3 mmol) in 1 mL MeOH for 12 h afforded target product **41** as a colourless oil.

Procedure for the Cross-Over Experiment

Following the standard procedure for allylations, the reaction of **16** (26.7 mg, 0.1 mmol), **42** (15.8 mg, 0.1 mmol) and allyl sulfone **2** (76.2 mg, 0.3 mmol) for 6 h.

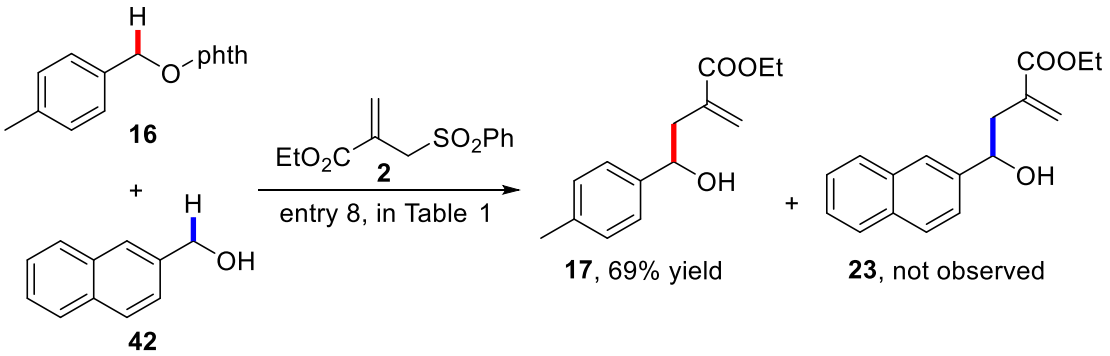

Scheme S24. Cross-Over Experiment, Related to Scheme 3

Procedure for the KIE experiments

A solution of *N*-alkoxyphthalimides **1/ D-1** (0.3 mmol, 1.0 equiv.), allyl sulfone **2** (0.9 mmol, 3.0 equiv.), Hantzsch ester (0.45 mmol, 1.5 equiv.) and 1,3,5-trimethoxybenzene (0.3 mmol, 1.0 equiv.) was placed in an 8 mL clear-colored glass vial. After 3.0 mL MeOH was added, the vial was sealed and exposed to 4W blue LED at room temperature with stirring. The reaction mixture was tested at different time points by ^{1}H-NMR.

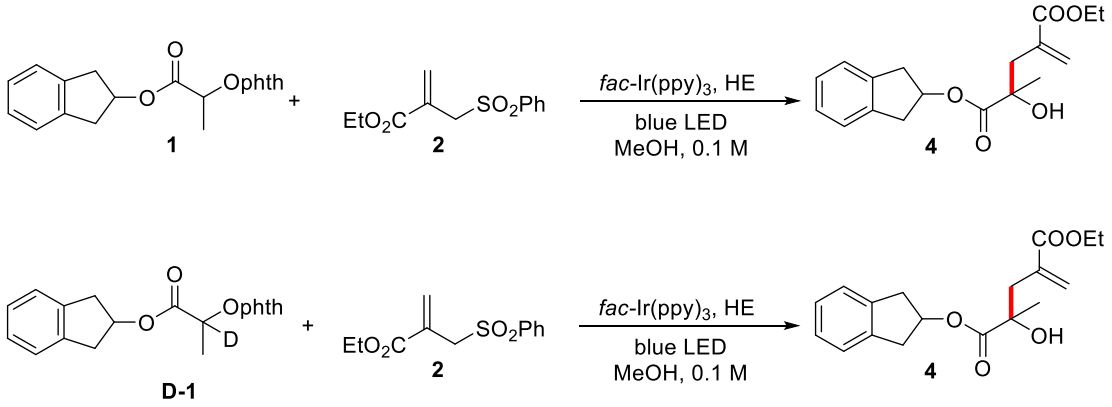

Scheme S25. KIE experiments, Related to Scheme 3.

Procedure for the 1,2-HAT Competes with Other Alkoxyl Radical Reaction Pathways

Following the standard procedure without the addition of allyl sulfone, the reaction of **42** (29.5 mg, 0.1 mmol) and Hantzsch ester (0.30 mmol, 3.0 equiv.) in 1 mL 1,4-dioxane for 12 h.

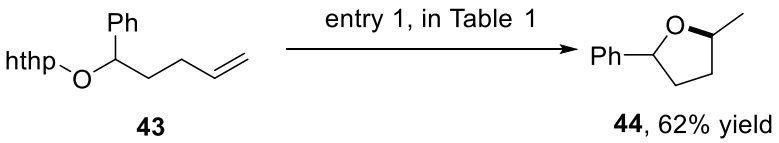

43 **44**, 62% yield

Scheme S26. 1,2-HAT Competition Experimrnts, Related to Scheme 3.

Following the standard procedure, the reaction of **46** (29.7 mg, 0.1 mmol) and Hantzsch ester (0.30 mmol, 3.0 equiv.) in 1 mL MeOH for 6 h afforded an unseperable mixture of **47** and **48** as a colorless oil after flash chromatography (90% hexanes : 10% EtOAc). Then the mixture of X and X was dissolved in 2 mL DCM and treated with Dess-Martin Periodinan (0.2 mmol, 2.0 equiv.) at room temperature for 3 hours. The saturated $Na_2S_2O_3$ aqueous solution was then added to quench the reaction, after which the mixture was washed with brine, dried over Na_2SO_4, and concentrated in vacuo. The crude product was puried by preparative thin layer chromatography (75% hexanes : 25% EtOAc).

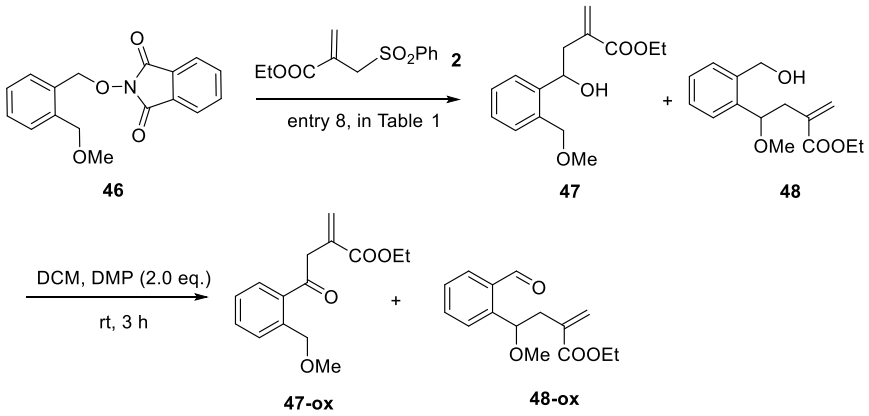

Scheme S27. 1,2-HAT Competition Experimrnts, Related to Scheme 3.

Procedure for the Luminescence Quenching Experiments

Emission intensities were recorded using Microplate Accessory 5JO-0139 spectrometer for all experiments. All *fac*-Ir(ppy)$_3$ solutions were excited at 320 nm and the emission intensity was collected at 518 nm. In a typical experiment, the 1,4-dioxane solution of *fac*-Ir(ppy)$_3$ (100 μM) was added the appropriate amount of quencher in a screw-top 1.0 cm quartz cuvette. After degassing with nitrogen for 10 min, the emission spectra of the samples were collected.

Procedure for the Cyclic Voltammetry

Cyclic Voltammetry was performed on a CH Instruments Electrochemical Workstation model CHI600E. A 0.001 M MeCN solution of the sample was prepared with 0.1 M Bu_4NPF_6 as the supporting electrolyte, using a glassy carbon working electrode, a Pt counter electrode, and a saturated calomel electrode reference electrode. Scan rate = 0.05 V/s, 2 sweep segments, a sample interval of 0.001 V.

Proceure for the Quantum Yield Measurement

n_x is the amount of photochemical or photophysical events during irradiation, n_p is the amount of photons aborbed by the reactant. n_x was calculated by NMR analysis, n_p was measured by Handy FZ-A Portable Radiometer/Photometer.

N-alkoxyphthalimides **1** (0.10 mmol, 1.0 equiv.), allyl sulfone **2**, *fac*-Ir(ppy)$_3$ (0.7 mg, 0.001 mmol, 0.01 equiv.) and Hantzsch eater (38.0 mg, 0.15 mmol, 1.5 equiv.) were placed in a 5 mL tube vial equipped with a magnetic stir bar. After 1.0 mL MeOH (treated by 4 Å MS) was added into the tube via a syringe, the reaction mixture was

exposed to blue LEDs at room temperature for 60 min and analyzed by ^{1}H-NMR

Produce for the On-Off-Light Experiments

Following the standard procedure, to a solution of **1** (105.2 mg, 0.3 mmol), **2** (232.2 mg, 0.9 mmol), *fac*-Ir(ppy)$_3$ (1.9 mg, 0.003 mmol), and HE (113.8 mg, 0.45 mmol) in MeOH (3 mL). The reaction mixture was stirred at 25 ^{o}C using 4W blue LED with on-off-light. 500 μL of the reaction mixture aliquot was collected at different points and concentrated in vacuo. The ^{1}H NMR analysis was calculated using 1,3,5-Trimethoxybenzene as the internal standard.

Proceduce for EPR studies

EPR experiments were performed on a Bruker E500 CW-EPR spectrometer at 298 K. A solution of *N*-alkoxyphthalimides **45** (0.1 mmol, 1.0 equiv.), Hantzsch ester (38.0 mg, 0.15 mmol, 1.5 equiv.) and DMPO **46** (5,5-dimethyl-pyrroline N-oxide) (13 μL 0.12 mmol, 1.2 equiv.) was placed in a 5 mL clear-colored glass vial. After 1.0 mL MeOH or dioxane (bubbled with nitrogen gas for 30 seconds to remove oxygen) was added, the vial was sealed and exposed to 4W blue LED at room temperature with stirring for 45 min. The reaction mixture was diluted 10 times and transferred to a sealed melting point tube in the glove box. The EPR signals were subsequently tested.

Computational methods for DFT caculations

All DFT calculations were performed with the GAUSSIAN 09 series of programs. Density functional B3-LYP (Becke, 1993; Lee et al., 1988) with a standard 6-31G(d) basis set was used for geometry optimizations. Harmonic frequency calculations were

performed at all stationary points to confirm them as local minima or transition structures and to derive the thermochemical corrections for the enthalpies and free energies. The DFT method M11 functional was used to calculate the single point energies in methanol and 1,4-dioxane. (Peverati and Truhlar, 2011) The solvent effects were considered by single point calculations on the gas-phase stationary points with a continuum solvation model SMD. (Cossi et al., 1996; Cances et al., 1997; Barone et al., 1998; Marenich et al., 2009; Liu et al., 2018) The larger basis set 6-311+G(d) was used in the solvation single point calculations. The energies given in this report are the M11 calculated Gibbs free energies in methanol and 1,4-dioxane solvent.

Complete reference for Gaussian 09

Frisch, M. J.; Trucks, G. W.; Schlegel, H. B.; Scuseria, G. E.; Robb, M. A.; Cheeseman, J. R.; Scalmani, G.; Barone, V.; Mennucci, B.; Petersson, G. A.; Nakatsuji, H.; Caricato, M.; Li, X.; Hratchian, H. P.; Izmaylov, A. F.; Bloino, J.; Zheng, G.; Sonnenberg, J. L.; Hada, M.; Ehara, M.; Toyota, K.; Fukuda, R.; Hasegawa, J.; Ishida, M.; Nakajima, T.; Honda, Y.; Kitao, O.; Nakai, H.; Vreven, T.; Montgomery, Jr., J. A.; Peralta, J. E.; Ogliaro, F.; Bearpark, M.; Heyd, J. J.; Brothers, E.; Kudin, K. N.; Staroverov, V. N.; Keith, T.; Kobayashi, R.; Normand, J.; Raghavachari, K.; Rendell, A.; Burant, J. C.; Iyengar, S. S.; Tomasi, J.; Cossi, M.; Rega, N.; Millam, J. M.; Klene, M.; Knox, J. E.; Cross, J. B.; Bakken, V.; Adamo, C.; Jaramillo, J.; Gomperts, R.; Stratmann, R. E.; Yazyev, O.; Austin, A. J.; Cammi, R.; Pomelli, C.; Ochterski, J. W.; Martin, R. L.; Morokuma, K.; Zakrzewski, V. G.; Voth, G. A.; Salvador, P.; Dannenberg, J. J.; Dapprich, S.; Daniels, A. D.; Farkas, O.; Foresman, J. B.; Ortiz, J. V.; Cioslowski, J.; and Fox, D. J. Gaussian 09, revision D.01; Gaussian, Inc.: Wallingford, CT, **2013**.

IV. Substrate And Product Characterizations

Characterizations of *N*-alkoxyphthalimide Precursors

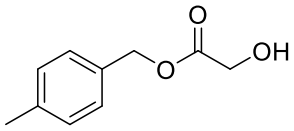

4-Methylbenzyl 2-hydroxyacetate (A1).

Colorless oil (0.62 g, 57% yield): TLC R_f = 0.43 (EtOAc/hexanes = 1/5); ^{1}H NMR (400 MHz, $CDCl_3$) δ 7.26 (d, *J* = 8.0 Hz, 2H), 7.18 (d, *J* = 8.0 Hz, 2H), 5.19 (s, 2H), 4.18 (d, *J* = 5.3 Hz, 2H), 2.36 (s, 3H); ^{13}C NMR (100 MHz, $CDCl_3$) δ 173.4, 138.8, 132.2, 129.5, 128.8, 67.4, 60.8, 21.4.

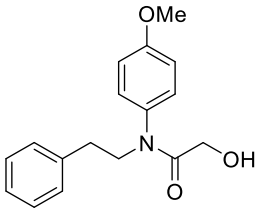

2-Hydroxy-*N*-(4-methoxyphenyl)-N-phenethylacetamide (A2).

Colorless oil (0.43 g, 62% yield): TLC R_f = 0.27 (EtOAc/hexanes = 1/2); ^{1}H NMR (500 MHz, $CDCl_3$) δ 7.29 – 7.26 (m, 2H), 7.23 – 7.16 (m, 3H), 6.96 – 6.94 (m, 2H), 6.92 – 6.89 (m, 2H), 3.96 – 3.93 (m, 2H), 3.84 (s, 3H), 3.73 (d, *J* = 4.5 Hz, 2H), 3.39 (t, *J* = 4.5 Hz, 1H, -OH), 2.91 – 2.87 (m, 2H); ^{13}C NMR (125 MHz, $CDCl_3$) δ 172.2, 159.8, 138.5, 132.3, 129.3, 129.0, 128.7, 126.6, 115.2, 60.7, 55.7, 51.4, 34.0; IR (KBr, thin film): 3436, 2933, 1655, 1512, 1386, 1250, 1030, 840, 743, 700 cm^{-1}; HRMS-ESI (m/z) [M+Na^+]: calcd. for $C_{17}H_{19}NNaO_3$ 308.1257, found 308.1258.

Characterizations of *N*-alkoxyphthalimide substrates

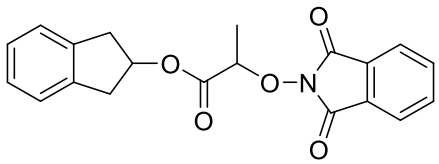

2,3-Dihydro-1*H*-inden-2-yl 2-((1,3-dioxoisoindolin-2-yl)oxy)propanoate (1).

White solid (2.36 g, 67% yield): TLC R_f = 0.46 (EtOAc/hexanes = 1/3); ^{1}H NMR (500 MHz, $CDCl_3$) δ 7.80 (dd, *J* = 5.5, 3.1 Hz, 2H), 7.74 (dd, *J* = 5.5, 3.1 Hz, 2H), 7.20 – 7.14 (m, 4H), 5.62 – 5.58 (m, 1H), 4.84 (q, *J* = 6.8 Hz, 1H), 3.37 – 3.30 (m, 2H), 3.08 – 3.02 (m, 2H), 1.61 (d, *J* = 6.8 Hz, 3H); ^{13}C NMR (125 MHz, $CDCl_3$) δ 169.8, 163.3, 140.2, 140.2, 134.7, 128.9, 126.9, 124.7, 124.7, 123.8, 81.3, 76.8, 39.5 , 39.4, 16.4; IR (KBr, thin film): 3073, 2943, 1792, 1737, 1467, 1375, 1188, 978, 747, 701 cm^{-1}; HRMS-ESI (m/z) [M+H$^+$]: calcd. for $C_{20}H_{18}NO_5$ 352.1179, found 352.1188.

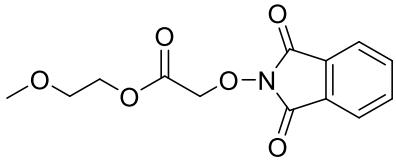

2-Methoxyethyl 2-((1,3-dioxoisoindolin-2-yl)oxy)acetate (6).

White solid (0.21 g, 27% yield): TLC R_f = 0.47 (EtOAc/hexanes = 1/4); ^{1}H NMR (500 MHz, $CDCl_3$) δ 7.85 (dd, *J* = 5.5, 3.1 Hz, 2H), 7.76 (dd, *J* = 5.5, 3.1 Hz, 2H), 4.87 (s, 2H), 4.36 – 4.34 (m, 2H), 3.63 – 3.61 (m, 2H), 3.35 (s, 3H); ^{13}C NMR (125 MHz, $CDCl_3$) δ 167.1, 163.1, 134.8, 129.0, 123.9, 73.1, 70.1, 64.6, 59.1; IR (KBr, thin film): 2987, 1793, 1733, 1276, 1260, 1187, 1130, 1054, 764, 702 cm^{-1}; HRMS-ESI (m/z) [M+Na$^+$]: calcd. for $C_{13}H_{13}NnaO_6$ 302.0635, found 302.0642.

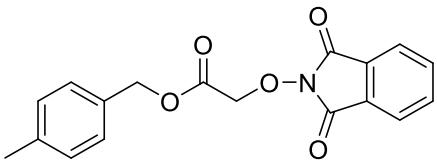

4-Methylbenzyl 2-((1,3-dioxoisoindolin-2-yl)oxy)acetate (8).

White solid (0.26 g, 24% yield over two steps): TLC R_f = 0.51 (EtOAc/hexanes = 1/4); ^{1}H NMR (500 MHz, $CDCl_3$) δ 7.84 (dd, *J* = 5.5, 3.1 Hz, 2H), 7.75 (dd, *J* = 5.5, 3.1 Hz, 2H), 7.25 (d, *J* = 7.8 Hz, 2H), 7.15 (d, *J* = 7.8 Hz, 2H), 5.19 (s, 2H), 4.84 (s, 2H), 2.34 (s, 3H); ^{13}C NMR (125 MHz, $CDCl_3$) δ 166.9, 163.1, 138.7, 134.8, 132.0, 129.4, 129.0, 128.9, 123.9, 73.2, 67.4, 21.4; IR (KBr, thin film): 3032, 2946, 1755, 1732, 1466, 1378, 1187, 1054, 878, 700 cm^{-1}; HRMS-ESI (m/z) [M+Na$^+$]: calcd. for $C_{18}H_{15}NNaO_5$ 348.0842, found 348.0844.

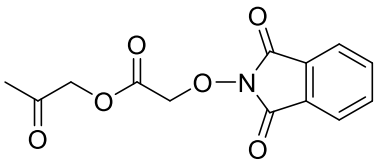

2-Oxopropyl 2-((1,3-dioxoisoindolin-2-yl)oxy)acetate (10).

White solid (0.19 g, 68% yield): TLC R_f = 0.38 (EtOAc/hexanes = 1/1); ^{1}H NMR (500 MHz, $CDCl_3$) δ 7.86 (dd, *J* = 5.5, 3.1 Hz, 2H), 7.77 (dd, *J* = 5.5, 3.1 Hz, 2H), 4.96 (s, 2H), 4.79 (s, 2H), 2.17 (s, 3H); ^{13}C NMR (125 MHz, $CDCl_3$) δ 200.2, 166.4, 163.1, 134.8, 128.9, 123.9, 72.9, 68.9, 26.1; IR (KBr, thin film): 3326, 2923, 1770, 1732, 1625, 1373, 1173, 1064, 877, 701 cm^{-1}; HRMS-ESI (m/z) [M+Na$^+$]: calcd. for $C_{13}H_{11}NNaO_6$ 300.0479, found 300.0484.

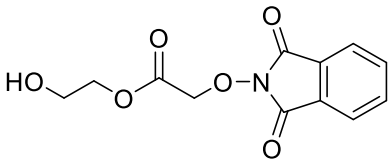

2-Hydroxyethyl 2-((1,3-dioxoisoindolin-2-yl)oxy)acetate (12).

White solid (0.24 g, 24% yield): TLC R_f = 0.44 (EtOAc/hexanes = 1/1); ^{1}H NMR (500 MHz, $CDCl_3$) δ 7.86 (dd, *J* = 5.5, 3.1 Hz, 2H), 7.78 (dd, *J* = 5.5, 3.1 Hz, 2H),

4.86 (s, 2H), 4.35 – 4.33 (m, 2H), 3.89 – 3.87 (m, 2H); ^{13}C NMR (125 MHz, $CDCl_3$) δ 167.5, 163.4, 135.0, 128.8, 124.0, 73.9, 67.6, 60.7 ; IR (KBr, thin film): 3505, 1732, 1375, 1276, 1187, 1082, 1050, 877, 750, 701 cm^{-1}; HRMS-ESI (m/z) [M+Na$^+$]: calcd. for $C_{12}H_{11}NO_6$ 288.0479, found 288.0478.

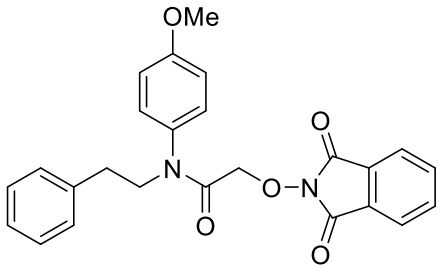

2-((1,3-Dioxoisoindolin-2-yl)oxy)-*N*-(4-methoxyphenyl)-N-phenethylacetamide (14).

White solid (0.46 g, 69% yield): TLC R_f = 0.24 (EtOAc/hexanes = 1/2); ^{1}H NMR (500 MHz, $CDCl_3$) δ 7.82 (dd, *J* = 5.5, 3.1 Hz, 2H), 7.73 (dd, *J* = 5.5, 3.1 Hz, 2H), 7.24 (t, *J* = 7.6 Hz, 2H), 7.19 – 7.12 (m, 5H), 6.91 (d, *J* = 8.8 Hz, 2H), 4.51 (s, 2H), 3.91 – 3.88 (m, 2H), 3.83 (s, 3H), 2.91 – 2.88 (m, 2H); ^{13}C NMR (125 MHz, $CDCl_3$) δ 165.8, 163.2, 159.6, 138.7, 134.6, 133.3, 129.5, 129.1, 129.0, 128.5, 126.4, 123.7, 115.2, 73.8, 55.6, 51.2, 33.7; IR (KBr, thin film): 3058, 2931, 1734, 1676, 1511, 1375, 1249, 1185, 877, 700 cm^{-1}; HRMS-ESI (m/z) [M+Na$^+$]: calcd. for $C_{25}H_{22}N_2NaO_5$ 453.1421, found 453.1423.

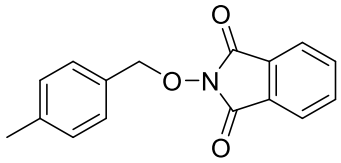

2-((4-Methylbenzyl)oxy)isoindoline-1,3-dione (16).

White solid (2.23 g, 83% yield): TLC R_f = 0.43 (EtOAc/hexanes = 1/4); ^{1}H NMR (500 MHz, $CDCl_3$) δ 7.81 (dd, *J* = 5.5, 3.1 Hz, 2H), 7.73 (dd, *J* = 5.5, 3.1 Hz, 2H), 7.42 (d, *J* = 8.0 Hz, 2H), 7.18 (d, *J* = 8.0 Hz, 2H), 5.17 (s, 2H), 2.35 (s, 3H); ^{13}C NMR (125 MHz, $CDCl_3$) δ 163.6, 139.4, 134.5, 130.8, 130.1, 129.4, 129.0, 123.6, 79.8, 21.5; IR (KBr, thin film): 3093, 1785, 1737, 1466, 1391, 1186, 1142, 975, 880, 699

cm^{-1}; HRMS-ESI (m/z) [M+Na$^+$]: calcd. for $C_{16}H_{13}NNaO_3$ 290.0788, found 290.0795.

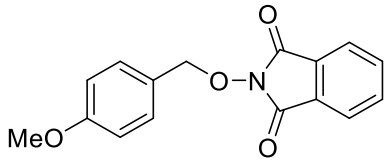

2-((4-Methoxybenzyl)oxy)isoindoline-1,3-dione (18).

White solid (2.30 g, 81% yield): TLC R_f = 0.27 (EtOAc/hexanes = 1/4); ^{1}H NMR (500 MHz, $CDCl_3$) δ 7.80 (dd, *J* = 5.5, 3.1 Hz, 2H), 7.72 (dd, *J* = 5.5, 3.1 Hz, 2H), 7.47 – 7.44 (m, 2H), 6.90 – 6.87 (m, 2H), 5.15 (s, 2H), 3.80 (s, 3H); ^{13}C NMR (125 MHz, $CDCl_3$) δ 163.7, 160.6, 134.5, 131.8, 129.0, 126.0, 123.6, 114.1, 79.6, 55.4; IR (KBr, thin film): 2963, 1786, 1736, 1612, 1515, 1392, 1253, 1143, 879, 698 cm^{-1}; HRMS-ESI (m/z) [M+Na$^+$]: calcd. for $C_{16}H_{13}NNaO_4$ 306.0737, found 306.0744.

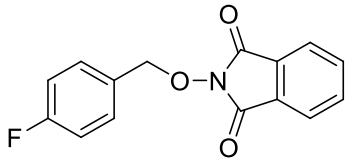

2-(4-fluorobenzyloxy)isoindoline-1,3-dione (20).

White solid (0.85 g, 31% yield): TLC R_f = 0.57 (EtOAc/hexanes = 1/5); ^{1}H NMR (400 MHz, $CDCl_3$) δ 7.82 (dd, *J* = 5.5, 3.1 Hz, 2H), 7.74 (dd, *J* = 5.5, 3.1 Hz, 2H), 7.52 (dd, *J* = 8.6, 5.4 Hz, 2H), 7.06 (t, *J* = 8.6 Hz, 2H), 5.18 (s, 2H); ^{13}C NMR (125 MHz, $CDCl_3$) δ 164.5, 163.6, 162.5, 134.6, 132.1, 132.0, 129.8, 129.8, 128.9, 123.7, 115.8, 115.6, 79.1; ^{19}F NMR (376 MHz, $CDCl_3$) δ -111.9 (m); IR (KBr, thin film): 3647, 3098, 1726, 1466, 1389, 1187, 1127, 975, 878, 696 cm^{-1}; HRMS-ESI (m/z) [M+NH$_4^+$]: calcd. for $C_{15}H_{14}FN_2O_3$ 289.0983, found 289.0987.

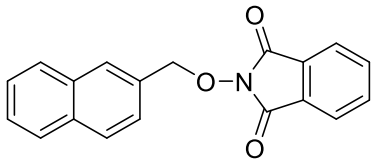

2-(Naphthalen-2-ylmethoxy)isoindoline-1,3-dione (22).

White solid (1.33 g, 88% yield): TLC R_f = 0.42 (EtOAc/hexanes = 1/4); ^{1}H NMR (500 MHz, $CDCl_3$) δ 7.93 (s, 1H), 7.88 (d, *J* = 8.4 Hz, 1H), 7.84 (dd, *J* = 6.5, 3.0 Hz, 2H), 7.79 (dd, *J* = 5.5, 3.1 Hz, 2H), 7.74 – 7.70 (m, 3H), 7.52 – 7.46 (m, 2H), 5.38 (s, 2H); ^{13}C NMR (125 MHz, $CDCl_3$) δ 163.7, 134.6, 133.8, 133.1, 131.4, 129.5, 129.0, 128.6, 128.3, 127.9, 127.2, 126.8, 126.4, 123.6, 80.1; IR (KBr, thin film): 3093, 1739, 1466, 1383, 1275, 1261, 1139, 972, 750, 699 cm^{-1}; HRMS-ESI (m/z) [M+Na^+]: calcd. for $C_{19}H_{13}NNaO_3$ 326.0788, found 326.0793.

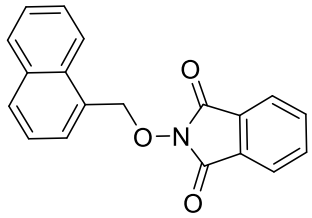

2-(Naphthalen-1-ylmethoxy)isoindoline-1,3-dione (24).

White solid (0.83 g, 54% yield): TLC R_f = 0.36 (EtOAc/hexanes = 1/4); ^{1}H NMR (500 MHz, $CDCl_3$) δ 8.63 (dd, *J* = 8.5, 1.1 Hz, 1H), 7.90 – 7.87 (m, 2H), 7.82 (dd, *J* = 5.5, 3.1 Hz, 2H), 7.72 (dd, *J* = 5.5, 3.1 Hz, 2H), 7.67 (ddd, *J* = 8.4, 6.8, 1.3 Hz, 1H), 7.61 (dd, *J* = 7.0, 1.1 Hz, 1H), 7.54 (ddd, *J* = 8.0, 6.8, 1.1 Hz, 1H), 7.43 (dd, *J* = 8.4, 6.8 Hz, 1H), 5.64 (s, 2H); ^{13}C NMR (125 MHz, $CDCl_3$) δ 163.7, 134.6, 133.8, 132.6, 130.7, 129.7, 129.6, 129.1, 128.6, 127.1, 126.3, 125.2, 124.6, 123.6, 78.2; IR (KBr, thin film): 3043, 2896, 1786, 1729, 1383, 1186, 1131, 971, 877, 699 cm^{-1}; HRMS-ESI (m/z) [M+Na^+]: calcd. for $C_{19}H_{13}NNaO_3$ 326.0788, found 326.0795.

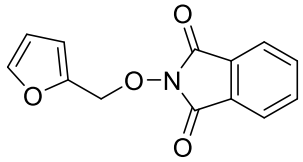

2-(Furan-2-ylmethoxy)isoindoline-1,3-dione (26).

White solid (0.70 g, 29% yield): TLC R_f = 0.50 (EtOAc/hexanes = 1/4); ^{1}H NMR (500 MHz, $CDCl_3$) δ 7.81 (dd, *J* = 5.5, 3.1 Hz, 2H), 7.74 (dd, *J* = 5.5, 3.1 Hz, 2H),

7.48 – 7.47 (m, 1H), 6.49 (dd, *J* = 3.3, 0.8 Hz, 1H), 6.35 (dd, *J* = 3.3, 1.8 Hz, 1H), 5.16 (s, 2H); ^{13}C NMR (125 MHz, $CDCl_3$) δ 163.4, 148.1, 144.6, 134.6, 128.9, 123.6, 113.3, 110.9, 70.4; IR (KBr, thin film): 3123, 1786, 1742, 1380, 1185, 1137, 976, 925, 759, 700 cm^{-1}; HRMS-ESI (m/z) [M+H$^+$]: calcd. for $C_{13}H_{10}NO_4$ 244.0604, found 244.0607.

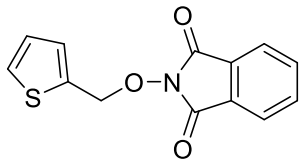

2-(Thiophen-2-ylmethoxy)isoindoline-1,3-dione (28).

White solid (0.61 g, 23% yield): TLC R_f = 0.49 (EtOAc/hexanes = 1/4); ^{1}H NMR (500 MHz, $CDCl_3$) δ 7.81 (dd, *J* = 5.5, 3.1 Hz, 2H), 7.74 (dd, *J* = 5.5, 3.1 Hz, 2H), 7.40 (dd, *J* = 5.1, 1.2 Hz, 1H), 7.20 – 7.19 (m, 1H), 6.99 (dd, *J* = 5.1, 3.5 Hz, 1H), 5.38 (s, 2H); ^{13}C NMR (125 MHz, $CDCl_3$) δ 163.6,

135.5, 134.6, 130.5, 129.0, 128.7, 127.2, 123.7, 73.1; IR (KBr, thin film): 3102, 3040, 1719, 1465, 1386, 1185, 1132, 1084, 875, 699 cm^{-1}; HRMS-ESI (m/z) [M+Na$^+$]: calcd. for $C_{13}H_9NNaO_3S$ 282.0195, found 282.0202.

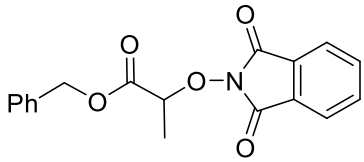

Benzyl 2-((1,3-dioxoisoindolin-2-yl)oxy)propanoate (30).

White solid (0.57 g, 38 % yield): TLC R_f = 0.35 (EtOAc/hexanes = 1/4); ^{1}H NMR (500 MHz, $CDCl_3$) δ 7.82 (dd, *J* = 5.5, 3.1 Hz, 2H), 7.74 (dd, *J* = 5.5, 3.1 Hz, 2H), 7.37 – 7.27 (m, 5H), 5.26 – 5.14 (m, 2H), 4.92 (q, *J* = 6.8 Hz, 1H), 1.66 (d, *J* = 6.8 Hz, 3H); ^{13}C NMR (125 MHz, $CDCl_3$) δ 169.7, 163.4, 135.2, 134.7, 129.0, 128.7, 128.6, 128.6, 123.8, 81.4, 67.5, 16.4; IR (KBr, thin film): 3446, 1734, 1620, 1384, 1187, 1080, 977, 877, 698, 664 cm^{-1}; HRMS-ESI (m/z) [M+H$^+$]: calcd. for $C_{18}H_{16}NO_5$ 326.1023, found 326.1021.

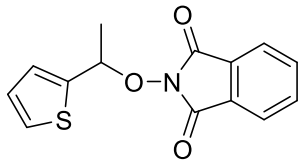

2-(1-(thiophen-2-yl)ethoxy)isoindoline-1,3-dione (32).

White solid (2.10 g, 77 % yield): TLC R_f = 0.52 (EtOAc/hexanes = 1/4): ^{1}H NMR (500 MHz, $CDCl_3$) δ 7.78 (dd, *J* = 5.5, 3.1 Hz, 2H), 7.72 (dd, *J* = 5.5, 3.1 Hz, 2H), 7.35 (d, *J* = 5.0 Hz, 1H), 7.11 (d, *J* = 4.4 Hz, 1H), 6.93 (dd, *J* = 5.0, 3.6 Hz, 1H), 5.68 (q, *J* = 6.5 Hz, 1H), 1.85 (d, *J* = 6.5 Hz, 3H); ^{13}C NMR (125 MHz, $CDCl_3$) δ 163.8, 141.8, 134.5, 128.9, 127.9, 127.2, 126.7, 123.6, 80.0, 20.7; IR (KBr, thin film): 1789, 1831, 1466, 1373, 1186, 1128, 1081, 971, 878, 699 cm^{-1}; HRMS-ESI (m/z) [M+Na^+]: calcd. for $C_{14}H_{11}NNaO_3S$ 296.0352, found 296.0357.

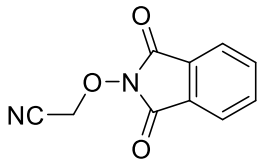

2-((1,3-Dioxoisoindolin-2-yl)oxy)acetonitrile (34).

White solid (1.38 g, 68% yield): TLC R_f = 0.29 (EtOAc/hexanes = 1/2); ^{1}H NMR (500 MHz, $CDCl_3$) δ 7.90 (dd, *J* = 5.5, 3.1 Hz, 2H), 7.82 (dd, *J* = 5.5, 3.1 Hz, 2H), 4.96 (s, 2H); ^{13}C NMR (125 MHz, $CDCl_3$) δ 162.8, 135.3, 128.7, 124.3, 113.8, 62.0; IR (KBr, thin film): 2993, 1793, 1735, 1362, 1276, 1187, 1021, 876, 750, 701 cm^{-1}; HRMS-ESI (m/z) [M+Na^+]: calcd. for $C_{10}H_6N_2NaO_3$ 225.0271, found 225.0278.

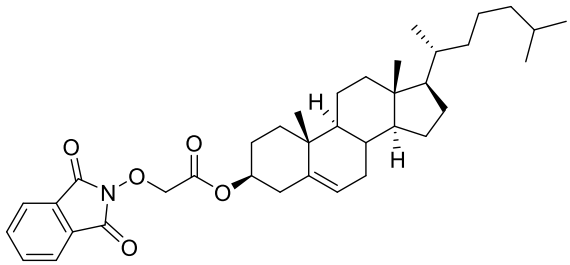

(3S,9S,10R,13R,14S,17R)-10,13-dimethyl-17-(6-methylheptan-2-yl)-2,3,4,7,8,9,10,

11,12,13,14,15,16,17-tetradecahydro-1H-cyclopenta[a]phenanthren-3-yl 2-((1,3-dioxoisoindolin-2-yl)oxy)acetate (40).

White solid (0.73 g, 62 % yield): TLC R_f = 0.48 (EtOAc/hexanes = 1/4): ^{1}H NMR (500 MHz, $CDCl_3$) δ 7.86 (dd, *J* = 5.4, 3.1 Hz, 2H), 7.76 (dd, *J* = 5.4, 3.1 Hz, 2H), 5.37 (d, *J* = 4.2 Hz, 1H), 4.80 (s, 2H), 4.74 (dtd, *J* = 12.5, 8.0, 4.3 Hz, 1H), 2.36 (d, *J* = 7.8 Hz, 2H), 2.04 – 1.78 (m, 5H), 1.65 (ddd, *J* = 14.0, 8.7, 2.9 Hz, 1H), 1.49 (dtdd, *J* = 37.3, 16.2, 12.4, 10.3 Hz, 6H), 1.39 – 1.30 (m, 3H), 1.24 (ddd, *J* = 13.2, 9.8, 3.1 Hz, 1H), 1.20 – 1.03 (m, 7H), 1.03 – 0.94 (m, 6H), 0.91 (d, *J* = 6.5 Hz, 3H), 0.86 (dd, *J* = 6.6, 2.3 Hz, 6H), 0.67 (s, 3H); ^{13}C NMR (125 MHz, $CDCl_3$) δ 166.5, 163.1, 139.3, 134.8, 129.0, 123.8, 123.2, 75.8, 73.3, 56.8, 56.3, 50.1, 42.4, 39.8, 39.7, 38.0, 37.0, 36.7, 36.3, 35.9, 32.0, 32.0, 28.4, 28.2, 27.7, 24.4, 24.0, 23.0, 22.7, 21.2, 19.4, 18.9, 12.0. IR (KBr, thin film): 3445, 2944, 1731, 1466, 1383, 1188, 1135, 1052, 877, 696 cm^{-1}; HRMS-ESI (m/z) [M+Na^+]: calcd. for $C_{37}H_{51}NNaO_5$ 612.3659, found 612.3665.

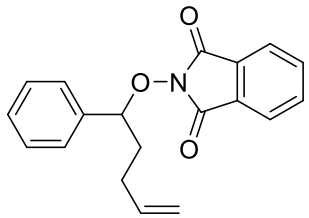

2-((1-Phenylpent-4-en-1-yl)oxy)isoindoline-1,3-dione (43).

White solid (1.53 g, 62% yield): TLC R_f = 0.51 (EtOAc/hexanes = 1/4); ^{1}H NMR (500 MHz, $CDCl_3$) δ 7.71 (dd, *J* = 5.3, 3.2 Hz, 2H), 7.66 (dd, *J* = 5.3, 3.2 Hz, 2H), 7.46 (d, *J* = 6.4 Hz, 2H), 7.31 (q, *J* = 5.9 Hz, 3H), 5.85 (ddt, *J* = 16.8, 10.2, 6.5 Hz, 1H), 5.34 (t, *J* = 6.9 Hz, 1H), 5.03 (dd, *J* = 26.7, 13.7 Hz, 2H), 2.29 (ddd, *J* = 13.1, 8.6, 6.7 Hz, 1H), 2.23 – 2.15 (m, 2H), 2.00 (dq, *J* = 14.8, 6.8 Hz, 1H); ^{13}C NMR (125 MHz, $CDCl_3$) δ 163.8, 138.1, 137.5, 134.4, 129.1, 128.9, 128.4, 128.2, 123.4, 115.5, 88.7, 34.1, 29.9.

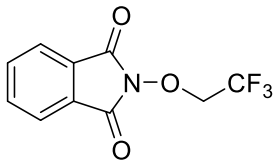

2-(2,2,2-trifluoroethoxy)isoindoline-1,3-dione(37).

White solid (1.64 g, 67% yield): TLC R_f = 0.53 (EtOAc/hexanes = 1/4);^{1}H NMR (500 MHz, $CDCl_3$) δ 7.86 (dd, *J* = 5.5, 3.1 Hz, 2H), 7.78 (dd, *J* = 5.4, 3.1 Hz, 2H), 4.55 (q, *J* = 8.0 Hz, 2H). ^{13}C NMR (126 MHz, $cdcl_3$) δ 162.5, 134.9, 128.6, 123.9, 73.5, 73.2, 72.9, 72.7. ^{19}F NMR (376 MHz, $CDCl_3$) δ -73.94 (t, *J* = 8.0 Hz).

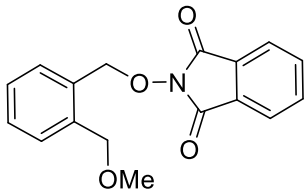

2-((2-(methoxymethyl)benzyl)oxy)isoindoline-1,3-dione. (46)

White solid (1.40 g, 47% yield): TLC R_f = 0.43 (EtOAc/hexanes = 1/4); ^{1}H NMR (500 MHz, $CDCl_3$) δ 7.81 (dd, *J* = 5.5, 3.0 Hz, 2H), 7.73 (dd, *J* = 5.5, 3.1 Hz, 2H), 7.50 – 7.46 (m, 1H), 7.45 – 7.42 (m, 1H), 7.38 (td, *J* = 7.5, 1.3 Hz, 1H), 7.30 (td, *J* = 7.5, 1.4 Hz, 1H), 5.31 (s, 2H), 4.79 (s, 2H), 3.45 (s, 3H). ^{13}C NMR (126 MHz, $CDCl_3$) δ 163.5 138.4 134.4, 131.9, 131.6 129.7 129.3, 128.9, 127.9, 123.6, 77.2 72.2, 58.4; IR (KBr, thin film): 1731, 1464, 1386, 1184, 1136, 1087, 928, 877, 753 cm^{-1}; HRMS-ESI (m/z) [$M+NH_4^+$]: calcd. for $C_{17}H_{16}N_2O_4$ 315.1339, found 315.1339.

Characterization of Allyl Sulfones

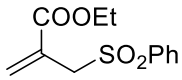

Ethyl-2-((phenylsulfonyl)methyl)acrylate (2).

Viscous oil (1.94 g, 74% yield): TLC R_f = 0.50 (EtOAc/hexanes = 1/4); ^{1}H NMR (400 MHz, $CDCl_3$) δ 7.86 (d, *J* = 7.6 Hz, 2H), 7.64 (t, *J* = 7.6 Hz, 1H), 7.54 (t, *J* = 7.6 Hz, 2H), 6.51 (s, 1H), 5.92(s, 1H), 4.17(s, 2H), 4.01(q, *J* = 7.2 Hz, 2H), 1.17(t, *J* = 7.2 Hz, 3H); ^{13}C NMR (100 MHz, $CDCl_3$) δ 164.7, 138.4, 133.9, 133.3, 129.1, 129.0, 128.8, 61.5, 57.5, 14.0.

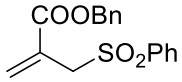

Benzyl-2-((phenylsulfonyl)methyl)acrylate (2-a).

White solid (1.3 g, 20% yield over three steps): TLC R_f = 0.49 (EtOAc/hexanes = 1/4); ^{1}H NMR (400 MHz, $CDCl_3$) δ 7.82 (d, *J* = 7.2 Hz, 2H), 7.59 (t, *J* = 6.9 Hz, 1H), 7.46 (t, *J* = 7.9 Hz, 2H), 7.42 – 7.15 (m, 5H), 6.54 (s, 1H), 5.94 (s, 1H), 4.99 (s, 2H), 4.16 (s, 2H); ^{13}C NMR (125 MHz, $CDCl_3$) δ 164.7, 138.4, 135.4, 134.0, 133.9, 129.1, 129.0, 128.8, 128.7, 128.5, 128.3, 67.3, 57.6; IR (KBr, thin film) 2938, 1721, 1447, 1309, 1246, 1177, 1145, 1084, 967, 750, 689 cm^{-1}; HRMS-ESI (m/z) [$M+H^+$]: calcd. for $C_{17}H_{17}O_4S$ 317.0841, found 317.0842.

Characterization of Allylation Product

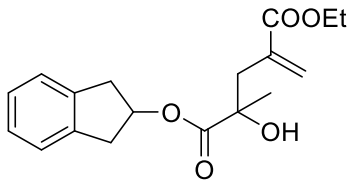

1-(2,3-Dihydro-1*H*-inden-2-yl) 5-ethyl 2-hydroxy-2-methyl-4-methylenepentane-dioate (4).

Colorless oil (29.5 mg, 93% yield) after flash chromatography (95% hexanes : 5% EtOAc): TLC R_f = 0.48 (EtOAc/hexanes = 1/4); ^{1}H NMR (500 MHz, $CDCl_3$) δ 7.24 – 7.18 (m, 4H), 6.22 (d, *J* = 1.5 Hz, 1H), 5.60 (d, *J* = 1.3 Hz, 1H), 5.60 – 5.50 (m, 1H), 4.17 (qd, *J* = 7.1, 5.6 Hz, 2H), 3.64 (s, 1H, -OH), 3.37 – 3.31 (m, 2H), 3.08 – 2.98 (m, 2H), 2.80 (dd, *J* = 14.0, 1.0 Hz, 1H), 2.64 (dd, *J* = 14.0, 1.0 Hz, 1H), 1.40 (s, 3H), 1.28 (t, *J* = 7.1 Hz, 3H); ^{13}C NMR (125 MHz, $CDCl_3$) δ 175.9, 167.9, 140.2, 140.2, 136.0, 128.9, 127.0, 127.0, 124.7, 74.3, 61.2, 41.8, 39.7, 39.5, 25.9, 14.2; IR (KBr, thin film): 3502, 2981, 1720, 1628, 1483, 1370, 1177, 1024, 965, 743 cm^{-1}; HRMS-ESI (m/z) [M+Na^+]: calcd. for $C_{18}H_{22}NaO_5$ 341.1359, found 341.1360.

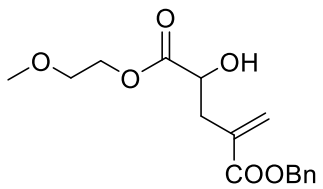

1-Benzyl 5-(2-methoxyethyl) 4-hydroxy-2-methylenepentanedioate (7).

Light yellow oil (27.5 mg, 89% yield) after flash chromatography (95% DCM : 5% EtOAc): TLC R_f = 0.14 (EtOAc/DCM = 1/10); ^{1}H NMR (500 MHz, $CDCl_3$) δ 7.38 – 7.31 (m, 5H), 6.35 (d, *J* = 1.2 Hz, 1H), 5.77 (d, *J* = 1.2 Hz, 1H), 5.24 – 5.18 (m, 2H), 4.47 – 4.43 (m, 1H), 4.34 – 4.25 (m, 2H), 3.59 (t, *J* = 4.7 Hz, 2H), 3.36 (s, 3H), 3.03 (d, *J* = 6.5 Hz, 1H, -OH), 2.91 – 2.87 (m, 1H), 2.72 – 2.67 (m, 1H); ^{13}C NMR (125 MHz, $CDCl_3$) δ 174.3, 167.0, 135.9, 135.6, 129.1, 128.7, 128.4, 128.2, 70.3, 69.6,

66.9, 64.6, 59.1, 37.2; IR (KBr, thin film): 3492, 2930, 1720, 1630, 1456, 1272, 1140, 1039, 742, 699 cm^{-1}; HRMS-ESI (m/z) [M+Na^+]: calcd. for $C_{16}H_{20}NaO_6$ 331.1152, found 331.1158.

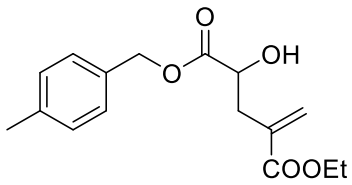

1-Ethyl 5-(4-methylbenzyl) 4-hydroxy-2-methylenepentanedioate (9).

Light yellow oil (26.8 mg, 92% yield) after preparative thin layer chromatography separation (75% hexanes : 12.5% acetone : 12.5% EtOAc): TLC R_f = 0.49 (DCM /acetone/hexanes = 1/1/6); ^{1}H NMR (500 MHz, $CDCl_3$) δ 7.25 (d, *J* = 7.8 Hz, 2H), 7.17 (d, *J* = 7.8 Hz, 2H), 6.24 (d, *J* = 1.3 Hz, 1H), 5.64 (d, *J* = 1.2 Hz, 1H), 5.19 – 5.12 (m, 2H), 4.44 – 4.40 (m, 1H), 4.20 (qd, *J* = 7.1, 2.4 Hz, 2H), 3.09 (d, *J* = 6.6 Hz, 1H, -OH), 2.87 – 2.83 (m, 1H), 2.67 – 2.62 (m, 1H), 2.36 (s, 3H), 1.29 (t, *J* = 7.1 Hz, 3H); ^{13}C NMR (125 MHz, $CDCl_3$) δ 174.2, 167.2, 138.6, 135.8, 132.3, 129.4, 128.7, 128.5, 69.8, 67.4, 61.2, 37.3, 21.3, 14.3; IR (KBr, thin film): 3487, 2981, 1716, 1632, 1447, 1206, 1148, 1098, 1031, 808 cm^{-1}; HRMS-ESI (m/z) [M+Na^+]: calcd. for $C_{16}H_{20}NaO_5$ 315.1203, found 315.1205.

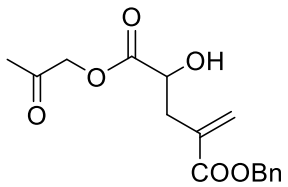

1-Benzyl 5-(2-oxopropyl) (*S*)-4-hydroxy-2-methylenepentanedioate (11).

Light yellow oil (26.8 mg, 88% yield) after flash chromatography (95% DCM : 5% EtOAc): TLC R_f = 0.15 (EtOAc/DCM = 1/10); ^{1}H NMR (500 MHz, $CDCl_3$) δ 7.39 – 7.32 (m, 5H), 6.37 (d, *J* = 1.2 Hz, 1H), 5.82 (d, *J* = 1.1 Hz, 1H), 5.24 – 5.18 (m, 2H), 4.69 (d, *J* = 1.3 Hz, 2H), 4.56 – 4.52 (m, 1H), 3.06 (d, *J* = 6.4 Hz, 1H, -OH), 3.00 – 2.96 (m, 1H), 2.77 – 2.72 (m, 1H), 2.16 (s, 3H); ^{13}C NMR (125 MHz, $CDCl_3$) δ 200.5, 173.5, 167.1, 135.9, 135.3, 129.6, 128.7, 128.4, 128.3, 69.7, 68.9, 67.0, 37.4, 26.2; IR

(KBr, thin film): 3473, 2929, 1719, 1633, 1423, 1274, 1171, 960, 742, 699 cm^{-1}; HRMS-ESI (m/z) [M+Na^+]: calcd. for $C_{16}H_{18}NaO_6$ 329.0996, found 329.0998.

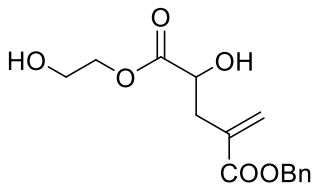

1-Benzyl 5-(2-hydroxyethyl) 4-hydroxy-2-methylenepentanedioate (13).

Light yellow oil (27.9 mg, 95% yield) after flash chromatography (50% hexanes : 50% EtOAc): TLC R_f = 0.32 (EtOAc/hexanes = 2/1); ^{1}H NMR (500 MHz, $CDCl_3$) δ 7.38 – 7.33 (m, 5H), 6.36 (d, *J* = 1.3 Hz, 1H), 5.80 (d, *J* = 1.1 Hz, 1H), 5.21 (s, 2H), 4.44 (td, *J* = 6.5, 5.5 Hz, 1H), 4.35 – 4.30 (m, 1H), 4.21 – 4.17 (m, 1H), 3.79 (q, *J* = 4.9 Hz, 2H), 3.02 (d, *J* = 6.7 Hz, 1H, -OH), 2.87 – 2.79 (m, 2H), 2.32 (d, *J* = 5.9 Hz, 1H, -OH); ^{13}C NMR (125 MHz, $CDCl_3$) δ 174.5, 167.3, 135.7, 135.1, 129.8, 128.8, 128.5, 128.3, 69.5, 67.6, 67.2, 60.9, 37.1; IR (KBr, thin film): 3400, 2954, 1719, 1632, 1455, 1210, 1145, 1083, 748, 699 cm^{-1}; HRMS-ESI (m/z) [M+Na^+]: calcd. for $C_{15}H_{18}NaO_6$ 317.0996, found 317.0996.

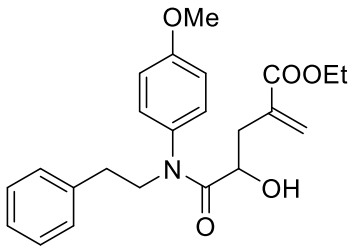

Ethyl 4-hydroxy-5-((4-methoxyphenyl)(phenethyl)amino)-2-methylene-5-oxopentanoate (15).

Light yellow oil (20.7 mg, 52% yield) after flash chromatography (70% hexanes : 30% EtOAc): TLC R_f = 0.29 (EtOAc/hexanes = 1/2); ^{1}H NMR (500 MHz, $CDCl_3$) δ 7.28 – 7.25 (m, 2H), 7.21 – 7.17 (m, 3H), 7.11 (d, *J* = 8.6 Hz, 2H), 6.92 (d, *J* = 8.6 Hz, 2H), 6.20 (d, *J* = 1.5 Hz, 1H), 5.54 (d, *J* = 1.5 Hz, 1H), 4.25 – 4.21 (m, 1H), 4.11 – 4.04 (m, 2H), 4.02 – 3.98 (m, 1H), 3.84 (s, 3H), 3.78 – 3.73 (m, 1H), 3.31 (d, *J* = 9.3

Hz, 1H, -OH), 2.93 – 2.81 (m, 2H), 2.46 (dd, *J* = 13.9, 7.0 Hz, 1H), 2.36 (dd, *J* = 13.9, 4.4 Hz, 1H), 1.21 (t, *J* = 7.1 Hz, 3H); ^{13}C NMR (125 MHz, $CDCl_3$) δ 173.8, 166.8, 159.5, 138.7, 135.5, 133.6, 129.7, 129.0, 128.6, 128.4, 126.5, 115.0, 67.1, 60.8, 55.6, 52.0, 37.1, 33.8, 14.3; IR (KBr, thin film): 3417, 2934, 1714, 1650, 1512, 1455, 1249, 1145, 1029, 701 cm^{-1}; HRMS-ESI (m/z) [M+Na^+]: calcd. for $C_{23}H_{27}NNaO_5$ 420.1781, found 420.1786.

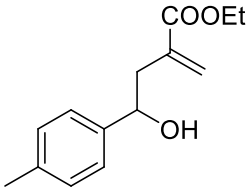

Ethyl 4-hydroxy-2-methylene-4-(p-tolyl)butanoate (17).

Light yellow oil (15.5 mg, 66% yield) after flash chromatography (90% hexanes : 10% acetone): TLC R_f = 0.36 (EtOAc/hexanes = 1/3); ^{1}H NMR (500 MHz, $CDCl_3$) δ 7.25 (d, *J* = 7.8 Hz, 2H), 7.15 (d, *J* = 7.8 Hz, 2H), 6.24 (d, *J* = 1.5 Hz, 1H), 5.60 (d, *J* = 1.3 Hz, 1H), 4.86 (dt, *J* = 8.1, 3.7 Hz, 1H), 4.23 (qd, *J* = 7.1, 1.0 Hz, 2H), 2.80 – 2.76 (m, 1H), 2.69 – 2.65 (m, 1H), 2.54 (d, *J* = 3.5 Hz, 1H, -OH), 2.34 (s, 3H), 1.32 (t, *J* = 7.1 Hz, 3H); ^{13}C NMR (125 MHz, $CDCl_3$) δ 167.8, 141.2, 137.4, 137.3, 129.2, 128.2, 125.8, 73.2, 61.2, 42.6, 21.3, 14.3; IR (KBr, thin film): 3486, 2981, 1713, 1631, 1370, 1305, 1192, 1144, 1028, 816 cm^{-1}; HRMS-ESI (m/z) [M+Na^+]: calcd. for $C_{14}H_{18}NaO_3$ 257.1148, found 257.1151.

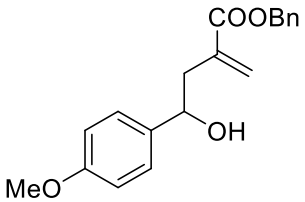

Benzyl 4-hydroxy-4-(4-methoxyphenyl)-2-methylenebutanoate (19).

Light yellow oil (22.1 mg, 71% yield) after preparative thin layer chromatography separation (75% hexanes : 12.5% acetone : 12.5% DCM): TLC R_f = 0.30 (DCM/acetone/hexanes = 1/1/6); ^{1}H NMR (500 MHz, $CDCl_3$) δ 7.38 – 7.33 (m, 5H), 7.27 – 7.24 (m, 2H), 6.87 – 6.84 (m, 2H), 6.28 (d, *J* = 1.4 Hz, 1H), 5.62 (d, *J* = 1.2 Hz,

1H), 5.21 (d, *J* = 3.2 Hz, 2H), 4.84 (dt, *J* = 8.0, 3.8 Hz, 1H), 3.79 (s, 3H), 2.79 – 2.75 (m, 1H), 2.72 – 2.67 (m, 1H), 2.43 (d, *J* = 3.3 Hz, 1H, -OH); ^{13}C NMR (125 MHz, $CDCl_3$) δ 167.5, 159.2, 137.1, 136.2, 136.0, 128.7, 128.4, 128.3, 127.1, 113.9, 72.9, 66.9, 55.4, 42.6; IR (KBr, thin film): 3485, 2955, 1715, 1513, 1456, 1177, 1034, 832, 739, 698 cm^{-1}; HRMS-ESI (m/z) [M+Na$^+$]: calcd. for $C_{19}H_{20}NaO_4$ 335.1254, found 335.1258.

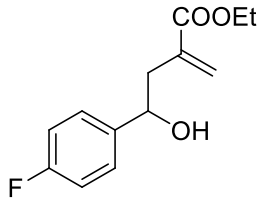

Ethyl 4-(4-fluorophenyl)-4-hydroxy-2-methylenebutanoate (21).

Light yellow oil (12.3 mg, 52% yield) after preparative thin layer chromatography separation (80% hexanes : 20% EtOAc): TLC R_f = 0.52 (EtOAc/hexanes = 1/5); ^{1}H NMR (500 MHz, $CDCl_3$) δ 7.36 – 7.30 (m, 2H), 7.06 – 6.99 (m, 2H), 6.23 (d, *J* = 1.5 Hz, 1H), 5.58 (q, *J* = 1.2 Hz, 1H), 4.88 (dd, *J* = 8.3, 4.0 Hz, 1H), 4.23 (qd, *J* = 7.1, 0.9 Hz, 2H), 2.81 (s, 1H), 2.76 (ddd, *J* = 13.9, 4.2, 1.1 Hz, 1H), 2.64 (ddd, *J* = 14.1, 8.4, 0.9 Hz, 1H), 1.32 (t, *J* = 7.2 Hz, 3H); ^{13}C NMR (125 MHz, $CDCl_3$) δ 167.9, 163.2, 161.3, 139.8, 139.8, 137.1, 128.5, 127.5, 127.5, 115.4, 115.2, 72.7, 61.3, 42.8, 14.3; ^{19}F NMR (376 MHz, $CDCl_3$) δ -115.4 (m); IR (KBr, thin film): 3081, 2955, 1730, 1574, 1451, 1189, 1065, 952, 750, 661 cm^{-1}; HRMS-ESI (m/z) [M-H_2O+H$^+$]: calcd. for $C_{13}H_{13}FO_2$ 221.0972, found 221.0976.

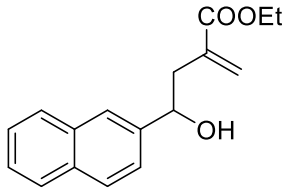

Ethyl 4-hydroxy-2-methylene-4-(naphthalen-2-yl)butanoate (23).

Light yellow oil (19.8 mg, 73% yield) after preparative thin layer chromatography separation (80% hexanes : 20% EtOAc): TLC R_f = 0.36 (EtOAc/hexanes = 1/4); ^{1}H

NMR (500 MHz, $CDCl_3$) δ 7.84 – 7.81 (m, 4H), 7.50 – 7.44 (m, 3H), 6.24 (d, *J* = 1.4 Hz, 1H), 5.61 (d, *J* = 1.2 Hz, 1H), 5.07 (dd, *J* = 8.4, 4.0 Hz, 1H), 4.23 (qd, *J* = 7.2, 1.1 Hz, 2H), 2.91 – 2.87 (m, 1H), 2.84 (s, 1H, -OH), 2.78 – 2.73 (m, 1H), 1.31 (t, *J* = 7.2 Hz, 3H); ^{13}C NMR (125 MHz, $CDCl_3$) δ 168.0, 141.5, 137.3, 133.4, 133.1, 128.4, 128.3, 128.1, 127.8, 126.2, 125.9, 124.5, 124.1, 73.5, 61.3, 42.7, 14.3; IR (KBr, thin film): 3464, 2981, 1710, 1630, 1321, 1142, 1028, 858, 819, 747 cm^{-1}; HRMS-ESI (m/z) $[M+Na^+]$: calcd. for $C_{17}H_{18}NaO_3$ 293.1148, found 293.1155.

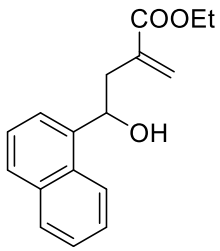

Ethyl 4-hydroxy-2-methylene-4-(naphthalen-1-yl)butanoate (25).

Light yellow oil (18.3 mg, 68% yield) after preparative thin layer chromatography separation (80% hexanes : 20% EtOAc): TLC R_f = 0.39 (EtOAc/hexanes = 1/4); ^1H NMR (500 MHz, $CDCl_3$) δ 8.22 (d, *J* = 8.5 Hz, 1H), 7.88 (d, *J* = 8.0 Hz, 1H), 7.78 (d, *J* = 8.2 Hz, 1H), 7.73 (d, *J* = 7.2 Hz, 1H), 7.56 – 7.53 (m, 1H), 7.50 – 7.47 (m, 2H), 6.31 (d, *J* = 1.4 Hz, 1H), 5.70 – 5.68 (m, 2H), 4.28 (qd, *J* = 7.1, 4.5 Hz, 2H), 3.09 – 3.06 (m, 1H), 2.77 (s, 1H, -OH), 2.68 – 2.64 (m, 1H), 1.36 (t, *J* = 7.1 Hz, 3H); ^{13}C NMR (125 MHz, $CDCl_3$) δ 167.9, 139.9, 137.5, 133.8, 130.3, 129.0, 128.6, 128.0, 126.2, 125.6, 125.6, 123.2, 122.7, 69.7, 61.3, 42.3, 14.3; IR (KBr, thin film): 3472, 2981, 1708, 1630, 1512, 1325, 1144, 1028, 802, 779 cm^{-1}; HRMS-ESI (m/z) $[M+Na^+]$: calcd. for $C_{17}H_{18}NaO_3$ 293.1148, found 293.1152.

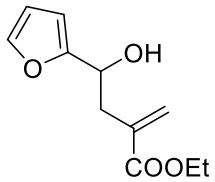

Ethyl 4-(furan-2-yl)-4-hydroxy-2-methylenebutanoate (27).

Light yellow oil (15.7 mg, 75% yield) after preparative thin layer chromatography

separation (75% hexanes : 12.5% acetone : 12.5% EtOAc): TLC R_f = 0.30 (EtOAc /acetone/hexanes = 1/1/6); ^{1}H NMR (500 MHz, $CDCl_3$) δ 7.37 (dd, *J* = 1.8, 0.8 Hz, 1H), 6.32 (dd, *J* = 3.3, 1.8 Hz, 1H), 6.26 – 6.25 (m, 2H), 5.64 (d, *J* = 1.2 Hz, 1H), 4.91 (dt, *J* = 8.2, 4.9 Hz, 1H), 4.23 (q, *J* = 7.1 Hz, 2H), 2.92 – 2.88 (m, 1H), 2.86 – 2.81 (m, 1H), 2.65 (d, *J* = 5.0 Hz, 1H, -OH), 1.31 (t, *J* = 7.1 Hz, 4H); ^{13}C NMR (125 MHz, $CDCl_3$) δ 167.7, 156.1, 142.1, 136.8, 128.4, 110.3, 106.3, 67.2, 61.3, 39.0, 14.3; IR (KBr, thin film): 3448, 2983, 1713, 1630, 1370, 1275, 1190, 1012, 949, 748 cm^{-1}; HRMS-EI (m/z) [M$^+$]: calcd. for $C_{11}H_{14}O_4$ 210.0892, found 210.0891.

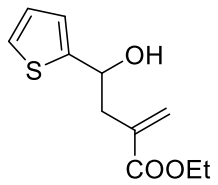

Ethyl 4-hydroxy-2-methylene-4-(thiophen-2-yl)butanoate (29).

Light yellow oil (16.0 mg, 71% yield) after preparative thin layer chromatography separation (75% hexanes : 25% acetone): TLC R_f = 0.50 (acetone/hexanes = 1/3); ^{1}H NMR (500 MHz, $CDCl_3$) δ 7.23 (dd, *J* = 4.6, 1.7 Hz, 1H), 6.97 – 6.95 (m, 2H), 6.26 (d, *J* = 1.4 Hz, 1H), 5.65 (d, *J* = 1.2 Hz, 1H), 5.15 (dd, *J* = 8.3, 4.5 Hz, 1H), 4.23 (q, *J* = 7.1 Hz, 2H), 2.91 – 2.84 (m, 2H), 2.82 – 2.78 (m, 1H), 1.32 (t, *J* = 7.1 Hz, 3H); ^{13}C NMR (125 MHz, $CDCl_3$) δ 167.7, 148.1, 136.8, 128.7, 126.8, 124.5, 123.7, 69.5, 61.3, 42.8, 14.3; IR (KBr, thin film): 3469, 2982, 2931, 1712, 1630, 1443, 1306, 1200, 1028, 700 cm^{-1}; HRMS-ESI (m/z) [M+Na$^+$]: calcd. for $C_{11}H_{14}NaO_3S$ 249.0556, found 249.0555.

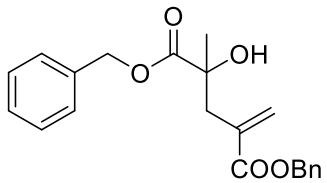

Dibenzyl 2-hydroxy-2-methyl-4-methylenepentanedioate (31).

Colourless oil (17.9 mg, 51 % yield) after preparative thin layer chromatography separation (75% hexanes : 12.5% acetone : 12.5% EtOAc): TLC R_f = 0.68

(EtOAc/acetone/hexanes = 1/1/6); ^{1}H NMR (500 MHz, $CDCl_3$) δ 7.38 – 7.30 (m, 8H), 6.26 (d, *J* = 1.3 Hz, 1H), 5.65 – 5.60 (m, 1H), 5.19 – 5.04 (m, 4H), 3.58 (s, 1H), 2.88 (d, *J* = 13.9 Hz, 1H), 2.70 (d, *J* = 13.9 Hz, 1H), 1.46 (s, 3H); ^{13}C NMR (125 MHz, $CDCl_3$) δ 175.8, 167.6, 135.9, 135.5, 135.4, 129.7, 128.7, 128.7, 128.6, 128.4, 128.4, 128.2, 74.5, 67.6, 67.0, 42.1, 25.7; IR (KBr, thin film): 3445, 2935, 1721, 1627, 1455, 1267, 1214, 1160, 962, 697 cm^{-1}; HRMS-ESI (m/z) [M+H$^+$]: calcd. for $C_{21}H_{23}O_5$ 355.1540, found 355.1538.

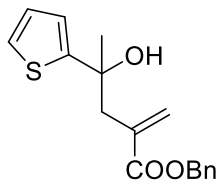

Benzyl 4-hydroxy-2-methylene-4-(thiophen-2-yl)pentanoate (33).

Colourless oil (14.4 mg, 53 % yield) after preparative thin layer chromatography separation (75% hexanes : 12.5% acetone : 12.5% EtOAc): TLC R_f = 0.74 (EtOAc/acetone/hexanes = 1/1/6); ^{1}H NMR (500 MHz, $CDCl_3$) δ 7.44 – 7.30 (m, 5H), 7.15 (dd, *J* = 5.1, 1.2 Hz, 1H), 6.92 (dd, *J* = 5.1, 3.5 Hz, 1H), 6.86 (dd, *J* = 3.5, 1.2 Hz, 1H), 6.27 (d, *J* = 1.3 Hz, 1H), 5.53 (d, *J* = 1.1 Hz, 1H), 5.18 (s, 2H), 3.83 (s, 1H), 2.91 (s, 2H), 1.61 (s, 3H); ^{13}C NMR (125 MHz, $CDCl_3$) δ 168.8, 153.3, 136.1, 135.7, 130.2, 128.7, 128.5, 128.3, 126.8, 123.8, 122.4, 73.6, 67.2, 47.2, 30.6; IR (KBr, thin film): 3445, 3066, 2975, 1714, 1625, 1455, 1383, 1164, 750, 697 cm^{-1}; HRMS-ESI (m/z) [M+Na$^+$]: calcd. for $C_{17}H_{18}NaO_3S$ 325.0869, found 325.0874.

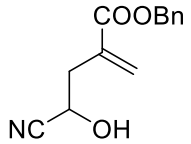

Benzyl 4-cyano-4-hydroxy-2-methylenebutanoate (35).

Light yellow oil (13.7 mg, 59% yield) after preparative thin layer chromatography separation (75% hexanes : 12.5% acetone : 12.5% DCM): TLC R_f = 0.27 (DCM /acetone/hexanes = 1/1/6); ^{1}H NMR (500 MHz, $CDCl_3$) δ 7.40 – 7.36 (m, 5H), 6.48 (d, *J* = 0.8 Hz, 1H), 5.92 (d, *J* = 1.0 Hz, 1H), 5.24 (d, *J* = 1.7 Hz, 2H), 4.74 (td, *J* = 6.8,

4.9 Hz, 1H), 3.86 (d, J = 6.9 Hz, 1H, -OH), 2.92 – 2.88 (m, 1H), 2.85 – 2.81 (m, 1H); ^{13}C NMR (125 MHz, $CDCl_3$) δ 167.9. 135.3, 134.1, 131.8, 128.9, 128.8, 128.5, 118.9, 67.8, 61.4, 38.6; IR (KBr, thin film): 3456, 2924, 1713, 1456, 1304, 1148, 1074, 913, 743, 699 cm^{-1}; HRMS-ESI (m/z) [M+Na$^+$]: calcd. for $C_{13}H_{13}NNaO_3$ 254.0788, found 254.0784.

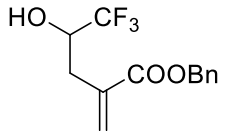

Benzyl 5,5,5-trifluoro-4-hydroxy-2-methylenepentanoate (38).

Colourless oil (10.9 mg, 39 % yield) after preparative thin layer chromatography separation (75% hexanes : 12.5% acetone : 12.5% EtOAc): TLC R_f = 0.63 (EtOAc /hexanes = 1/4); ^{1}H NMR (500 MHz, $CDCl_3$) δ 7.46 – 7.29 (m, 4H), 6.40 (s, 1H), 5.83 (s, 1H), 5.24 (s, 2H), 4.14 (th, J = 9.5, 3.3 Hz, 1H), 3.30 (d, J = 5.9 Hz, 1H), 2.79 (dd, J = 14.3, 2.8 Hz, 1H), 2.63 (dd, J = 14.4, 9.6 Hz, 1H). ^{13}C NMR (126 MHz, $CDCl_3$) δ 167.55, 135.34, 134.87, 130.03, 128.64, 128.46, 128.17, 70.25, 70.00, 69.80, 69.75, 69.50, 67.24, 33.38. ^{19}F NMR (376 MHz, Chloroform-*d*) δ -79.78 (d, J = 6.5 Hz); IR (KBr, thin film): 3446, 1714, 1697, 1455, 1415, 1318, 1213, 1171, 1127, 696 cm^{-1}; HRMS-ESI (m/z) [M+NH$_4^+$]: calcd. for $C_{13}H_{17}F_3NO_3$ 292.1155, found 292.1155.

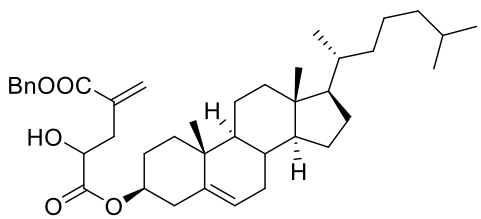

1-Benzyl 5-((3S,9S,10R,13R,14S,17R)-10,13-dimethyl-17-(6-methylheptan-2-yl)-2,3,4,7,8,9,10,11,12,13,14,15,16,17-tetradecahydro-1H-cyclopenta[a]phenanthren-3-yl) 4-hydroxy-2-methylenepentanedioate (41).

Colourless oil (38.4 mg, 62 % yield) after flash chromatography separation (EtOAc/hexanes = 1/10): TLC R_f = 0.71 (EtOAc /acetone/hexanes = 1/1/6); ^{1}H NMR (500 MHz, $CDCl_3$) δ 7.41 – 7.31 (m, 4H), 6.35 (d, J = 1.3 Hz, 1H), 5.76 (t, J = 1.3 Hz,

1H), 5.42 – 5.34 (m, 1H), 5.27 – 5.16 (m, 2H), 4.68 (dq, *J* = 10.7, 6.0, 5.3 Hz, 1H), 4.38 (dd, *J* = 8.2, 4.3 Hz, 1H), 2.88 (dd, *J* = 14.4, 4.3 Hz, 1H), 2.64 (dd, *J* = 14.3, 8.2 Hz, 1H), 2.32 (t, *J* = 6.7 Hz, 2H), 2.04 – 1.94 (m, 2H), 1.85 (tdd, *J* = 13.0, 6.7, 3.4 Hz, 3H), 1.64 – 1.41 (m, 8H), 1.39 – 1.21 (m, 5H), 1.20 – 1.05 (m, 7H), 1.01 (s, 6H), 0.91 (d, *J* = 6.5 Hz, 3H), 0.86 (dd, *J* = 6.6, 2.4 Hz, 6H), 0.68 (s, 3H); ^{13}C NMR (125 MHz, $CDCl_3$) δ 173.9, 166.9, 139.3, 135.9, 135.7, 129.0, 128.7, 128.4, 128.2, 123.2, 75.9, 69.5, 66.9, 56.8, 56.2, 50.1, 42.4, 39.8, 39.6, 38.1, 37.4, 37.0, 36.7, 36.3, 35.9, 32.0, 31.9, 28.4, 28.2, 27.8, 24.4, 23.9, 23.0, 22.7, 21.1, 19.4, 18.8, 12.0; IR (KBr, thin film): 3446, 2947, 2867, 1723, 1466, 1383, 1210, 1101, 749, 696 cm^{-1}; HRMS-ESI (m/z) [M+Na$^+$]: calcd. for $C_{40}H_{58}NaO_5$ 641.4176, found 641.4180.

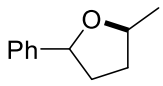

2-Methyl-5-phenyltetrahydrofuran (44).

Colorless oil (10.1 mg, 62 % yield) after flash chromatography (90% hexanes : 10% EtOAc): TLC R_f = 0.87 (EtOAc/hexanes = 1/9); ^{1}H NMR (500 MHz, $CDCl_3$) δ 8.36 – 8.23 (m, 5H), 6.05 – 5.86 (m, 1H), 5.39 – 5.14 (m, 1H), 3.39 – 3.28 (m, 1H), 3.17 – 3.07 (m, 1H), 2.90 – 2.82 (m, 1H), 2.64 – 2.59 (m, 1H), 2.34 (dd, *J* = 25.1, 6.1 Hz, 3H); ^{13}C NMR (125 MHz, $CDCl_3$) δ 144.1, 143.7, 128.4, 128.4, 127.3, 127.2, 126.0, 125.7, 81.2, 80.4, 76.1, 76.1, 35.7, 34.8, 34.4, 33.2, 21.7, 21.5.

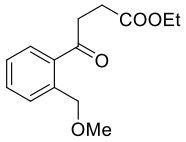

Ethyl 4-(2-(methoxymethyl)phenyl)-2-methylene-4-oxobutanoate (47-ox).

Colorless oil (7.9 mg, 30 % yield): TLC R_f = 0.65 (EtOAc/hexane = 1/4); ^{1}H NMR (500 MHz, $CDCl_3$) δ 7.79 (d, *J* = 7.7 Hz, 1H), 7.65 (d, *J* = 7.8 Hz, 1H), 7.51 (t, *J* = 7.6 Hz, 1H), 7.37 (t, *J* = 7.6 Hz, 1H), 6.41 (s, 1H), 5.69 (s, 1H), 4.71 (s, 2H), 4.21 (q, *J* = 7.1 Hz, 2H), 3.94 (s, 2H), 3.43 (s, 3H), 1.27 (t, *J* = 7.1 Hz, 3H). ^{13}C NMR (126 MHz, $CDCl_3$) δ 200.26, 166.39, 139.49, 135.97, 134.85, 131.88, 128.65, 128.54, 127.73,

126.94, 72.48, 61.03, 58.63, 44.26, 14.12. IR (KBr, thin film) 2982, 2930, 1716, 1685, 1312, 1198, 1146, 1100, 1026, 1003, 950, 760 cm^{-1}; HRMS-ESI (m/z) $[M+H^+]$: calcd. for $C_{15}H_{18}O_4$ 263.1278, found 263.1278.

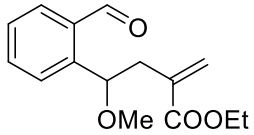

Ethyl 4-(2-formylphenyl)-4-methoxy-2-methylenebutanoate (48-ox)

Colorless oil (2.6 mg, 10 % yield): TLC Rf = 0.68 (EtOAc/hexane = 1/4); ^{1}H NMR (500 MHz, Chloroform-*d*) δ 10.36 (s, 1H), 7.86 (d, *J* = 7.6 Hz, 1H), 7.61 (d, *J* = 5.9 Hz, 2H), 7.45 (t, *J* = 7.0 Hz, 1H), 6.20 (s, 1H), 5.57 (s, 1H), 5.27 (dd, *J* = 8.1, 4.8 Hz, 1H), 4.18 (q, *J* = 7.1 Hz, 2H), 3.24 (s, 3H), 2.86 – 2.61 (m, 2H), 1.29 (t, *J* = 7.1 Hz, 3H). ^{13}C NMR (126 MHz, $cdcl_3$) δ 192.52, 167.03, 144.41, 136.89, 133.98, 133.91, 131.74, 127.74, 127.22, 127.21, 78.45, 60.72, 57.17, 40.51, 14.17. IR (KBr, thin film) 2982 2933 1713 1693 1599 1310 1188 1144 1098 1027 763 cm^{-1}; HRMS-ESI (m/z) $[M+H^+]$: calcd. for $C_{15}H_{18}O_4$ 263.1278, found 263.1279.

V. References

Barone, V.; Cossi, M.; Tomasi, J. (1998) Geometry optimization of molecular structures in solution by the polarizable continuum model. J. Comput. Chem. *19*, 404.

Becke, A. D. (1993) Density-functional thermochemistry. III. The role of exact exchange. J. Chem. Phys. *98*, 5648.

Cances, E.; Mennucci, B.; Tomasi, J. (1997) A new integral equation formalism for the polarizable continuum model: Theoretical background and applications to isotropic and anisotropic dielectrics. J. Chem. Phys. *107*, 3032.

Cossi, M.; Barone, V.; Cammi, R.; Tomasi, J. (1996) Ab initio study of solvated molecules: a new implementation of the polarizable continuum model. Chem. Phys. Lett. *255*, 327.

Lee, C.; Yang, W.; Parr, R. G. (1988) Development of the Colle-Salvetti correlation-energy formula into a functional of the electron density. Phys. Rev. B: Condens. Matter Mater. Phys. *37*, 785.

Liu, S.; Qi, X.; Qu, L.-B.; Bai, R. B.; Lan, Y. (2018) C–H bond cleavage occurring on a Rh(V) intermediate: a theoretical study of Rh-catalyzed arene azidation. Catal. Sci. Technol. *8*, 1645.

Marenich, A. V.; Cramer, C. J.; Truhlar, D. G. (2009) Universal Solvation Model Based on Solute Electron Density and on a Continuum Model of the Solvent Defined by the Bulk Dielectric Constant and Atomic Surface Tensions. J. Phys. Chem. B *113*, 6378.

Peverati, R.; Truhlar, D. G. (2011) Improving the accuracy of hybrid meta-GGA density functionals by range separation. J. Phys. Chem. Lett. *2*, 2810.